INVESTIGATION OF MAGNETOGENIC POLLUTANTS USING ENVIRONMENTAL MAGNETISM TECHNIQUES AND ATOMIC ABSORPTION ANALYSIS IN ABUJA METROPOLIS, NIGERIA

BY

JATTO, SOLOMON SUNDAY

DEPARTMENT OF PHYSICS

FACULTY OF SCIENCE

AHMADU BELLO UNIVERSITY,

ZARIA

JULY, 2018

INVESTIGATION OF MAGNETOGENIC POLLUTANTS USING ENVIRONMENTAL MAGNETISM TECHNIQUES AND ATOMIC ABSORPTION ANALYSIS IN ABUJA METROPOLIS, NIGERIA

BY

JATTO, SOLOMON SUNDAY B.Sc (UNIJOS) 2005, MSc. (ABU) 2011

Ph.D/SCI/4757/2011-2012

A DISSERTATION SUBMITTED TO THE POSTGRADUATE SCHOOL

AHMADU BELLO UNIVERSITY (ABU), ZARIA

NIGERIA IN PARTIAL FULFILLMENT FOR THE AWARD OF THE DOCTOR OF PHILOSOPHY IN APPLIED GEOPHYSICS

DEPARTMENT OF PHYSICS

AHMADU BELLO UNIVERSITY,

ZARIA, NIGERIA

JULY, 2018

DECLARATION

I declare that the work in the thesis entitled **'Investigation of Magnetogenic Pollutants using Environmental Magnetism Techniques and Atomic Absorption Analysis in Abuja Metropolis, Nigeria' has** been performed by me in the Department of Physics under the supervision of Dr. P. O. Sule, A.L. Ahmed and A. S. Arabi.

The information derived from literature has been duly acknowledged in the text and a list of references provided. No part of this dissertation was previously presented for another degree or diploma at any university.

Name of student	Signature	Date

CERTIFICATION

This thesis entitled **'Investigation of Magnetogenic Pollutants using Environmental Magnetism Techniques and Atomic Absorption Analysis in Abuja Metropolis, Nigeria'**by Jatto, Solomon Sunday meets the regulations governing the award of Doctor of Philosophy of the Ahmadu Bello University, Zaria and is approved for its contribution to knowledge and literacy presentation.

Chairman Supervisory committee	Sign/Date
Member, Supervisory committee	Sign/Date
Member, Supervisory committee	Sign/Date
HOD Physics Department	Sign/Date
Dean, Postgraduate School	Sign/Date

DEDICATION

To my lovely Mother, whose love is beyond measure, the words of her mouth are life indeed.

I love you greatly.

ACKNOWLEDGEMENTS

At this moment of accomplishment, first of all I wish to extend my profound gratitude to my supervisor Dr. P. O. Sule for picking me as a student in my pursuit of Ph. D and providing necessary infrastructure and resources to accomplish this work under strong criticism and fatherly advice. I am very much thankful to him for his scholarly inputs, ideas and boundless optimism and contributions of time to make my Ph. D experience productive, stimulating and exciting.

It is my great pleasure to acknowledge Dr. A. L. Ahmed, for his valuable advice, constructive criticism and his extensive discussions of my work. It is a superb experience to be with him and learn how to face, think, and evaluate different kinds of problems. He has a wonderful ability to see and find beautiful things from what looks somewhat boring and unimportant.

I will like to extend my profound gratitude to Dr. A S. Arabi for his mentorship contributions to this dissertation. It is really a great privilege working as a student under you.

I would like to thank the former Head of Physics Department, Late Dr. Zakari for providing me the facilities and administrative support to carry out my Ph. D. work smoothly. Appreciation is due to the former HOD, Dr. Umar Sadiq, and the Postgraduate Coordinator, Dr Onoja for their support and fair dealing at various important phases of this Ph.D. programme.

My special thanks go to Prof. N. Basavaiah of the National Centre for Geophysical research India where I was first introduced to the applications of environmental magnetism.

I will also like to extend my appreciation to Prof. Kola Lawal of the Department of Physics, Ahmadu Bello University, Zaria, indeed his constructive criticism brought out the beauty of this work.

I wish to acknowledge a friend and master in the field, Mr. B. Kasal, who I also called upon whenever I have problems with operating an instrument.

I am forever grateful to my Director; Prof. Babatunde Rabiu for his kind support, encouragement, fatherly advice and opportunity he gave me to undergo this programme. I also wish to extend my appreciation to all the staff of the Center for Atmospheric Research, National Space Research and Development Ageny, Anyigba, for their kind support most especially, Dr. Daniel Okoh, who I easily ran to when I find it difficult with Matlab programme, Mr. Enoch Elemo for his brotherly support; Mr. Najib Yusuf who willingly give me the opportunity to travel in and out of office for my research and Mr. Suleiman Abdulraham who assisted me in editing some of the maps and Miss Oluwatobiloba Johnson for her assistance in typing part of the notes.

I take this opportunity to thank Mr. Ezekiel Josiah, Dr. Kizito Musa, Dr Afuwai Cyril and the FCT Police for making my field investigations smooth and enjoyable at Abuja. Thanks are due to Miss Rose Matthew, Mr. Steve Onoja and Mr. Isaac James for all their efforts in road dust sample collection.

My appreciation will not be complete without paying tribute to Mr. B. Nwosu of blessed memory who first took me through geophysical field experience; you still live fresh in my heart.

My time at Ahmadu Bello University, Zaria was made enjoyable in large part due to the many friends and groups that became a part of my life. I am deeply thankful to my friends Cyril, Kizito and George who had always supported me through thick and thin.

I would like to thank my family for all their love, support, encouragement and their belief in me. I am forever grateful for their sacrifices without which I could not have made it here.

I really do not know how to express my gratitude to my loving and beautiful wife; Mrs. Olayinka Deborah Jatto who stood by me through all the darkest moment of this research and with wisdom she always told me ‘it is possible’. I love you greatly.

At the end, it is a pleasant task to express my thanks to all those who contributed in many ways to the success of this study and made it an unforgettable experience for me. Above all, I owe it all to Almighty God for granting me the wisdom, health and strength to undertake this research task and enabling me complete it.

ABSTRACT

In this study, the use of environmental magnetism techniques were applied both as a proxy and as a fast and time efficient method to investigate the spatial and vertical distribution of these magnetic grains within some road networks and soils of Abuja. Results from these methods where complimented with Atomic Absorption Spectrometer analysis of some roadside and urban soils of Abuja. The susceptibility test on rock samples and background soil samples within the study area show a low magnetic susceptibility values of about (40.0-120.0) x 10^{-5}SI, with an average of about 112.0 x 10^{-5}SI. The magnetic susceptibility results around the city of Abuja shows magnetic susceptibility enhancement of about (350.0-700.0) x 10^{-5}SI. These values were dominant along the road networks and commercial areas at the surface to a depth of about 30.0cm in soil profiles. The susceptibility also decreases with increasing distance away from roads and commercial places and highly reduced in residential areas of Abuja. The 2D spatial distribution of magnetic susceptibility with depth reveals the pattern theses magnetic grains are distributed in the subsurface. From the profiles obtained, it is evidenced that the anthropogenic boundary is about 20.0-30.0cm of depth. From the field measurements it is observed that the frequency-dependence of magnetic susceptibility (χ_{fd}%) values are very low (0-5.0%) in most of the areas on the surface soil. Low frequency-dependence susceptibility values indicate that the magnetic properties are predominantly contributed by the coarse multidomian (MD) and stable single domain (SSD) grains of anthropogenic rather than super paramagnetic grains. From the surface map, low frequency-susceptibility is mostly observed in Wuse, Garki and Part of Central districts, these districts have high commercial activities and vehicle movement. In Asokoro district, the frequency-dependence susceptibility is mostly above 6%, this is due to the contribution of the super paramagnetic grains from the parent rocks. At a depth of 30.0 cm, the subsurface map clearly show frequency-dependence susceptibility greater than 6% in almost all the area with exception of few portions. This indicates that, super paramagnetic grains are the main contributors to the magnetic susceptibility at that depth. These super paramagnetic grains are mostly from pedogenic origin rather than anthropogenic source. From most of the samples, magnetite, pyrrhotite and hematite were evidenced in the susceptibility variation with temperature. Atomic Absorption Spectrometer analysis of these soil samples indicates the presence of Iron, Chromium, Lead, Zinc, Cadmium and Nickel in large concentration at the surface soil but decreases with depth. A strong positive correlation exists between concentration of Fe, Pb, and Cd with the spatial magnetic susceptibility measurements. From the research obtained in this study, high magnetic enhancements are attributed to vehicular/industrial activities within the areas and mostly deposited at the surface with the boundary depth between anthropogenic pollutants and pedogenic influenced susceptibility placed at 30.0cm. The frequency-dependence less than 5.0 percent predominantly found near road networks and most of the commercial areas at the surface but almost not all observed at the depth of 30.0cm. These indicate the contribution of vehicular/industrial emission to the deposition of these particles in the environment. The strong correlation between magnetic susceptibility and the concentration of Lead, Iron and Chromium indicates that these heavy metals contribute most of the high magnetic susceptibility observed around Abuja city. From the results obtained here, it is clear only magnetic method can be an effective

and efficient tool to map out anthropogenic magnetic pollutants at the surface and at various depths.

TABLE OF CONTENTS

Cover Page …… …… …… …… …… …… …… …… …… i

Fly Leaf ….. ……. …… …… …… …… …… …… …… …… ii

Title Page …..…… …… …… …… …… …… …… …… …… iii

Declaration …..……. …… …… …… …… …… …… …… …… iv

Certification ……. …… …… …… …… …… …… …… …… v

Dedication…..…… …… …… …… …… …… …… …… …… vi

Acknowledgement … ……. …… …… …… …… …… …… ……. vii

Abstract ….. …… …… …… …… …… …… …… …… x

Table of Contents …..…… ……. …… …… …… …… …… …… xii

List of Figures ….. …… …… …… …… …… …… …… …… xvi

List of Tables ….. …… ……. …… …… …… …… …… …… xxi

List of Plates ….. …… …… …… …… …… …… …… …… xxii

List of Appendices … ……. …… …… …… …… …… …… …… xxiv

List of Abbreviation ….. …… …… …… …… …… …… …… xxv

CHAPTER ONE GENERAL INTRODUCTION… ……. …… 1

1.1 Brief Overview….. …… …… …… …… …… …… 1

1.2 Heavy metals in soil… …… …… …… ……. …… 4

1.3 Atomic Absorption Spectrometer …… … ….. ……. …… 5

1.4 Health effects associated with urban environmental pollution…. ….. 6

1.5 Justification of the Research ….. …… ……. …… …… …… 9

1.6 Aims and Objectives of the Study… ……. … …… …… …… 10

1.7 Study Area ….. …… ……. …… …… …… …… …… 12

1.8 General Geology of Federal Capital Territory (FCT)…… …… …… 15

CHAPTER TWO LITERATURE REVIEW….. …… …… 16

2.1 Introduction ……. …… …… …… …… …… …… …… 16

2.2 Previous environmental magnetism studies on pollution…..……. …… 16

2.3 Basic magnetic properties…..….. …… …… …… …… ……. 27

2.3.1 Diamagnetism ….. …… ……. …… …… …… …… …… 28

2.3.2 Paramagnetism ….. …… ……. …… …… …… …… …… 28

2.3.3 Ferromagnetism ….. …… …… …… …… …… …… 29

2.4 Hysteresis …..…… ……..…… …… …… …… …… …… 30

2.4.1 The Hysteresis loop and magnetic properties ….. ……. …… …… 31

2.5 Magnetic susceptibility ….. …… …… …… …… …… …… 34

2.5.1 Anisotropy of magnetic susceptibility …. ……. …… …… …… 35

2.5.2 Factors that affect the magnetic susceptibility ….. ……. …… …… 36

2.6 Magnetic properties of materials ….. …… …… …… …… 39

2.7 Low and high temperature dependence susceptibility … ……. …… 42

2.7.1 Thermal disordering ….. …… …… …… …… …… …… 42

2.7.2 Magnetocrystalline anisotropy phase transitions ……. …… …… 43

2.7.3 Mineral destruction and formation ….. …… …… …… …… 44

CHAPTER THREE INSTRUMENTATION AND METHODOLOGY… 45

3.1 Introduction ….. … …… …… …… …… …… …… 45

3.2 Geology Mapping…. ….. …… …… …… …… …… …. 45

3.3 Bartington MS2 Magnetic Susceptibility Meter ….. …… …… …… 46

3.3.1 Principle of operation of Bartington MS2 meter …. ……. …… …… 48

3.4 Field measurement ….. … …… …… …… …… …… 49

3.5 Sample collection method selected in this work ……. …… …… 53

3.5.1 Sampling….. …… …… …… …… ….. …… …… ……. 54

3.5.2 Sample Digestion……. …… ……. …… …… …… ……. 54

CHAPTER FOUR DATA PROCESSING AND INTERPRETATIONS….. 56

4.1 Introduction ….. …… …… …… ….. …… ….. …… 56

4.2 Background magnetic susceptibility ….. …… …… …… …… 57

4.3 Magnetic Susceptibility data processing and interpretation….. …… 60

4.3.1 Central district magnetic susceptibility data …… …… …… ……. 61

4.3.2 Garki district magnetic susceptibility data ……. …… …… …… 67

4.3.3 Wuse district magnetic susceptibility data ……. …… …… …… 72

4.3.4 Maitama magnetic susceptibility data ….. … …… …… …… 77

4.3.5 Asokoro magnetic susceptibility data ….. …… …… …… …… 82

4.4 Vertical soil and sediment profiles along road sections ……. …… 87

4.4.1 Background areas of soil profiles ……. …… …… …… …… 87

4.4.2 Vertical soil profiles along selected roads in wuse area …… …… 90

4.4.3 Vertical soil profiles along selected roads in garki area ……. …… 90

4.4.4 Vertical soil profiles along selected roads in central area …… …… 91

4.4.5 Vertical soil profiles along selected roads in maitama area …… …… 92

4.4.6 Vertical soil profiles along selected roads in asokoro area …… …… 93

4.5 2D spatial distributions of magnetic susceptibility variation with depth… 94

4.5.1 2D data Interpretation ….. …… ……. … …… ……. 95

4.5.2 Interpretation of magnetic susceptibility profiles line ….. …… 102

4.6 Frequency dependent magnetic susceptibility ….. …… …… 106

4.6.1 Spatial frequency dependent magnetic susceptibility distribution in Abuja with depth ……. ….. …… …… ….. 108

4.7 Temperature dependence of magnetic susceptibility ……. …… …… 114

4.7.1 Low temperature dependence of magnetic susceptibility ……. …… 115

4.7.2 High temperature dependence of magnetic susceptibility ……. …… 118

CHAPTER FIVE HEAVY METALS CONCENTRATION IN ABUJA SOIL. 123

5.1 Introduction ….. …… …… …… …… …… …… …… 123

5.1.1 Concentration of Iron (Fe) within Abuja surface and subsurface soil ….. …… ……. ….. ….. ….. ….. ….. 123

5.1.2 Concentration of Cadmium (Cd) within Abuja surface and subsurface soil ….. …… …… …… …… ….. …… …. 126

5.1.3 Concentration of Chromium (Cr) within Abuja surface and subsurface soil ….. …… …… …… …… ….. …. 128

5.1.4 Concentration of Lead (Pb) within Abuja surface and subsurface soil ….. …… ……. …… …… ……. ……. ….. 130

5.1.5 Concentration of Zinc (Zn) within Abuja surface and subsurface soil ….. …… ……. …… …… ….. ….. ….. 133

5.1.6 Concentration of Nickel (Ni) within Abuja surface and subsurface ….. …… ……. …… ……. …… ….. …. 136

5.2 Correlation between magnetic susceptibility and heavy metals … ……. 138

CHAPTER SIX DISCUSSION SUMMARY AND RECCOMENDATION… 142

6.1 Discussion ….. …… …… …… …… …… …… …… 142

6.1.1 Discussion on magnetic susceptibility measurements …. ……. …… 143

6.1.2 Discussion on AAS analysis ….. …… …… …… …… 149

6.2 Conclusion ….. …… ……. …… …… …… …… …… 151

6.3 Recommendations ….. …… …… …… …… …… …… 151

REFERENCES ….. …… …… …… …… …… …… …… 154

Appendices ….. …… …… …… …… …… …… …… …… 170

LIST OF FIGURES

Figure	Title	
1.1	Map of Abuja, Federal Capital Territory (FCT), Nigeria ……	22
1.2	Map of Abuja, Phase 1, showing the study area ….. …… ……	23
2.1	Four types of ferromagnetic materials ….. …… …… ……	29
2.2	Example of Hysteresis loop and its Parameter ….. …… ……	31
3.1	Map of Abuja showing the study area (edited by the author) …….	46
3.2	Illustration of the profile layouts for this work (Source: the author) ….. …… …… …… …… ……	52
3.3	Map of Abuja showing the location of the vertical Magnetic susceptibility soil profile (Source: the author) …..	52
4.1	Geological Map of the study Area showing Rocks distributions ….. ……. ……. ……. …… …….	60
4.2	Magnetic susceptibility distribution of rock types within the study area….. ……. ….. …… ……. …… ……	62
4.3	Background Magnetic Susceptibility profile at different locations in Abuja….. ….. …… …… ….. …..	64
4.4	Magnetic Susceptibility profiles line variation with distancealong selected roads in Central District of Abuja …..	67
4.5	High-resolution magnetic contour maps in a vicinity of selected roads in Central District, showing clearly, spatial distribution of MS affected by road traffic….. …… ……	69
4.6	Magnetic Susceptibility profiles line variation with distance along selected roads in Garki District of Abuja….. ……	70
4.7	High-resolution magnetic contour maps in a vicinity of selected roads in Garki District, showing clearly spatial distribution of MS affected by road traffic… …… …… ……	73
4.8	Magnetic Susceptibility profiles line variation with distance along selected roads in Wuse District of Abuja….. ……	74

4.9	High-resolution magnetic contour maps in a vicinity of selected roads in Wuse District, showing clearly, spatial distribution of MS affected by road traffic….. …… …….	76
4.10	Magnetic Susceptibility profiles line variation with distance along selected roads in Asokoro District of Abuja ….. ……	78
4.11	High-resolution magnetic contour maps in a vicinity of selected roadin Maitama District , showing clearly, spatial distribution of MS affected by road traffic ….. …… …….	80
4.12	Magnetic Susceptibility profiles line variation with distance along selected roads in Asokoro District of Abuja …..	82
4.13	High-resolution magnetic contour maps in a vicinity of selected road roads in Asokoro District, showing clearly, spatial distribution of MS affected by road traffic ….. …… …….	84
4.14	Background magnetic susceptibility profile from the surface to a depth of 35.0cm ….. …… ……. …… …… ……	87
4.15	Vertical magnetic susceptibility distribution with depth along selectedroads in Wuse District ….. …… ……. …	88
4.16	Vertical magnetic susceptibility distribution with depth along selected roads in Garki District ….. …… …… ……	89
4.17	Vertical magnetic susceptibility distribution with depth along selected roads in Central District…… …… ……	90
4.18	Vertical magnetic susceptibility distribution with depth along selectedroads in Maitama District ….. …… …….	91
4.19	Vertical magnetic susceptibility distribution with depth along selected road in Asokoro District ….. …… …….	91
4.20	(a) 2D contour (3D) surface map of Abuja showing magnetic susceptibility distribution at the surface….. …… ……. ……	95
4.21	(a) 2D contour (3D) surface map of Abuja showing magnetic susceptibility distribution at the depth of 10.0cm…… …….	96
4.22	(a) 2D contour (3D) surface map of Abuja showing magnetic susceptibility distribution at the depth of 20.0cm ……. ……	97

4.23	(a) 2D contour (3D) surface map of Abuja showing magnetic susceptibility distribution at the depth of 30.0cm…… …….	98
4.24	(a) 2D contour (3D) surface map of Abuja showing magnetic susceptibility distribution at the depth 40.0cm …… …….	99
4.25	Magnetic Susceptibility profile lines taken on the map ……	101
4.26	Magnetic Susceptibility profile lines with depth in Abuja……	103
4.27	Distribution of frequency dependence magnetic susceptibility alongselected road profile in Central District…… ……. ……	105
4.28	Distribution of frequency dependence magnetic susceptibility alongselected road profile in Garki District …… ……. ……	106
4.29	Distribution of frequency dependence magnetic susceptibility alongselected road profile in Wuse District …… …… ……	106
4.30	Distribution of frequency dependence magnetic susceptibility alongselected road profile in Maitama District …… ……	107
4.31	Distribution of frequency dependence magnetic susceptibility alongselected road profile in Asokoro District…… …… ……	107
4.32	Distribution of frequency-dependence magnetic susceptibility valuesat the surface soil of Abuja…. …… …… ……	109
4.33	Distribution of frequency-dependence magnetic susceptibility valuesat the depth of 30.0cm…. …… …… ……. ……	110
4.34	A χlf-χhf % scattergram showing typical position of samples dominated by various domains and sources at a road in Central district, Abuja …… …… …… …… …… ….. …..	112
4.35	A χlf-χhf % scattergram showing typical position of samples dominated by various domains and sources at a road in Garki district, Abuja …… …… ….. ….. ….. ….. …..	112
4.36	A χlf-χhf % scattergram showing typical position of samples dominated by various domains and sources at a road in Wuse district, Abuja …… …… …… ……. ……. .	113

4.37	A χlf-χhf % scattergram showing typical position of samples dominated by various domains and sources at a road in Maitama district, Abuja …… …… ….. ….. ….. ……	113
4.38	A χlf-χhf % scattergram showing typical position of samples dominated by various domains and sources at a road in Asokoro district, Abuja …… …… ….. ….. ….. ….. ….	114
4.39	Interface for Magnetic susceptibility variation with temperature analysis…… …… …… …… …… …… ….. …..	115
4.40	Variation of low magnetic susceptibility with low temperature fromsamples collected at different locations in various districts of Abuja….. …… …… ….. ….. ….. ……	119
4.41	Variation of low magnetic susceptibility with high temperature from samples collected at different locations in various districts of Abuja….. …… ….. …… ….. ……	123
5.1	(a) Iron (Fe) distribution maps showing high Fe concentration in theboundaries of Maitama, Wuse and Central area and (b) at the depth of 30.0cm … …… …… ….. ….. …..	128
5.2	(a) Cadmium (Cd) distribution maps showing high Cd concentration at the surface soil and (b) at a depth of 30.0cm in Abuja….. …… …… …… …… …..	130
5.3	(a) Chromium (Cr) distribution maps showing Cr concentrations at the surface soil and (b) at depth 30.0cm in Abuja….. ……. ……. …… ….. …… ……	132
5.4	(a) Lead (Pb) distribution maps showing high Pb concentrations at the surface soil and (b) at depth of 30.0cm in Abuja….. ……. ……. ……. ….. …… ……	135
5.5	(a) Zinc (Zn) distribution maps showing high Zn concentrations in Wuse district at the surface soil and (b) at depth of 30.0cm in Abuja…… …… …… …… …..	138
5.6	(a) Nickel (Ni) distribution maps showing Ni concentrations at the surface soil and (b) at a depth of 30.0cm…… ……. …	140
5.7	Correlation plots between Magnetic Susceptibility and concentration of Heavy metals at the surface soil. …… ……	144

LIST OF TABLES

Table	Title	
3.1	Route locations were Magnetic Susceptibility measurements are carried out….. …… …… …… ….. ….. ……	51
3.2	Traffic volume in different areas of Abuja (FME, 2015)….. ….	55
3.3	Road deposited sediment, collection methodology of previous studies (taken from Christopher, 2012) ……. ……	56
4.1	Rock types and their Magnetic Susceptibility within the study area….. …… …… …… …… …… …… …..	59
4.2	Background Magnetic Susceptibility values obtained from undisturbed soil in different locations in Abuja…… ……. ……. ……. …….. ……. ….. ……	63
4.3	Background magnetic susceptibility range in different locations within Abuja…. …… …… …… …… …….	64
4.4	Interpretation of χfd% values (according to Dearing, 1999 and Michal, 2012)…… ….. …… …… …… ……	104
4.5	Origins of magnetite/maghemite and greigite with domain size (Dearing, 1999 and modified by the author)…….	110
4.6	Curie and Neel temperature of iron and common Fe-bearing minerals(Dearing, 1999)…… …… …… …… …… ……	116
4.7	Low Magnetic susceptibility characteristics at low temperature of samples collected on the work….. ……. …… …… ……	117
4.8	Low magnetic susceptibility characteristics of samples at high temperature….. …… ……. …… …… …… ……	120
5.1	Background concentration of heavy metals used for this study….	124
5.2	Correlation Parameters of selected heavy metals with magnetic susceptibility measurements in Abuja ……. ……. …….	143
6.1	Classification of magnetic susceptibility effect on the Environment… …….. …… …… …… ……	146

6.2 Comparison of Anthropogenic Boundaries in some cities across the world with the present study… ……. ……. …….149

LIST OF PLATES

Plate	Title	
3.1	MS2 Magnetic susceptibility meter (Source: the author)…. ……	48
3.2	Field work in progress…… …… ……. …… …… ……	53
4.1	Geological Field Mapping in Progress…..…… ……. ……	58
4.2	Gneiss Rocks collected from the study Area…. …… …….	61

LIST OF APPENDICES

Appendix A Magnetic Susceptibility data obtained along roads in Central district…… …… ……. …… …… …… … 172

Appendix B Magnetic Susceptibility data obtained along roads in Garki district….. ….. …… …… …… …… ….. .176

Appendix C Magnetic Susceptibility data obtained along roads in Wuse district…. …….. …… …… ….. …… …… 179

Appendix D Magnetic Susceptibility data obtained along roads in Maitama district…. …….. …… ……. …… …… …… 182

Appendix E Magnetic Susceptibility data obtained along roads in Asokoro district…. …….. …… ……. …… …… …… 184

Appendix F Low frequency magnetic susceptibility measurement in vertical profiles along road networks…… ……. …… … …… …….. 186

Appendix G Magnetic Susceptibility data obtained from surface and various depths indifferent locations in Abuja … …… 187

Appendix H Concentration of heavy metals at surface and depth of 30.0cm obtained from different locations in Abuja ……. ……. 203

LIST OF ABBREVIATION AND SYMBOLS

A1	Kwame-Nkrumah Crescent
A2	Yakubu Gowon Crescent
A3	Nelson Mandela Street
A4	Maitama Sule Street
AAS	Atomic Absorption Spectrometer
BSE	Backscattered Electrons
BSED	Backscattered Electrons Detector
C1	Independence Avenue Road
C2	Olusegun Obasanjo Road
C3	Ahmadu Bello Way
C4	Constitution Avenue
CNG	Compressed Natural Gas
Cr	Chromium
CO	Carbon monoxide
Cd	Cadmium
Cu	Copper
Co	Cobalt
COMEAP	Committee of Medical Effects of Air Pollution
CVD	Cardiovascular Disease
EC	Element of Carbon
EDS	Energy Dispersed Spectrometry
FCT	Federal Capital Territory

Fe	Iron
G1	Nnamdi Azikwe Way
G2	Moshood Abiola Road
G3	Fumilayo Ransome Kuti Road
G4	Kam Salem Street
GIS	Geographical Information System
GMR	Giant Magnetoresistance
IRM	Isothermal Remanent Magnetization
LPG	Liquefied Natural Gas
M1	Mban Close
M2	Ibrahim Babangida Way
M3	Gana Street
M4	Shehu Shagari Way
Mn	Manganese
MD	Multidomain
Ms-T	Curve- temperature dependence measurement of magnetization
Nm	Nano meter
NO_2	Nitrogen dioxide
Ni	Nickel
PM	Particulate Matter
PGE	Platinum Groups Elements
PAHs	Polycyclic Aromatic Hydrocarbons
Pb	Lead

PSD	Pseudo-single domain
RDS	Road Deposited Sediments
SEM	Scanning Electron Microscopy
SP	Super paramagnetic
SPM	Suspended Particulate Matter
SIRM	Saturated Isothermal Remanance Magnetization
SSD	Single State Domain
UK	United Kingdom
USA	United State of America
VOCs	Volatile Organic Compounds
W1	Herbert Macaulay Way
W2	Kashim Ibrahim Way
W3	Sani Abacha Way
W4	Bissau Street
XDR	X-ray Diffraction
Zn	Zinc
χlf	Low frequency magnetic susceptibility
χhf	High frequency magnetic susceptibility
χfd	Frequency-dependent susceptibility
μ	Permeability

CHAPTER ONE

GENERAL INTRODUCTION

1.1 BRIEF OVERVIEW

The origin of environmental magnetism (also called minerals magnetism) was first brought to limelight in the work of Thompson and Oldfield (1986). Environmental magnetism involves the application of rocks and minerals magnetic techniques to situations in which the transport, deposition or transformation of magnetic grains are influenced by the environmental processes in the atmosphere, hydrosphere and lithosphere (Verosub and Roberts, 1995).

As one of the branch of geophysics, Evans and Heller (2003) introduced it to a wider audience by the book 'Environmental Magnetism'. Since then, it has been gaining relevance because the techniques are simple, rapid, non-destructive, and inexpensive and can be applied to a wide range of materials including rocks, sediment, soil, atmospheric particulates, and biological materials. Environment magnetism has found applications in and is making major contributions to a range of diverse fields especially paleoclimate, sedimentology, paleoceanography, archaeology and more recently in particulates pollution especially in anthropogenic pollution studies (Maher, 1988; Maher and Thompson, 1999).

In environmental magnetism, the inherent magnetic mineralogy and granulometry of natural samples are investigated; hence the parameters used in environmental magnetism are independent of the earth's magnetic field at any point, and are largely a function of the volume of magnetic minerals (O' Reilly, 1976). Environmental magnetic techniques are designed to measure the response of natural materials to a range of artificially applied

magnetic field. These non-naturally remanent characteristic (also called non-directional magnetic measurements) is the foundation of this branch of geophysical (Basavaiah and Aniruddha, 2004).

Environmental issues (especially pollution) have top the world agenda of recent, thus data based monitoring and assessment of environmental pollution becomes important in providing crucial information to policy makers, managers, technicians and indeed to the public in order to improve the environmental situation. The basis of the present work is based on the following:

i. The rate at which anthropogenic ferromagnetic particles (Dekkers and Pietersen, 1992; Vassilev, 1992) accumulate results in significant enhancement of topsoil and road dust susceptibility, implying, under favorable condition magnetic signatures of soils and dusts could be used for assessment of pollutants in th environment.

ii. The need for fast, effective and efficient mapping and monitoring tools for environmental pollution makes magnetic methods a suitable and reliable option to determine and characterize contamination level (Dearing *et al*., 1996; Hoffmann *et al*., 1999;Petrovsky *et al*., 2001;). Given the recent attention to heavy metals in urban soils, the use of magnetic measurements have notbeing fully utilized in examining magnetic properties and their correlation with heavy metals in Nigeria, and

iii. Magnetic susceptibility mapping on highly metamorphic background has not been done in Nigeria.

Generally, chemical methods are used to determine the level of environmental pollution. However, such methods are expensive, tedious and time consuming. In contrast, magnetic method becomes generally acceptable as a fast and cost-effective screening tool for pollution mapping of heavy metals in surface and subsurface soils and sediments. For quantification of the degree of environmental pollution, new techniques using environmental magnetic methods have been developed and reported in many literatures. It is demonstrated that magnetic methods should be considered as a first choice, as an appropriate strategy for conducting surveys, which can be a helpful indicator when targeting and selecting sampling sites for subsequent geochemical analyses.

The magnetic method for pollution studies is validated through correlation with geochemical measurements. The correlations between magnetic parameters and the contents of heavy metals can be used as a proxy to determine different degrees of pollution by heavy metals in urban dust as well as in industrial soils. Because of their genetical origin, the concentration of magnetic minerals not only reflect magnetogenic pollutants, but also provides the relative content of toxic metals in environmental samples.

Vehicle emissions, commercialand industrial activities form a major and a significant contributor to environmental pollution. This is because they release directly into the atmosphere, magnetic particles, heavy metals and other compounds that can be incorporated for a long time either in the environment or in living organisms, especially in urban areas (Palmgren *et al.*,2003). These emissions comprises different fraction of particles like the ultrafine particles (<30 nm, 30-100 nm) formed in the engine, in the exhaust pipe or immediately after the emission; fine particles (0.1-2 μm) formed by

chemical reactions or other processes; and coarse mode (>2 μm) formed mechanically by abrasion of road material, tyres and brake lining (Palmgren *et al.*,2003).

According to Petrovsky and Ellwood (1999) and Gautam *et al*., (2004) urban area roadsides, commercial and industrial places are greatly polluted by particulate matter (PM) released mostly from trafficactivities: motor vehicle emissions, abrasion of tyres, brake linings as well as road surface, cycling of dust in suspension due to vehicular movement, dispersion of construction material, etc. When released initially into the atmosphere, these PM may remain airborne for some time, before finally settling along the narrow roadside corridor and urban soil; thus forming an integral part of the urban city soil, especially in the vicinity of roads. Hence, urban soil dusts may serve as an archive of elevated concentrations of trace metals and their compounds.

Over the last 60 years topsoil has been found to exhibit high values of magnetic susceptibility compared to the subsoil (Mullins, 1977; Maher, 1986; Williams and Cooper, 1990). Magnetic susceptibility shows this relationship because of its ability to detect ultra-fine ferrimagnetic particles (Maher 1986; Eyre 1997; Dearing 1999) that occur in the topsoil.(Thompson *et al., 1980;* Maher 1986 and Dearing *et al.,* 1996). From this, one can presume magnetic susceptibility can be used to determine the characteristics or magnetic signature of the topsoil compared to the subsoil.

1.2 HEAVY METALS IN SOIL

Chemically, heavy metals are defined as elements which conduct electricity, have a metallic luster, are malleable and ductile, form cations, and have basic oxides (Atkins and Jones, 1997). The term heavy metals refer to any metallic chemical element that has a relatively high density and is toxic or poisonous at low concentration. Heavy metals are naturally formed in the Earth's crust and as such formed a natural background

value(Table 1.1); however, human activities tend to raise the concentration of these metals relative to the background values and hence pose a risk to the environment.

Heavy metals which are found in urban soil dust are Pb, Cr, Cu, Zn, Cd, Ni e.t.c. play a significant role in environmental pollution and degradation. Thus, high concentration of metals for example Pb, Cd, Zn etc., needs to be investigated for their environmental and health implications.

Table 1.1: Background Concentration of selected Heavy Metals for this study (weppi.gtk.fi/publ/foregsatlas/text/hm.pdf)

Heavy Metal	Background concentration (ppm)
Lead (Pb)	20.0
Zinc (Zn)	52.0
Nickel (Ni)	20.0
Chromium (Cr)	80.0
Cadmium (Cd)	0.40
Iron (Fe)	550.0

1.3 ATOMIC ABSORPTION SPECTROMETER

The Atomic absorption spectrometer (AAS) is a spectro-analytical procedure for the quantitative determination of chemical elements concentration using the absorption of optical radiation (light) by free atoms in the gaseous state.

In analytical chemistry the technique is used for determining the concentration of a particular element (the analyte) in a sample to be analyzed. AAS can be used to determine over 70 different elements in solution or directly in solid samples used in pharmacology, biophysics, geology, toxicology researches and environmental researches.

The technique makes use of absorption spectrometry to assess the concentration of an analyte in a sample. It requires standards with known analyte content to establish the relation between the measured absorbance and the analyte concentration and relies therefore on the Beer-Lambert Law.

In short, the electrons of the atoms in the atomizer can be promoted to higher orbitals (excited state) for a short period of time (nanoseconds) by absorbing a defined quantity of energy (radiation of a given wavelength). This amount of energy, i.e., wavelength, is specific to a particular electron transition in a particular element. In general, each wavelength corresponds to only one element, and the width of an absorption line is only of the order of a few picometers (pm), which gives the technique its elemental selectivity. The radiation flux without a sample and with a sample in the atomizer is measured using a detector, and the ratio between the two values (the absorbance) is converted to analye concentration or mass using the Beer-Lambert Law.

In this work, the concentration of Iron (Fe), Cronium (Cr), Cadiunm (Cd), Nickel (Ni), Zinc (Zn) and Lead (Pb) were determined using the Atomic Absorption Spectrometer analysis.

1.4 HEALTH EFFECTS ASSOCIATED WITH URBAN ENVIRONMENTAL POLLUTION

According to Briggs *et al*., (1997) and Wrobel *et al*., (2000), Industrial/traffic-generated emissions are estimated to account for more than 50% of the total emission of PM in the urban areas of highly industrialized countries. These emissions pose serious threats to human health since they are emitted at ground level.

Emissions of PM from exhaust as well as non-exhaust sources have an impact on air quality in urban areas. The physical and chemical properties of urban particulates are associated with several health risks such as respiratory problems, skin irritation, eye inflammation, blood clotting and various types of allergy. Salonen *et al*., (2004) found that re-suspension particles caused pro-inflammatory activity in cells due to their endotoxin concentrations and they hypothesized that this might be the reason for irritative symptoms in the respiratory system frequently reported by both asthmatic and healthy people during re-suspension episodes. Miguel *et al*., (1999) reported that road dust contains pollen and other allergens which are capable of causing allergic disease in humans.

PM can affect our health and particle size is considered to be a primary concern in terms of health effects (COMEAP, 2009). Decreasing PM particle size generally creates greater probability of inhalation and deep penetration of the lungs. It is when the smallest particles enter the sensitive lung areas that a secondary concern becomes apparent over time, with composition and toxicity of particles. Evidence suggests that it is the fine components of PM, which have a diameter <2.5μm and are formed by combustion, that are the main cause of the harmful effects of PM (COMEAP, 2009) causing triggering mechanisms linked to respiratory problems (such as asthma) (Hetland *et al*., 2001; Perera, 2008). These fine particles consist of carbon, trace metals (such as Cu and Zn) and organic compounds, which are potentially toxic and pose a greater risk to health with decreasing particle size (Dockery *et al*., 1993; Kelly and Fussell, 2012). Studies in the USA (Dockery *et al.*, 1993) showed that individuals living in less air polluted cities live longer than those living in more air polluted cities. There is less evidence to connect

secondary inorganic PM (such as sulphates and nitrates) or larger particles with adverse health effects, although they cannot be eliminated as probable causes. Particles cause the most serious health problems among those susceptible groups with pre-existing lung or heart disease and/or the elderly and children. There is evidence that short and long-term exposure to particulate matter cause respiratory and cardiovascular illness and even death. It is likely that the most severe effects on health are caused by exposure to particles over long periods of time. However, UK estimates indicate that short-term exposure to the levels of PM_{10} that was experienced in 2002 led to 6,500 deaths and 6,400 hospital admissions being brought forward that year, although it is not possible to know by what length of time those deaths were brought forward (COMEAP, 2001). Studies conducted by the Committee on Medical Effects of Air Pollution (COMEAP) found that for every 1 μg/m3 decrease in PM2.5 over the lifetime of the current population of England and Wales, between 0.2-0.5 million years of life will be gained (COMEAP, 2010). This is equivalent, on average, to 1.5–3.5 days for every individual in England and Wales. The effect is unlikely to be evenly spread across the population, however, and some people will gain much more.

Increased presence of heavy metal content in urban soil may affect the microbial activities which reduce the soil fertility (Ahmed *et al*., 2005). Environmental stress arising from soil contamination may affect biodiversity of the micro-organisms and hence disturb the ecological balance. It has also been proven that soil with high concentration of heavy metals affect the growth of plants in the environment.

1.5 JUSTIFICATION OF THE RESEARCH

The rise in urbanizationand development along with population growth has adversely affected the environment (atmosphere, hydrosphere, lithosphere and biosphere). In developing countries like Nigeria, the problem is more acute due to weakness in most of the environment enforcement agencies, the lack of pollution control measures, inadequate technical, economic as well as legislative provisions.

Soil is essential for plant, animal and human survival. However, this important natural resource is non-renewable andhence, the increased pressure due to rises in human population growth is likely to threaten soil sustainability (Doran *et al.*,1998). Topsoil erosion causes the soil system to lose its input of organic matter and nutrients, therefore it can eventually lead to desertification (United Nations, 1998). This has important implications for agriculture and thus food security..

Topsoil forms at a rate of approximately 10mm of soil per 100 to 400 years (Doran *et al.*,1999), while natural or geological erosion of the soil occurs at approximately the same rate. Soil degradation due to anthropogenic factors, known as 'man-accelerated' erosion, is at a rate higher than that of soil formation (Bennett, 1939). It is therefore essential that we recognize topsoil as a resource in Nigeria and develop methods to conserve it.

The soil also plays an important role in the evolution of the subsurface and the exchange of matter between the bedrock and the atmosphere and, as such, the understanding of its properties is a prerequisite in numerous fundamental problems and environmental applications (Musy and Soutter, 1991). Reconstructing the past history of deposition and erosion of a given soil, for example, is useful for the reconstruction of past climates (Gu*et al.*, 1997; Lagroix and Banerjee, 2002). To assess the history of a given soil or its

ability to store, release or transmit pollutants, some knowledge of its physical and chemical properties are needed. Unfortunately, soil is a complex multiphase time-dependent non-linear system, difficult to characterize and model (Musy and Soutter, 1991). While numerous empirical methods have been developed since the nineteenth century, it is difficult in practice to measure extensively all known soil parameters. Methods that are both easy to implement, as well as efficient and unambiguous, might therefore be of great help, in particular in a context of the planet's threatened soils (Banwart, 2011).

Today environmental issues top the world agenda, from climate change, drought and flood, there is therefore a need to look into the environmental pollution. In Nigeria today different vehicles are found moving in all nooks and crannies of our country without anybody checking the standard and road worthiness of such vehicles; industrial activities are in the increase without effective regulation. Besides monitoring, we see an urgent need for characterization and quantification of the particles in different environmental system (atmosphere, soil, vegetation, water e.t.c) using rapid and cost-effective techniques such as combined environmental magnetic and analytical chemical methods similar to those applied in European countries.

This research is necessary as it will expose the pollution implication of urbanization, thereby sets awareness and alert on the danger associated with pollution.

1.6 AIM AND OBJECTIVES OF THE STUDY

The aim of this study is to map out areas with high concentration of magnetic grains on the surface and subsurface soil of Abuja municipal (Phase 1) using environmental magnetism techniques, with the following objectives:

i. to determine the different magnetic susceptibility of the topsoil and the subsoil.

ii. to identify and characterize magnetic particulates.

iii. to investigate the spatial distributions of traffic pollution on roadside and soils with different traffic volumes.

iv. to establish any correlation between the magnetic susceptibility measurements and the concentration of selected heavy metals in the urban surface and sub-surface soil of Abuja city (Phase 1).

v. to generate basic data from magnetic and mineral magnetic analysis from prospective source materials to determine their relative contribution to soil dust composition and urban topsoil for the city of Abuja.

vi. to determine trace metals present in the soil.

To achieve these objectives, this research work will develop from previous research in the following ways:

i. Establishing mineral magnetic and particle size associations over time and at varying spatial scales (road, city and regional) as a review of literature suggests that previous research has not fully explored road sediments relationships and only concentrates on small sampling areas.

ii. Investigating linkages of roadside particle size, airborne PM and mineral magnetic associations, as there is a lack of research and available data in this area.

iii. Establishing and investigating the reliability of mineral magnetic measurements as an urban geochemical pollution indicator within road deposited sediment (RDS) at a number of spatial scales, as only small scales have been investigated in previous research.

iv. Investigate the anthropogenic depth penetration of magnetic grains in the soil of Abuja as most research focus on spatial surface distribution.

v. Examine the relationship between magnetic susceptibility and topsoil in Nigeria as a base for developing an indicator for topsoil loss. Past research shows distinct different magnetic susceptibility measurements of the soil in topsoil and in subsoil, but the applicability of this in Nigeria is yet to be fully utilize.

1.7 THE STUDY AREA

Abuja is the capital city of Nigeria (Figures 1.1). It is located in the north central Nigeria and bounded between latitude 9.0 and 9.1 and longitude 7.4 and 7.6 within the Federal Capital Territory (FCT). Abuja is a planned city, and was built mainly in the 1980s. It officially became Nigeria's capital on 12 December, 1991, replacing Lagos, though the latter remains the country's most populous city. At the 2006 census, the city of Abuja had a population of 1,776,298, making it one of the ten most populous cities in Nigeria. Abuja has witnessed a huge influx of people into the city; this has led to the emergence of satellite towns such as Karu Urban Area, Suleja, Gwagwalada, Lugbe, Kuje and smaller settlements to which the planned city is sprawling.

Previous researchhas indicated that urbanization has drastically increased in the last ten years, with the population almost doubling especially during working hours. This has made the city jam-parked and polluted. The city (Phase 1) is divided into five major districts namely; Wuse, Garki, Central Area, Maitama and Asokoro.

Within the City of Abuja, (Phase 1) as with most urban environments, the principal source of these environmental pollutants are exhaust from vehicular movement, commercial activities and fuel combustion. While in recent years, there has been

increasing use of emissions control technology in vehicles (for example catalytic converters) the number of vehicles on roads is continually increasing. In short, technological improvements only partially mitigate the effects of increased road traffic.

The area chosen for this work has taken into account areas noted for business and commercial activities and also residential and reserved areas. This work will assess the appropriateness for using magnetic susceptibility and mineral magnetic techniques in determining the spatial and particle size associations of deposited sediments within road (RDS) and soils of Abuja.

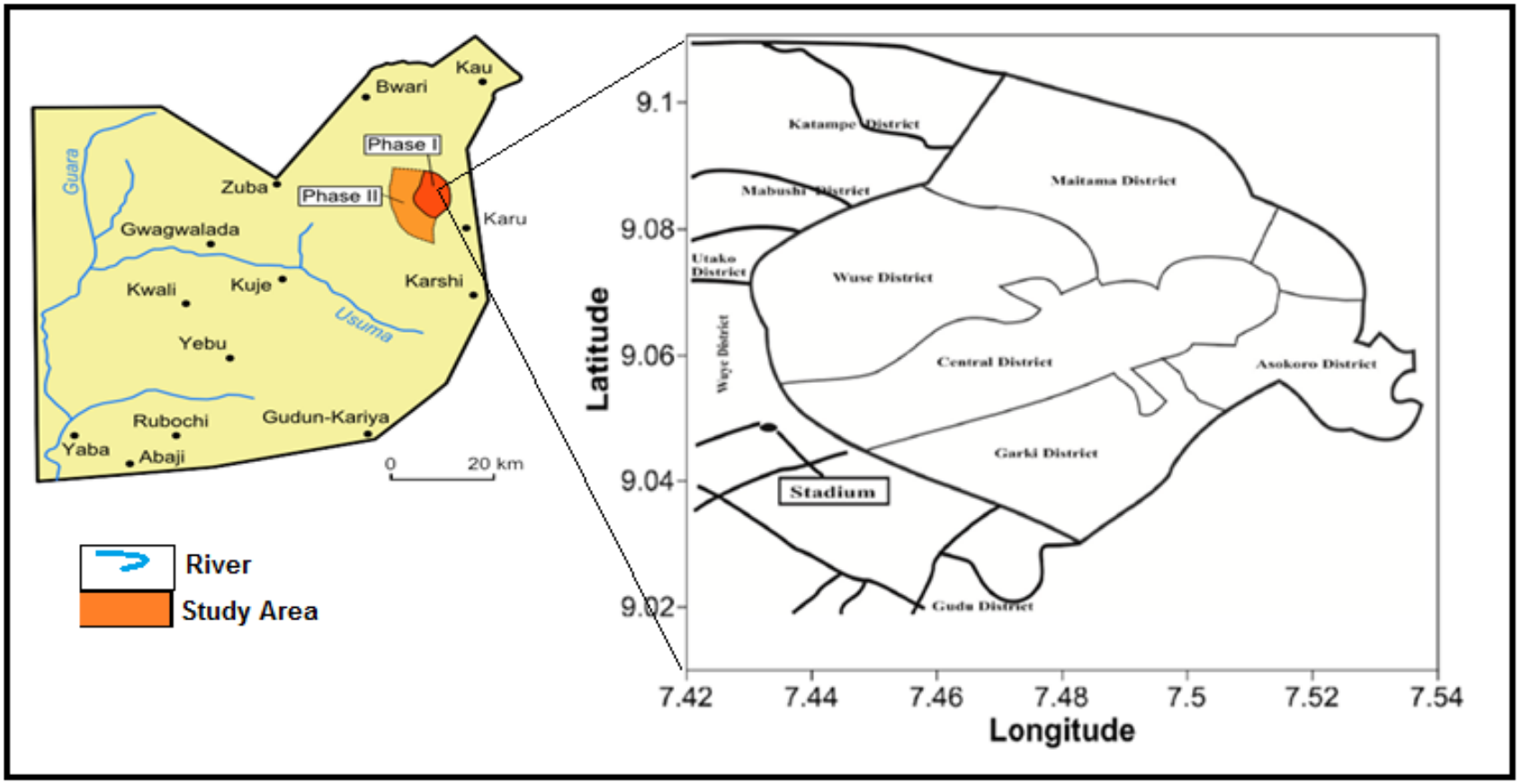


Figure 1.1 Map of Federal Capital Territory showing the study area (modified after NGSA 1985-1985)

1.8 GENERAL GEOLOGY OF FEDERAL CAPITAL TERRITORY (FCT)

Abuja is almost predominantly underlain by crystalline rocks of north-central basement complex. The Nigerian basement complex lies within the Pan-African mobile belt which has been affected by Pan-African events through the ages of orogenic, tectonic and metamorphic cycles (Oyawoye 1964). Lithological units present within the FCT, Abuja include migmatite, granite gneiss, Quartzo-fedspathic gneiss, Undefferentiated schist, porphyritic biotite, marble and Nupe sandstone of lower Turonian age covering less than 5% within the FCT, Abuja (Figure 1.2). The study area which falls within the FCT (Figure 1.2 in box) is underlain by high grade metamorphic and igneous rocks of Precambrian age. Generally trending NNE-SSW, these rocks consist of gneiss, migmatites and granites. A schist belt outcrops along the eastern margin of the area. The belt broadens southwards and attains a maximum development to the southeastern sector of the area where the topography is rugged and the relief is high.

Abuja has two main seasons, rainy (April to October) and dry (November to March). The high altitude and undulating terrain of the territory act to provide a regulating influence on its weather. During the dry season, the typical month being March, the temperature varies between 30°C in the northeast to about 37°C in the southwest.

The two main types of soils in FCT are the sedimentary belt in the southern and south-western extremities of the territory and the pre-Cambrian Basement soil country which accounts for more than 80 percent of the territory.

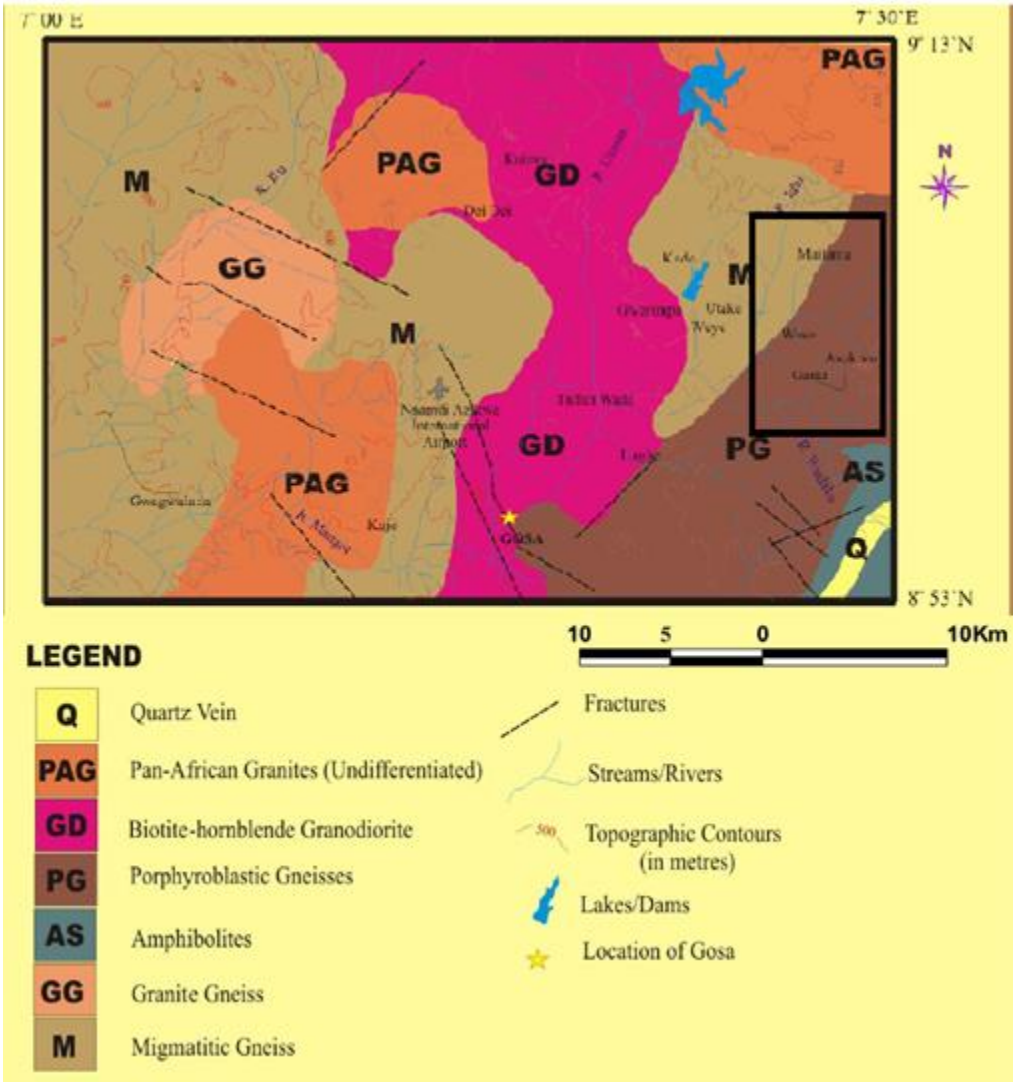


Figure 1.2 Geological map of FCT, Abuja Nigeria (insert box, the study area) modified after Omeje et al., 2013.

CHAPTER 2

LITERATURE REVIEW

2.1 INTRODUCTION

The role of environmental magnetism in understanding past climate change through the study of loess, lake and marine sediments magnetic properties (Walden*et al*., 1999) cannot be over emphasised. Furthermore, environmental magnetism offers a more rapid and non-destructive means of assessing pollution history of sediments (Charlesworth and Lees, 2001). Moreover, Shilton*et al*., (2005) found positive relationship between magnetic contents and organic matter in dust samples.

2.2 PREVIOUS ENVIRONMENTAL MAGNETISM STUDIES ON POLLUTION

Several studies exist in literature on environmental magnetism as it applies to pollution most especially, the one employing the use of magnetic susceptibility mapping. This arise from the fact that a good relationship exist between the magnetic parameters and heavy metal concentration based on generic relationship from simultaneous production of both particles sources (Beckwith *et al,*. 1986; Georgeaud *et al.*,1997; Petrovský *et al.*, 1998; Knab *et al.*,2001; Spiteri *et al.*,2005; Chaparro *et al.*, 2006)

Magnetic measurements have been used comprehensively to investigate the relationship between heavy metal content, magnetic lithological and pedological properties as a measure of heavy contamination (Hanesch *et al*., 2001; Jordanova *et al*., 2004 and Schmidt *et al*., 2005). The correlation between magnetic susceptibility of contaminated soil and the presence of hydrocarbons, as well as certain heavy metals such as Pb and Zinc have also been confirmed (Morris *et al*., 1995).

The use of magnetic susceptibility measurements to investigate industrial and urban pollution in different environments (soil, rivers/stream and lakes, road and vegetation species) has been carried out by Hunt *et al*., (1984), Hoffmann *et al*., (1999), Matzka and Maher (1999), Jordanova *et al*., (2003), Amereih *et al*., (2005), Lu *et al*., (2005); Zhang *et al*., (2006), Kim *et al*., (2007), Chaparro *et al*., (2005) and Maher *et al*., 2008).

Kucer *et al*., (2011) have carried out an investigation on environment pollution in an industrial area using magnetic susceptibility measurements in Gaziemin district in Turkey. Using the Barthington MS2 system, measurements carried out on soil samples indicated that the susceptibility values in the entire sample are high and thus suggest that the soil may contain iron, nickel, lead, zinc etc.

Magnetometric techniques were used to determine the contamination of the forest soil in the Orlicke Hory Region, Easter Bohenia from fly-ash (Semelova *et al*., 2009). The magnetic susceptibility of the topsoil was measured on the field using the Bartington MS2 instrument, while detailed laboratory magnetic analysis of some samples collected in the field were carried out to identify the origin and translocation history of magnetic particles in the soil horizon. Also identified by the magnetic measurements on Kappa Bridge was the dominant ferromagnetic fraction in the forest floor. IRM curves identified two types of magnetic contributions which are the topsoil magnetic particles generally derived from the atmospheric deposition and the soil from which arise from the lithology. [Evaluating the result of the magnetic susceptibility with concentrations of chosen heavy metals (Fe, Mn, Zn, Cu, Co and Cr)] the results confirmed that magnetometry is a suitable and effective proxy method for the evaluation of soil contamination.

Magnetic susceptibility measurements aimed to investigate the suitability of such field measurement for indicating heavy metal pollution were carried out at a former industrial iron production and processing site (Schmidt *et al*., 2005). The result from geochemical analysis of the soil samples indicated a close correlation of concentration between Fe, Cu, Mn and Ni. The concentration of Fe was also found to correlate with the magnetic susceptibility field measurements. The study also revealed a better correlation for magnetic susceptibility values higher than a site-specific threshold. These results demonstrate the potential of magnetic susceptibility field mapping for fast preliminary site assessment and hence reducing the scale of subsequent geochemical sampling and analysis.

Lu *et al*., (2012) performed magnetic and geochemical analyses on soil collected from Lishiu city, a highly industrialized area in China. Low frequency magnetic susceptibility (χlf), saturation isothermal remanent magnetization (SIRM) and concentration of metals (Cd, Cu, Pb and Zn) were measured on samples of urban soils. Concentration-dependent magnetic parameters (χlf and SIRM) were significantly positively correlated to the concentration of heavy metals (Cr, Ni, Cu, Zn, Cd and Pb), but not correlated with V, Co and As. The χlf and SIRM also have strong linear correlation with integrated pollution index (IPI), indicating that χlf and SIRM can be used as effective proxy indicators for the pollution degree of heavy metals in urban soils. Magnetite was identified as the possible dominant magnetic carrier using temperature-dependent measurements of saturation magnetization (Ms-T curve). The results proved the applicability of the magnetic method in detecting heavy metals pollution in urban soils.

A soil profile of 74cm depth was sampled on a hillside close to Beijing Muslim cemetery near the Shijingshan industrial area (Shen *et al*., 2006) to study the magnetic pollution within the soil profile. Magnetic measurements, grain size and geochemical analyses as well as multivariate statistics were performed. The magnetic proxies showed similar trends compared to heavy metal elements with high concentration at the top and lower concentration in the lower part. The anthropogenic dust input from the industrial activities is predominantly the cause of strong magnetic signals in the uppermost soil horizon. The main magnetic component is magnetite contained in the grain size fractions of 4-16µm and 16-32µm, and they are observed up to a depth of 10cm. Multivariate statistic and fuzzy C-mean cluster analysis showed a reasonable correlation of magnetic susceptibility, ARM, SIRM and Mn, Cu, Fe, Pb, Zn, Al,. Hence, they concluded that magnetic parameters can be used as an indicator for screening heavy metal pollution.

Various mechanisms for the correlation of heavy metals with iron-oxides in soils have been identified, especially adsorption and incorporation. It was found that the individual contributions depend strongly on the source of contamination, local soil geology and geochemistry (Petrovský and Ellwood, 1999 and Wehland *et al.*, 2002). Where iron-oxide particles are discharged from industrial processes, associated heavy metals can either be incorporated into their atomic lattice or be adsorbed to their surfaces and their concentrations are therefore correlated. For example, Scholger, (1998) found that iron producing and manufacturing industries in Styria (Austria) emitted Zn, Pb, Ni, Cu and Cr together with macroscopic scale particles, which were easily quantified in river sediments through magnetic measurements.

In another study, Hoffmann *et al.,* (1999) successfully measured road traffic pollution by evaluating the spatial distribution of magnetic susceptibility in the nearby soils. Only a fraction of the pollutants are airborne. The strongest enhancement was found at the road's verge, indicating washed-down abrasion particles.

In order to determine the environmental damages caused by Izmit waste treatment in the (soil province of Kocaeli) Turkey, the magnetic susceptibility method was used to detect the heavy metal concentrations in an area of $1km^2$ (Debora, 2010). Samplings were carried out periodically in order to investigate the pollution trends with time. Magnetic susceptibility measurements both at the site and the laboratory show that the soil is contaminated with heavy metals. The value of the magnetic susceptibility observed varies between 12.0×10^{-0} SI and 84.0×10^{-5} SI in mostly the upper layers of the soil. The geochemical analysis indicates the presence of some heavy metal like Pb, Cu, Zn, Co, and Ni.

In another study, in Denizli, Turkey, on pollution analysis using magnetic susceptibility measurements, Aydin et al., in 2009), investigated the distribution of heavy metals pollution by taking 50 samples near the road. These were used to show the distribution of heavy metallic elements deposited from exhaust gases and fumes chimney in areas near the highway and around. Contour maps were then used to show the pollutants distribution and also their sources were determined to assess their environmental threats.

Matzka and Maher, (1999) found that the isothermal remanent magnetization (IRM) imparted on leaves of birch (Betulapendule) in urban and suburban areas, around the city of Norwich (UK), are useful as a proxy of traffic pollution. Suitability of both susceptibility and IRM of dust-loaded leaves of deciduous trees (Platanus sp. and

Quercus Ilex) for mapping vehicular traffic emissions in the city of Rome in Italy was described by Moreno *et al*., (2003). Similarly, Hanesch *et al*., (2003) demonstrated the potential of susceptibility and IRM to susceptibility ratio of maple tree leaves in and around Austrian industrial site in Leoben for monitoring short-term (up to several months) dust deposition.

In a research to identify and characterize magnetic vehicle-derived particulates, Michal(2012), used combination of magnetic, geochemical and micro-morphological methods to discriminate sources of particulate anthropogenic particles. Spatial and temporal distributions of traffic pollution were collected by the application of various collectors (roadside soil, snow, lichen and moss bags). The spatial distribution of magnetic parameters of road dust accumulated in roadside soil, snow, lichens and moss bags indicates that the highest concentration of magnetic particles is in the sampling points situated closest to the road edge. Magnetic particles concentration decreases with increasing distance from the road; indicating vehicles as a major source of emission. Significant differences in horizontal distribution of magnetic susceptibility were observed between soil and snow. Magnetic particles derived from road traffic deposit on soil within a few meters from the road, but on snow up to 60 m from the road. The values of magnetic susceptibility of road dust deposited near busy urban motorway are significantly higher than in the case of road with low traffic. These differences are attributed to traffic volume, which is 30 times higher on motorway than on local roads. Enhanced concentrations of heavy metals (e.g. Fe, Mn, Zn, Cu, Cr, Ni and Co) were observed in the studied samples (Michal 2012). This may be associated with specific sources of vehicle emissions (e.g. exhaust and non-exhaust emissions) and/or grain size

of the accumulated particles (large active surface of ultrafine particles). Significant correlations were found between magnetic susceptibility and the concentration of selected heavy metals in the case of moss bags exposed to road traffic. Low-coercivity magnetite was identified as a major magnetic phase in all studied roadside collectors (soil, snow, moss bags and lichens). However, magnetic minerals such as titanomagnetite, ilmenite, pyrite and pyrrhotite were also observed in the studied samples. The identified magnetite particles are mostly pseudo-single-domain (PSD) with a predominant MD fraction (>10 µm). The ultrafine iron oxides (>10 nm) were found in road dust extracted from roadside snow. Large magnetic particles mostly originate from non-exhaust emissions, while ultrafine particles originate from exhaust emissions.

To investigate the environmental pollution of Beni Mellal city, Morocco, Mohammed *et al*., (2011) carried out a joint magnetic and geochemical investigation of road side urban soil materials. Twenty three soils magnetic susceptibility profiles were made along 5km peripheral national road. High magnetic susceptibility values and high contents of heavy metals were found near the paved edge of the road and within the place reserved as large engine park. Magnetic extracts of highly polluted areas and unpolluted soil were also analyzed by SEM coupled with X-ray Diffraction (XDR) in order to discriminate anthropogenic magnetic spherules and pedo-lithogenic magnetite-like minerals. The magnetic mineralogy suggests the presence of hematite, magnetite and goethite in highly polluted areas.

A preliminary study of traffic-derived pollutant from primary sources (vehicles) and on road (paved area), road border, and surrounding areas was carried out (Debora *et al*., 2008) in order to identify the pollutants with their distribution and concentration. The

results of the magnetic parameter and its analysis suggests that the magnetic signal of the vehicle-derived emission is controlled by a magnetic-like phase, the magnetic grain size estimation reveal the presence of fine particles (0-1.5μm) that can be inhaled and therefore are dangerous to human health. Results from the magnetic susceptibility measurements show higher magnetic concentration in the central area of the tollbooth line that is related to higher traffic. Magnetic susceptibility on several roadside along the 120 km was computed and a contour map generated. Higher magnetic values near the edge of the road indicate the magnetic particles emitted by vehicles are accumulating and mainly concentrated within a distance of a couple of metres (1-2m) along the road.

The ability to map spatial distributions of anthropogenic pollution by measuring the magnetization of tree leaves has been demonstrated in different European cities (Hannam and Heller, 2001 and Moreno *et al.,* 2003). High susceptibility is often observed in the city centre near busy roads and railway stations. In contrast, low values are found in rural regions with almost no traffic.

Sangode *et al.,* (2010) carried out magnetic susceptibility measurements to investigate the susceptibility distribution in soil of the Pune Metropolitan Region based on the linkages between ferrimagnetism and heavy metal concentration of anthropogenic particulates. A total of 118 samples were collected in a 3.0 x 3.0 km grid during the pre and post moonsoon seasons for surface soil, bedrock, dust and rain water. These were analyzed for magnetic susceptibility and isothermal remanent magnetization. The magnetic susceptibility in the soil profiles decreases from bedrock to intermediate soil horizons but notably increases towards the top. Spatial variations based on the fundamental rock magnetic parameters and knowledge of the polluting sources show significant

anthropogenic loading for the topsoil. The distribution of the frequency dependence magnetic susceptibility infers wind as another important agent for dispersal of finer ferromagnetic particulate matters predominantly controlled by the metrological amongst other factors.

In another study, Tadeusz *et al.*, (2013) collected dust samples from the acoustic barriers of E-77 expressway (Poland). Chemical analysis was performed by means of Atomic Absorption Spectrometer with flame atomization (F-AAS). Fe, Al and Zn metals dominate in the investigated road dusts. Mossbauer spectra collected at room temperature enabled the identification of several iron-containing phases in the dust. Some traces of hematite and magnetite have been found as well as α-Fe phase in ferromagnetic state. A significant component could be interpreted as pure iron in paramagnetic state. The dominating doublet in the spectrum of high quadrupole splitting could correspond to iron carbonates. Complementary measurements of low-field AC magnetic susceptibility confirmed a different metal content in the road dust samples collected from different altitudes of acoustic barriers.

The combination of morphological, geochemical and magnetic methods was used to characterize urban road dust properties of the city of Thessaloniki, the second largest of Greece and one of the largest urban agglomerations in Balkans (Bourliva et al., 2011). Samples of road dust were collected from accumulated matter at the edges of major roads from eight selected sites in the historic center of the city. In order to compare the results obtained, samples from selected industrial areas were also collected. SEM-EDS of the samples identified two groups of magnetic materials (angular/aggregate particles derived from motor vehicles circulation and spherules possibly originating from industrial and

domestic heating systems. The magnetic susceptibility shows high value ranging from 331.7-591.7 x 10^{-8} SI. The magnetic susceptibility correlated significantly with the Cr and Cu obtained from the chemical analysis. Furthermore, the frequency dependent susceptibility indicates that the presence of super paramagnetic ferromagnetic minerals is not significant.

A detailed magnetic study of urban soils in Hangzhou City, China, was carried out using combined environmental magnetism and rock magnetism techniques (Lu and Bai, 2008). Magnetic measurements showed that the urban soils have a significant magnetic enhancement, which were characterized by higher magnetic susceptibility. Magnetic susceptibility values of urban soils showed highly significant negative correlation with frequency-dependent susceptibility, indicating that the mechanism of the magnetic enhancement of urban soils is different from contribution of pedogenic ferrimagnetic minerals in nature soils. Magnetic susceptibility values of urban soils, on the other hand, have significantly positive correlation with Soft IRM (IRM 20mT) and saturation isothermal remanent magnetization (SIRM), suggesting that ferrimagnetic minerals are the main magnetic carriers. The combined rock magnetism (acquisition curves of IRM, temperature-dependent susceptibility and hysteresis measurement) and SEM/EDX (scanning electron microscopy and energy dispersive X-ray analysis) revealed that magnetic mineralogy of urban soils is dominated by magnetite-like and hematite-like phases. The hysteresis parameters suggested that they are present mainly in the pseudo-single domain (PSD) and multidomain (MD) grains, which is attributed to input of anthropogenic magnetic grains from industrial activity, fuel combustion and traffic pollution. This finding suggested that magnetic measurements could be used as potential

tools for monitoring soil pollution, mapping spatial distribution of pollution, and differentiating source of pollutants in urban soils.

Maria *et al*., (2008) investigated the magnetic properties of soil profiles taken from polluted regions of Eastern Ukraine around the industrial centres Krivyj Rig, Mariupol and Komsomolsk. Soils represent chernozem and podzoluvisol. The low-field magnetic susceptibility shows enhancement in the topsoil caused by contamination by coarse-grain magnetite connected with industrial pollution. Magnetic mineralogy was determined by means of thermal demagnetisation of *SIRM*, monitoring of susceptibility changes during warming from –196°C to room temperature and heating to 700°C, and Mössbauer analysis. Granulometry of magnetic particles was investigated by determination of hysteresis parameters, susceptibility, *Ms*, *SIRM* and *ARM* ratios and frequency dependence of susceptibility.

The chemical parameters, namely , organic carbon and iron content in different pedogenic and lithogenic minerals, measured for particular horizons determined pedogenic characteristic of soil profiles. The results showed that differences in magnetic parameters of non-polluted and polluted soil profiles are not limited to the topsoil, but reach deep layers of the parent material. Industrial pollution promotes formation of the so-called "pedogenic" SP and SD particles in these layers.

2.3 BASIC MAGNETIC PROPERTIES

The dependency of magnetic behavior of materials on the magnetic moments of its atom or ions describes its magnetic properties. Not all materials have the same magnetic properties.

2.3.1 Diamagnetism

Diamagnetism is a fundamental magnetic property: it is extremely weak compared with other magnetic effects and so it tends to be swamped by all other types of magnetic behavior. In diamagnetic materials, all the electron shells are filled and no impaired electrons exist. When such material is placed in a magnetic field, the orbital path of the electrons rotates so as to produce a magnetic field in opposition to the applied field. This is called Larmor precession. The magnetization of diamagnetic materials is lost as soon as the magnetic field is removed.

Diamagnetism is for all practical purposes independent of temperature. Examples are quartz, calcite, marble and salt.

2.3.2 Paramagnetism

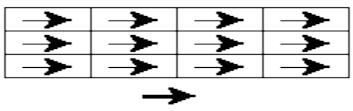
In some materials the shells are not completely filled so that a magnetic field results from the spin of their impaired “electrons” or “magnetic moment “can align with the external magnetic field. Magnetization is then induced that is proportional to the strength (and parallel to the direction) of the applied field. However, the magnetization of paramagnetic material is lost once the field is removed because of thermal effects. When magnetic field is applied to paramagnetic substances the spin magnetic moments tends to order and to orientate parallel to the applied field direction. However, the magnetic energy involved are small and thermal agitation constantly attempts to break down the magnetic ordering. A balance is reached between these two competing processes of thermal randomization and magnetic ordering. The magnetic moment which depends on this balance is thus a

direction of both the applied field and the absolute temperature. Examples are olivine, biotitic, pyroxene and garnet.

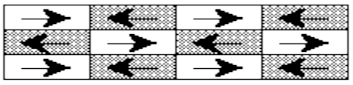
2.3.3 Ferromagnetism

In ferromagnetic material, the dipoles are parallel giving rise to a strong spontaneous magnetization which can exist even if the ferromagnetic materials are characterized by the way in which their magnetic properties change dramatically at a particular critical temperature, called the curie temperature. Below the Curie temperature, a ferromagnetic material can carry a strong remanent magnetization, but above the Curie temperature, its ferromagnetic ordering is broken down by the thermal energy and it behaves as paramagnet.

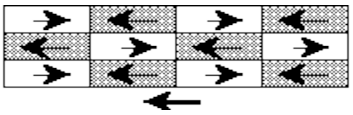
The remanent magnetization of these types of materials results from the principles of spontaneous magnetization (magnetization that exist when in the absence of a material field). Spontaneous magnetization arises from the group-magnetic phenomenon of exchange interactions. In these interactions, all elementary magnetic moments of neighbor electrons are aligned parallel with one another by quantum mechanical effects. The most important factor influencing rock magnetism is the type of ferromagnetic minerals, its grain size and the manner in which it acquires a remanent magnetization or isothermal magnetization. There are four types of ferromagnetic materials (Figure 2.1)



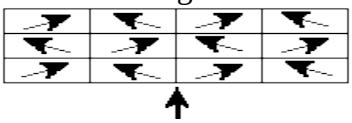
(a) True Ferromagnetic: alignment within lattice. Net resultant field. Examples are iron, nickel, cobalt.



(b) Antiferromagnetic: sub-lattices aligned but anti-parallel and equal strength. No net resultant field.



(c) Ferrimagnetic: sub-lattices aligned anti-parallel but unequal strength. Examples are magnetite



(d) Canted antiferromagnetic: sub-lattices equal strength, canted.

Figure 2.1 Four types of ferromagnetic material

2.4. HYSTERESIS

The magnetic state of an iron bar depends on both its magnetic field to which it is subjected and the history of the bar. The field dependence of magnetization can be described with the aid of diagram which plots magnetization on the vertical axis starting with an unmagnetized piece of iron. It is found that its magnetization increases slowly as a small field is applied and that if this field is removed, the magnetization returns to zero. However, on applying a stronger field, beyond a certain critical field, it is found that an important change in magnetic behavior take place. The magnetization is now no longer reversible in the straightforward way of the very low fields; instead, on removal of the field, a phenomenon referred to as hysteresis develops. In short, change in magnetization associated with the removal of the field now differs from those that occurred during the preceding increase of the field, in such a way that the magnetization changes lag behind

the field. Furthermore, it is found that on complete removal of the field i.e. in zero fields, the iron is no longer un-magnetized but has a remanent magnetization. At moderate fields magnetization rises sharply with increasing field and at still higher fields, saturation of the magnetization sets in and the magnetization curve flattens out. A complete hysteresis loop is obtained by cycling the magnetic field from an extreme applied field in one direction to an extreme in the opposite direction and back again.

2.4.1 The Hysteresis Loop and Magnetic Properties

A great deal of information can be learned about the magnetic properties of a material by studying its hysteresis loop. A hysteresis loop shows the relationship between the induced magnetic flux density (*B*) and the magnetizing force (*H*). It is often referred to as the *B*-*H* loop. An example of hysteresis loop is shown below.

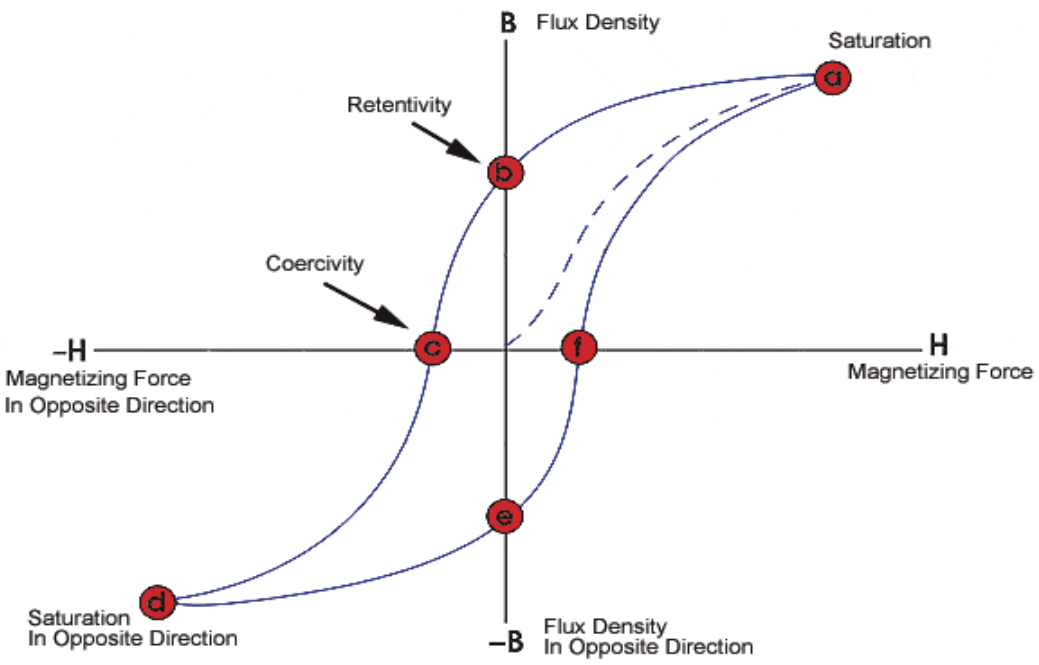


Figure 2.2: Example of Hysteresis loop and its parameter

The loop is generated by measuring the magnetic flux of a ferromagnetic material while the magnetizing force is changed. A ferromagnetic material that has never been previously magnetized or has been thoroughly demagnetized will follow the dashed line as *H* is increased. As the line demonstrates, the greater the amount of current applied (*H*+), the stronger the magnetic field in the component (*B*+). At point "*a*" almost all of the magnetic domains are aligned and an additional increase in the magnetizing force will produce very little increase in magnetic flux. The material has reached the point of magnetic saturation. When H is reduced to zero, the curve will move from point *"a"* to point *"b"* At this point, it can be seen that some magnetic flux remains in the material even though the magnetizing force is zero. This is referred to as the point of retentivity on the graph and indicates the remanence or level of residual magnetism in the material. (Some of the magnetic domains remain aligned but some have lost their alignment). As the magnetizing force is reversed, the curve moves to point *"c"*, where the flux has been reduced to zero. This is called the point of coercivityon the curve. (The reversed magnetizing force has flipped enough of the domains so that the net flux within the material is zero). The force required to remove the residual magnetism from the material is called the coercive force or coercivity of the material.

As the magnetizing force is increased in the negative direction, the material will again become magnetically saturated but in the opposite direction (point *"d"*). Reducing *H* to zero brings the curve to point *"e."* It will have a level of residual magnetism equal to that achieved in the other direction. Increasing *H* back in the positive direction will return *B*to zero. Notice that the curve did not return to the origin of the graph because some force is

required to remove the residual magnetism. The curve will take a different path from point *"f"* back to the saturation point where it will complete the loop.

From the hysteresis loop, a number of primary magnetic properties of a material can be determined.

i. **Retentivity** - A measure of the residual flux density corresponding to the saturation induction of a magnetic material. In other words, it is a material's ability to retain a certain amount of residual magnetic field when the magnetizing force is removed after achieving saturation. (The value of *B*at point *b* on the hysteresis curve.)
ii. **Residual Magnetism** or **Residual Flux** - the magnetic flux density that remains in a material when the magnetizing force is zero. Note that residual magnetism and retentivity are the same when the material has been magnetized to the saturation point. However, the level of residual magnetism may be lower than the retentivity value when the magnetizing force did not reach the saturation level.
iii. **Coercive Force** - The amount of reverse magnetic field which must be applied to a magnetic material to make the magnetic flux return to zero. (The value of *H*at point *c* on the hysteresis curve.)
iv. **Permeability** - A property of a material that describes the ease with which a magnetic flux is established in the component.
v. **Reluctance** - Is the opposition that a ferromagnetic material shows to the establishment of a magnetic field. Reluctance is analogous to the resistance in an electrical circuit.

2.5 MAGNETIC SUSCEPTIBILITY

All materials, including minerals, possess the property of becoming magnetized or polarized in the presence of an applied magnetic field and also altering the applied field. This property is called magnetic susceptibility. In weak fields, like the Earth's main magnetic field, the magnetization is approximately linearly proportional to the magnetizing field.

Magnetic Susceptibility, *k*, is a measure of the ease with which a material can be magnetized. Volume susceptibility, k_v is defined by the relation

$$k_v = \frac{M}{H} \qquad 2.1$$

where*M* is the volume of magnetization induced in a material of susceptibility *k*, by an applied field *H*. By using this definition we have volume susceptibility as a dimensionless quantity. Specific susceptibility, *x*, is defined as volume susceptibility divided by density and has units of m^3kg^{-1}

$$\chi = \frac{k_v}{\rho} \qquad 2.2$$

Susceptibility is generally measured in small fields of strength less than $1mT$. At these low fields it is found that magnetic susceptibility is reasonably independent of the applied field intensity.

Magnetic susceptibility measured by the usual methods is an apparent value because of the self-demagnetizing effect. When a material is magnetized, its internal magnetic field is less than the externally applied field.The intrinsic susceptibility,$k_{i,}$ relates the induced

magnetization to the internal magnetic field, whereas, the extrinsic susceptibility, k_e, which we actually observe, relates the induced magnetization to the external field. The relationship between the two susceptibilities can be expressed as

$$\kappa_e = \frac{\kappa_i}{(1+N\kappa_i)} \qquad 2.3$$

where$N$ is the demagnetization factor.

In strongly magnetic mineral, such as pure magnetite, $N_{ki} > 1$, hence, we have $k_e \sim 1/\infty$ and if N is known then there is a very simple relationship between the susceptibility measured and the concentration of ferromagnetic grains in a sample. This is the situation for natural samples where the concentration of ferromagnetic grains is generally small, being a few percent or less. In terms of a volume fraction of ferrimagnetic grains, f, the measured magnetic susceptibility, k is given by

$$\kappa = fk_e \qquad 2.4$$

Many studies have established that the magnetic susceptibility of natural materials mainly depends on their magnetite content (Mooney and Bleifuss, 1953; Puranen, 1977 and Currie and Bornhold, 1983).

2.5.1 Anisotropy of magnetic susceptibility

The relative ease with which a material can be magnetized in various directions is expressed by its anisotropy of susceptibility. Such anisotropy in natural sample can arise through external stresses, such as at most technic stresses, or be intrinsic due to the shape or crystalline structure of ferromagnetic minerals in the samples. The first type of anisotropy is of practical interest because of its contributions to change in the local

geomagnetic field (Johnston and Stacey, 1969). The second type has application in fabric analysis (Hamiton and Rees, 1970).

For natural samples to be anisotropic, the shape or crystalline axes of the assemblage of magnetic grains must be aligned to form a fabric. The effect of grains shape alignment will dominate when the magnetic anisotropy is due to ferromagnetic grains such as magnetite.

2.5.2 Factors that affect the magnetic susceptibility

In natural rocks the susceptibility depends on a variety of factors, among them are the composition of the actual rock, the shape and distribution of the ferromagnetic minerals, as well as possible magnetic grain interaction and sample shape.

Important factors other than those mentioned above are:

i. ***Magnetic Field Strength***

It has been found that the susceptibility of ferromagnetic materials increases with an increase in the applied field up to a point (typically ~150 Oe for magnetite-bearing rocks) and then decreases again.

Worldwide measurements of paleointensities suggest that the amplitude of the Earth's magnetic field has not changed substantially over most of geological history (Tarling, 1971). Thus, rocks which are used would have come under the influence of this field, and therefore it is advantageous to measure susceptibility in applied fields of the order of magnitude of the present field. In such low fields, susceptibility can be considered to be nearly, but not completely, independent of the field.

ii. Grain Size

For a given material the susceptibility tends to increase with increasing grain size. This is especially important for diameters less than 50 microns and the rate of increase of magnetic susceptibility is greatest when this size approaches a value determined by the transition from single domain to multi-domain structure, since single-domain grains are magnetically hard and so tend to have low susceptibilities. Multi-domain grains are easier to magnetize since it is easier to move domain walls than to rotate magnetization vectors.

iii. *Temperature*

The changes in susceptibility produced by changes in the temperature depend on the type of material used. For diamagnetic materials, there is no temperature dependence, whereas paramagnetic substances obey the Curie law. Ferromagnetic materials are strongly temperature dependent. For single crystals, the susceptibility generally decreases with increasing temperature until the Curie temperature, Tc.Above Tc, the materials are paramagnetic, obeying the Curie-Weiss law.

Since rocks are much more complex than a single crystal, the susceptibility variation as a function of temperature fits no simple expression. It has been found, however, that susceptibility generally increases on heating, occasionally by a large factor, before falling off sharply at the Curie temperature. Generally, if this increase is reversible, it will be due to the 'Hopkinson Effect'.

iv. *Previous Magnetic History of the Rock*

This depends largely upon the age and mode of formation of the rock, and hence its thermal history and upon the origin and subsequent modifications of its remanent magnetism.

v. ***Mineralogical Composition***

The presence of ferromagnetic minerals other than magnetite, and hence with different susceptibilities will, of course, affect a susceptibility estimate based upon magnetite content alone. Another mineralogical factor is crystalline anisotropy, which can give rise to susceptibility anisotropy. This is generally negligible in cubic minerals such as titanomagnetite, but can be important when the susceptibility of rocks containing predominantly pyrrhotite or minerals in the ilmenite-hematite series is to be measured, as these minerals exhibit strong crystalline anisotropy with the minimum susceptibility being directed perpendicular to the basal plane of the crystal. In an assemblage of particles the directions of the axes of the susceptibility ellipsoid (which corresponds to the property of anisotropic susceptibility as a second-rank tensor) are not necessarily randomized, so that crystal anisotropy may have caused the remanent magnetization direction in rocks containing the above minerals to be deflected from that of the original magnetizing field (Lowrie 1990).

vi. ***Petrological Characteristics***

Factors such as homogeneity in rock composition, the presence of fractures, or the degree of metamorphism, may have varying influence on the value of bulk susceptibility. Again an important factor can be susceptibility anisotropy, as this may be caused not only by crystalline anisotropy, but also by anisotropy of shape; i.e., elongated ferromagnetic grains can have a shape controlled direction of remanence even when crystalline anisotropy is negligible. Hence anisotropy in the bulk rock susceptibility may be caused by non-random packing of the grains. While igneous rocks are usually magnetically

isotropic, the susceptibility of some sedimentary rocks as measured parallel to the bedding planes can be appreciably different from that measured perpendicular to it.

2.6 MAGNETIC PROPERTIES OF MATERIALS

Many magnetic properties of materials are expressed in terms of the magnetic field strength *H*, magnetic flux density *B* and the magnetic polarization *J*. The SI units of *H* and *B* are respectively, ampere per metre (A m^{-1}) and tesla (T).

The relation between the quantities expressed in SI units is:

$$B = \mu_0 H + J \qquad 2.5$$

in which μ_0 is $4\pi \times 10^{-7}$ H m^{-1}, the magnetic constant (permeability of free space). The absolute permeability, μ(= *B/H*) and the volume susceptibility κ (= $J/\mu_0 H$), are thus related by the equation:

$$\mu = \mu_0(1 + k) \qquad 2.6$$

The mass susceptibility χ is equal to κ/ρ, where ρ is the density. The relative permeability $\mu_r = \mu/\mu_0$ is the permeability of the material relative to that of a vacuum.

In ferromagnetic materials, as *H* is increased steadily from zero the permeability changes and is at first relatively small, its value being defined as the initial permeability, then reaches a maximum value, and finally decreases towards μ_0 as the polarization tends towards a limiting value ($B - \mu_0 H$). The flux density remaining when *H* is reduced to zero is the remanent flux density and the negative *H* needed to reduce *B* to zero is the coercive

force. The remanent flux density and coercive force for a cycle which proceeds to saturation are called the remanence, B_r, and the coercivity, H_{cB}. In an open magnetic circuit the variation of J with H is usually measured and the coercivity is then denoted by H_{cJ}.

When a ferromagnetic material is taken through a cycle of magnetization there is a loss of energy as heat due to the combined effects of hysteresis, induces eddy currents and domain wall motion. The hysteresis loss per unit volume, $Q_h = \oint HdB$, has been shown empirically to vary as $B^{1.6}_{max}$ over a limited range of peak flux density of up to about 1.0 T for high saturation materials, and 0.5 T for low saturation materials (Parthasaradhy and Ranganayakulu 2014). This relationship, known as the Steinmetz law, is nevertheless only approximate. Some indication of the second loss, namely the eddy current power loss, may be calculated from standard formulae once certain relevant physical parameters are known. In their present forms, however, these formulae are only approximate. The total power losses that will be dissipated in laminar material when an alternating flux is developed in it has a direct bearing on the efficiency that can be realized in equipment such as transformers and electric motors and should therefore be known accurately. Accordingly the power losses of representative forms of typical materials are measured in terms of power loss per unit mass.

Many magnetic properties of ferromagnetic materials depend greatly on previous history, state of strain, temperature, size, perfection and orientation of crystals, and the effect of small traces of impurity may be enormous.

Ferrimagnetic materials (ferrites) have all of the above characteristics of ferromagnetic materials. However, due to their high resistivity, soft (low coercivity) ferrites are widely used in high frequency applications, in which case the following parameters are also of interest:

Power loss density- this is another name for specific total power loss, but for ferrite materials the loss is usually expressed per unit volume

Disaccommodation factor- the permeability of a magnetic material can also change with time after magnetization. This phenomenon is often called *disaccommodation*. If the permeabilities μ_1 and μ_2 correspond to times t_1 and t_2 then the disaccommodation is given by:

$$\frac{\mu_1-\mu_2}{\mu_1} \times 100\% \qquad 2.7$$

As with the loss and temperature factors, the disaccommodation factor is normalized to unit permeability and is given by:

$$Disaccommodation\ factor = \frac{\mu_1-\mu_2}{\square} \times 100\% \qquad 2.8$$

Apart from changes in their magnetic permeability, some materials have other responses to changes in magnetic field strength. All conducting materials exhibit the *Hall Effect*, of which there are two forms. In the transverse Hall Effect, a voltage is developed in a direction at right angles to a current passing through the material when a magnetic field is applied in a mutually perpendicular direction. The relationship between the current

flowing through the material I_x, the output voltage, V_y, the thickness of the material, t_z, and the applied magnetic field strength, H_z, is given by:

$$V_y = \frac{(K_H I_x \mu_0 H_Z)}{t_z} \qquad 2.9$$

where K_H is the transverse Hall coefficient of the material.

2.7 LOW AND HIGH TEMPERATURE MAGNETIC SUSCEPTIBILITY

The *MS2* temperature-dependence system is able to detect minerals and domains in samples that have been cooled below or heated above room temperature because the magnetic behaviour of many minerals and domain states varies with temperature. Three different sequences of susceptibility temperature measurements are possible: warming from liquid nitrogen temperature (-196°C) to room temperature (25°C); heating from room temperature to high temperature (up to ~800°C); and cooling from high temperature to room temperature (25°C). Three types of thermal effect may be observed (France and Oldfield 2000).

2.7.1 Thermal disordering

In simple terms, the magnetisation and hence χ_{lf} of a material is a competition between the ordering of atomic magnetic moments and their disordering by thermal energies. As a sample is heated, internal thermal energies are aided by external energy, which as a general rule causes the χ_{lf} to reduce. Paramagnetic substances show a decline in χ_{lf} with increasing temperature (°C) according to the Curie-Weiss Law. With the exception of superparamagnetic domains, ferrimagnetic and canted antiferromagnetic minerals undergo abrupt transitions at Curie (T_C) and Néel (T_N) temperatures respectively from magnetically ordered states below and disordered states above where they behave as

paramagnetic substances. T_C and T_N values for common iron-bearing minerals range from +770°C to -218°C, but it should be noted that many T_C and T_N values are approximate and may vary according to the precise crystalline structure, degree of oxidation and presence of impurities (France and Oldfield 2000). In superparamagnetic grains (SP), external heat also aids the destruction of magnetisation by internal thermal energies, but cooling opposes internal thermal energies and shifts the grains towards stable single domain(SSD)behavior, with a lower κ_{lf}. The temperature of the transition point between SP and SSD behavior is known as the blocking temperature (T_B) which is close to room temperature for large (0.03 μm) SP magnetite crystals (Hakon 2008).

2.7.2 Magnetocrystalline anisotropy phase transitions

In addition to changes in the ordering of magnetic behavior there are also two significant changes caused by transitions in the crystalline structure of minerals. The Verwey transition takes place in multidomain MD magnetite at about -155°C as a result of thermally activated changes to the crystal lattice structure. At this transition there is a reduction in the χ_{lf} values towards higher temperatures, the magnitude of which increases with decreasing oxidation state and large domain sizes(Hakon 2008). Pure maghemite shows no Verwey transition. The Morin transition takes place in haematite at about -10 °C as the spin-canted moment disappear giving rise to a drop in χ_{lf} at lower temperatures. The actual temperature at which the Morin transition takes place can vary widely down to temperatures as low as -90°C depending on the amount of titanium substitution and domain status. Large (MD) haematite grains and zero substitution give rise to the clearest transitions.

2.7.3 Mineral destruction and formation

Below room temperature, most of the thermal changes are reversible with little permanent change to crystal structures and magnetic states. A major disadvantage of high temperature measurements is the frequent occurrence of irreversible changes in magnetic mineralogy through oxidation, reduction and dehydration leading to the destruction of original minerals and the formation of new ones.

Importantly, the thermal transformation of minerals may invalidate the diagnostic use of theoretical Curie point temperatures. The nature of mineral changes may be highly unpredictable because they are often related to other properties of the sample, such as the amount of water, organic matter, and the presence and intensity of a reducing atmosphere. As a consequence, curves of χ_{lf} during cooling from high temperature are not usually diagnostic of the original room temperature minerals.

CHATPER THREE

INSTRUMENTATION AND METHODOLOGY

3.1 INTRODUCTION

In almost every aspect of geophysical investigation, measurement are carried out in the field and data processing done in the lab. In this work the Bartington MS2 magnetic susceptibility meter was use in taking measurement in the field. Aside measurements carried out in the field, samples of roadside dust and sediments were also collected and laboratory investigation were done on them.

3.2 GEOLOGICAL MAPPING

Twenty two outcrops (site) located within the study area were considered for the study. Two samples were collected from each site, in conformity with the normal procedure of sample collection in paleomagnetic studies using a Garmin GPS device to get the coordinates point where the rock samples are collected. The magnetic susceptibility for each of the 22 specimens was measured using the Bartington MS2B sensor, operated at low frequency, and connected to MS2 meter linked to a computer operated using the Multisus2 for windows software.



Plate 4.1: Geological field mapping in Progress

3.3 BARTINGTON MS2 MAGNETIC SUSCEPTIBILITY METER

The Bartington MS2 is a portable meter (Plate 3.1) with an integral four-digit display. It operates with all MS2 sensors. Powered by internal batteries, it is rechargeable from the mains or a vehicle charging point, with indicators for battery status and charging. Push buttons or toggle switches are used for control and acquisition of data. A range switches allows the user to select high or low resolution. All sockets and switches are environmentally sealed for outdoor use.



Plate 3.2Bartington MS2 Magnetic Susceptibility meter

The Bartington MS2 system is a reliable and high quality instrument used in most countries of the world for environmental magnetic susceptibility measurements. The system comes with wide varieties of sensors that suits different purposes; this makes the system adaptable to different applications on different materials. The system can perform high precision measurements in the following areas of study:

i. Geology and soil surveys
ii. Palaeomagnetics
iii. Archaeological prospecting
iv. Palaeoclimatic studies
v. Sedimentology
vi. Core logging and correlation

vii. Soil and airborne pollution surveys

viii. Analysis of ferrites and magnetic inks

ix. Study of micro/nano magnetic particles and fluids

Softwares are provided to integrate the system with desktop PCs, laptop and handheld GPS/PDA devices.

3.3.1 Principle of Operation of Bartington MS2 meter

The MS2 system operates by generating a low frequency (Bartington, 2010), low intensity, AC magnetic field around the sensor. When a material is placed near the sensor, the resulting change in the generated field is sensed by the system and converted to magnetic susceptibility readings for both positive and negative (diamagnetic) values, to a resolution of 2.0 x 10^{-5} SI units. The measurement are non-destructive, retaining the sample's magnetic properties, and relatively unaffected by the sample conductivity. The sensors are temperature compensated to minimize drift during use.

The MS2 instrument measures the magnetic susceptibility in the following ways:

The sensor consists of a very high thermal stability oscillator for which a wound inductor is the principal frequency-determining component. When the inductor contains only air the value of μ_0 determines the frequency of oscillation.

When the inductor is placed within the influence of the specimen to be measured, the value of μ determines the frequency of oscillation. The meter to which the sensor is connected digitizes the μ_0 andμ dependent frequency values with a resolution of better than one part in a million and computes the values of magnetic susceptibility. The value

of μ_0 is constant but the variable of interest is relatively small. Therefore any thermally induced sensor drift needs to be eliminated by occasionally obtaining a new "air" value by depressing the "zero" button on the MS2 meter. The μ value is obtained by pressing the "measure" button. The magnetic susceptibility value is displayed digitally and output via a serial interface.

3.4 FIELD MEASUREMENT

Single magnetic susceptibility (χ) measurements were made using a Bartington MS2 magnetic susceptibility meter connected to a Bartington MS2B dual frequency susceptibility sensor. Measurements were taken at low frequency (0.47 kHz; (χ_{LF})) and high frequency (4.65 kHz; (χ_{HF})). Both low and high frequency susceptibilities were measured (χ_{LF} and χ_{HF}) to allow frequency dependent susceptibility to be calculated (χ_{FD}%).

Field measurements were taken in different road locations within Abuja main city (Table 3.1)

Table 3.1 Route Location where Magnetic Susceptibility Measurements are carried out

Location	Road	Road	Road	Road
Central Area	Independence Avenue	Olusegun Obasanjo way	Ahmadu Bello Way	Constitution Avenue
Wuse	Kashim Ibrahim Way	Herbert Macauley Way	Bissau Street	Sani Abacha Way
Asokoro	Kwane-Nkrumah cresent	Yakubu Gowon Cresent	Nelson Mandela street	Maitama Sule Street
Maitama	Mban Close	Ibrahim Babangida Way	Gana Street	Shehu Shagari Way
Garki	Kam Salem Street	Nnamdi Azikwe Way	Moshood Abiola Road	Fumilayo-Ransome Kuti Road

At each district, measurements were taken in four different road networks. At each road a profile distance of 100.0 m was mapped parallel to the road pavement, while distance off the road is determined by the availability of space within the road sections. Several profile lines separated by 1.0 m from each other were taken along the road pavement (Figure 3.1).

Also,random magnetic susceptibility measurements were taken at 324 points at the surface and down to a depth of 40.0cm using 10.0cm intervals (Figure 3.2). Measurements were conducted in the vertical soil profiles usings a specially designed device SM 400 (Petrovsky *et al*., 2009). The main part of the SM 400 is a plastic tube with the magnetic sensor inside that is being moved upward and downward during the measurement. Before the measurement, the 40.0cm deep drilling was made using HUMAX SH 300 sampler, thereafter, the tube of SM 400 was inserted into the prepared hole, and the measurement of soil magnetic susceptibility was performed at interval of 10.0cm

In this work we integrate both measurements and obtained a 2 dimensional surface spatial distributions of magnetic susceptibility map of Abuja (phase 1).

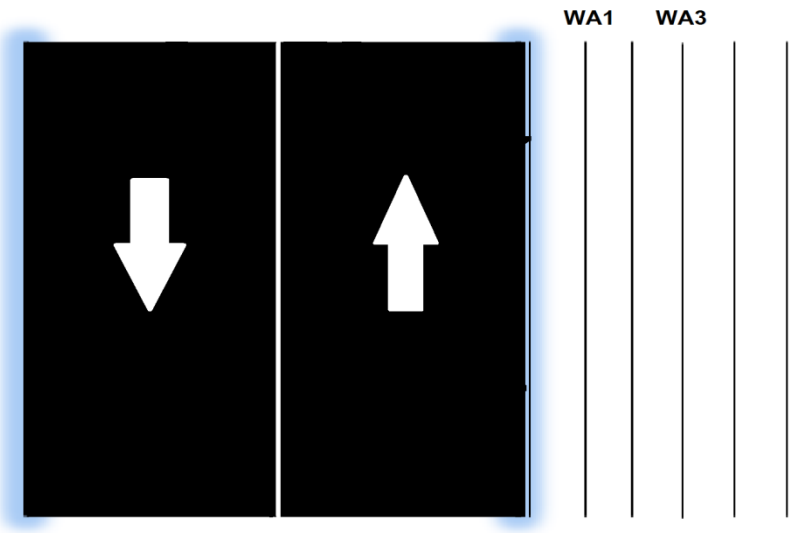


Figure 3.1 Illustration of the profile layouts for this work, the arrows indicates the direction of traffic movement (WA1….are the profile lines)

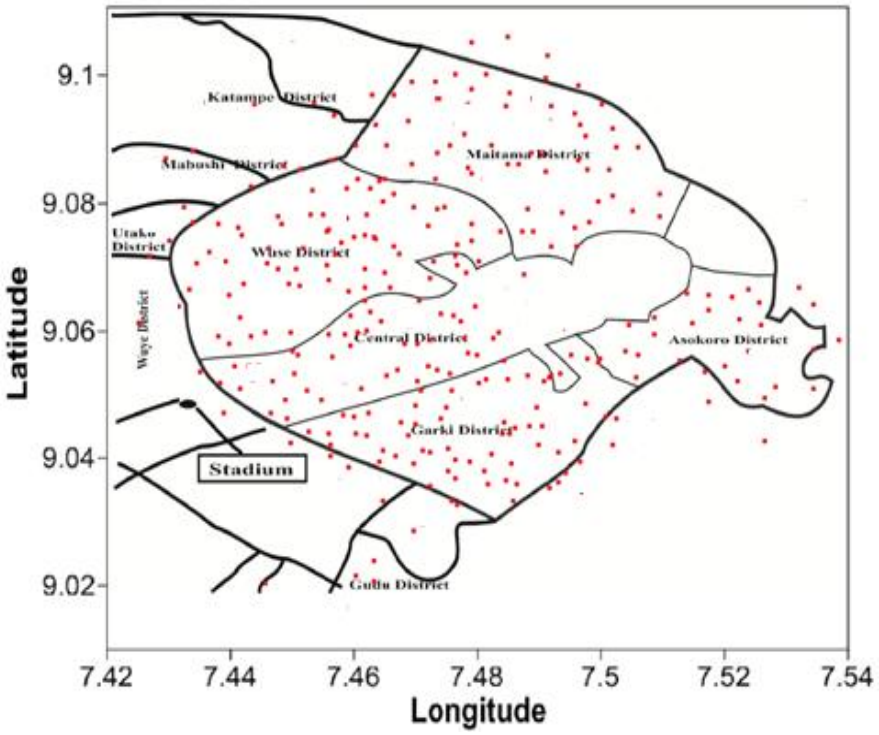


Figure 3.2: Map of Abuja with the red dots indicating the location of the surface and vertical magnetic susceptibilitysoil profilesmeasured points(modified after NGSA 1985-1986)



Plate 3.3 The researcher on the field

3.4 SAMPLING STRATEGY SELECTED IN THIS WORK

In previous studies, suitable methods for sampling and mapping have been used to understand the best way to distinguish anthropogenic pollutants from lithological signals. Several studies have used spatial design to identify sites of specific interest, Booth *et al.*, (2006) used city roads to contrast with rural roads. Yin *et al.,* (2005), Banerjee, (2003) and Yang *et al*., (2010) used industrial and residential areas to analyse differences in urban soil within unique environments. Some studies have investigated high volume traffic areas to develop a study area, with sampling taking place along busy urban roads (Abu-Allaban *et al.,* 2003; Giugliano *et al.,* 2005; Harrison *et al.,* 1981; Kim *et al.,* 2007), city centres (Charlesworth *et al.,* 2003; Anagnostopoulou and Day, 2006; Haugland *et al.,* 2007) and urban street canyons (Kumar and Britter, 2005). In addition to urban sampling design there have been numerous studies involving specific sites, such as schools, day care centres, parks and hospital gardens, which have been incorporated into sampling strategies (Anagnostopoulou and Day, 2006; Haugland *et al.,* 2007). Gautam *et al.,* (2005) used arterial and inner roads as a focus within urban areas, while Sutherland and Tolosa (2000) based their strategy on a representative mix of traffic conditions.

The sampling strategy used in this study include a combination of design features that have shown to work successfully in other studies (Sutherland and Tolosa, 2000; Banerjee, 2003; Charlesworth *et al.,* 2003; Gautam *et al.,* 2005; Yin *et al.,* 2005; Anagnostopoulou and Day, 2006; Booth *et al.,* 2006; Haugland *et al.,* 2007, and Yang *et al*. 2010). The urban area has been considered, with a mix of industrial, commercial, residential and reserved areas. Traffic volumes and vehicle movements within the study area have also been considered.

Table 3.2 shows high levels of traffic on the main area routes of the city. Wuse, Garki and Central Area have high traffic levels and suggest high commercial activities within the areas. In comparison, most of the roads in Maitama and Asokoro display low vehicle numbers and suggests considerably quieter traffic conditions. The data suggest that most side roads in Abuja with less traffic are access routes to homes, and that most vehicle traffic comes in from outside of the city.

Table 3.2: Traffic volume in different areas of Abuja (Federal Ministry of Environment, 2015)

No. of Vehicles	Wuse	Central Area	Garki	Maitama	Asokoro
Maximun	24,785	13,432	13,121	6,532	3,875
Minimum	17,432	7,231	6,377	3,444	1401
Average	21,108	19,331	18,749	9,988	6938
Time	6 am-11:59pm	6 am-11:59pm	6 am-11:59pm	6 am-11:59pm	6 am-11:59pm

3.5.1 Sampling

Soil samples were collected from 320 points (Appendix H) within Abuja metropolis (see Figure 3.3) in March, 2015. The samples were collected using a stainless steel spoon at the surface and at a depth of 30.0cm. The samples were packaged in laboratory sample container and analyzed in the Soil Science Department, Ahmadu Bello University, Zaria and National Geophysical Research Institute, India.

3.5.2 Sample Digestion

The samples were oven dried at 105^0C to constant weight for 6 hours (Galadima *et al*., 2010). The oven dried material was crushed and sieved through 2.00 mm mesh to obtain sample that were used in digestion. 1.0g of the sieved sample was then reacted with 15ml of concentrated HCl, 5ml of HNO_3 and 0.3 H_2SO_4.

The total concentrations of Cr, Cd, Fe, Pb, Ni and Zn in filtrate were then determined using a flame atomic absorption spectrometer (Varian SpectrAA 220 FS) at wavelengths, λ: Fe = 372.0 nm; Pb = 217.0 nm; Ni = 232.0 nm and Zn = 213.9 nm, using air acetylene flame.

CHAPTER FOUR

DATA PROCESSING AND INTERPRETATIONS

4.1 INTRODUCTION

The magnetic properties of the residual soil of an area depend largely on the lithological structure and weathering process of the parent rock types within the area (Enahoro and Ogbonnaya, 2015). The chemical inhomogeneity, depositional and/or crystallization, and post-deformation activities affect the magnetic properties of rocks greatly (Oniku*et al*., 2008).

The magnetic properties of rocks arise from the magnetic properties of the constituent mineral grains and crystals. Typically, only a small fraction of the rock consists of magnetic minerals, and hence this small portion determines the magnetic properties and the magnetization of the rock as a whole.

The contribution of these mineral to the magnetic susceptibility of a rock has been widely given in literature (Thompson and Oldfield, 1986; Lowrie, 1990; Schön, 1996). The values of magnetic susceptibility depend on the grain size, the presence of minute crystal lattice, such as dislocations, lattice vacancies, impurities, e.t.c., and amount of iron in a sample.

The study area falls within the basement complex of the North Central Nigeria. The rocks within the area are predominantly metamorphic rocks with magnetic susceptibility ranging between 65.0-140.0 x 10^{-5} SI, with an average value of 112.5 x 10^{-5}SI (Table 4.1). The mean susceptibility value of 112.0 × 10^{-5} SI is an indication that the magnetic susceptibility is controlled by paramagnetic minerals.

Table 4.1: Rock Types and their Magnetic Susceptibility within the Study Area

Sample No	Lat.	Long.	Class of Rock	Rock Type	Magnetic Susceptibility ($x10^{-5}$SI)
S1	9.082049	7.533087	Metamorphic	Gneiss	130.0
S2	9.099804	7.489976	Metamorphic	Gneiss	100.0
S3	9.119377	7.501350	Metamorphic	Gneiss	122.8
S4	9.062831	7.520868	Metamorphic	Gneiss	98.7
S5	9.045082	7.499997	Metamorphic	Migmatite	68.2
S6	9.057639	7.473580	Metamorphic	Migmatite	108.4
S7	9.042873	7.450074	Metamorphic	Migmatite	78.4
S8	9.077091	7.537106	Metamorphic	Gneiss	130.2
S9	9.053616	7.473431	Metamorphic	Migmatite	192.0
S10	9.061372	7.459516	Metamorphic	Migmatite	89.4
S11	9.006000	7.494668	Metamorphic	Gneiss	104.2
S12	9.036435	7.507745	Metamorphic	Migmatite	78.4
S13	9.104597	7.442601	Metamorphic	Gneiss	120.9
S14	9.032890	7.484586	Metamorphic	Gneiss	128.4
S15	9.041299	7.521963	Metamorphic	Migmatite	138.5
S16	9.067703	7.483311	Metamorphic	Gneiss	84.8
S17	9.088885	7.504010	Metamorphic	Gneiss	79.5
S18	9.056727	7.451534	Metamorphic	Migmatite	140.3
S19	9.036349	7.534051	Metamorphic	Gneiss	65.2
S20	9.052065	7.468310	Metamorphic	Migmatite	85.0
S21	9.075673	7.504588	Metamorphic	Migmatite	106.5
S22	9.073729	7.459441	Metamorphic	Migmatite	78.5

4.2 BACKGROUND MAGNETIC SUSCEPTIBILITY DATA

In using magnetic susceptibility measurements for pollution studies, there is need to collect a control data within the same geological area, but mostly, it should be located in an undisturbed location. In interpreting our results, several profiles of hundred metres were taken for five different undisturbed locations (Table 4.2), like football pitch, secondary/primary schools within Wuse, Garki, Central area, Maitama and Asokoro. The average for each area are determined and a single magnetic susceptibility profile is plotted against distance (Figure 4.1).

Table 4.2: Background Magnetic Susceptibilities Values obtained from undisturbed soil in different locations in Abuja

Distance along profile (m)	Maitama Magnetic Susceptibility (x 10^{-5} SI)	Wuse Magnetic Susceptibility (x 10^{-5} SI)	Central Area Magnetic Susceptibility (x 10^{-5} SI)	Garki Magnetic Susceptibility (x 10^{-5} SI)	Asokoro Magnetic Susceptibility (x 10^{-5} SI)
0	41.7	50.3	45.3	48.7	41.2
5	42.5	51.2	46.7	47.4	42.1
10	42.4	51.1	45.1	48.9	41.7
15	42.7	50.6	45.0	48.4	41.6
20	42.1	49.9	46.3	48.1	41.9
25	42.0	51.2	44.6	47.8	42.7
30	42.7	50.8	47.1	46.7	41.3
35	42.6	50.3	46.3	48.9	42.7
40	42.7	51.4	45.4	48.4	41.6
45	42.6	49.8	47.4	47.7	41.7
50	42.4	50.6	45.8	47.8	41.7
55	42.7	50.7	46.4	48.3	42.0
60	42.5	50.8	46.9	47.4	41.9
65	42.1	53.4	44.3	47.4	41.7
70	42.6	50.8	45.6	46.5	42.5
75	42.8	49.5	47.0	47.0	42.1
80	42.3	49.9	44.5	48.7	41.6

The magnetic susceptibility varies between 42.0 to53.4x 10^{-5}SI within these areas. Asokoro district has the lowest background values of (41.2-42.7) x 10^{-5}SI, while Wuse has the highest background value of (49.5-53.4) x 10^{-5}SI (Table 4.3).

From Figure 4.3, it is observed that the profiles have a linear trend all through the distance covered with little variations. This is an indication that there is no external control force or trend influencing the magnetic susceptibilities of the areas.

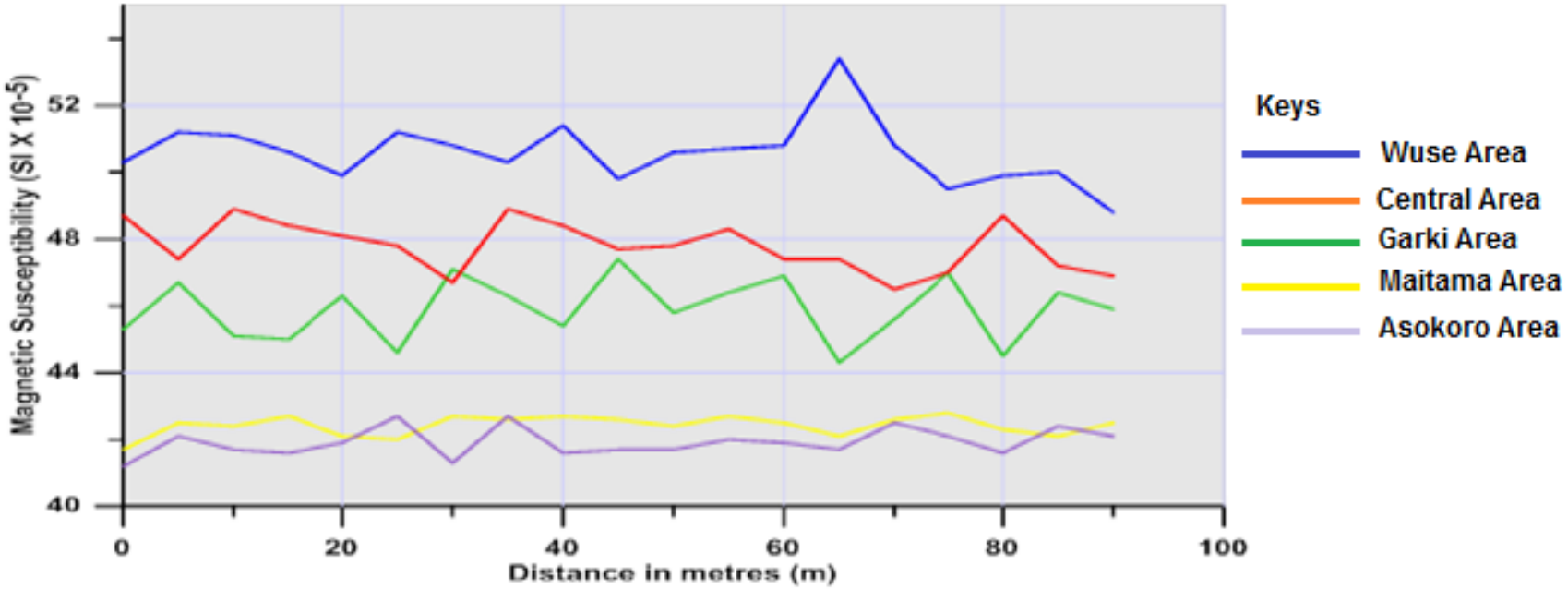


Figure 4.3: Background magnetic susceptibility profile at different locations in Abuja

Table 4.3: Magnetic susceptibility range in different location within Abuja

Location	Minimum (x 10^{-5}SI)	Maximum (x 10^{-5}SI)
Asokoro	41.2	42.7
Maitama	41.7	42.8
Central Area	44.3	47.4
Garki	46.5	48.9
Wuse	49.5	53.4

These magnetic susceptibilities arise from the natural geological and lithological processes of the parent bedrocks rather than from anthropogenic origin at the surface. The background magnetic susceptibility values are in agreement with the rock magnetic susceptibility values obtained from the geological mapping. This result serves as the control for our interpretation, as this will show the level of magnetic susceptibility along road networks and topsoilwithin the city deviated from the background values.

4.3 MAGNETIC SUSCEPTIBILITY DATA PROCESSING AND INTERPRETATION

In magnetic susceptibility measurements, as well as with other geophysical exploration/investigation methods, large volume of data are generated. These are mostly stored in the memory of the device used in the field work. In this research, tens of thousands data were collected by the Bartington MS2 magnetic susceptibility meter. These data collected in the field are stored in the memory of the device. Computer softwares are therefore needed to create a communication interface with a computer system, where the data can easily be downloaded and processed.

Many softwares were used in different stages of this work, these include;

Bartsoft, version 4.2.1.1, used to create interface between the device and a computer.

MatLab, version R2010a, used to further analyze the data and plot most of the graph

GeoLabsoft, version 1.0.0.1, used to analyze magnetic susceptibility variation with temperature

Surfur, version 11, used in plotting contour maps

and

ArcGIS 9 Software, used to edit maps.

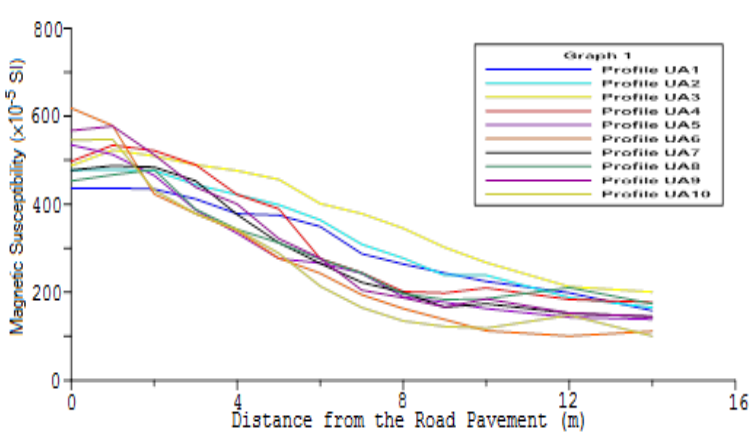
4.3.1 Central District magnetic susceptibility data along road networks

In the Central District of Abuja, magnetic susceptibility measurements were conducted in four selected road networks namely; C_1, C_2, C_3 and C_4. A maximum distance of 14.0m, 8.0m 9.0m and 7.0m was covered off the road pavements at road C_1, C_2 C_3 and C_4 respectively. At each of the road 1.0m separation along profile lines was observed.

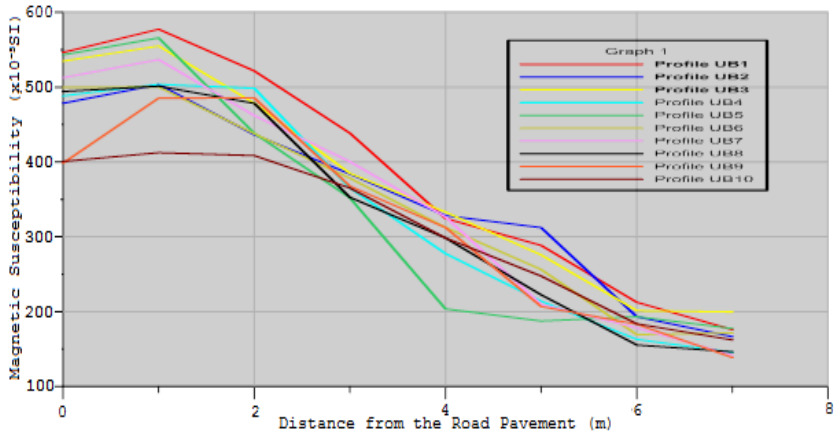
Magnetic susceptibility values vary considerably with road C_3 having the peak magnetic signal of about 650.0 x 10^{-5}SI (Appendix A).

From the graph of the profiles, magnetic susceptibilities decrease with increase in distance from the road pavement (Figure 4.4). At road C_1 the magnetic susceptibility decreases from the range of (437.5 - 618.4) x 10^{-5}SI to the range of (100.4-200.4) x 10^{-5}SI at a distance of 14.0m away from the road pavement (Figure 4.4a). At road C_2, it is observed that each of the profile lines have peak magnetic susceptibility signal at a distance of 1.0m from the road pavement (Figure 4.4b). However, the magnetic susceptibility strength decreases with distance from the pavement. Irregularities were observed at road C_3 as each of the four of the line profiles pecks at different distance from the road pavement. The first maximum value was observed at a distances of about 3.0m from the road pavement while the last maximum was observed at a distance of about 7.0m from the pavement (Figure 4.4c). For road C_4 maximum magnetic

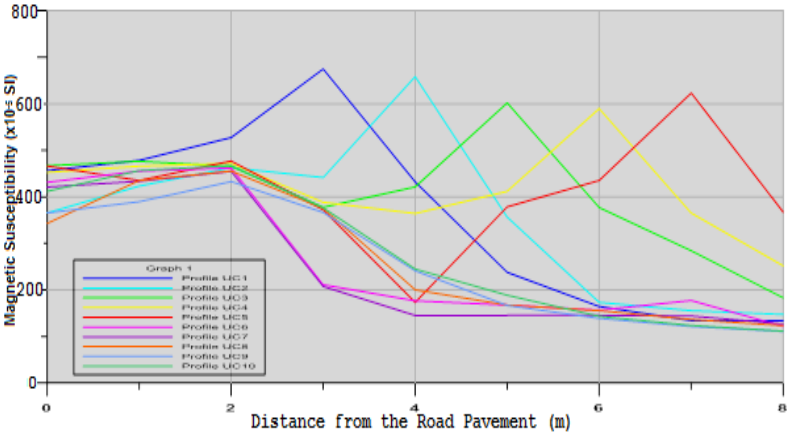
susceptibility was recorded on all the profile at a distance of 1.0m away from the pavement. The maximum signal obtained from this road is about 580.0 x 10^{-5}SI while the minimum of about 150.0 x 10^{-5}SI was recorded at a distance of about 7.0m from the road pavement (Figure 4.4d).



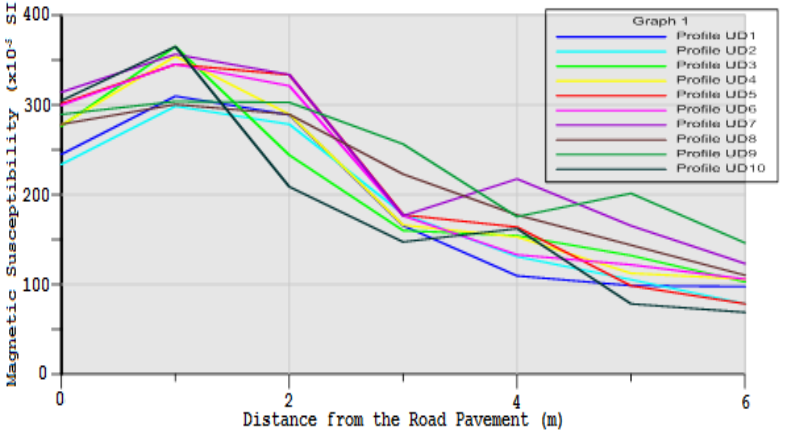
(a) Independence Avenue



(b) Olusegun Obasanjo Way



(c) Ahmadu Bello Way



(d) Constitution Avenue

Figure 4.4: Magnetic Susceptibility profile line variations with distance along selectedroads in Central District of Abuja

Figure 4.5 shows the spatial distribution of magnetic susceptibility along the four road pavements in Central District. Magnetic susceptibility enhancements were observed immediately after the road pavement at a distance of 1.0m . These enhancements decrease with increased distance from the road pavements. The maximum magnetic susceptibility value recorded immediately after the road pavements are 540.0 x 10^{-5}SI; 570.0 x 10^{-5}SI; 640.0 x 10^{-5}SI and 380.0 x 10^{-5}SI for road C_1, C_2, C_3 and C_4 respectively. In road C_3, (Figure 4.5c) magnetic enhancement was recorded diagonally from the beginning of the road pavement to a distance of about 40.0m along the road. This trend may be due to the presence of a metallic object very close to the surface or a depositional pathway for roadside dust. In Figure 4.5d, the maximum magnetic susceptibility value recorded was about 1.0 m from the road; this may be due to the presence of a linear depression along the road that serves as a collector of road side dust. It is also observed that the maximum magnetic susceptibility recorded in Figure 4.5d is about 350.0 x 10^{-5}SI, this is low compared with the other roads within the Central District. At a distance of 7.0m, the magnetic susceptibility 70.0 x 10^{-5}SI, almost correspond to the background value. The reason for this may be attributed to the fact that it is one of the roads that leads to residential areas; thus low traffic activities take place there.

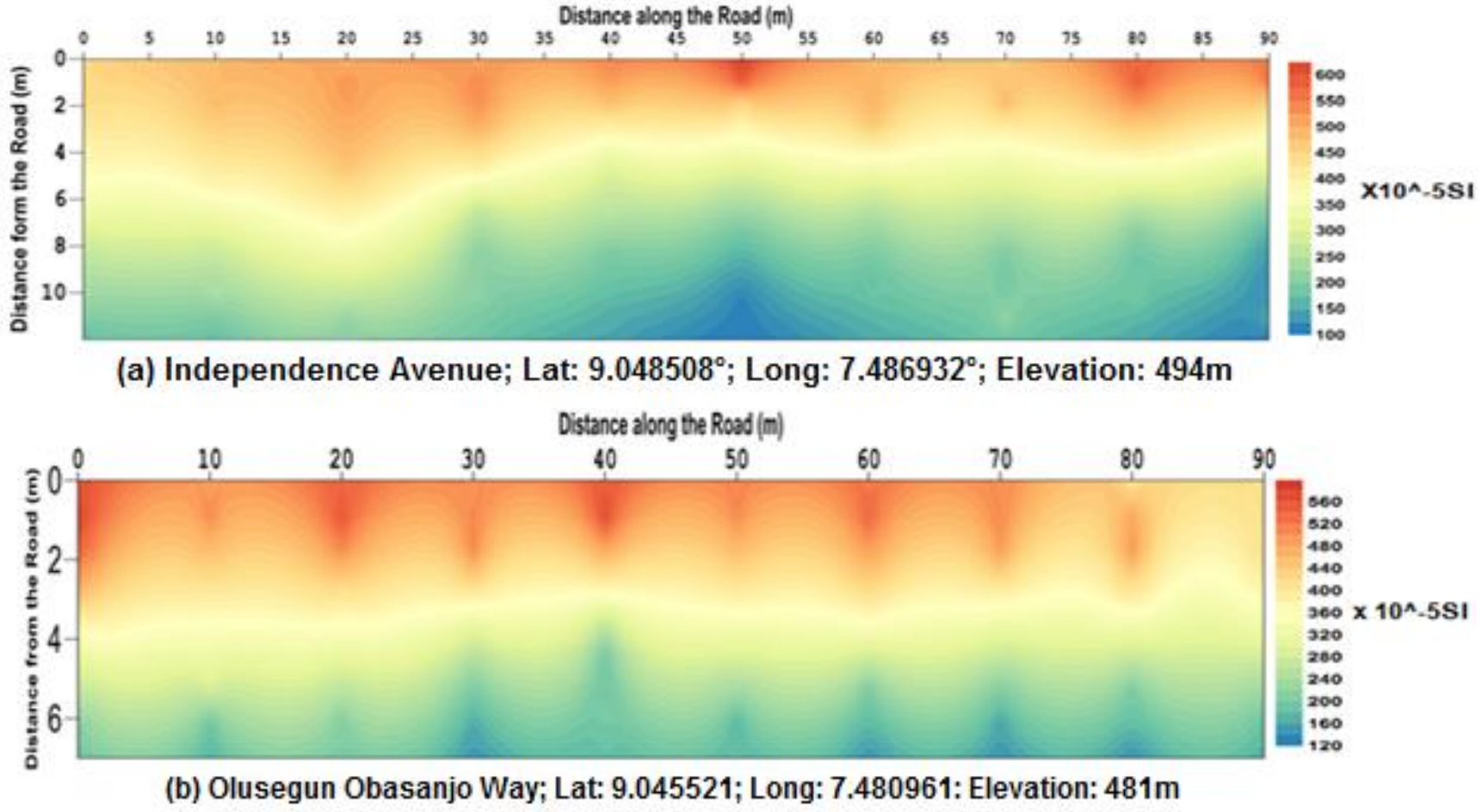
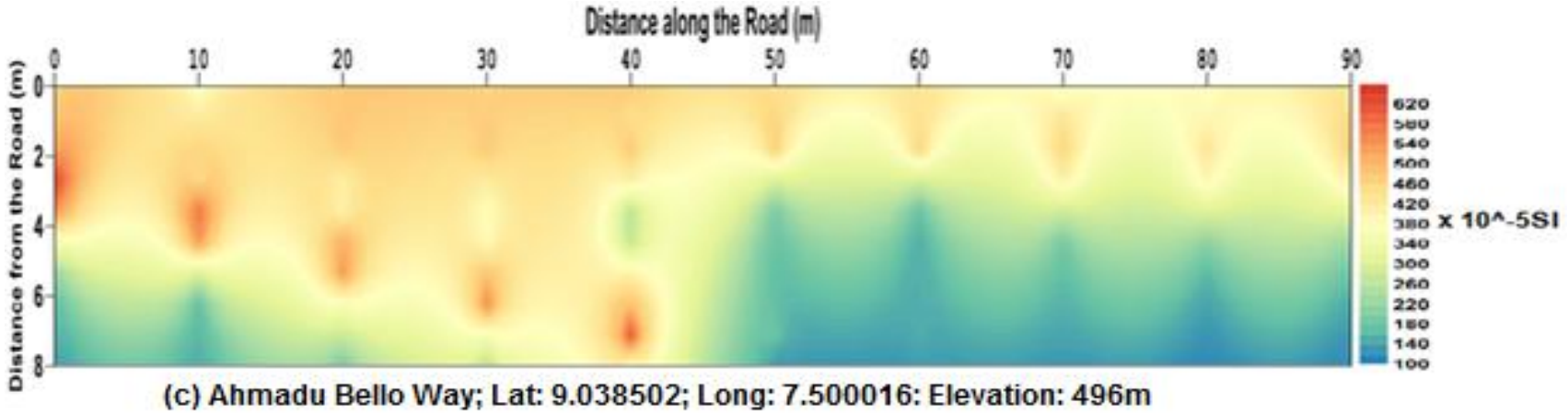
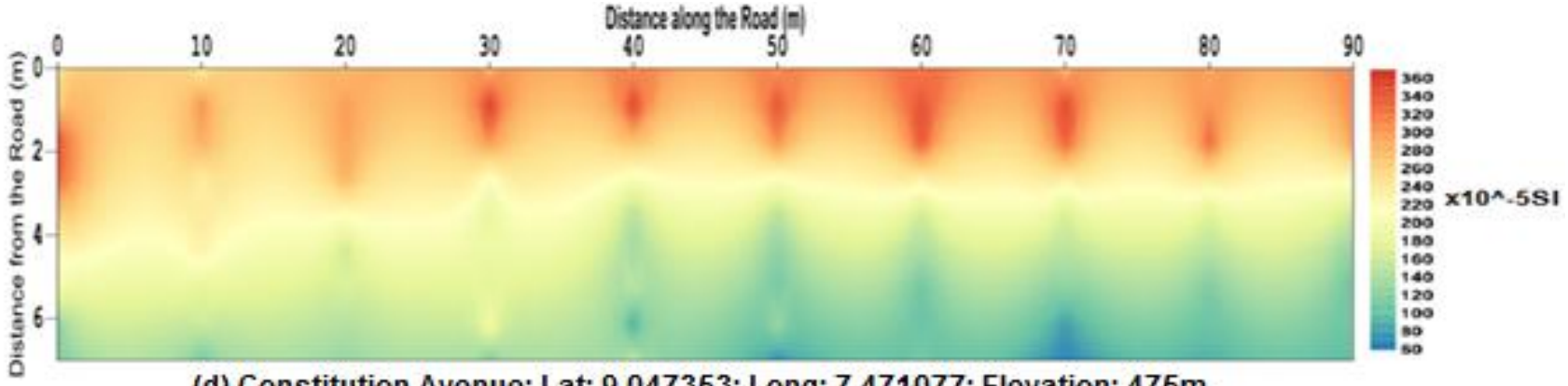


Figure 4.5: High-resolution magnetic contour maps in a vicinity of selected roads in Central District, showing clearly spatial distribution of MS affected by road traffic



(c) Ahmadu Bello Way; Lat: 9.038502; Long: 7.500016: Elevation: 496m



(d) Constitution Avenue; Lat: 9.047353; Long: 7.471077; Elevation: 475m

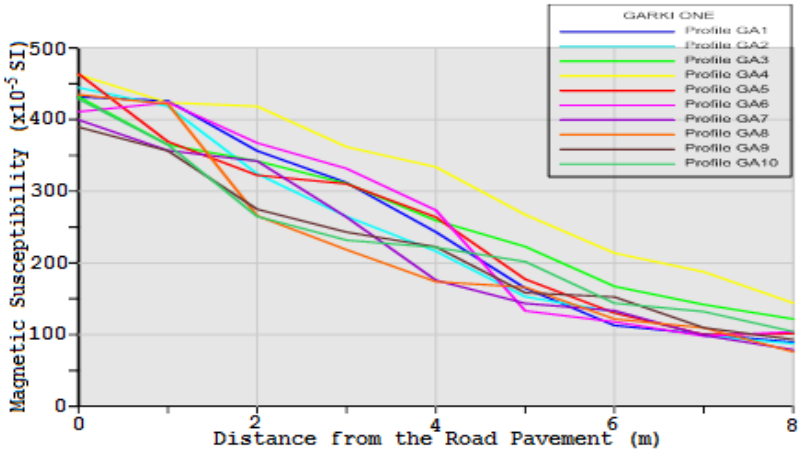
Figure 4.5: High-resolution magnetic contour maps in a vicinity of selected roads inCentral District, showing clearly spatial distribution of MS affected by road traffic (cont.)

4.3.2 Garki District magnetic susceptibility data along road networks

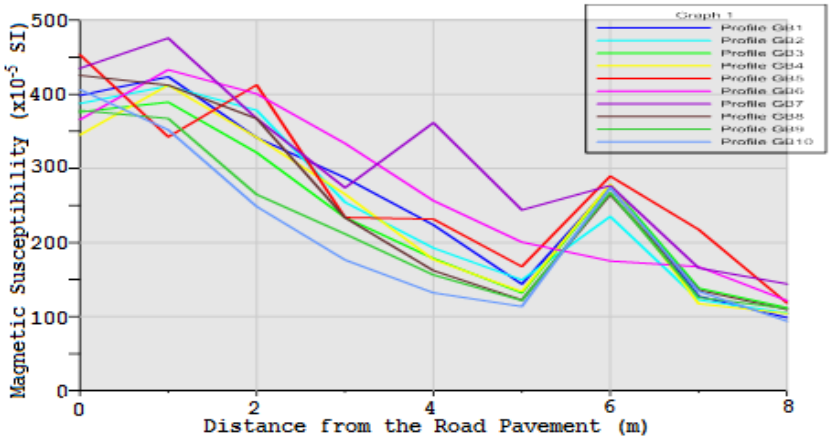
Magnetic susceptibility measurements were conducted in four selected road networks namely; G_1, G_2, G_3 and G_4 in Garki District. A maximum distance of 9.0mwas covered at road G_1, G_2 and G_4 while 8.0m was covered at road G_3 respectively. At each of the road 1.0m separation along profiles lines were observed.

Road G_4 has the highest maximum magnetic susceptibility of about 660.0 x 10^{-5}SI while road G_2 has the lowest maximum of about 450.0 x 10^{-5}SI respectively (Appendix B).

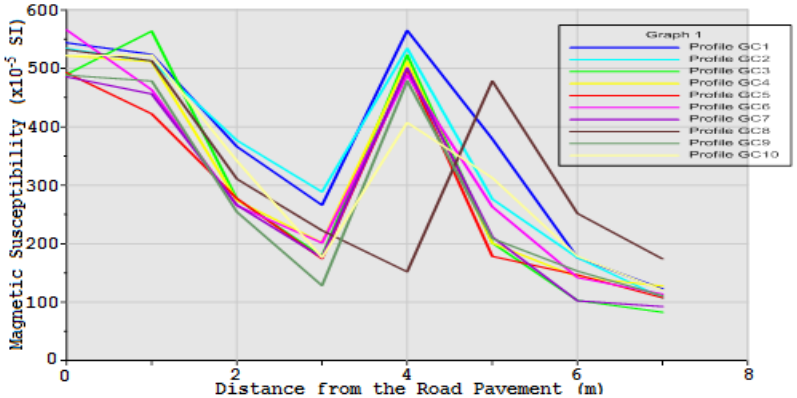
Figure 4.6 shows the graph of the various profiles obtained from the selected road networks. It is evidence from the graph that magnetic susceptibility decrease with increase distance from the road pavements. In Figure 4.6a, magnetic susceptibility decreases almost linearly with distance in all the profiles the maximum magnetic susceptibility values recorded are all observed immediately after the road pavement, while the minimum values obtained are at a distance of 9.0m from the road pavement. Irregular profile lines were observed in Figure 4.6b, with the maximum susceptibility values obtained immediately after the road pavement. At a distance of 6.0m from the road, magnetic susceptibility tends to increase. At this point redisposition of roadside dust or a walk path may likely be attributed to this sudden phenomenon. In Figure 4.6c, the redisposition of roadside dust or walk path may also be the cause of the magnetic susceptibility enhancement at a distance of 4.0m from the road. The profiles in Figure 4.6d, show a linearly decreasing trend with distance, however, maximum enhancement was observed at about 2.0m from the pavement.



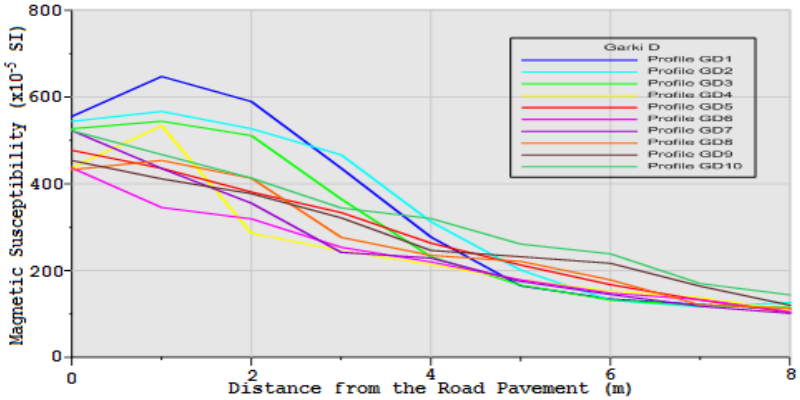
(a) **Kam Salem Street**



(b) Fumilayo Ransome Kuti Road



(c) Nnamdi Azikwe Way



(d) Moshood Abiola Road

Figure 4.6: Magnetic Susceptibility profile line variations with distance along selected roads in Garki District of Abuja

Figure 4.7shows the contour maps of the spatial distributions of magnetic susceptibility along selected road pavements in Garki District. The magnetic susceptibility decreases with increased distance from the road pavement as observed from the maps. The maximum average magnetic susceptibility values measured along the roads are 480.0 x 10^{-5}SI, 500.0 x 10^{-5}SI, 580.0 x 10^{-5}SI and 600.0 x 10^{-5}SI for road G_1, G_2, G_3 and G_4 respectively. Maximum enhancements were mostly observed immediately after the road pavement to a distance of about 3.0 m from the pavement.

The maximum magnetic susceptibility value recorded immediately after the road pavements are 480.0 x 10^{-5}SI; 470.0 x 10^{-5}SI; 560.0 x 10^{-5}SI and 640.0 x 10^{-5}SI for road G_1, G_2, G_3 and G_4 respectively.In Figure 4.8a, the maximum susceptibility value was obtained immediately after the road pavement and the minimum of about 70.0 x 10^{-5}SI was observed at the last profile a distance of 8.0m from the road pavement. This value at the last profile almost corresponds to the background value of the area. In Figure 4.7b, magnetic enhancement was observed immediately after the road pavement to a distance of about 3.0m form the pavement, however, the values observed at the end of the profile indicates that magnetic susceptibility decreases with distance from the pavement. Magnetic susceptibility enhancement was observed immediately after the road pavement and at a distance of about 4.0m from the pavement at road G_3 (Figure 4.7c). The reoccurrence of this magnetic enhancement at 4.0m may be attributed to the presence of a walk way rather than the re-depositional effect since the trend is linearly and parallel to the road pavement.

Road G_3 has the highest recorded magnetic susceptibility of about 640.0 x 10^{-5}SI within Garki District. Enhancement occurs from the road pavement to a distance of about 2.0m away from the road (Figure 4.7d)

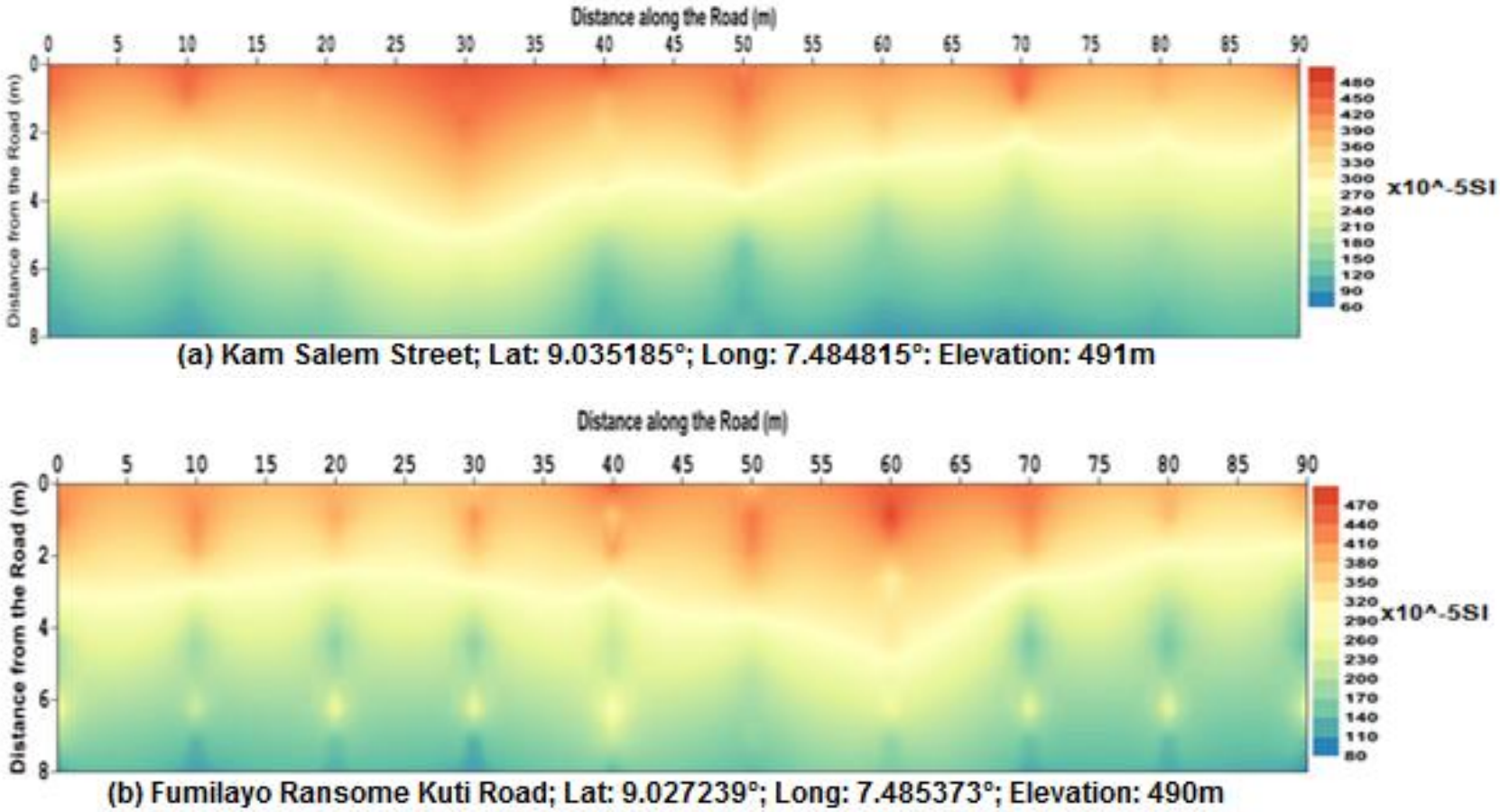
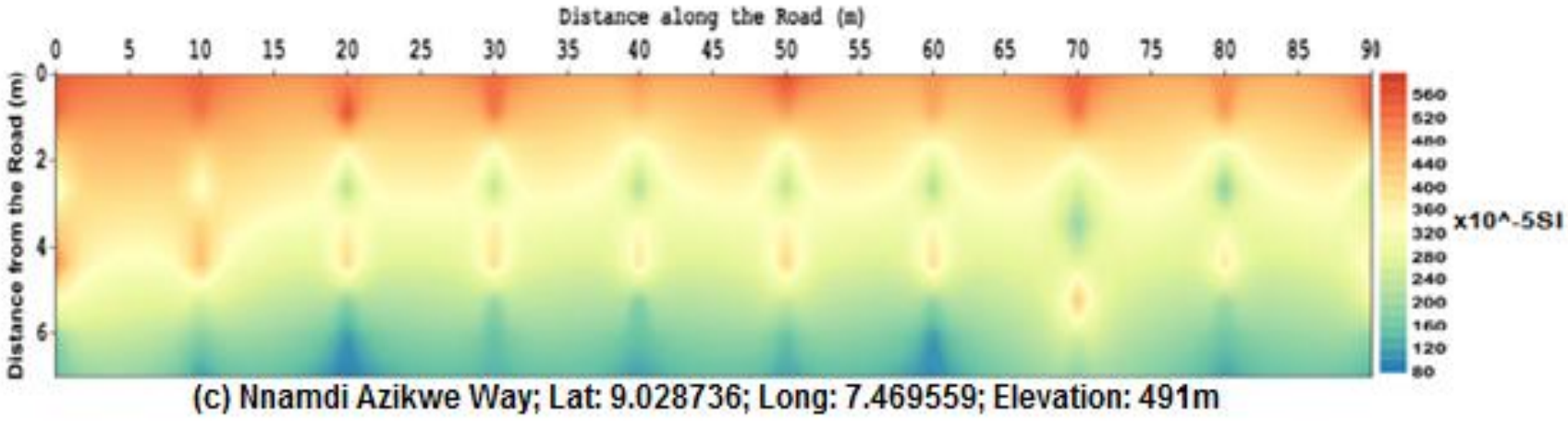
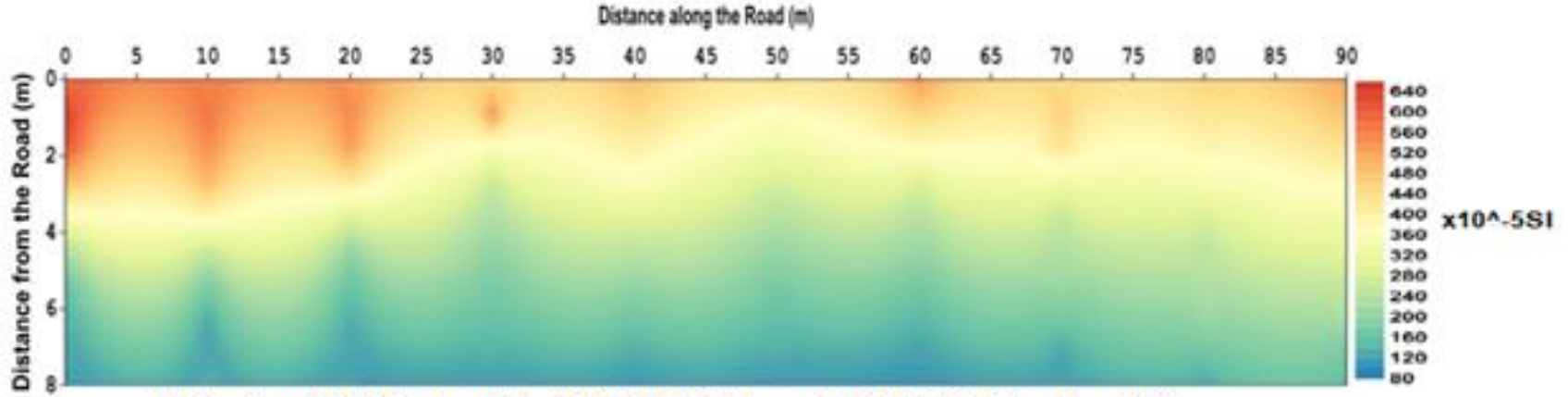


Figure 4.7: High-resolution magnetic contour maps in a vicinity of selected roads in Garki District, showing clearly spatial distribution of MS affected by road traffic



(c) Nnamdi Azikwe Way; Lat: 9.028736; Long: 7.469559; Elevation: 491m



(d) Moshood Abiola Road; Lat: 9.035059°; Long: 7.477783°; Elevation: 490m

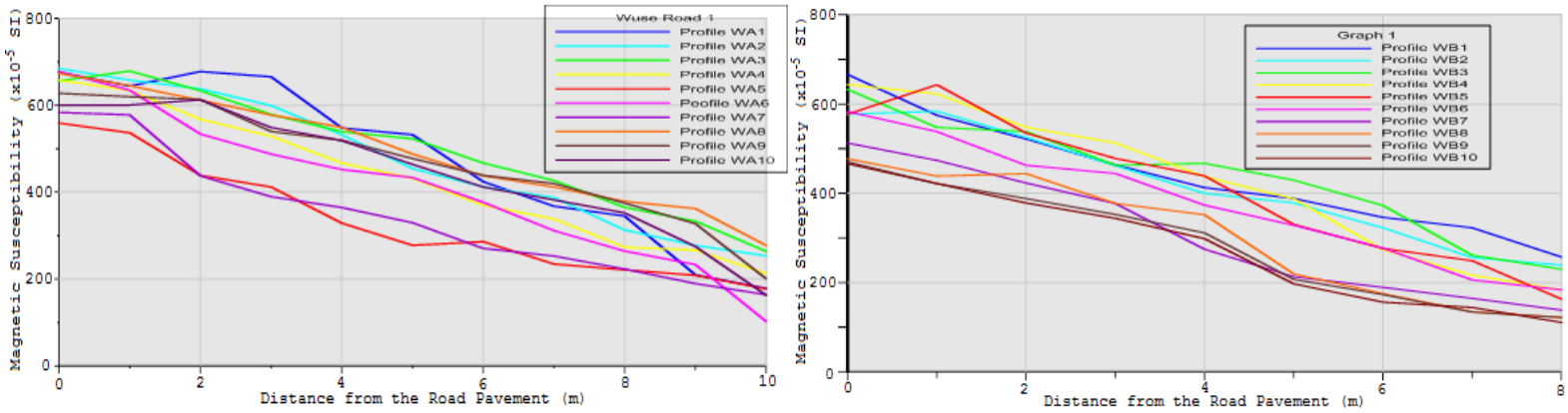
Figure 4.7: High-resolution magnetic contour maps in a vicinity of selected roads inGarkiDistrict, showing clearly spatial distribution of MS affected by road traffic (cont.)

4.3.3 Wuse magnetic susceptibility data along road networks

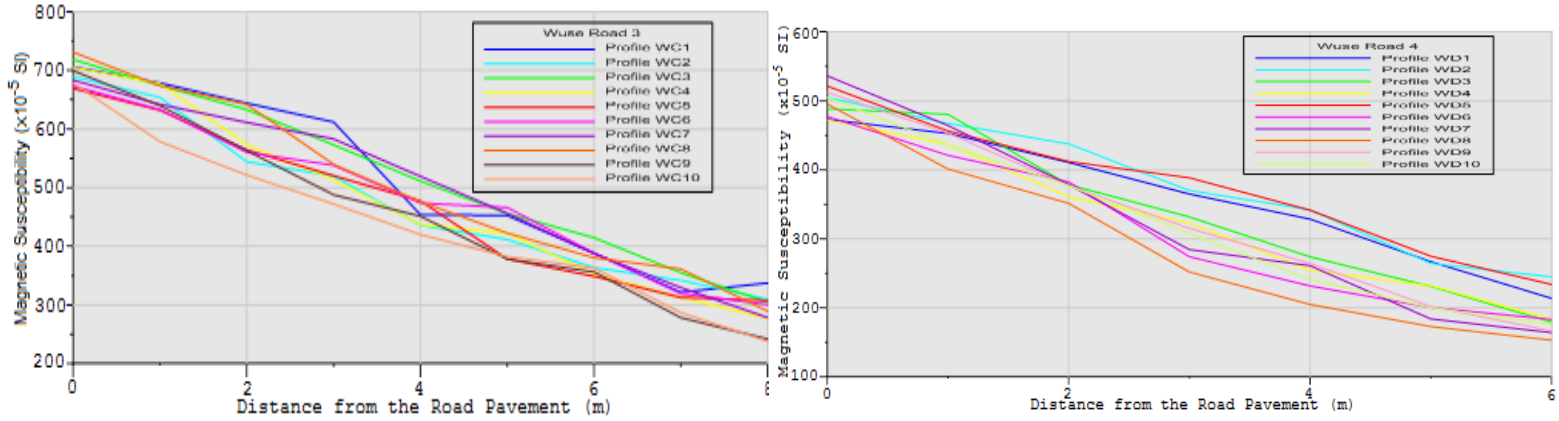
In Wuse District, magnetic susceptibility measurements were carried out along four selected roads network namely; W_1, W_2, W_3 and W_4.At road W_1, a maximum distance of 11.0 m was covered off the road, while in W_2 and W_3 a maximum distance of 9.0 m was covered, at W_4, 7.0 m was covered off the road pavement.

Highest maximum magnetic susceptibility recorded in the District is about 720.0 x 10^{-5}SI while the lowest maximum value recorded is about 480.0 x 10^{-5}SI (Appendix C). Generally, the high magnetic readings obtain in this district is attributed to the fact that this Wuse remained one of the busy district of Abuja city.

The graph of the various profiles obtained from the selected roads networks are shown in Figure 4.8. From all the profiles plots of the selected road network, it is observed that magnetic susceptibilities enhancement decrease linearly without any irregularities in the profile lines with increase distance from the road pavements. Maximum magnetic susceptibility values were recorded immediately after the road pavement. There is no evidence of magnetic susceptibility signal distortion along the profiles.



(a) Kashim Ibrahim Way **(b) Sani Abacha Way**



(c) Herbert Macauly Way **(d) Bissau Street**

Figure 4.8: Magnetic Susceptibility profile line variations with distance along selectedroads in Wuse District of Abuja

The magnetic susceptibility contour maps along the selected roads section are shown in Figure 4.9. Enhancements of magnetic susceptibilities were observed immediately after the road pavements. Figure 4.9a shows that the magnetic susceptibility enhancement occurs from the road pavement to a distance of about 4.0m away from the pavement. Maximum values observed immediately after the road pavement is about 700.0 x 10^{-5}SI, while the minimum value of about 100.0 x 10^{-5}SI were observed at a distance of about 10.0m away from the pavement. In Figure 4.9b, high magnetic susceptibilityvalue are recorded from 0-50.0m along the road and 0-4.0m off the road pavement. This indicates that the deposition factors move from right to left hand side of the map. The maximum magnetic signal observed is about 660 x 10^{-5}SI at the beginning of the profiles and the minimum of about 100.0 x 10^{-5}SI were observed at a distance of about 8.0m away from the road pavement. Figure 4.9c indicates a maximum of about 740 x 10^{-5}SI immediately after the pavement and a minimum of 220.0 x 10^{-5}SI at a distance of 9.0m form the road. Magnetic enhancement at the section of the road occurs immediately after the road pavement to a distance of about 5.0m away from the pavement. Generally, even though the magnetic susceptibility enhancement reduces with increase in distance, it is obvious that the overall magnetic susceptibility intensity is high in this road network. At road W_4, maximum magnetic susceptibility enhancement was observed immediately after the road pavement to a distance of about 2.0m from the road (Figure 4.9d). In all the road sections under investigation in Wuse District, no evidence of magnetic susceptibility anomaly was observed aside from the fact that high values are recorded at the sections of the roads.

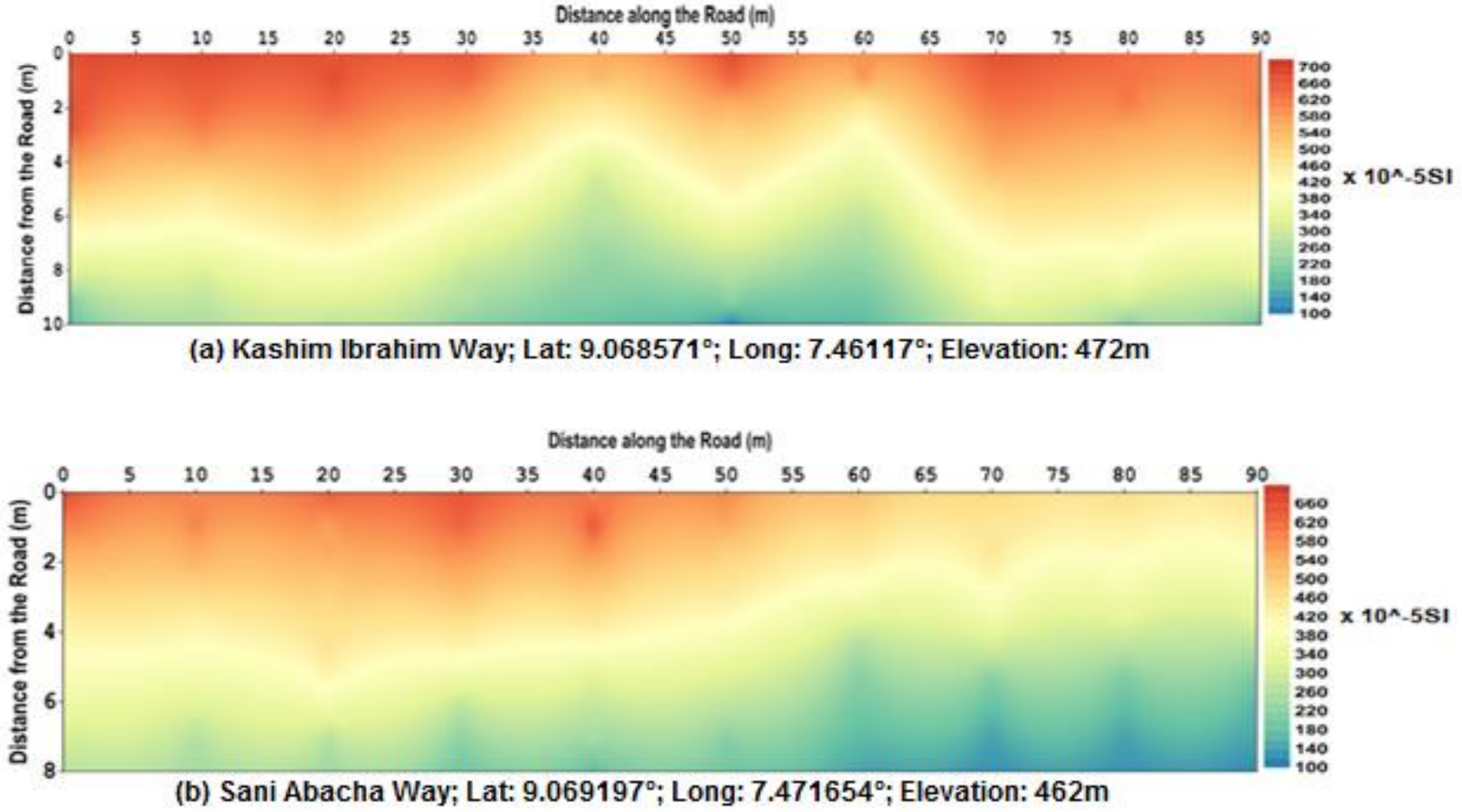
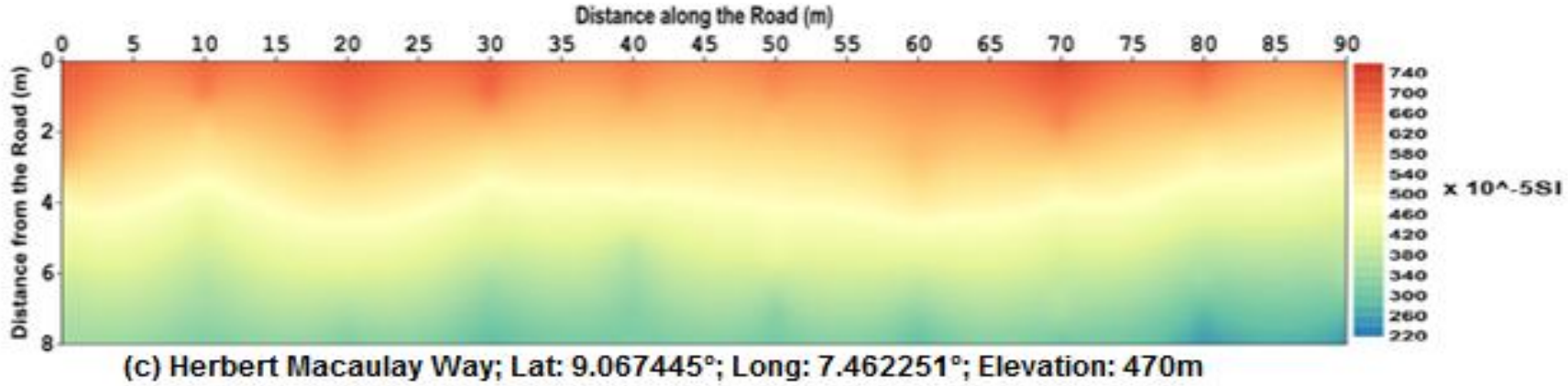


Figure 4.9: High-resolution magnetic contour maps in a vicinity of selected roads in Wuse District, showing clearly spatial distribution of MS affected by road traffic



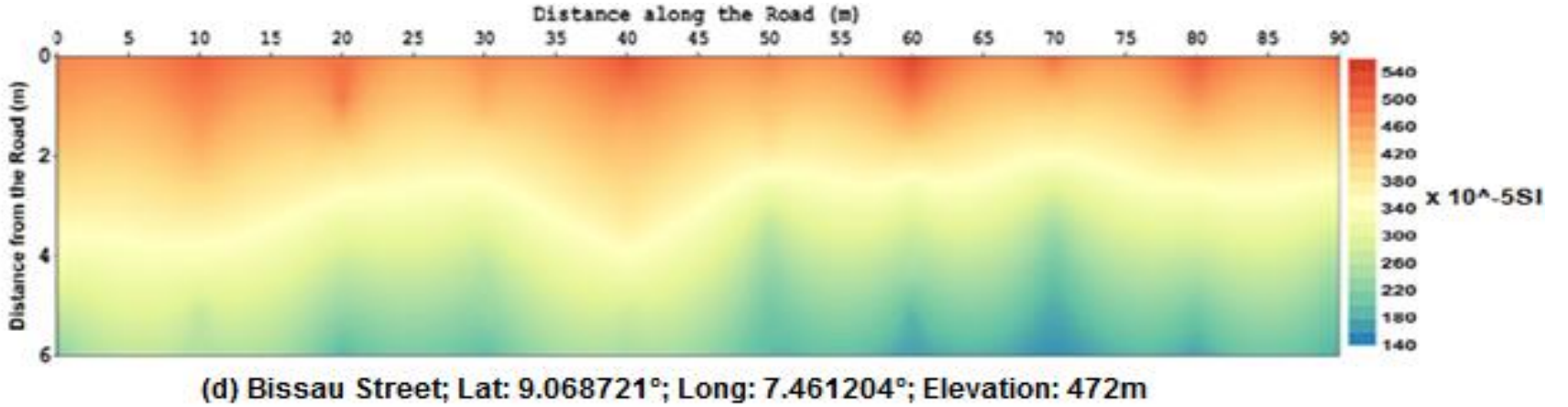


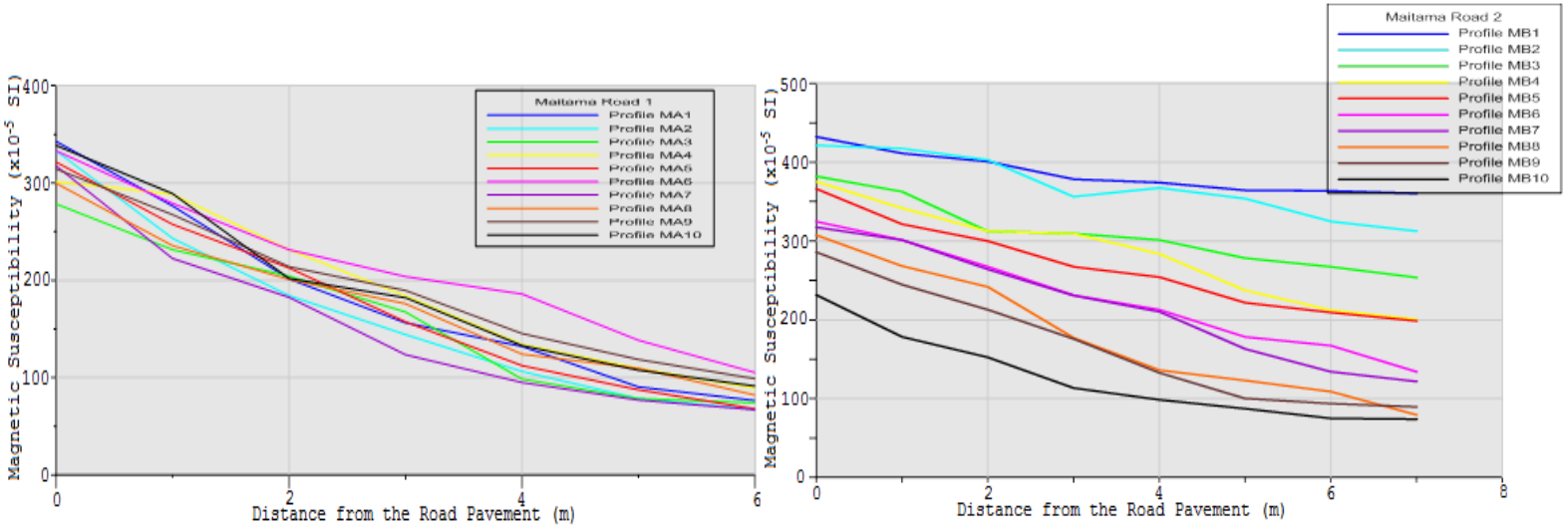
Figure 4.9: High-resolution magnetic contour maps in a vicinity of selected roads in Wuse District, showing clearly spatial distribution of MS affected by roadtraffic (cont.)

4.3.4 Maitama magnetic susceptibility data along road networks

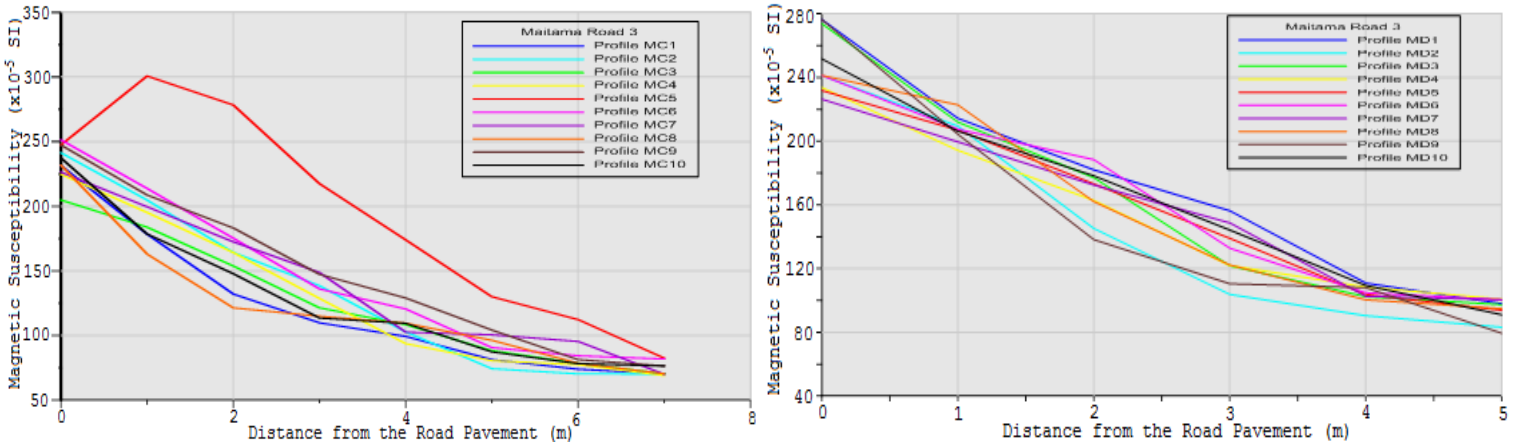
In Maitama district, magnetic susceptibility measurements were conducted along four selected roads namely; M_1, M_2, M_3 and M_4 respectively. A maximum distance from the road pavement in the road network covered was 7.0m, 8.0m, 8.0m and 6.0m for M_1, M_2, M_3 and M_4 respectively.

The maximum magnetic susceptibility value recorded at the District is about 420.0 x 10^{-5}SI and a minimum value recorded is about 70.0 x 10^{-5}SI respectively (Appendix D). The minimum values obtained are on the last profile lines and almost correspond to the background value recorded for this District.

Figure 4.10 shows the magnetic susceptibility variation with distance plots, aside from Figure 4.10c; linear variations are recorded in all the plots. This simple linear trend indicates that there are no magnetic susceptibility abnormalities within the section of roads in consideration, and most of the magnetic enhancement occurs immediately after the road pavement and extending to a distance of about 1.0-2.0m from the road pavement. On one of the profile in Figure 4.10c, maximum magnetic susceptibility enhancement occurs at a distance of about 1.0 m and 2.0m respectively from the road pavement



(a) Ibrahim Babagida Way **(b) Shehu Shagari Way**



(b) Gana Street **(d) Mban Close**

Figure 4.10: Magnetic Susceptibility profile line variations with distance along selected roads in Maitama District of Abuja

The contour map of the road sections are shown in Figure 4.11, the normal decreasing trends are observed in all the maps, but generally the maximum intensity is less than those in Wuse, Central and Garki District. Figures4.11a and 4.11d shows normal decreasing devoid of any abnormality, the magnetic enhancements are noticed immediately after the road pavements with values in the range of(240.0-350.0) x 10^{-5}SI. Towards the end of the map, the magnetic susceptibility decreases to about 100.0 x 10^{-5}SI. Figure 4.11b shows that the concentration of magnetic grains is high at the left hand side of the contour map. This may be attributed to the fact that wind or any other depositor control factor might have contributed to the high magnetic susceptibility intensity at that section. In Figure 4.11c, high magnetic susceptibility values were obtained at about 40.0m along the road, immediately after the road pavement. This indicates the presence of a metallic body at that portion. However, the decreasing susceptibility with distance is observed on the map.

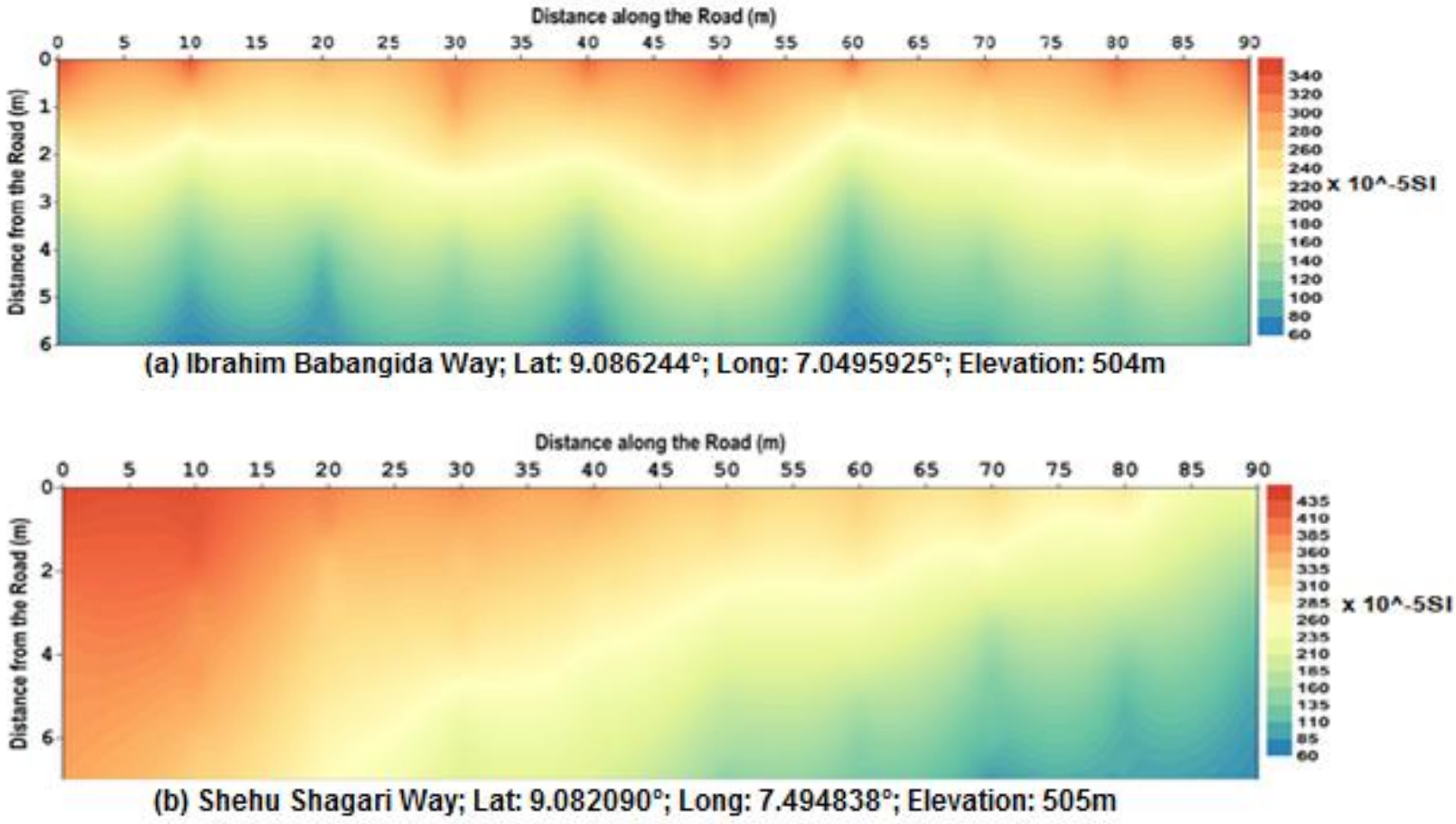


Figure 4.11: High-resolution magnetic contour maps in a vicinity of selected roads in Maitama District, showing clearly spatial distribution of MS affected by road traffic

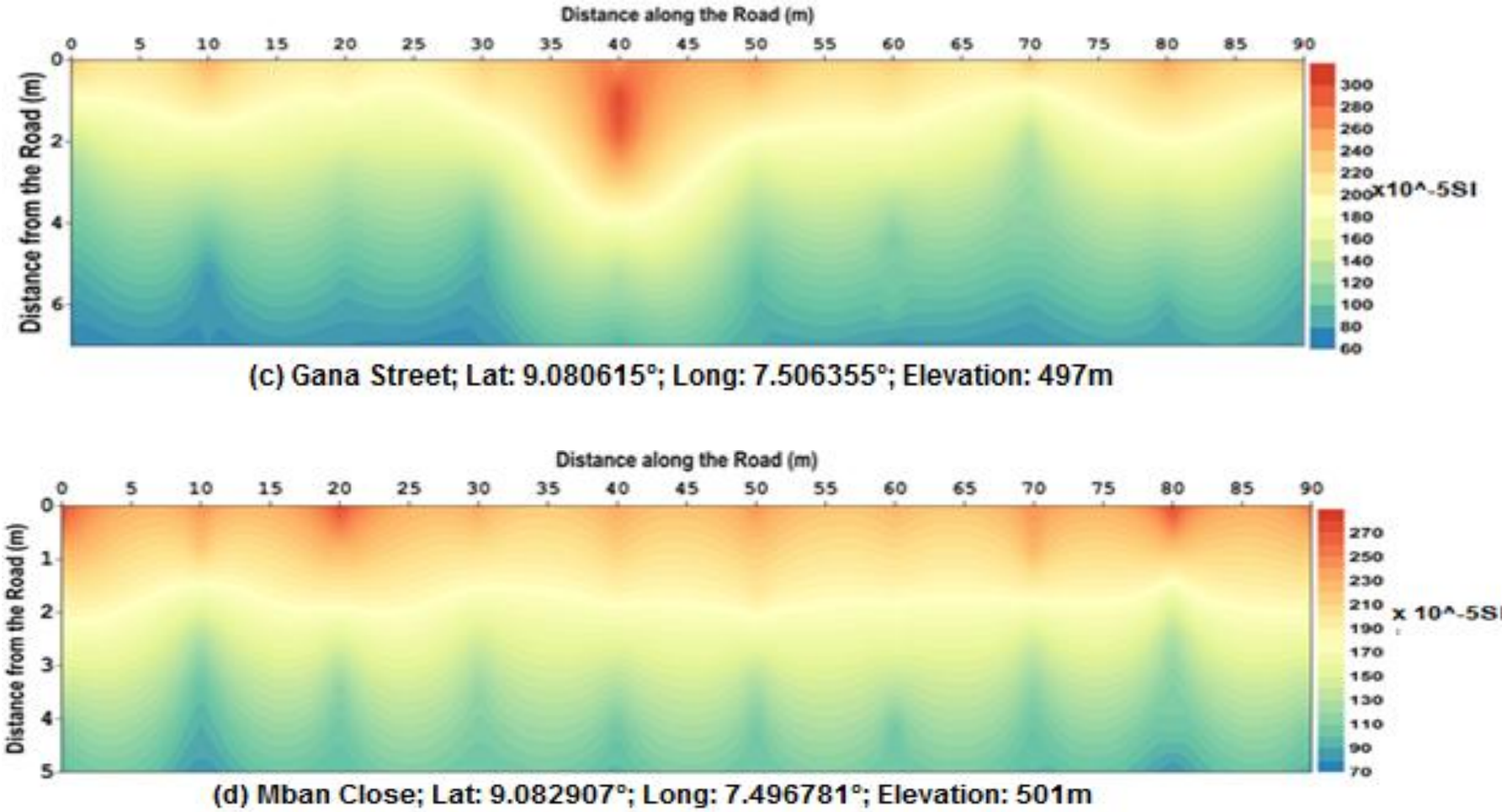


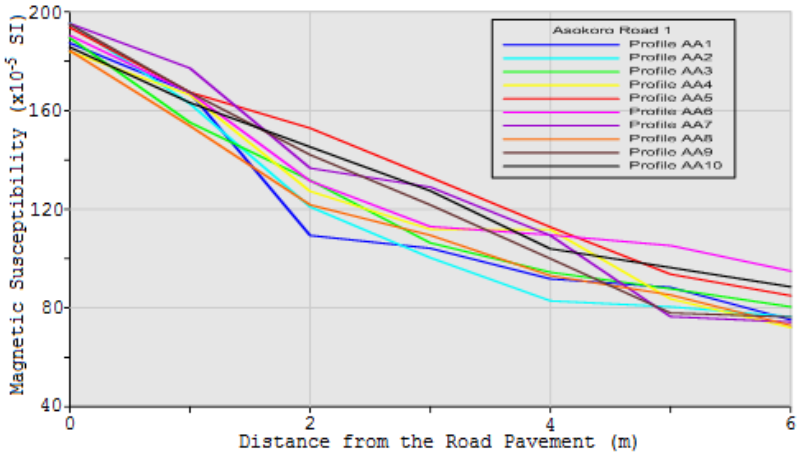
Figure 4.11: High-resolution magnetic contour maps in a vicinity of selected roads in Maitama District, showing clearly spatial distribution of MS affected by road traffic (cont.)

4.3.5 Asokoro magnetic susceptibility data along road networks

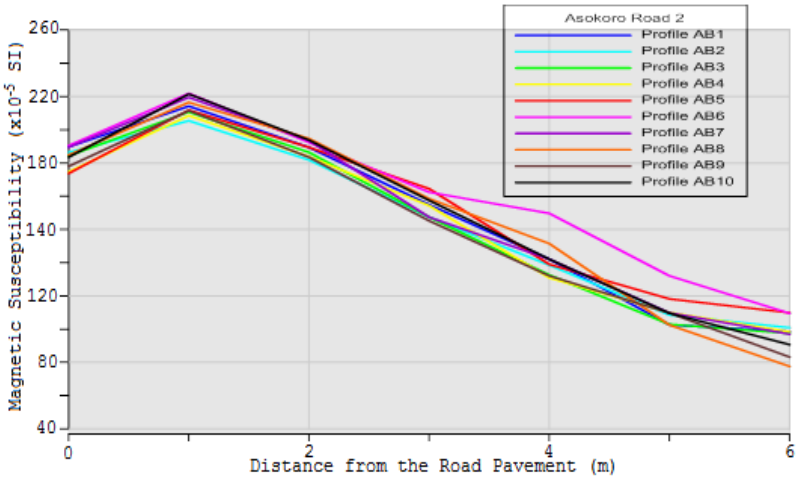
In Asokoro district, magnetic susceptibility measurements were conducted along four selected roads namely; A_1.A_2, A_3 and A_4. A maximum distance from the road pavement in the road network covered was 6.0m, for A_1, A_2 and A_3 respectively, while 7.0m covered along road A_4.

Magnetic susceptibility varies largely between 60.0 x 10^{-5}SI and 300.0 x 10^{-5}SI (Appendix E). The low magnetic susceptibility recorded at the District clearly indicates that commercial activities are less compared to the other district. The district is mostly residential housesand foreign mission buildings.

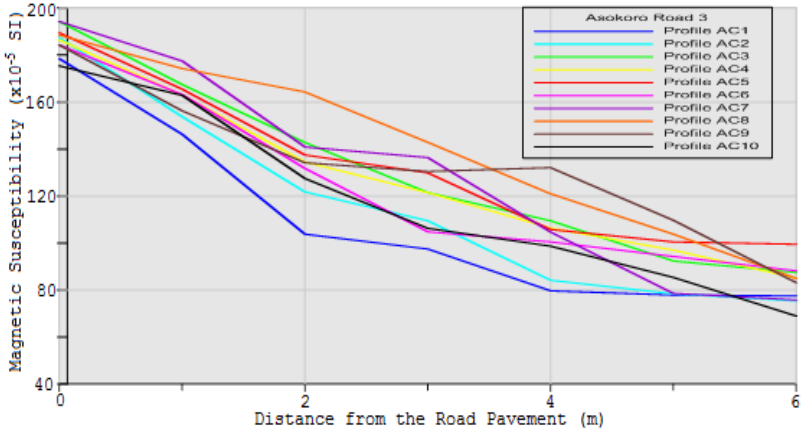
From the magnetic susceptibility variation with distance from the road sections (Figure 4.12), it was observed that magnetic susceptibility decreases with distance away from the road pavements. In Figure 4.12a, the maximum magnetic susceptibility of about 190.0 x 10^{-5}SI was recorded immediately after the pavement. No abnormalities trends were observed in the profile lines. Maximum magnetic susceptibility of about 220.0 x 10^{-5}SI was observed at a distance of 1.0m away from the road pavement in Figure 4.12b. In all the plots, it is evident that magnetic susceptibility decreases linearly with distance.



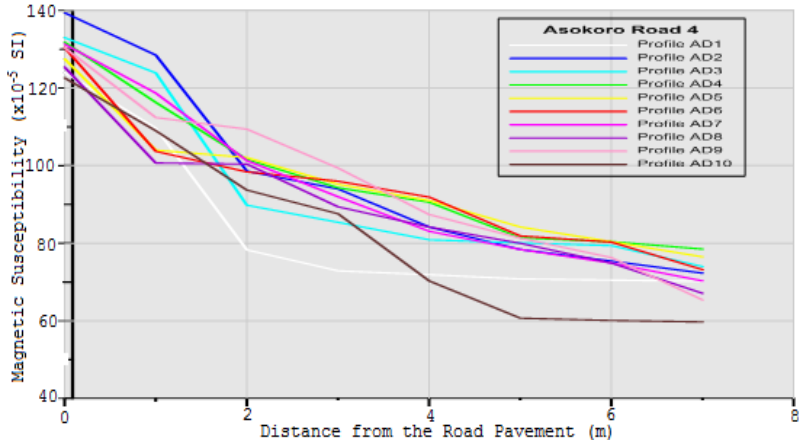
(a) Kwane-Nkrumah Cresent



(b) Yakubu Gowon Cresent



(c) Nelson Mandela Street



(d) Maitama Sule Street

Figure 4.12: Magnetic Susceptibility profile line variations with distance along selected roads in Asokoro District of Abuja

The contour map of the road sections are shown in Figure 4.13, the normal decreasing trends are observed in all the maps, but generally, the maximum intensity is less.Maximum magnetic susceptibility observed in Figure 4.13a is about 200.0 x 10^{-5}SI. This is observed immediately after the road pavement. In Figure 4.13b, the maximum value observed was at 1.0m away from the pavement.

In Figure 4.13c, the maximum magnetic susceptibility of about 195.0 x 10^{-5}SI was observed immediately after the road pavement. Enhancement of magnetic susceptibility was also observed even though with less intensity. Towards the last profile line, the minimum magnetic susceptibility of about 60.0 x10^{-5}SI was recorded. This almost corresponds to the background values obtained at the area. Figure 4.13d has the lowest magnetic susceptibility observed immediately after the road pavement.

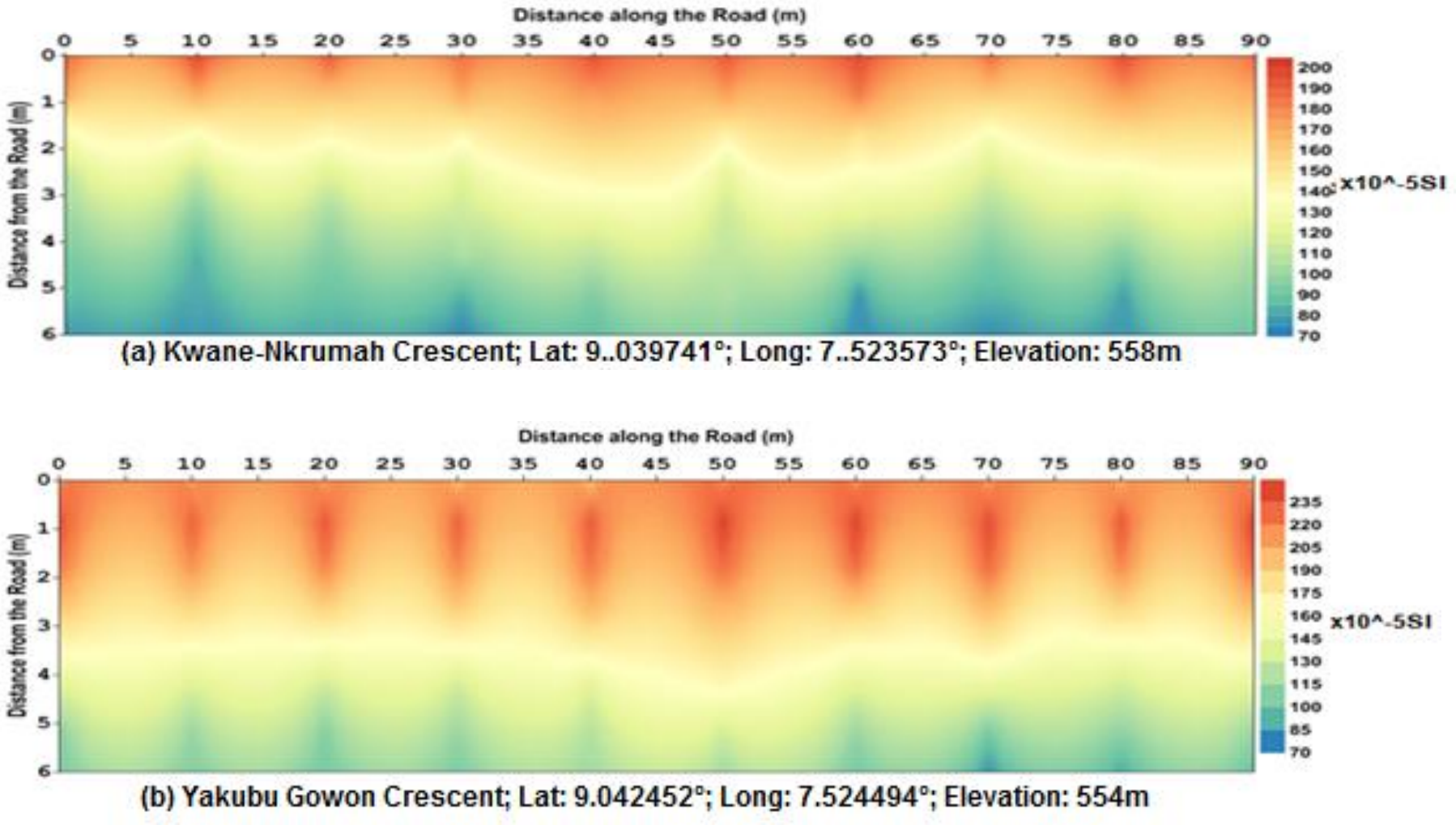


Figure 4.13: High-resolution magnetic contour maps in a vicinity of selected roads in Asokoro District, showing clearly spatial distribution of MS affected by road traffic

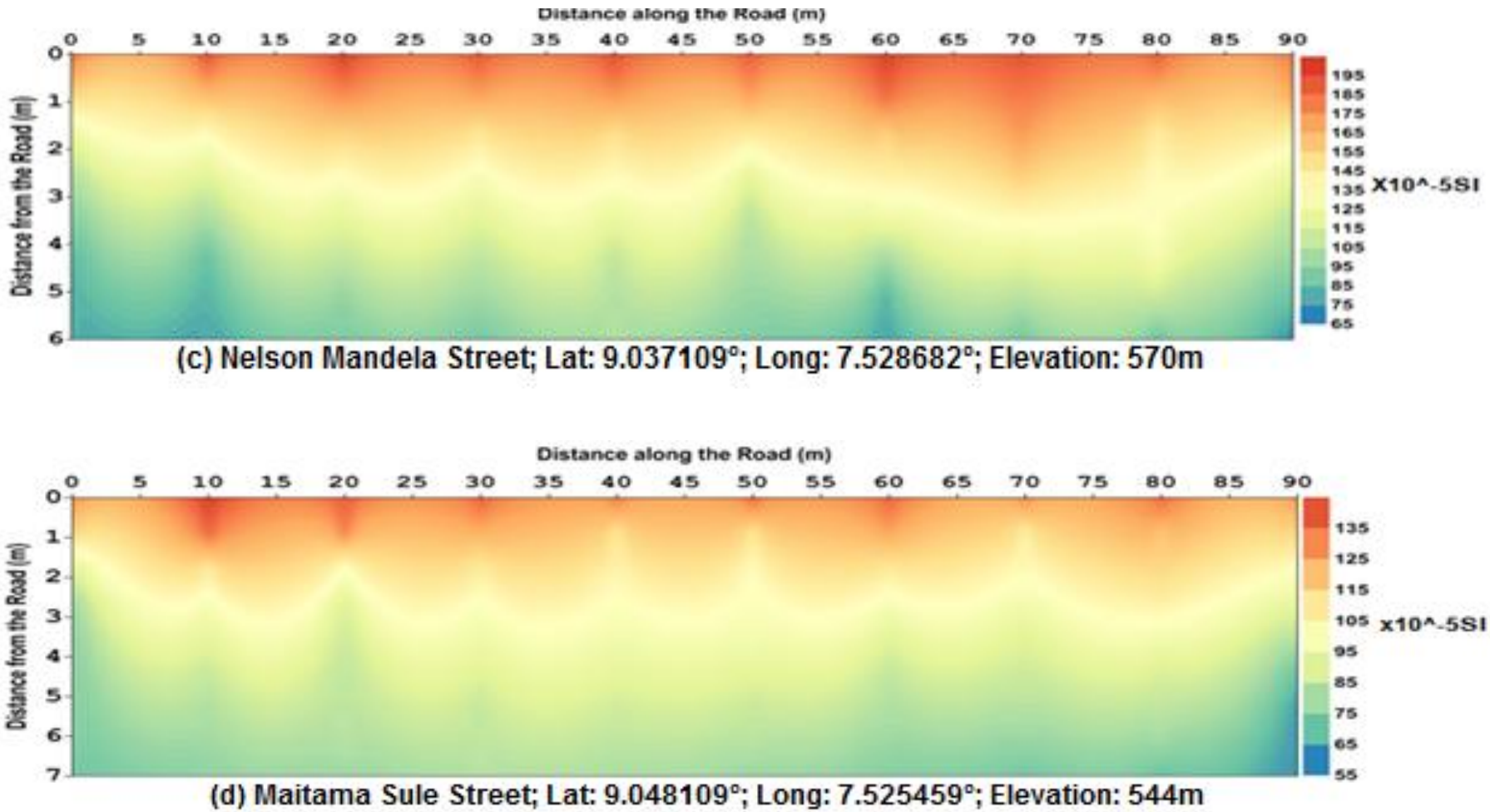


Figure 4.13: High-resolution magnetic contour maps in a vicinity of selected roads in Asokoro District, showing clearly spatial distribution of MS affected by road traffic (cont.)

4.4 VERTICAL SOIL AND SEDIMENT PROFILES ALONG ROAD SECTIONS

4.4.1. Background areas of soil profiles

A 35.0 cm deep magnetic susceptibility of soil profile from Asokoro, Maitama, Garki, Central and Wuse districts were collected (Figure 4.14). The soil profiles sequence, of Precambrain age (Yoshida and Gautam, 1988), has no signs of present-day environmental as there is no reasonable variable in the magnetic susceptibility from the top soil to the depth of 35.0 cm. The in situ susceptibility has a range of (28.0 – 52.0) x 10^{-5} SI. These profiles serve as a guide to the lithogenic background susceptibility in Abuja.

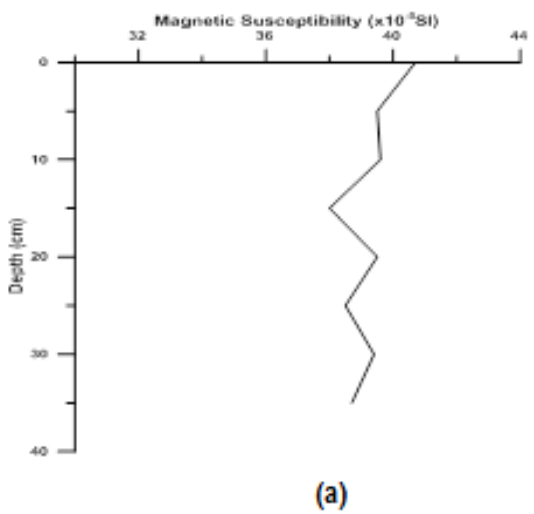


Figure 4.14a Background magnetic susceptibility profile from the surface to a depth of 35.0m at W1

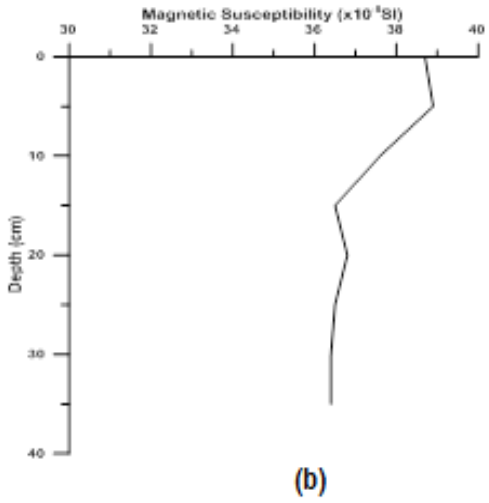


Figure 4.14b Background magnetic susceptibility profile from the surface to a depth of 35.0m at W2

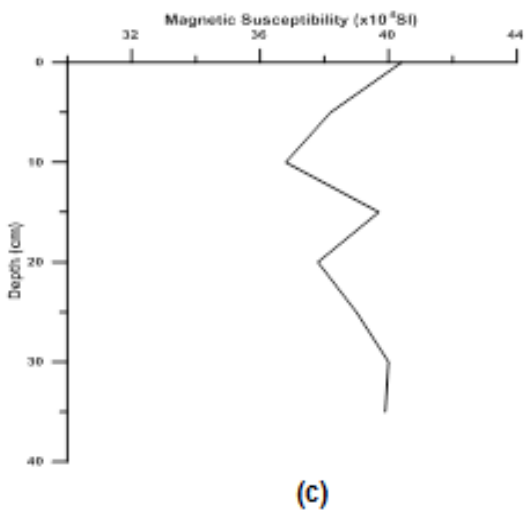


Figure 4.14c: Background magnetic susceptibility profile from the surface to a depth of 35.0m at G1

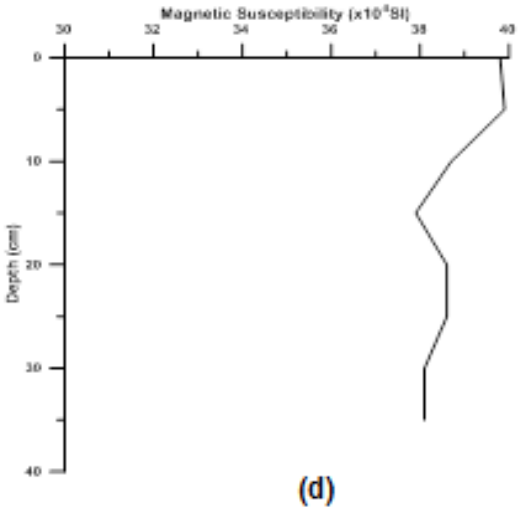


Figure 4.14d: Background magnetic susceptibility profile from the surface to a depth of 35.0m at G2

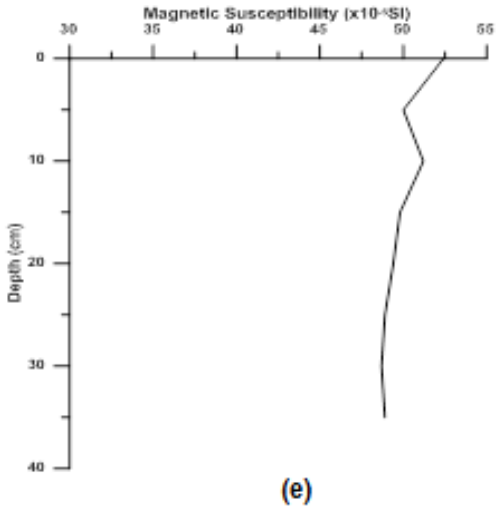


Figure 4.14e Background magnetic susceptibility profile from the surface to a depth of 35.0 m at C1

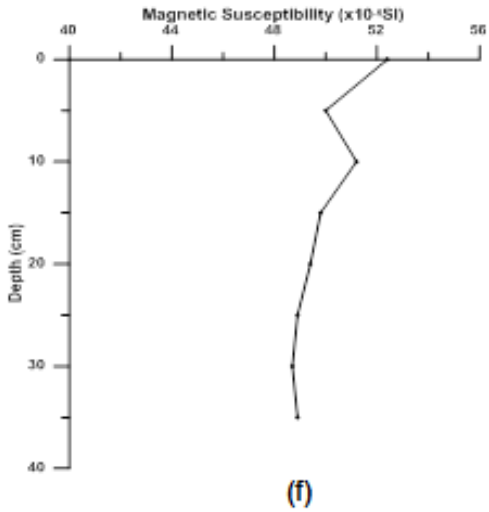
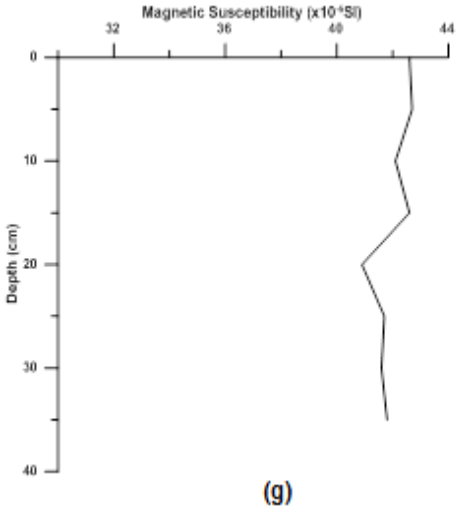
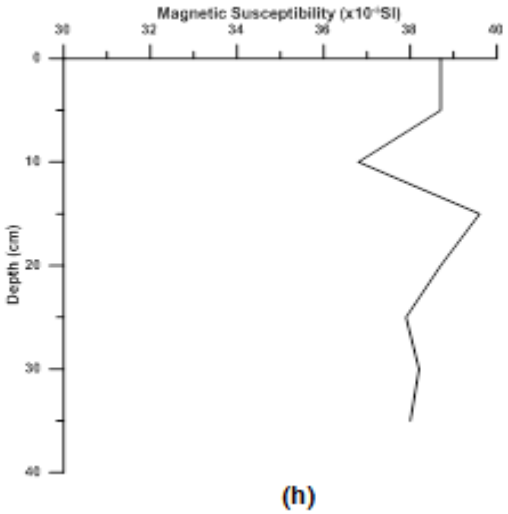


Figure 4.14f Background magnetic susceptibility profile from the surface to a depth of 35.0 m at C2



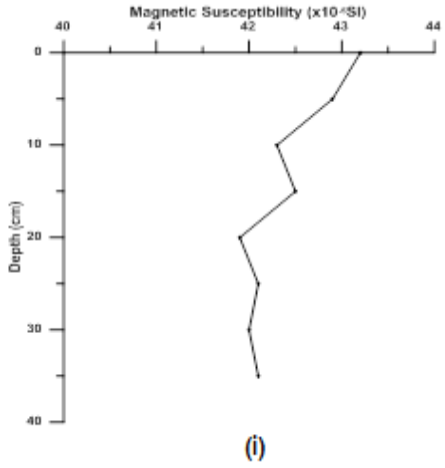
(g)

Figure 4.14g Background magnetic susceptibility profile from the surface to a depth of 35.0m at M1



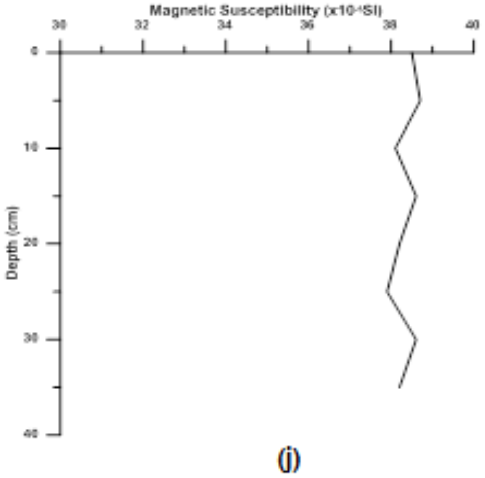
(h)

Figure 4.14h Background magnetic susceptibility profile from the surface to a depth of 35.0m at M2



(i)

Figure 4.14i Background magnetic susceptibility profile from the surface to a depth of 35.0m at A1



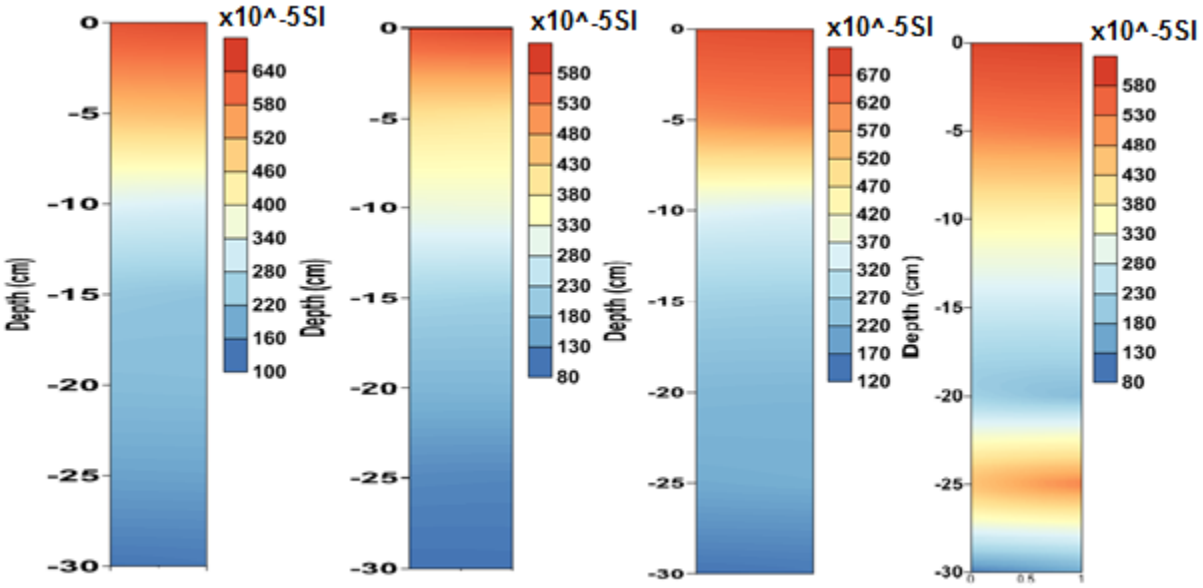
(j)

Figure 4.14j Background magnetic susceptibility profile from the surface to a depth of 35.0m at A2

The vertical profile measurements of the magnetic susceptibility with depth along the road pavements belonging to the four different areas are shown in Appendix F.

4.4.2 Vertical soil profiles along selected roads in Wuse District

Figure 4.15 shows the magnetic susceptibility of soil profiles variation with depth along selected roads obtained from Wuse district of Abuja. Enhanced magnetic susceptibility values greater than 400.0 x 10^{-5}SI were observed at the surface to a depth of about 10.0cm in most of the profiles. Magnetic susceptibility tends to decrease with depth down the ground as observed in the profiles. However, in Figure 4.15d, enhanced magnetic susceptibility with value of about 450.0 x 10^{-5}SI was observed at a depth of 23.0cm- 27.0cm below the surface. The reoccurrence of enhanced magnetic susceptibility at this depth may be an indication of contamination within the soil profile.



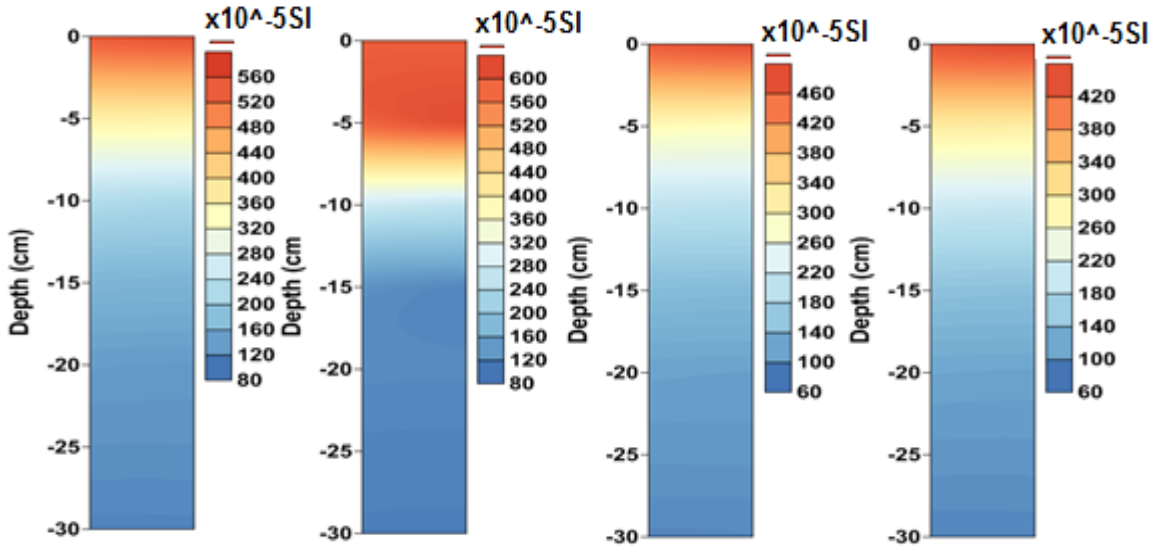
(a) (b) (c) (d)

Figure 4.15: Vertical magnetic susceptibility distribution with depth along selected roads inWuse district

4.4.3 Vertical soil profiles along selected roads in Garki area

Figure 4.16 shows the distribution of magnetic susceptibility obtained from Garki district of Abuja, Four soil profiles were obtained from different locations. It is observed from all the

profiles that magnetic susceptibility decreases with depth. At the top soil to a depth of about 7.0cm, enhanced magnetic susceptibility with value of about 400.0 x 10^{-5}SI were observed. At the depth of 30.0cm, it is clearly seen that the value obtained almost correspond to the background values obtained from the area and hence this may be attributed to lithological origin.



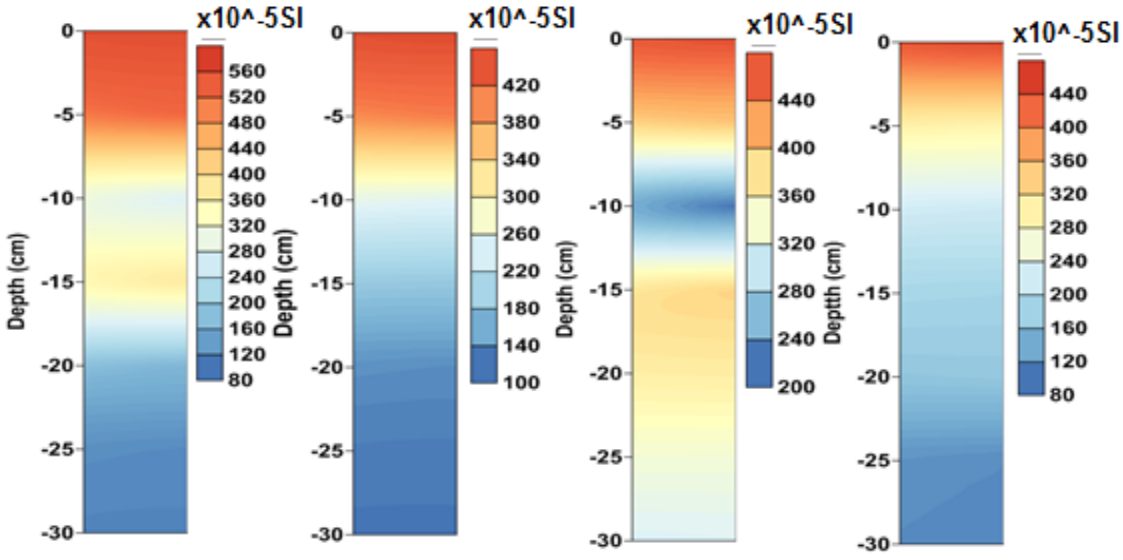
(a) (b)(c) (d)

Figure 4.16: Vertical magnetic susceptibility distribution with depth along selected roads inGarki district

4.4.4 Vertical soil profiles along selected roads in Central area

Figure 4.17 shows the magnetic susceptibility distribution in four profiles from different locations within the Central district. Figure 4.17a shows enhanced magnetic susceptibility at the top soil to a depth of about 5.0cm. At depth of 5.0cm to about 7.0cm the average magnetic susceptibility obtained is about 300.0 x 10^{-5}SI. However, magnetic susceptibility decreases further to depth of about 30.0cm with value of about 80.0 x 10^{-5}IS. In Figure 4.17c, magnetic susceptibility tends to decrease at a depth of 7.0 to 12.0cm and thereafter increases. This may be

attributed to the type of soil material which is dark brownish in colour, may likely be rich in iron oxides.

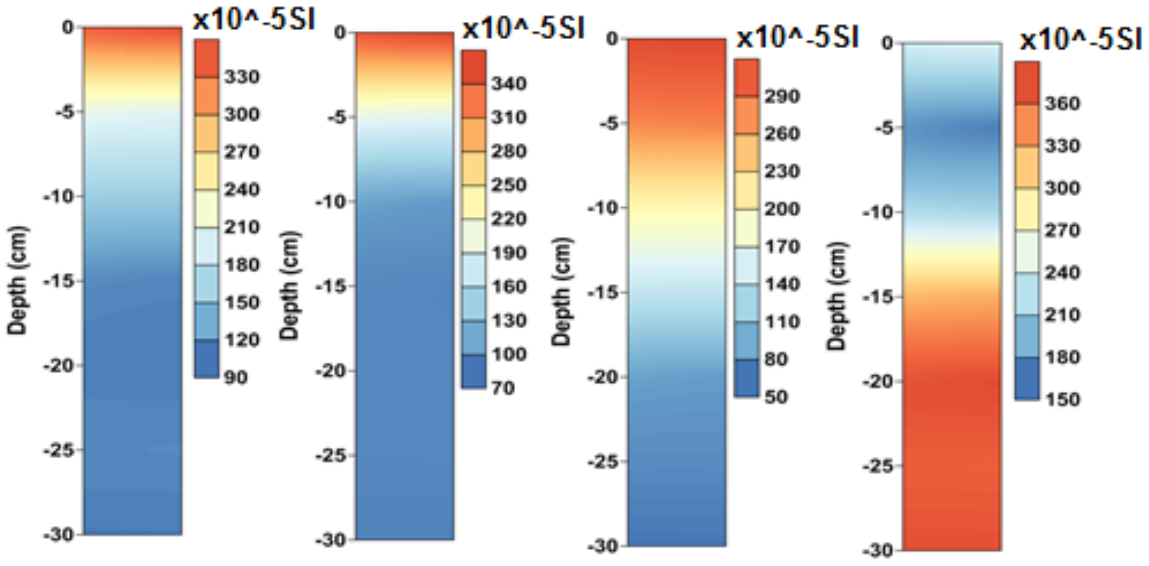


(a) (b) (c) (d)

Figure 4.17: Vertical magnetic susceptibility distribution with depth along selected roads in Central district

4.4.5 Vertical soil profiles along selected roads in Maitama area

In Figure 4.18, the magnetic susceptibility distribution obtained from the four profiles in Maitama district indicates that magnetic susceptibility decreases with depth, however, in Figure 4.18d, the opposite is the case, as it is observed that magnetic susceptibility increases with depth. This may be attributed to either the presence of metallic conductor or soil contamination along the profile.

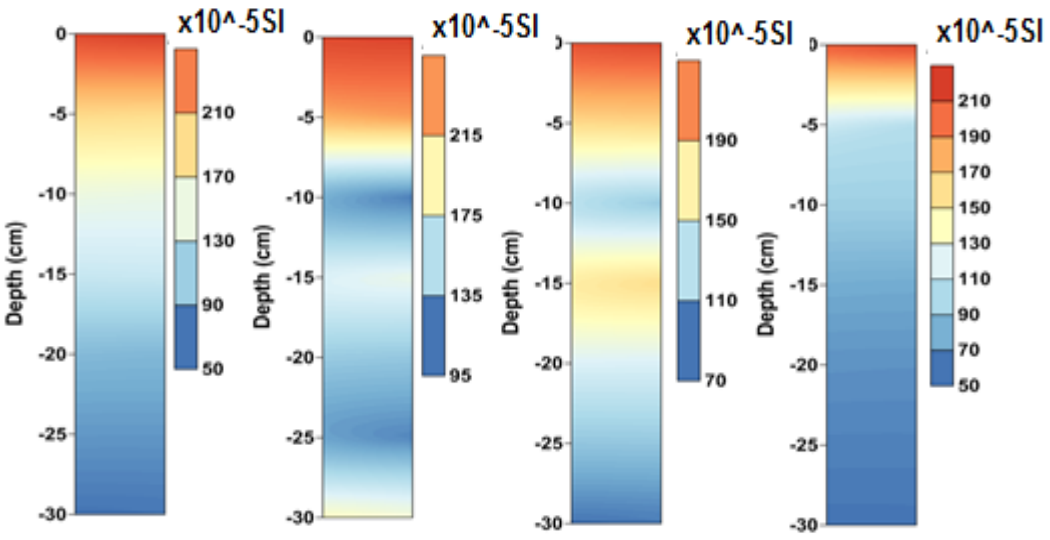


(a) (b) (c) (d)

Figure 4.18: Vertical magnetic susceptibility distribution with depth along selected roads inMaitama district

4.4.6 Vertical soil profiles selected road in Asokoro area

In Asokoro district, four vertical magnetic susceptibility soil profiles were obtained with maximum enhancement at the top soil (Figure 4.19).



(a) (b) (c) (d)

Figure 4.19: Vertical magnetic susceptibility distribution with depth along selected roads inAsokoro district

From the vertical distribution of magnetic susceptibility with depth in the all the profiles, it is clearly observed that the top soil has the highest magnetic susceptibility enhancement signal. This may be attributed to the deposition of anthropogenic metallic particulates matters on the soil.

4.5 2D SPATIAL DISTRIBUTIONS OF MAGNETIC SUSCEPTIBILITY VARIATION WITH DEPTH

Distributions of magnetic susceptibility in the soil profiles are often very similar to the distribution of heavy metals (Strzyszcz and Magiera1993; Strzyszcz and Magiera,1998; Hanesch and Scholger,2002; Spiteri *et al*.,2005). Commonly, the maximum magnetic susceptibility in the soil profile is observed at the same depth as the highest concentration of heavy metals. Additionally, using the distribution of magnetic susceptibility in the soil profile, it is possible to estimate the thickness of contaminated layer with the highest accumulation of anthropogenic magnetic particles and related heavy metals. Measurements of magnetic

susceptibility in soil profiles have been used effectively to distinguish between natural (lithogenic or pedogenic) and anthropogenic contributions to measured topsoil magnetic susceptibility values (Magiera *et al.*,2006). 2-D spatial distribution can be used to distinguish areas where the increased susceptibility value is a result of the influence of anthropogenic pollution from those areas where it is of lithogenic origin.

A total of 324 vertical profiles of 40.0cm depth were drilled across Abuja city. These vertical susceptibility data obtained was downloaded from the meter and a Matlab program (Appendix G) was written to indicate the measurement points and also remove points that are out of the boundary of Abuja phase one coordinates. In the end, we have a data set of 311 values of soil magnetic susceptibility within the study area (see Figure 3.3).

The magnetic susceptibility data collected in each of the soil profiles at 10.0cm intervals from the surface usually shows characteristic distribution in the soil profiles. This depth is directly connected with the thickness of the soil organic horizon. From each plot of the magnetic susceptibility in the soil profile, the maximum value was picked up and used in further analysis as a main variable using the Co-kriging Geostatistical method.

4.5.1 2-D Data Interpretation

From the 2-D surface contour map diagram (Figure 4.20), five major sections with enhanced magnetic susceptibility at the surface were delineated (blue circles). These sections are mostly areas with high vehicle and commercial activities. The magnetic susceptibility at the surface within these regions ranged from (400.0-600.0) x 10^{-5}SI. The top soil within these sections is considered highly magnetic according to Gautam*et al.* (2004). Figure 4.21 show the magnetic susceptibility distribution at a depth of 10.0cm. Highly magnetic soil with magnetic

susceptibility ranging from (400.0-600.0) $x10^{-5}$SI, are still observed though with reduced surface area when compared with Figure 4.20. At a depth of 20.0cm (Figure 4.22) only two main sections are delineated with high magnetic susceptibility values above 400.0 x 10^{-5}SI. These sections have less surface area compared to Figure 4.20 and 4.21 above. At 30.0cm Figure 4.23, an enhanced anomalous magnetic susceptibility which was not observed in the previous diagrams may be an indication of the presence of a highly magnetic material or near surface magnetic rock within the area. Figure 4.24shows that most of the sectionshave magnetic susceptibility values of less than 300.0x 10^{-5}SI with the exception of two places. These two place did not show enhanced magnetic susceptibility in the previous plots. Hence, it can be considered as a result of lithological enhancement or any other cause different from anthropogenic sources.

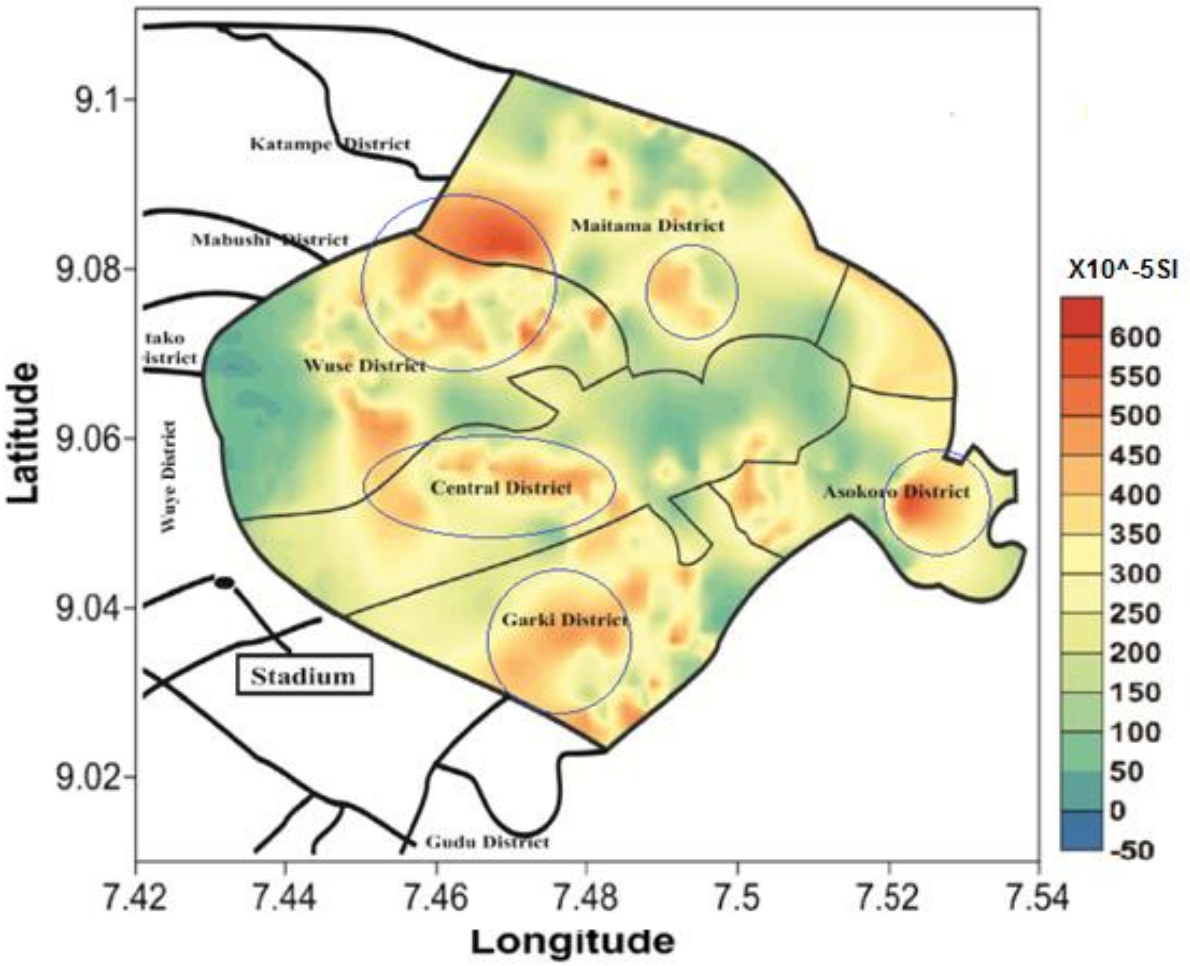


Figure 4.20: 2D contour map of Abuja showing magnetic susceptibility distribution at the surface.

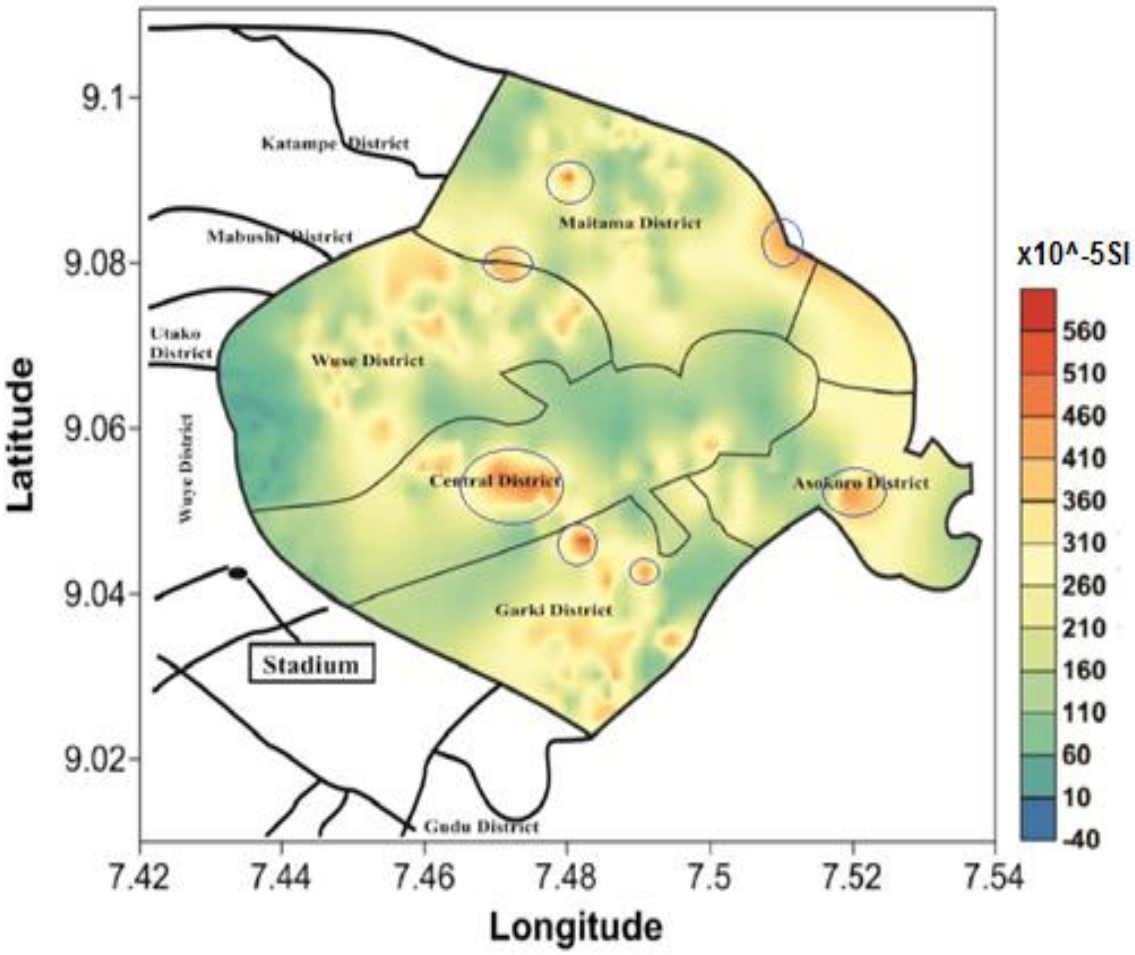


Figure 4.21: 2D contour map of Abuja showing magnetic susceptibility distribution at 10.0cm depth

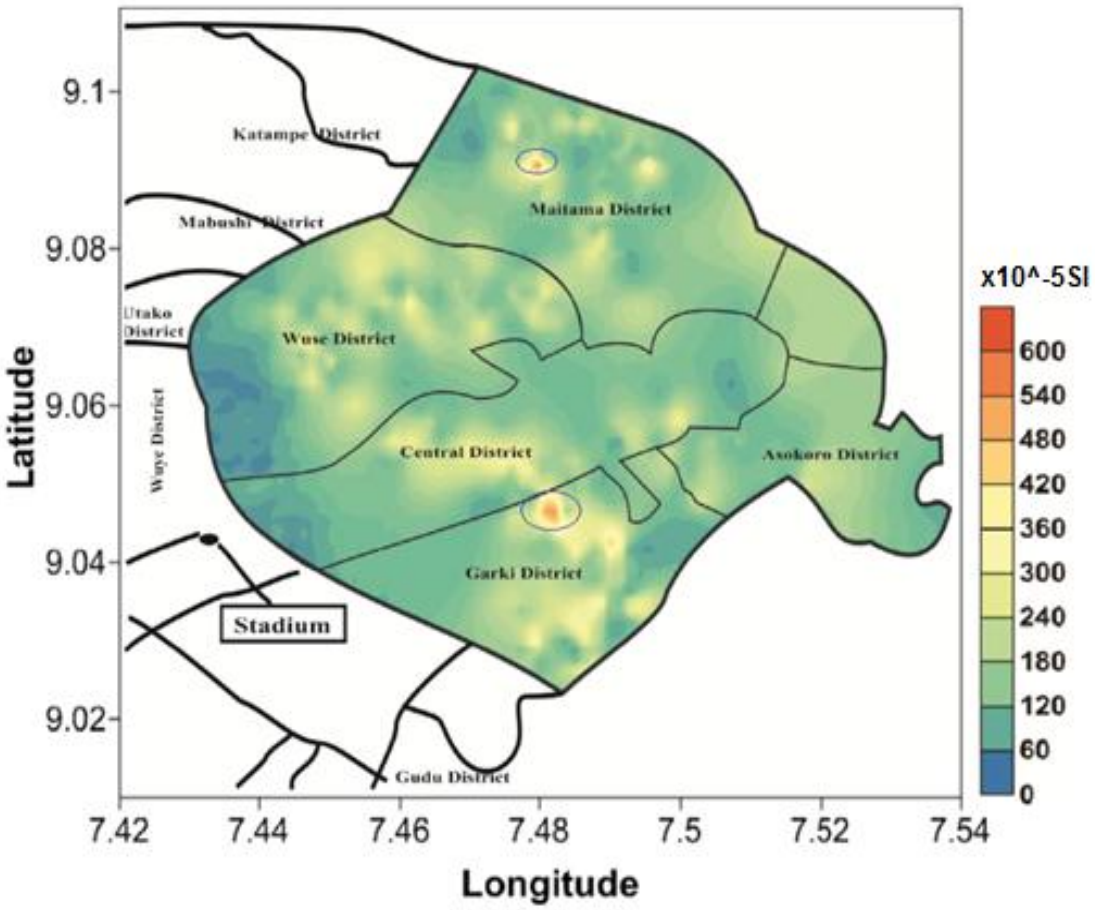


Figure 4.22: 2D contour map of Abuja showing magnetic susceptibility distribution at 20.0cm depth

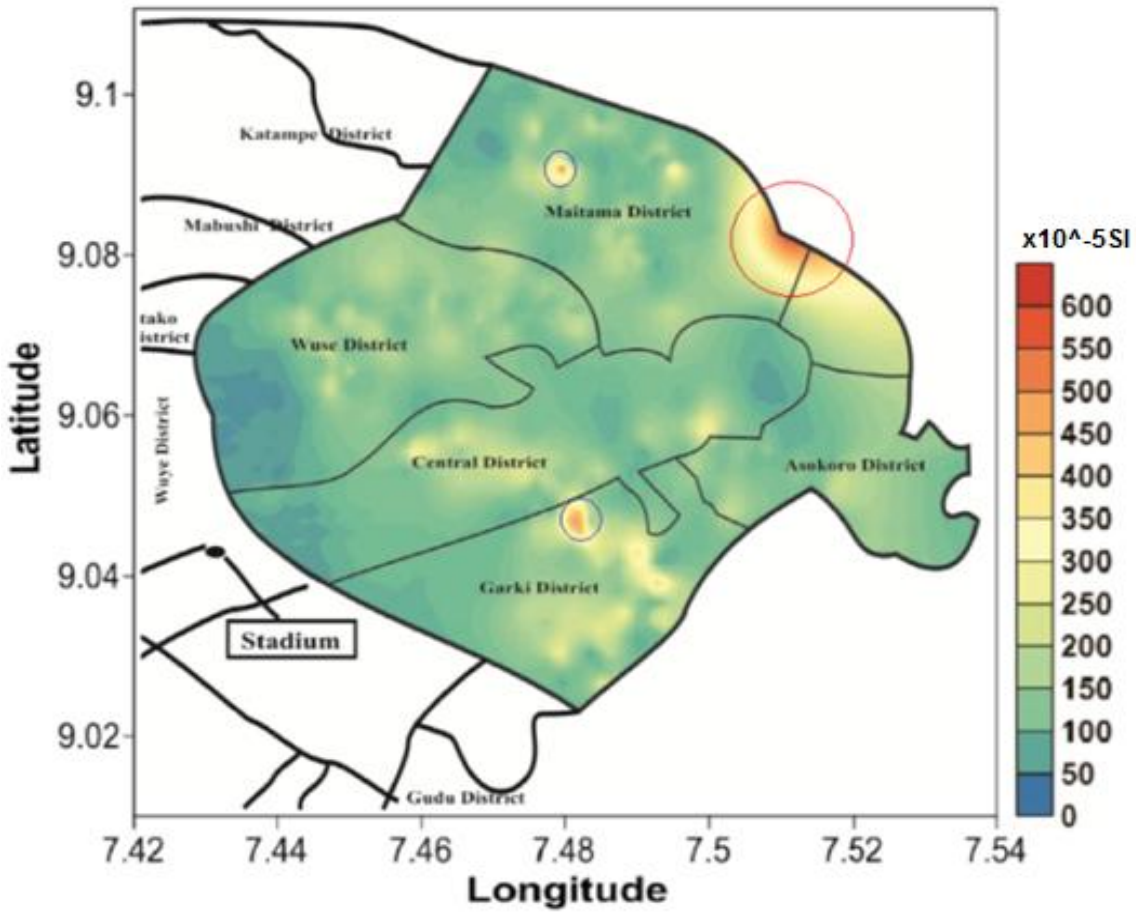


Figure 4.23: 2D contour map of Abuja showing magnetic susceptibility distribution at 30.0cm depth

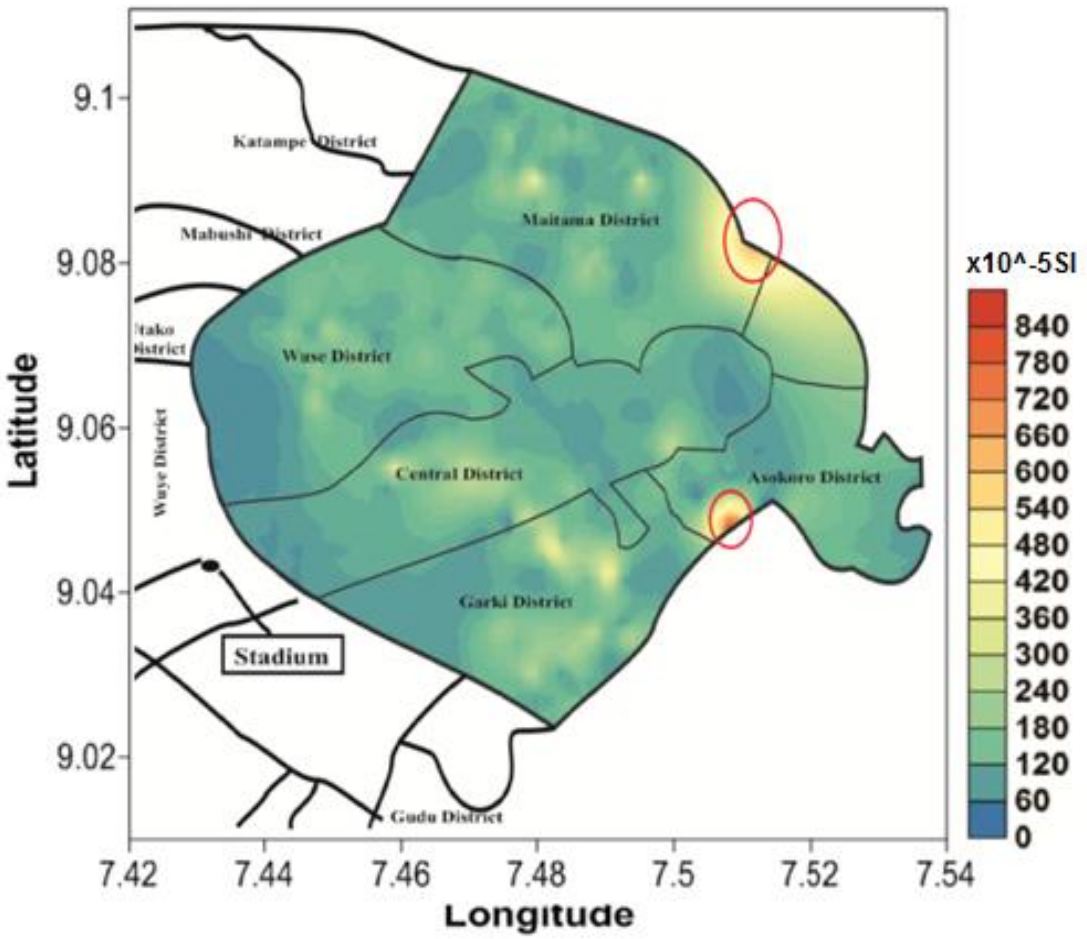


Figure 4.24: 2D contour map of Abuja showing magnetic susceptibility distribution at 40.0cm depth.

Moreover, the 2-D spatial distribution that is obtained shows the magnetic susceptibility of the top 20.0 cm of soil, which includes the soil horizons where most of the heavy metals are accumulated on the surface. The decreasing tendency towards the deeper horizons means that the magnetic particles were accumulated in the topsoil as a result of anthropogenic dust fall.

Previous studies showed that the magnetic susceptibility variations are caused by differences in geology (lithogenic/geogenic), soil forming processes (pedogenesis) and anthropogenic input of magnetic materials (Dearing *et al*., 1996 and Thompson and

Oldfield, 1986). Lithological enhanced magnetic susceptibility increased with depth while anthropogenic influenced magnetic susceptibility decreased with depth. We can therefore infer that the boundary between the two contributing factors is about 30.0cm in Abuja city.

4.5.2 Interpretation of Magnetic Susceptibility Profile Lines

The data used for the profiling was obtained from the digitization of 2-D maps of spatial distribution of magnetic susceptibility at different depths. The digitization method is based on interpolation using MagPix software. This method involves drawing 8 straight lines (A to H) running E-W direction and separated at an interval of 1.4km on each of the magnetic susceptibility distribution spatial maps (Figure 4.25). The maps are then imported into the MagPix software where the digitization was done at an interval of 50.0m on each line. The data from the process is then used to plot contour maps of each profile line using Surfer 11.

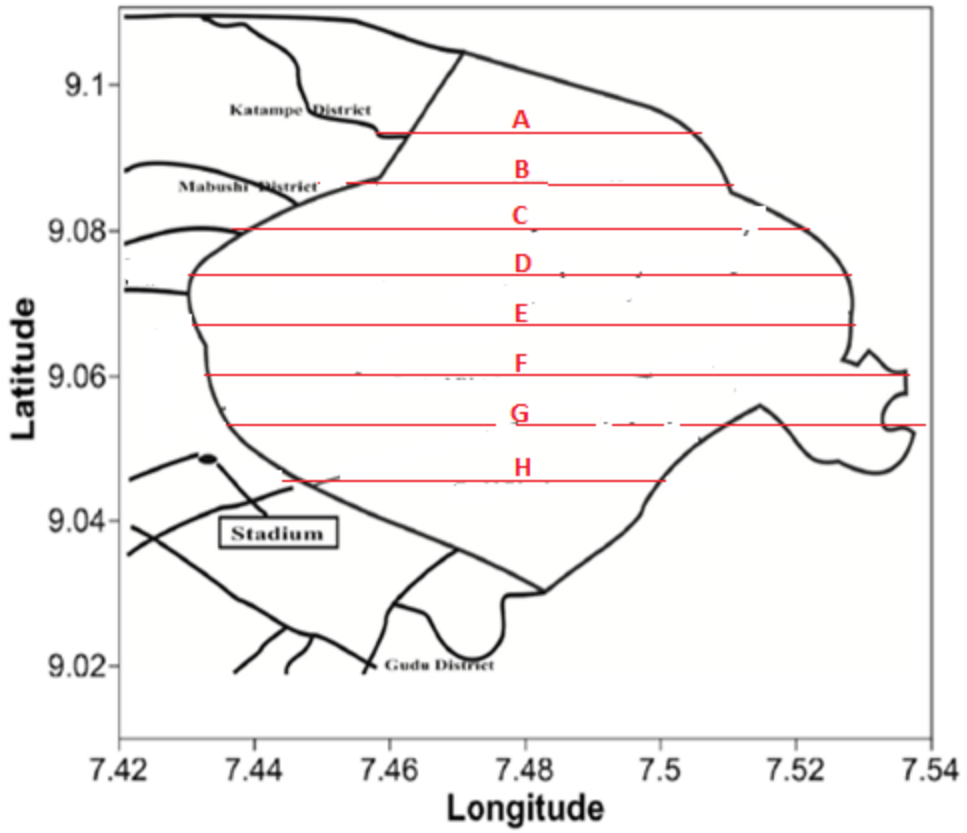
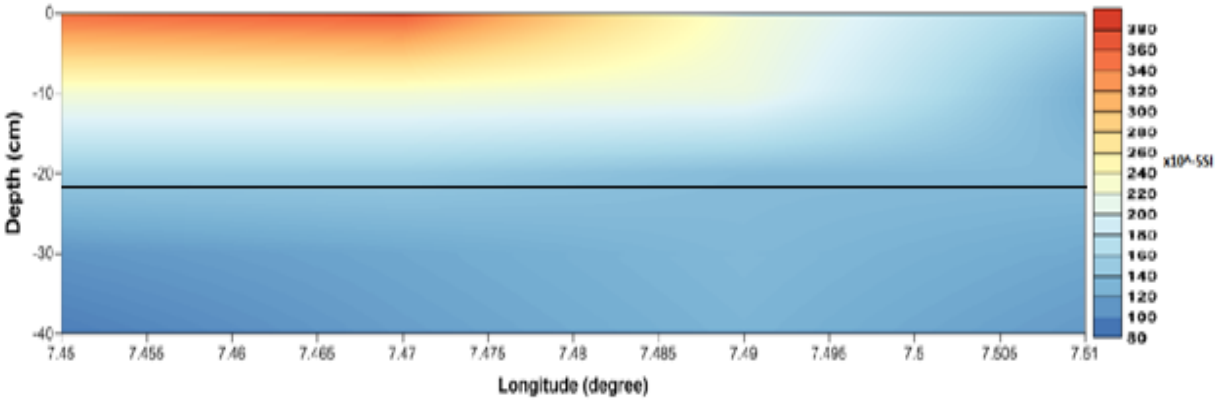


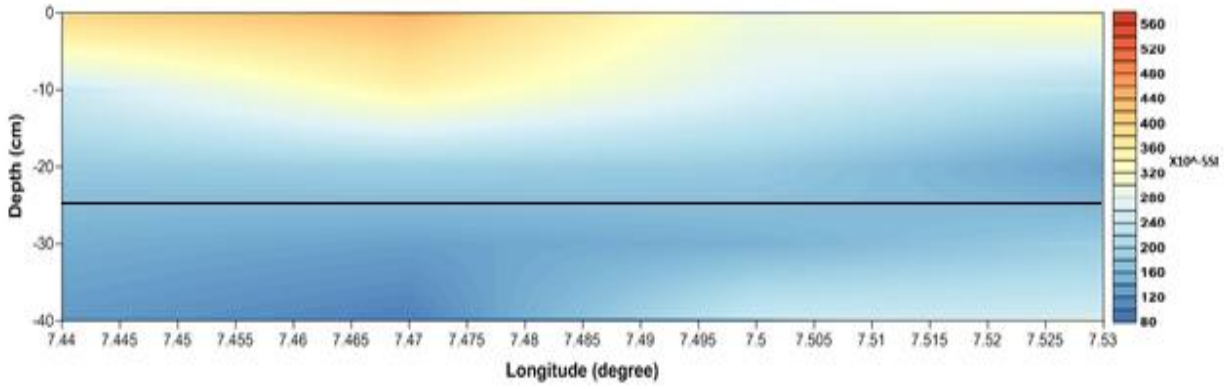
Figure 4.25: Magnetic Susceptibility Profile Lines taken on the map of Abuja

From the profiles (Figure 4.26), it is observed that the maximum thickness of soil affected by magnetogenic particles is about 20.0-30.0cm with magnetic susceptibility values ranging from 150.0 x 10^{-5}SI to 600.0 x10^{-5}SI.

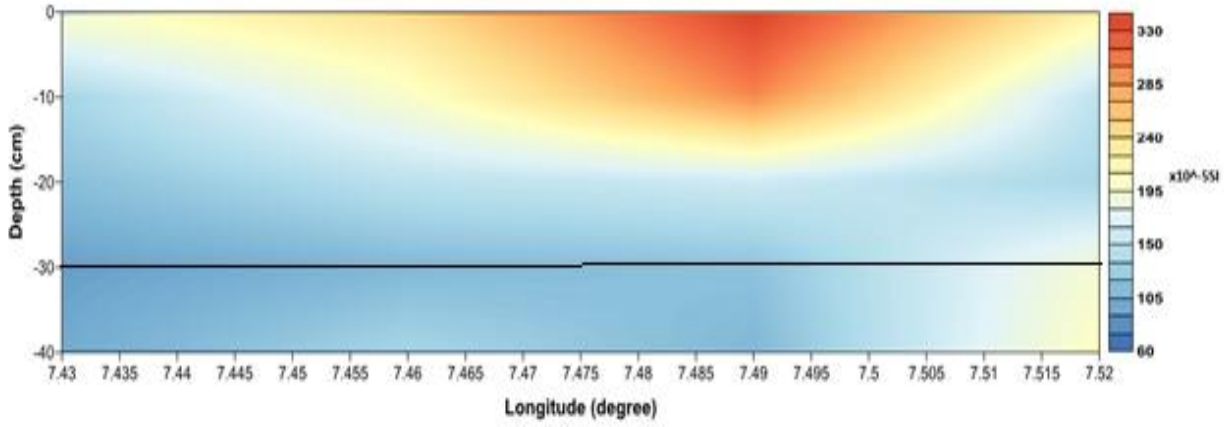
Figure 4.26f and 4.26g, shows intrusion of high magnetic susceptibility at a depth of about 40.0cm around longitudes 7.49-7.51. This may be the signature of an abnormalous body within that section of the study area.



(a)

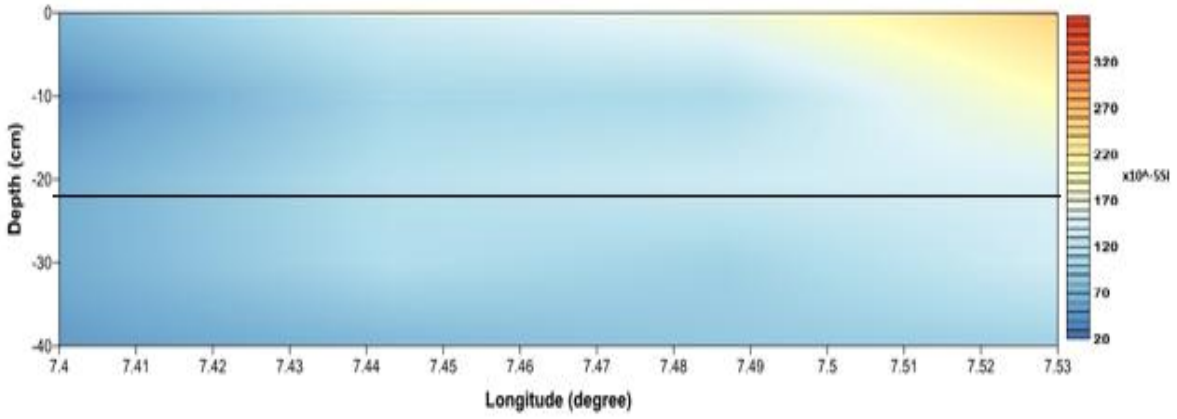


(b)

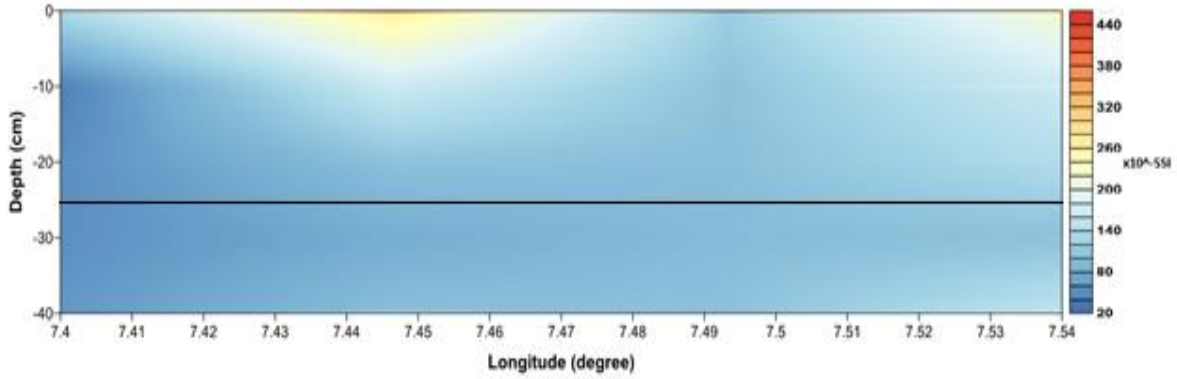


(c)

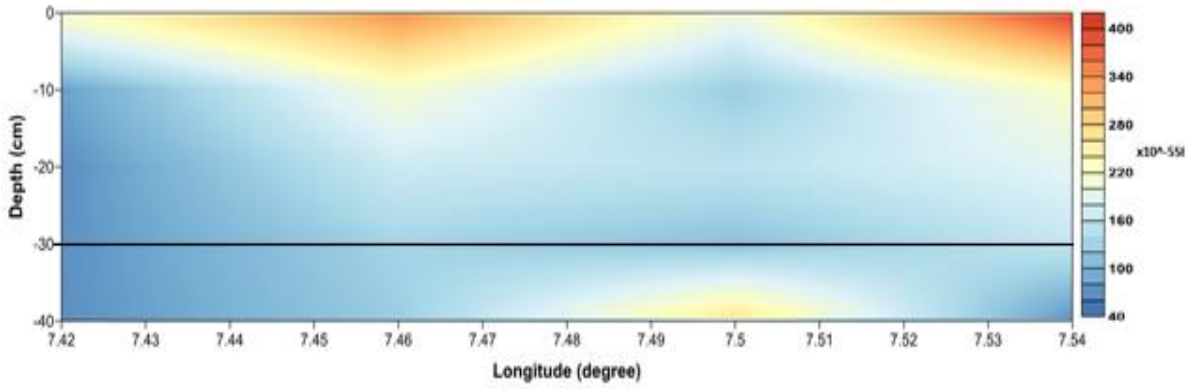
Figure 4.26: Magnetic Susceptibility Profile lines with depth in Abuja, Phase 1 (black line indicates the anthropogenic boundary)



(d)

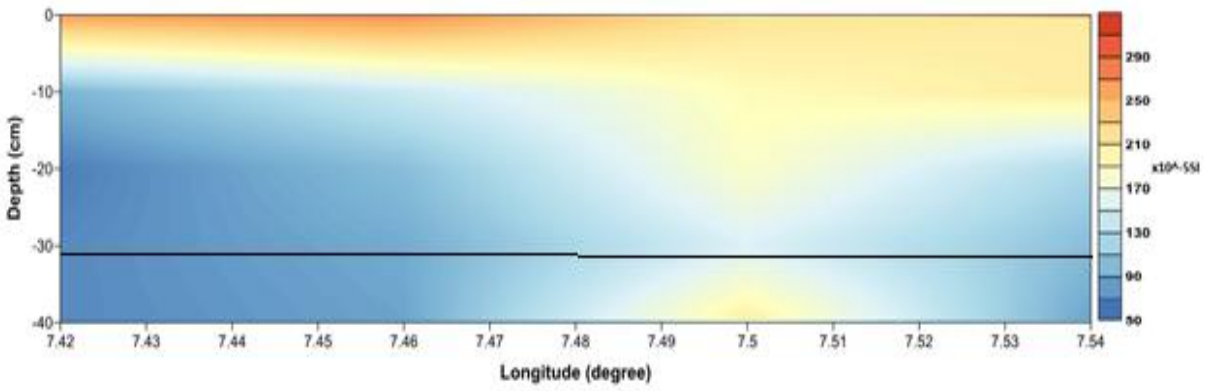


(e)

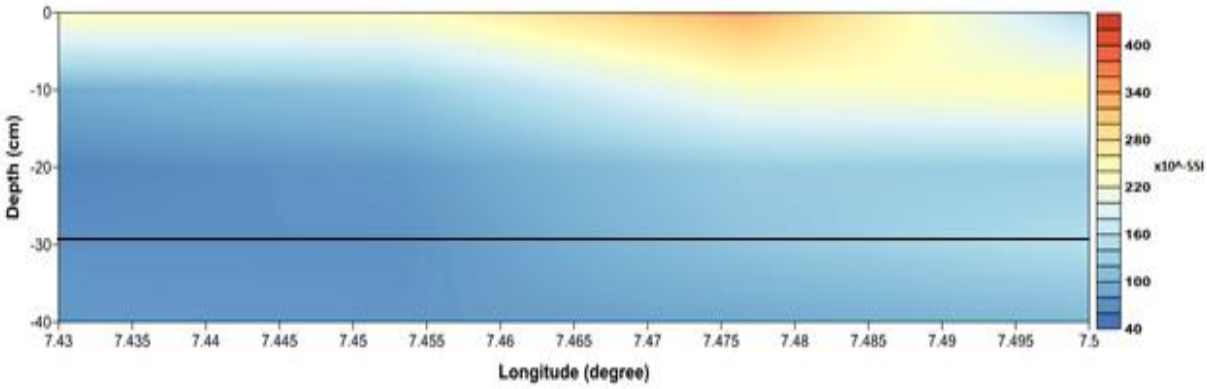


(f)

Figure 4.26: Magnetic Susceptibility Profile lines with depth in Abuja, Phase 1 (cont.) (black line indicates the anthropogenic boundary)



(g)



(h)

Figure 4.26: Magnetic Susceptibility Profile lines with depth in Abuja, Phase 1 (cont.) (black line indicates the anthropogenic boundaries)

4.6 FREQUENCY DEPENDENT MAGNETIC SUSCEPTIBILITY

Soil formed from lithological and weathering processes of parent rocks generally exhibit paramagnetic properties due to some minerals contained in the rocks and thus have significant value of magnetic susceptibility. This susceptibility arising from the influence of the parent rocks tend to mask anthropogenic grain pollutants released into the environment by human activities. Hence, it becomes difficult to identify the effect of the lithological and anthropogenic magnetic susceptibility in complex soil found in urban

areas. The superparamagnetic effect of lithological soil, a single state domain and multi-domain state of anthropogenic grains can easily be investigated by frequency dependent measurements where readings between 0 to2.0% indicates the absence of lithological influence, 2.0 to8.0% indicates multi-domain grains or mixture of both single stage and mulidomain grains and 8.0 to12% indicates the superparamagntic(SP) grain from lithological origin (Dearing, 1999; Michal, 2012).

This parameter is obtained from magnetic susceptibility measurements performed at two different frequencies: low (χ_{lf}) and high (χ_{hf}). Measurements made at these two frequencies are generally used to detect the presence of ultrafine (<0.03 μm) superparamagnetic (SP) minerals in samples. Samples where SP minerals are present will show slightly lower values when measured at high frequency; samples without superparamagnetic minerals will show identical magnetic susceptibility, χ, at both frequencies (Dearing, 1999). Frequency dependent susceptibility is mostly expressed as a percentage of the mass-specific frequency dependent susceptibility;

$$\chi_{fd}\% = \frac{\chi_{lf} - \chi_{hf}}{\chi_{hf}} X\ 100 \qquad 4.1$$

Table 4.4 shows values of χ_{fd}% indicating the presence of SP particles in the sample.

It has recently been suggested (Li *et al*., 2015) that all crystals smaller than ≈0.03μm show reduced susceptibility values at the high frequency measurement but there still remains an ongoing debate about the precise physical basis for frequency dependence.

Table 4.4: Interpretation of χ_{fd}% values (according to Dearing, 1999 and Michal, 2012)

Low χ_{fd}%	< 2.0	Virtually no SP grains
Medium χ_{fd}%	2.0-8.0	Mixture of SP and coarser grains, or SP grains <0.05μm
High χ_{fd}%	8.0-14.0	Virtually all SP grains
Very High χ_{fd}%	>14.0	Erroneous measurement, anisotropy, weak sample or contamination

4.6.1 Spatial Frequency Dependent Magnetic Susceptibility distribution in Abuja with depth

The frequency dependent magnetic susceptibility at the surface soil of Abuja is shown in Figure 4.32. From the Figure, it is observed that the frequency dependence varies between 0-14 percent. This large variation indicates the heterogenic composition of the top soil in Abuja.

From the field measurements it is observed that the frequency-dependence of magnetic susceptibility (χ_{fd}%) values are very low (0-5.0%) in most of the areas. Low frequency-dependence susceptibility values indicate that the magnetic propertices are predominantly contributed by the coarse multidomian (MD) and stable single domain (SSD) grains rather than super paramagnetic grains (Adyin and Akyol, 2015). Hence, this indicates the anthropogenic nature of the magnetic particles, which are derived from the phenomena associated with the movement of vehicles, industrial and precipitation of the particles floating in the air (Sylwia, 2014). From the surface map, low frequency-susceptibility is mostly observed in Wuse, Garki and Part of Central districts, these districts have high commercial activities and vehicle movement. In Asokoro district, the frequency-dependence susceptibility is mostly above 6%, this is due to the contribution of the super

paramagnetic grains from the parent rocks. Another likely cause of high frequency-dependence is the fact that the area is rocky and on higher altitude than any portion of Abuja. Other portions that show high frequency-dependence susceptibility are mostly around the boundaries of Abuja Phase 1, these areas are mostly reserved or undeveloped sections and thus commercial activity is less. Therefore the contributing factor is generally super paramagnetic of the pedogenic origin.

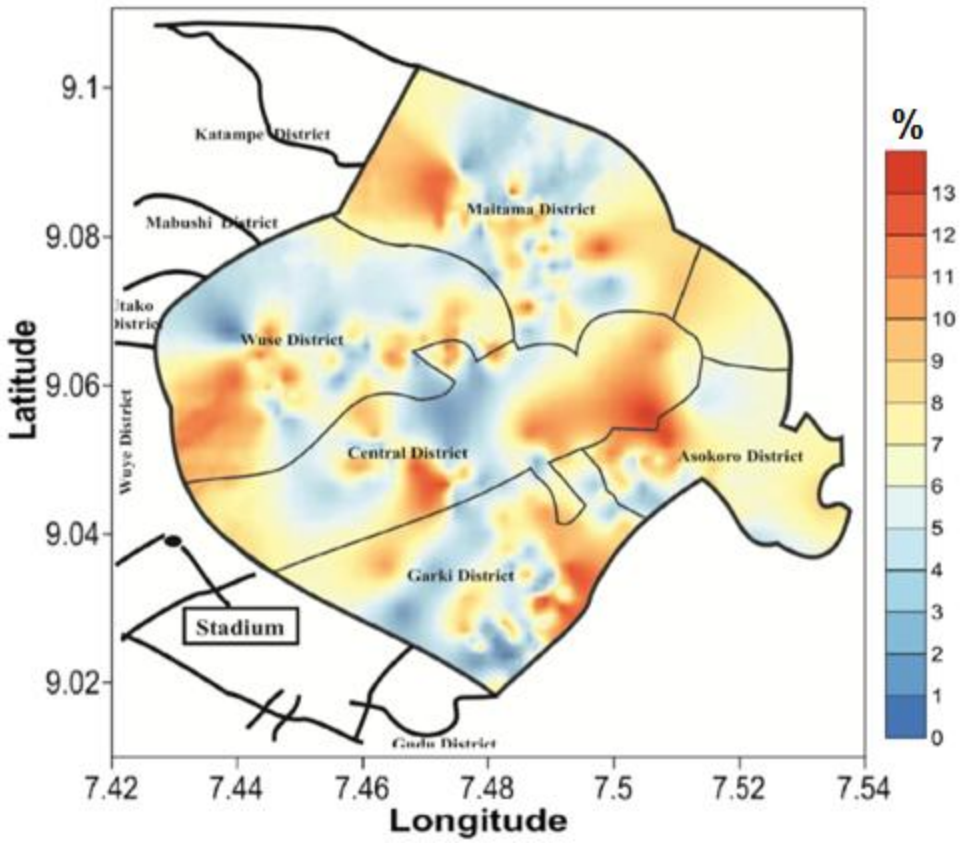


Figure 4.32: Distribution of frequency-dependence magnetic susceptibility values for the surface soil of Abuja

At a depth of 30.0cm (Figure 4.33), the subsurface map clearly show frequency-dependence susceptibility greater than 6% in almost all the area with exception of few portions. This indicates that, super paramagnetic grains are the main contributors to the

magnetic susceptibility at that depth. These super paramagnetic grains are mostly from pedogenic origin rather than anthropogenic source. From this, we can infer that magnetic grains do not penetrate through the soil except in some cases where over time they keep depositing and thus may form a record guide to understanding the activities of the place from ancient periods. However, this may only happen if there is no transportation means like running water or wind to move them from the surface as soon as they are released.

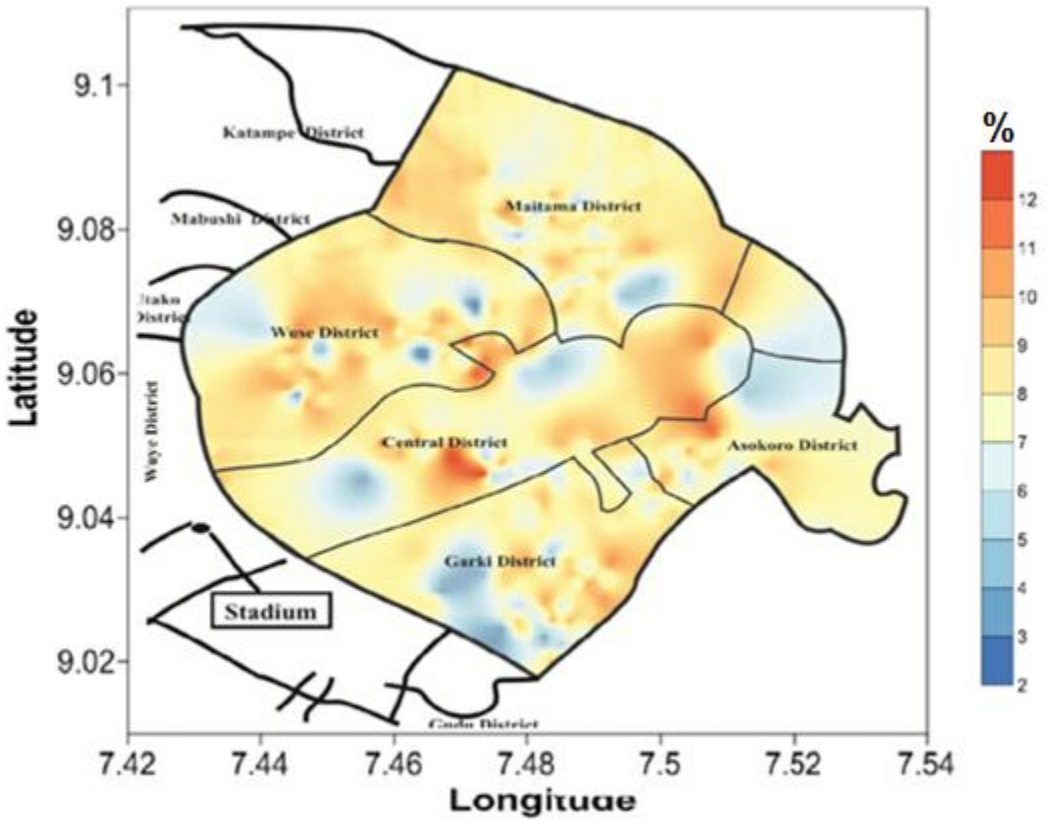


Figure 4.33: Distribution of frequency-dependence magnetic susceptibility values at the depth of 30.0cm

A plot of χ_{fd}% versus χ_{lf} may help to discriminate between grain-size and domain state, and may give a first order classification of magnetic properties and even sources (Table 4.5).

Table 4.5: Origins of magnetite/maghemite and greigite with domain size (Dearing, 1999 and modified by the author)

	MD	PSD	SSD	SP
Primary				
Magnetite/titanomagnetite	X	X	(X)	(X)
Secondary				
Fuel Combustion	X	X	(X)	(X)
Pedogenesis		(X)	X	X
Bacterial Magnetosomes		(X)	X	(X)
Burning			(X)	X

MD-multidomain, **PSD**-pseudo-single domain, **SSD**-stable single domain, **SP**- superparamagnetic, x - expected (x) - some evidence, but not normally expected

Figure 4.34-4.38 show the patterns of values plotted on a bivariate χ_{lf}-χ_{fd}% scattergram of different measurements from selected roadside in Central Area, Garki, Wuse, Maitama and Asokoro area in Abuja. Measurements dominated by relatively coarse-grained non-SP ferrimagnets from igneous rocks or combustion products show relatively high χ_{lf} but virtually zero χ_{fd}. Values of χ_{fd}% < 5% are typical where non-SP grains dominate the assemblage or where extremely fine grains (<0.005 μm) dominate the SP fraction. At present, it is prudent to interpret frequency dependence data semi-quantitatively as shown in Table 4.5.

Values of χ_{fd} % will be depressed by the presence of frequency-independent grains or grains with weak frequency-dependence and will be exaggerated by the presence of a significant diamagnetic component. Values of χ_{fd} % greater than 12 to 14 % are rare.

In this research, and in nature, it is unlikely that grains exist either independently of each other or in narrow size ranges of discrete grains. They will probably adhere to form clusters. It is probable, for instance, that low frequency-dependent values in relatively large crystals are caused by small numbers of SP crystals attached to their surfaces.

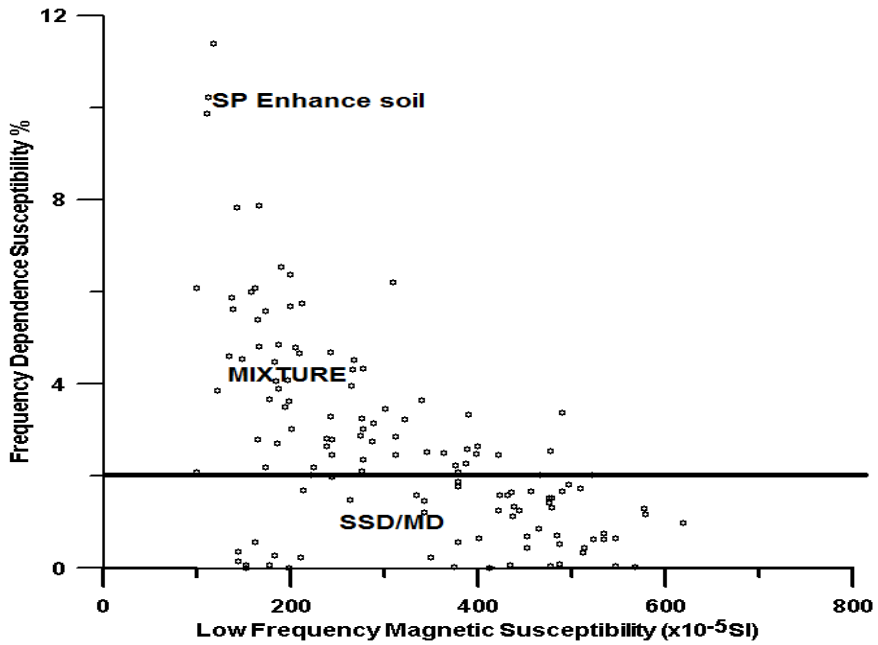


Figure 4.34:A χ_{lf} -χ_{fd} % scattergram showing typical positions of samples dominated by various domains and sources at a road in Central district, Abuja

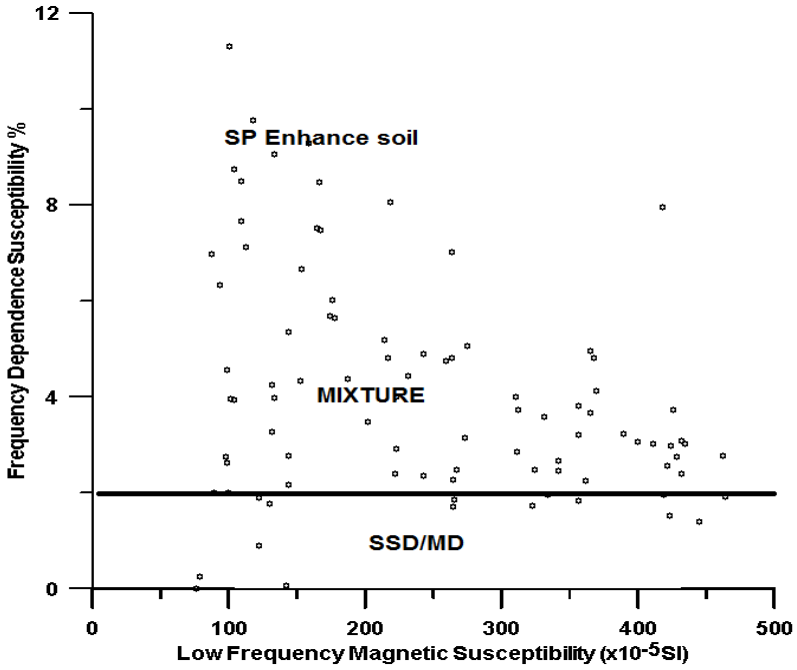


Figure 4.35:A χ_{lf} -χ_{fd} % scattergram showing typical positions of samples dominated byvarious domains and sources at a road in Garki area, Abuja

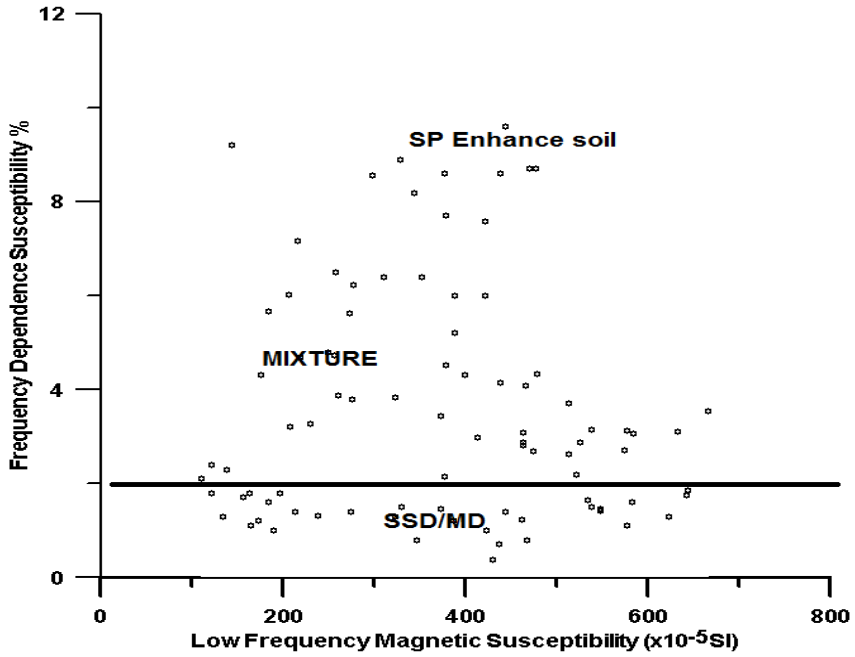


Figure 4.36:A χ_{lf} -χ_{fd} % scattergram showing typical positions of samples dominated by various domains and sources at a road in Wuse area, Abuja

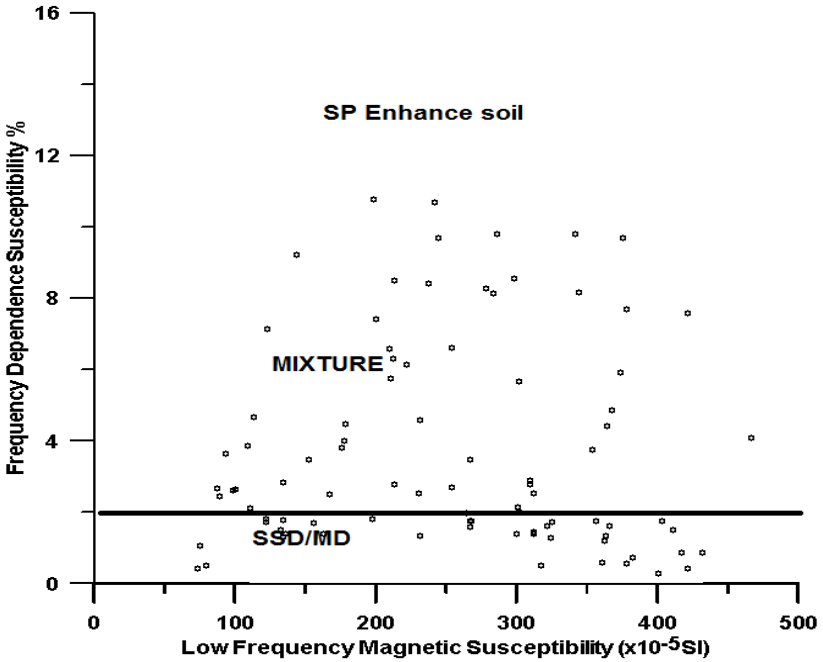


Figure 4.37:A χ_{lf} -χ_{fd} % scattergram showing typical positions of samples dominated byvarious domains and sources at a road in Maitama, Abuja

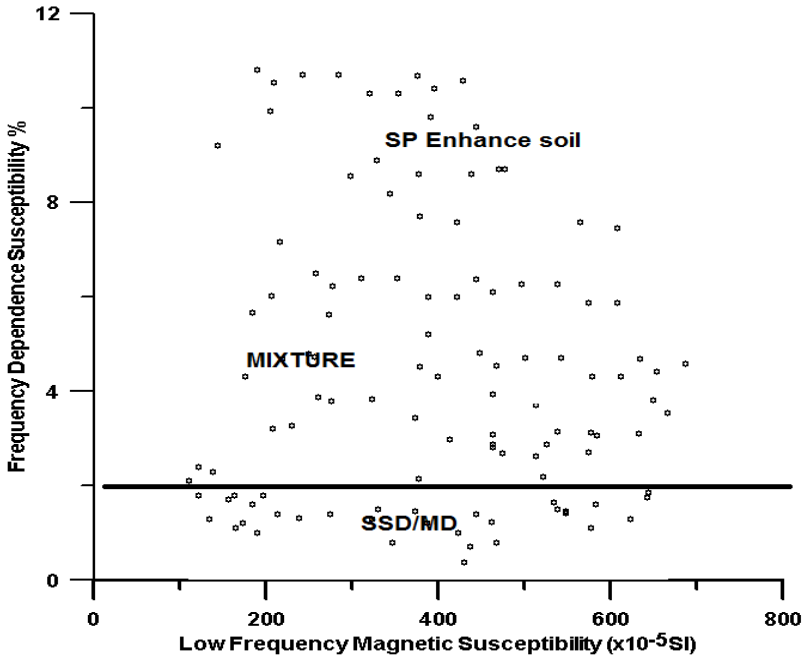


Figure 4.38:A χ_{lf} -χ_{fd} % scattergram showing typical positions of samples dominated byvarious domains and sources at a road in Asokoro, Abuja

4.7 TEMPERATURE DEPENDENCE OF MAGNETIC SUSCEPTIBILITY

The presence of minerals and domains is detected from the shapes of the temperature susceptibility curves and distinctive transition points. The lack of irreversible change and the presence of several diagnostic transitions mean that low temperature curves are easier to interpret than high temperature curves. At present, interpretations are usually qualitative and there still remain ambiguous curve shapes, especially where the sample contains a mixture of minerals. It is important to bear in mind the different magnitudes of χ_{lf} for the main minerals and the consequent likelihood that ferrimagnetic minerals may completely dominate the temperature curves even where other minerals are present in significant amounts. To some extent the curve shapes are additive, such that a mixture of SSD magnetite and paramagnetic minerals will produce an intermediate curve and major transitions are often found superimposed upon curves. But great care should be exercised

Table 4.6 was used in the interpretation of the temperature dependence magnetic susceptibility curve.

Table 4.6:Curie and Néel temperatures of iron and common Fe-bearing minerals (Dearing, 1999)

Curie Temperature (T_c) (Ferro-para)	
Iron	770°C
Magnetite	580°C
Maghemite	600°C
Titanomagnetites	580°C (magnetite) to -153°C (ilvospine)
Pyrrhotite	320°C
Greigite	330°C

4.7.1 Low temperature dependence of magnetic susceptibility

Measurement of low temperature dependenceallows the identification of magnetic minerals such as magnetite and hematite. The presence of magnetite is indicated by T_V, which occurs at about -150 °C and marks a change in the crystallographic distribution of the iron cations such that the previously cubic framework is slightly distorted to monoclinic symmetry (Evans and Heller, 2003). However, $T_V$indicates only the contribution of stoichiometric magnetite. The presence of non-stoichiometric (substituted) magnetite such as titanomagnetite cannot be recorded by low temperature dependence curves. At $T_M$of -15° C, hematite undergoes changes in magnetic properties, where it loses spin canting, and hence weak ferromagnetism (Evans and Heller, 2003).

Table 4.7 summaries the magnetic susceptibility characteristics of the different samples at low temperature in this work.

Table 4.7: Low Magnetic susceptibility characteristics of samples collected in the work at low temperature

Sample	Source	Low Magnetic Susceptibility ($x10^{-5}$SI)	Low Temperature Characteristics
S1	Soil collected from Central Area	565.4	The presence of stoichiometric magnetite (Özdemir and Dunlop, 1998). Magnetite is indicated by T_V, which occurs at about -150 °C (Figure 4.40a). It marks a change in the crystallographic distribution of the iron cations such that the previously cubic framework is slightly distorted to monoclinic symmetry (Evans and Heller, 2003).
S2	Roadside dust collected from the road pavement in Central District	613.6	Presence of magnetite is indicated by T_v, which occurs at about -150°C (Figure 4.40b). The observed rapid on the curve indicates instability in the measurement; this may be due to the presence of impurities in the sample. The change in slope at approximately -50°C may indicate the presence of Vivainite (Minyuk et al., 2012).
S3	Roadside dust, collected from the road pavement in Garki District	566.7	Magnetite presence is observed in the curve at about -150°C (Figure 4.40c). It marks a change in the crystallographic distribution of the iron cations such that the previously cubic framework is slightly distorted to monoclinic symmetry (Evans and Heller, 2003).
S4	Soil collected from Garki District	541.6	Instability is observed in the curve; however, magnetite presence is indicated slightly at about -150°C. it is evidence that the sample may have been contaminated or mix with so many minerals (Figure 4.40d)
S5	Roadside dust collected from Wuse District	588.6	The dominant mineral obtained in the sample is magnetite (Figure 4.40e).
S6	Brake dust, collected from Wuse District	654.3	From this curve (Figure 4.40f), the change from -200°C to about -175°C may be an indication of siderite (Frederichs et al., 2003). The Tv temperature observed at -150°C shows that magnetite is presence in the sample. Other minerals like pyrrhotite may also be in the sample as indicated by sharp drops at -75°C and -25°C.
S7	Soil collected from Maitama	564.3	The dominate mineral in the sample is magnetite as indicated by the Tv temperature at -150°C (Figure 4.40g).
S8	Roadside dust collected from Maitama	655.4	The dominate mineral in the sample is magnetite as indicated by the Tv temperature at -150°C. The slightly drop in susceptibility on the curve indicated the presence of other minerals not quite observed at low temperature (Figure 4.40h)
S9	Roadside dust collected from Asokoro	663.2	Siderite and magnetite are the dominate minerals observed at low temperature in the sample (Figure 4.40i)
S10	Soil collected from Asokoro District	465.7	It is observed from this curve that mix minerals are present, however, magnetite dominated the sample (Fig 4.40j)

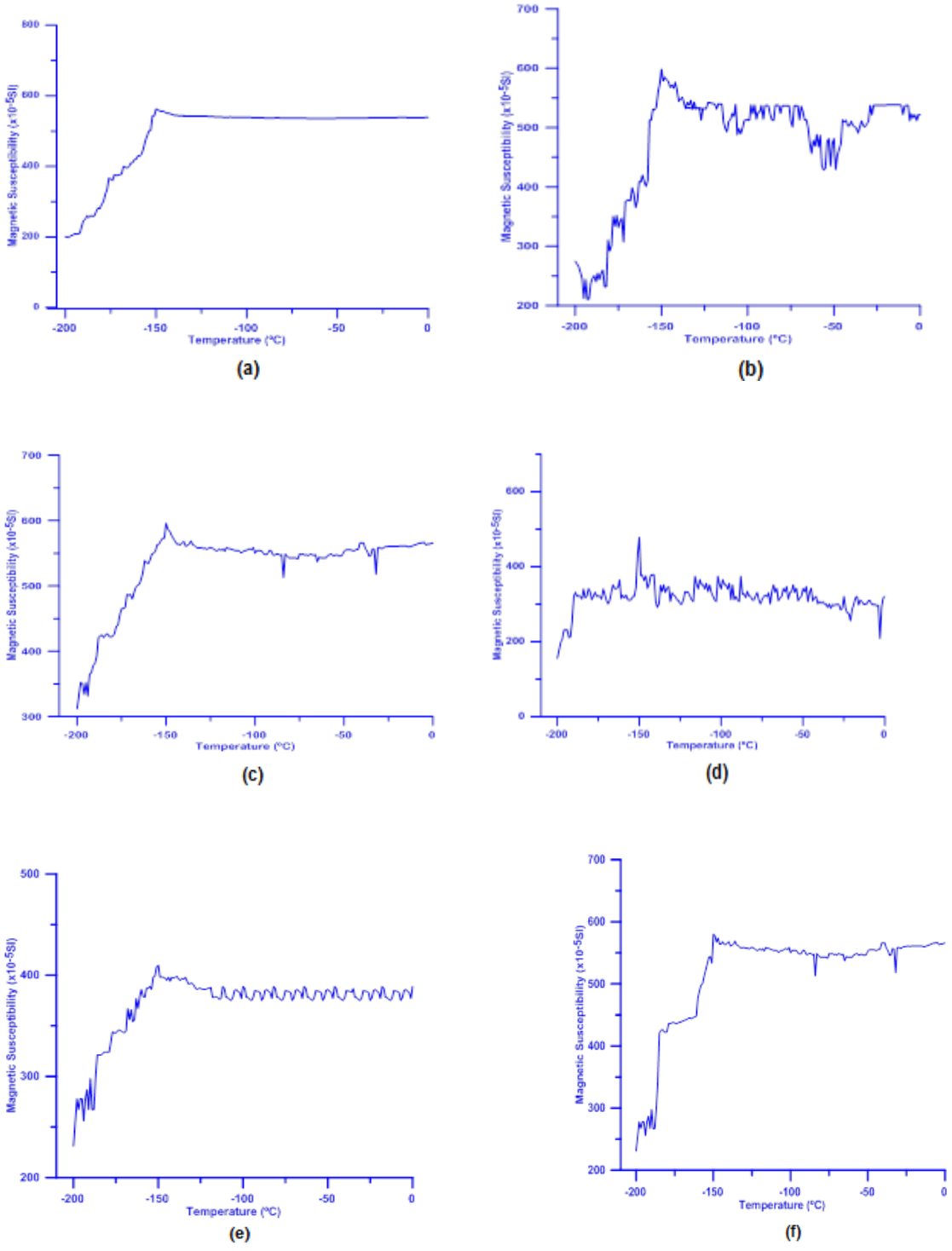


Figure 4.40: Variation of low magnetic susceptibility with low temperature from samples collected at different locations in various districts of Abuja Phase 1

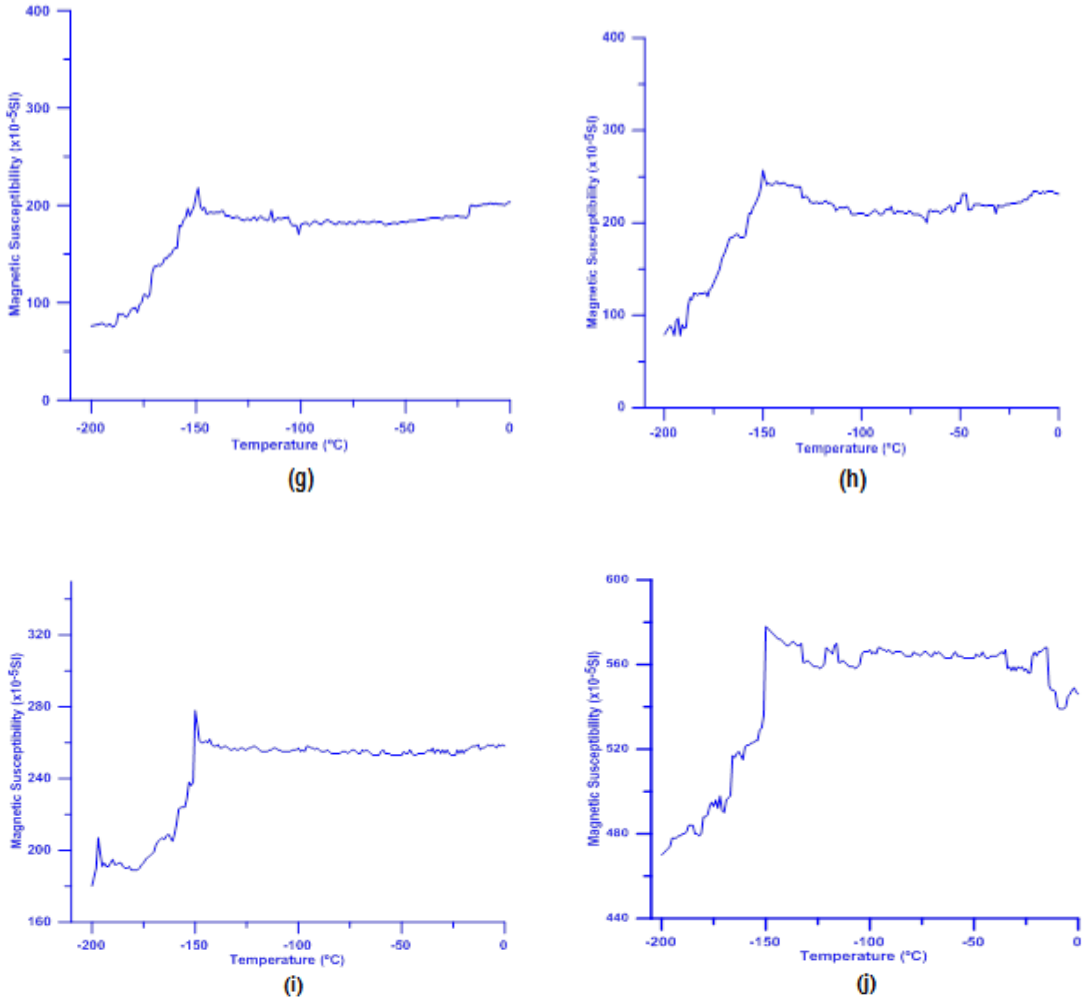


Figure 4.40: Variation of low magnetic susceptibility with low temperature from samples collected at different locations in various districts of Abuja Phase 1(cont.)

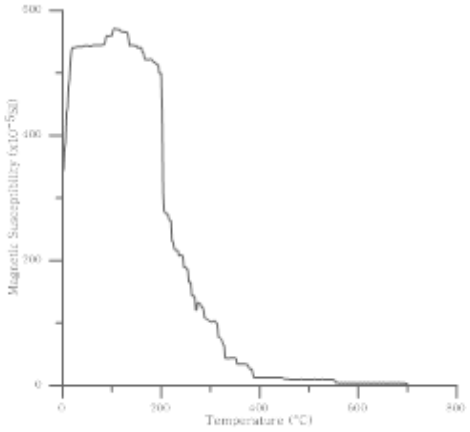
4.7.2 High temperature dependence of magnetic susceptibility

Table 4.8 summaries the magnetic susceptibility characteristics of the different samples at high temperature in this work.

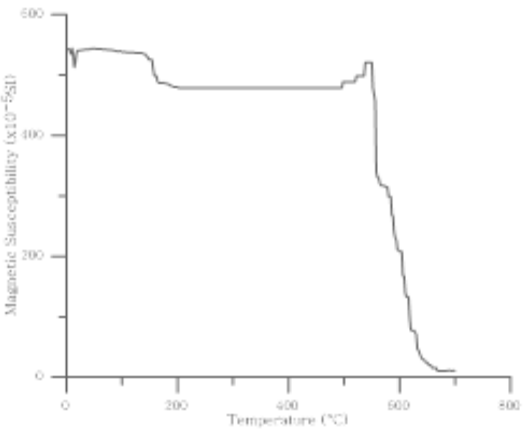
Table 4.8: Low Magnetic susceptibility characteristics of samples at high temperature

Sample	Source	Low Magnetic Susceptibility ($x10^{-5}$SI)	High Temperature Characteristics
S1	Soil collected from Central Area	565.4	The sudden drop in susceptibility at 400°C indicates that monoclinic pyrrhotite is the major contributor to the susceptibility. However, the susceptibility continue to drop with increase in temperature at about 600°C, on the heating curve, this suggest the presence of hematite (Ju et al., 2004) (Figure 4.41a).
S2	Roadside dust collected from the road pavement in Central District	613.6	In (Figure 4.41b), the clear susceptibility drop near 580°C indicates that magnetite is the major contributor to the susceptibility in the sample (Ju et al., 2004). Near 650°C, there is another susceptibility drop on the heating curve signaling the presence of hematite. The susceptibility have been flat from 0°C to about 400°C. This indicates the presence of a multidomain (MD)-like behavior (Ozdemir and Dunlop, 1998).
S3	Roadside dust, collected from the road pavement in Garki District	566.7	The cause of instability in the susceptibility variation with temperature in (Figure 4.41c) from 0°C to about 600°C is not clear. However, the susceptibility drop at about 620°C indicates the presence of magnetite in the sample, also the further drop above 620°C shows that hematite may be present in the sample.
S4	Soil collected from Garki District	541.6	In Figure 4.41d it is observed in the graph, creation of new minerals from magnetic phases due to heating at temperature of 240°C and above 400°C (Chadima, 2010). The clear susceptibility drop near 580°C indicates that magnetite is the major contributor to the susceptibility. The weakly rise in susceptibility from 0°C to about 400°C is an indication of a multidomain (MD)-like behavior (Ozdemir and Dunlop, 1998
S5	Roadside dust collected from Wuse District	588.6	The presence of ripples from 0°C to about 250°C is an indication of instability in susceptibility variation with temperature. However, at about 640°C, there is another sudden susceptibility drop signaling the presence of hematite in the sample (Figure 4.41e).
S6	Brake dust, collected from Wuse District	654.3	The heating curve of these samples is nearly flat from 0°C to about 400°C. The clear susceptibility drop near 580°C indicates that magnetite is the major contributor to the susceptibility. (Figure 4.40f) The weakly rise in susceptibility from 0°C to about 400°C is an indication of a multidomain (MD)-like behavior (Ozdemir and Dunlop, 1998)
S7	Soil collected from Maitama	564.3	The curve is almost independent of temperature from room temperature to about 250°C (Figure 4.41g); this indicates the presence of multidomain minerals. The sudden susceptibility drop at about 350°C is an indication of the Curie temperature of ferromagnetic pyrrhotite in the sample (Chadima, 2010).).
S8	Roadside dust collected from Maitama	655.4	There is an indication of the presence of amphibole in the sample due to the drop in susceptibility from room temperature to about 200°C. Susceptibility drop at 400°C is an indication of the presence of ferromagnetic pyrrhotite in the sample (Figure 4.41h).
S9	Roadside dust collected from Asokoro	663.2	(Figure 4.41i) the nearly flat susceptibility from room temperature to about 250°C is a clear indication of a multidomain like behavior (Chadima, 2010). The heating curve shows a rapid increase in susceptibility starting at 240°C with a marked peak at 270°C.

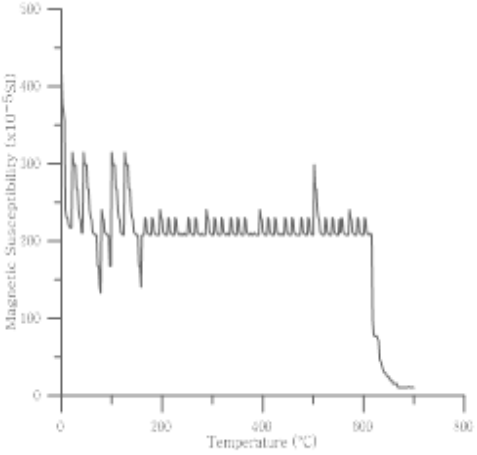
S10	Soil collected from Asokoro District	465.7	The dominate mineral in the sample is magnetite as indicated by the Tv temperature at -150°C. The slightly drop in susceptibility on the curve indicated the presence of other minerals not quite observed at low temperature (Fig 4.41j)


Magnetic Susceptibility (x10⁻⁵SI)
Temperature (°C)

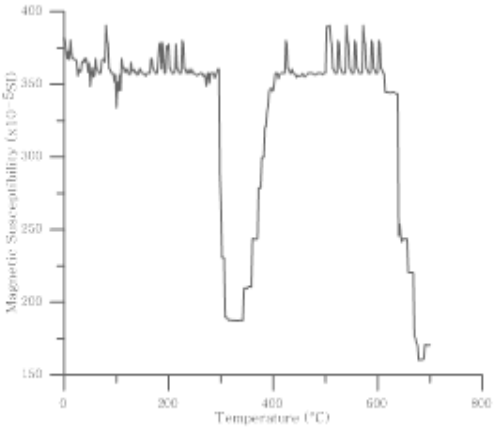
(a)


Magnetic Susceptibility (x10⁻⁵SI)
Temperature (°C)

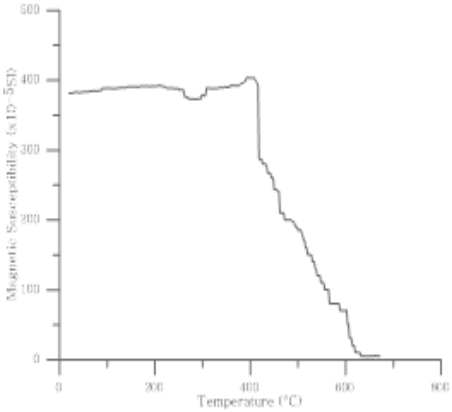
(b)


Magnetic Susceptibility (x10⁻⁵SI)
Temperature (°C)

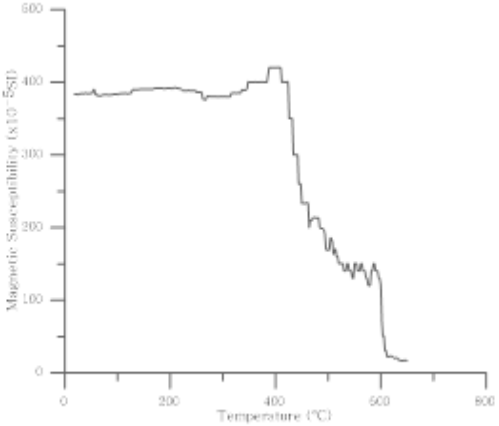
(c)


Magnetic Susceptibility (x10⁻⁵SI)
Temperature (°C)

(d)


Magnetic Susceptibility (x10⁻⁵SI)
Temperature (°C)

(e)


Magnetic Susceptibility (x10⁻⁵SI)
Temperature (°C)

(f)

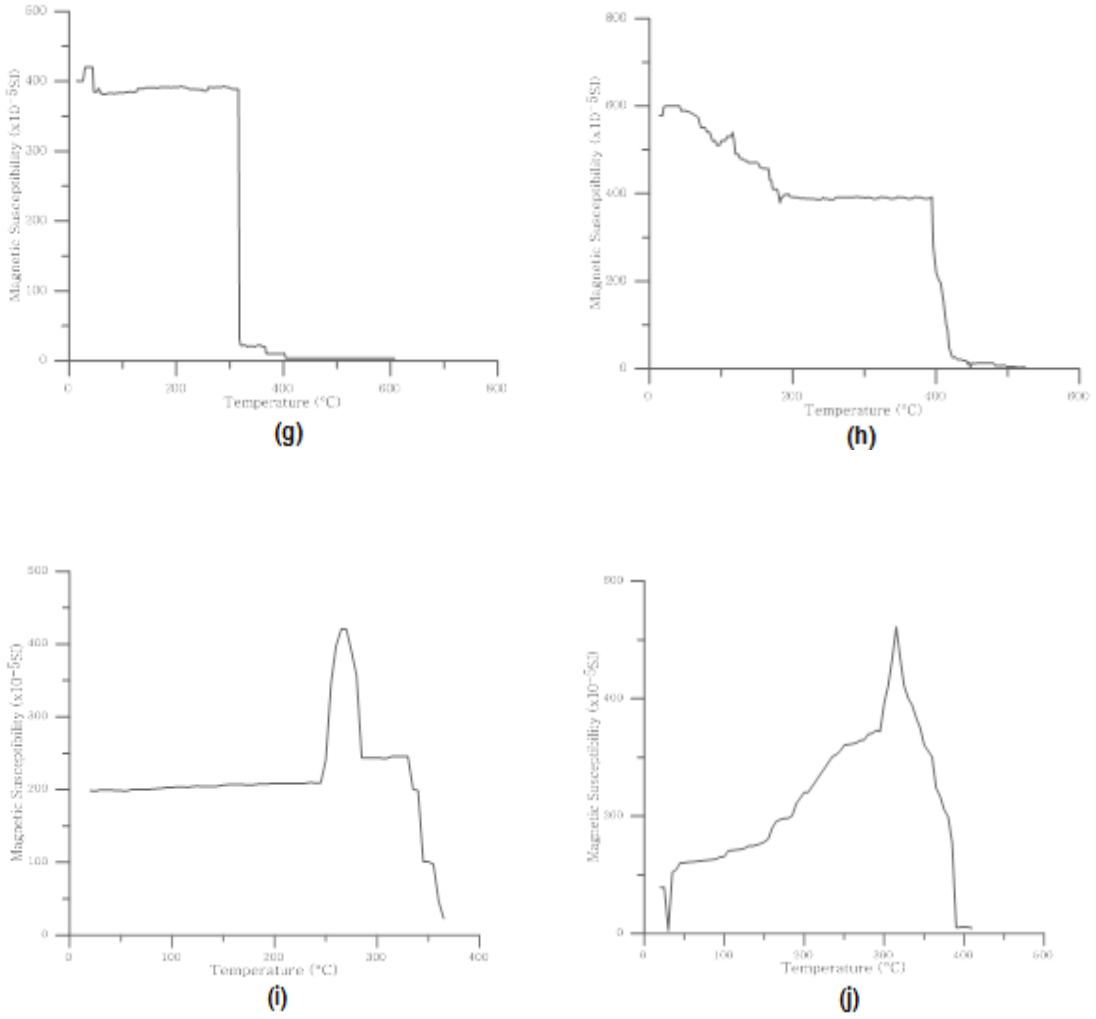


Figure 4.41: Variation of highmagnetic susceptibility with high temperature from samplescollected at different locations in various districts of Abuja Phase 1

CHAPTER FIVE

HEAVY METAL CONCENTRATION IN SOILS

5.1 INTRODUCTION

The actual concentrations of the selected heavy metals in the samples were measured in mg/l. These concentrations were used to plot a spatial contour map for each of the heavy metal at the surface and at a depth of 30.0cm respectively.

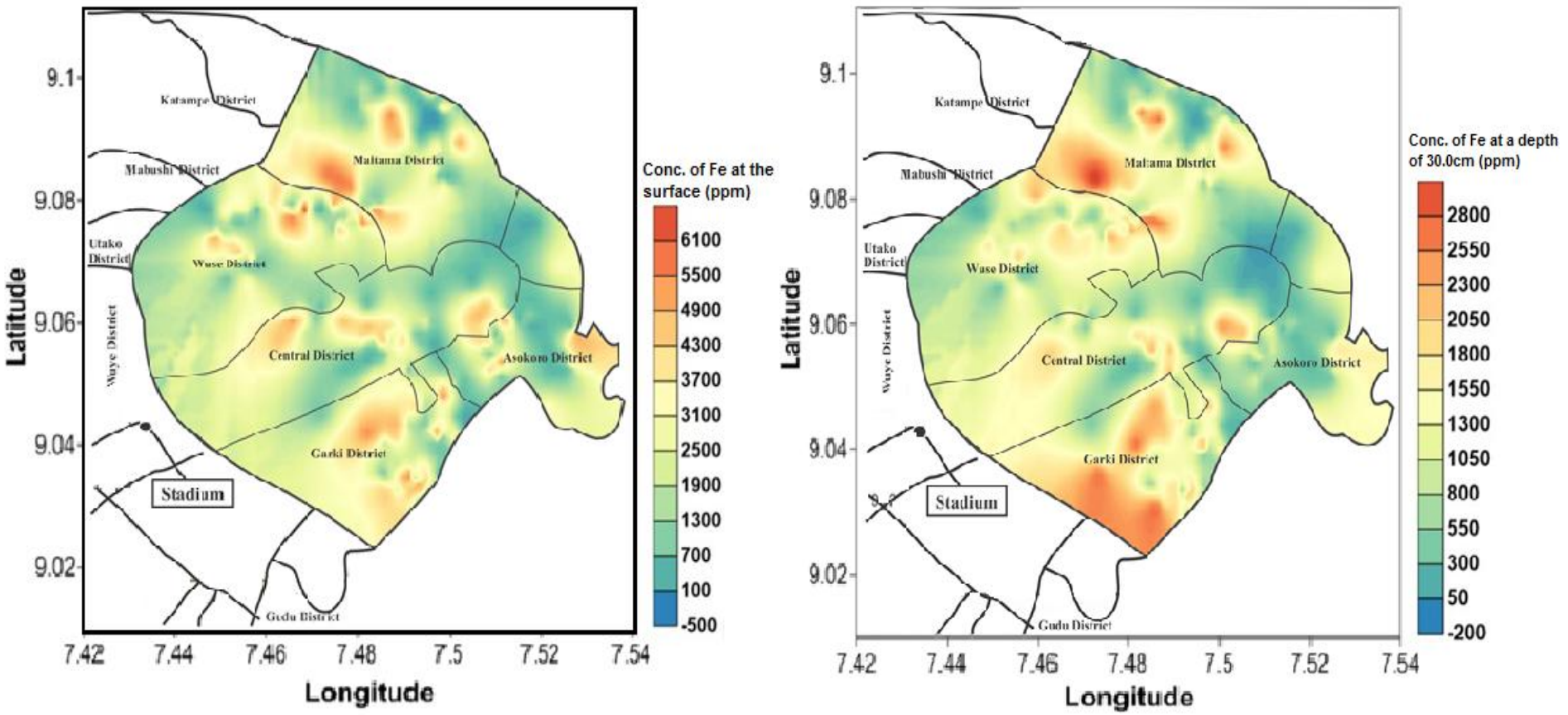
5.1.1 Concentration of Iron (Fe) within Abuja Surface and Subsurface Soil

Iron belongs to the group 8 of the periodic table and on the first row transition series consisting of Sc, Ti, V, Cr, Mn, Fe, Co, Ni, Cu and Zn. Iron has an atomic number of 26, an atomic mass of 56, two main oxidation states (+2 and +3) and four naturally occurring isotopes (^{54}Fe, ^{56}Fe, ^{57}Fe and ^{58}Fe), although ^{56}Fe is the major isotope at 92% of the total mass.

According to Rose et al., (1979), Iron is a major element in soil with a median value of 2.1%. It is present mostly as Fe^{2+} in ferro-magnesian silicates, such as olivine, pyroxene, amphibole and biotite, and as Fe^{3+} in iron oxides and hydroxides, as the result of weathering. The spatial distribution pattern of Fe (Figure 5.1) confirms the results obtained from magnetic susceptibility analysis.

The highest Fe concentration on the surface soil of about 6800mg/l was observed in major commercial areas of Wuse, Garki and Central district. At the depth of 30.0cm, (Figure 5.1b), the maximum concentration recorded is about 3000mg/l in Wuse and Garki districts. The decrease in subsurface concentration indicates that anthropogenic activities are the major factor contributing to the high concentration of Fe on the surface soil. There is a

considerable correlation between the concentration of Fe and magnetic susceptibility at the surface and at the depth of 30.0cm.



(a) **(b)**

Figure 5.1: Iron (Fe) distribution maps (a) at the surface (b) at the depth of 30.0cm

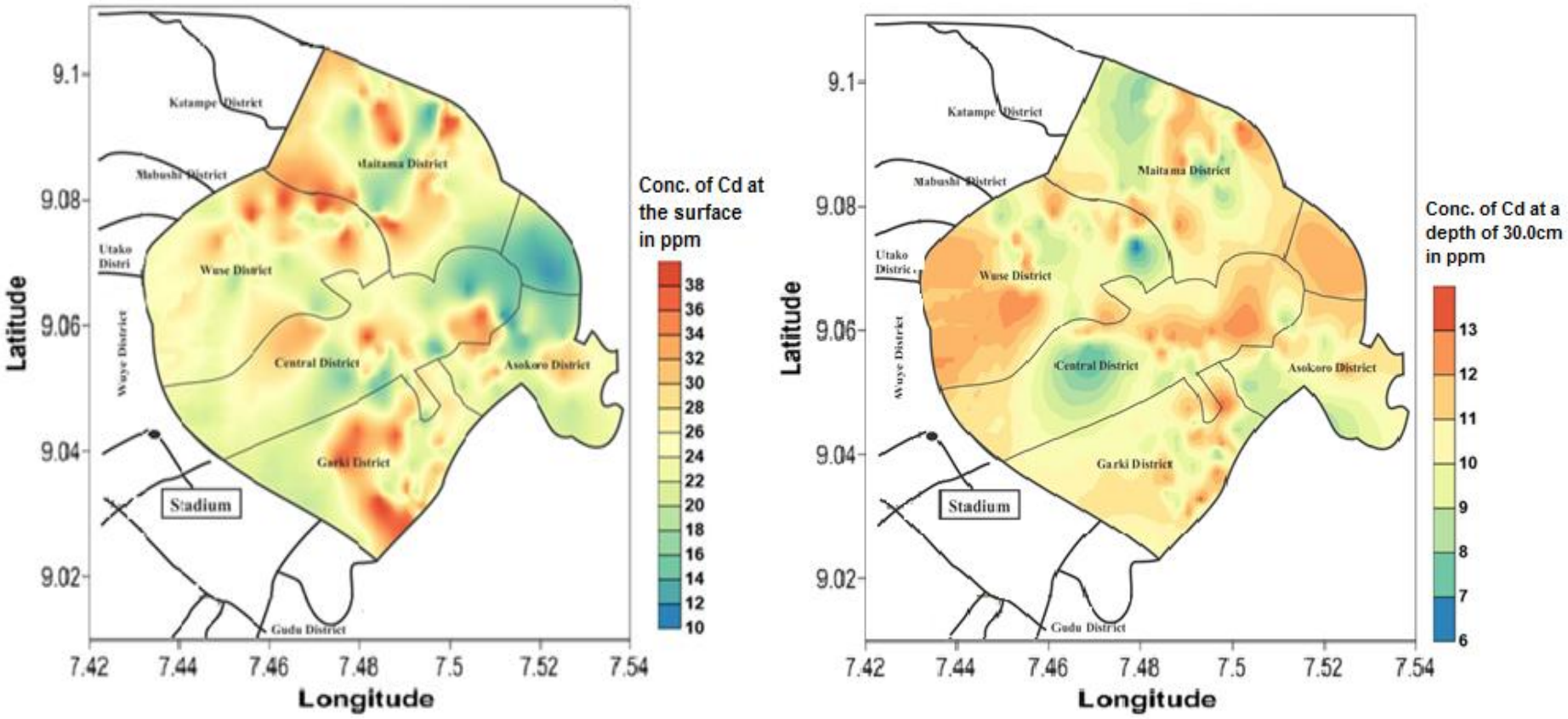
5.1.2 Concentration of Cadmium (Cd) within Abuja Surface and Subsurface Soil

Cadmium is a second row transition metal belonging to group 12 of the periodic table, along with Zn and Hg. The element has an atomic number of 48, an atomic mass of 112, one main oxidation state (+2) and eight naturally occurring isotopes (^{106}Cd, ^{108}Cd and ^{110}Cd to ^{116}Cd), of which ^{114}Cd, ^{112}Cd, ^{111}Cd, ^{110}Cd and ^{113}Cd have abundances of 28.73%, 24.13%, 12.80%, 12.49% and 12.22% respectively (Smith *et al.*,1995).

Cadmium is widely distributed in the Earth's crust, but is particularly associated with zinc and copper and is produced commercially only as a by-product of zinc smelting. Like mercury, cadmium and its compounds enter the environment only from geological or human activities (metal mining, smelting and fossil fuel combustion).

The average content of Cd in soil varies between 0.06 to 1.1 mg kg^{-1}, whereas the global mean for surface soil has been estimated to be 0.53 mg kg^{-1}, and apparently all higher values may reflect anthropogenic influences especially from tires wear (Kabata-Pendias *et al.*, 1992).

From Figure 5.2, it is evident that Cadmium is distributed evenly in almost all the areas at the surface (Figure 5.2a) with concentration range between 10.0-40.0mg/l. At the depth of 30.0cm, (Figure 5.2b) the concentration of Cd range from 5.0-15.0mg/l. The high concentration at the surface is mostly attributed to anthropogenic pollution. Comparing the surface spatial distribution of Cadmium and spatial magnetic susceptibility distribution map, there is a correlation between them. This indicates that Cadmium is among the contributors to the magnetic susceptibility at the surface.



(a) (b)

Figure 5.2: (a) Cadmium (Cd) distribution at the surface soil and (b) at depth of 30.0cm in Abuja

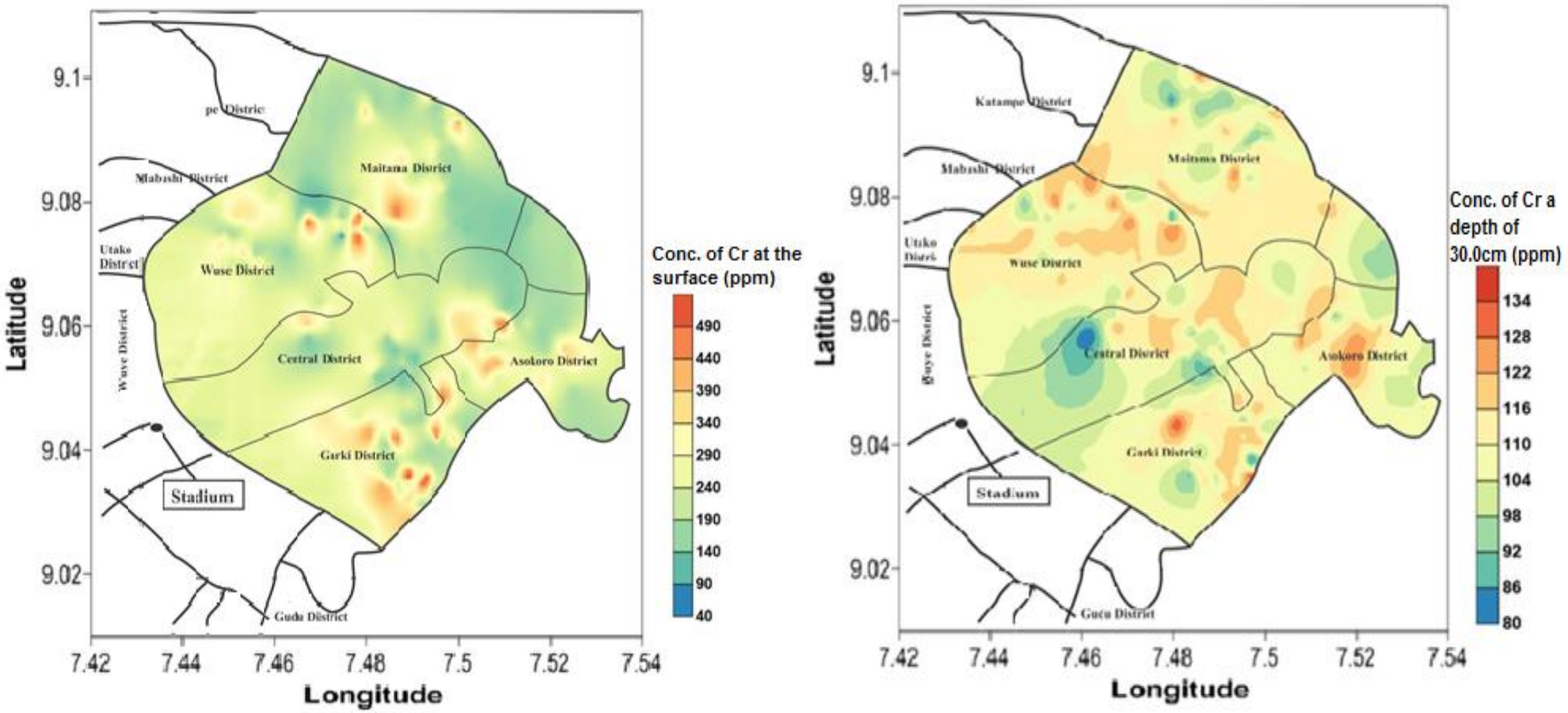
5.1.3 Concentration of Chromium (Cr) within Abuja Surface and Subsurface Soil

Chromium belong to the first row transition series of elements, which consists of Sc, Ti, V, Cr, Mn, Fe, Co, Ni, Cu and Zn, and belongs to group 6 of the periodic table, along with Mo and W. The element has an atomic number of 24, an atomic mass of 52, two main oxidation states (+3 and +6) and four naturally occurring isotopes (^{50}Cr, ^{52}Cr, ^{53}Cr and ^{54}Cr), of which ^{52}Cr represents 84% of the total mass (Kabata-Pendias *et al*., 1992).

Chromium is a major component of steel alloys (10–26%) and used for coating steel as chrome plating. Chromates and dichromates, containing Cr^{6+}, are sometimes released in industrial effluents, especially from leather tanning and electroplating operations, and are highly poisonous and readily soluble (Rai *et al*., 2005). However, because of their powerful oxidising properties they are rapidly reduced and absorbed by organic residues.

Most rocks and soils contain small amounts of chromium. Chromium in its naturally occurring state is in a highly insoluble form; however, most of the more common soluble forms found in soils are mainly the result of contamination by industrial emissions. The major uses of chromium are for chrome alloys, chrome plating, oxidizing agents, corrosion inhibitors, pigments for the textile glass and ceramic industries as well as in photography.

Concentration of Cr at the surface ranges between 0-300.0mg/l, with some points within the central area having concentration of about 400.0mg/l (Figure 5.3a). At the depth of 30.0cm, the concentration ranged from 10.0-150.0mg/l in most locations (Figure 5.3b). The decrease in the concentration with depth may be attributed to anthropogenic activities.



(a) (b)

Figure 5.3: (a) Chromium (Cr) distribution maps showing Cr concentrations at the surface soil and (b) at depth of 30.0cm in Abuja

5.1.4 Concentration of Lead (Pb) within Abuja Surface and Subsurface Soil

Lead belongs to group 14 of the periodic table, which also includes C, Si, Ge and Sn. Lead has the most metallic characteristics of this group. The element has an atomic number of 82, an atomic mass of 207, two oxidation states (+2 and +4) and four naturally occurring isotopes (^{204}Pb, ^{206}Pb, ^{207}Pb and ^{208}Pb), of which ^{208}Pb is the most abundant at 52% of the total mass. Lead is the most abundant of the transition metal elements (Greenwood and Earnshaw 1984).

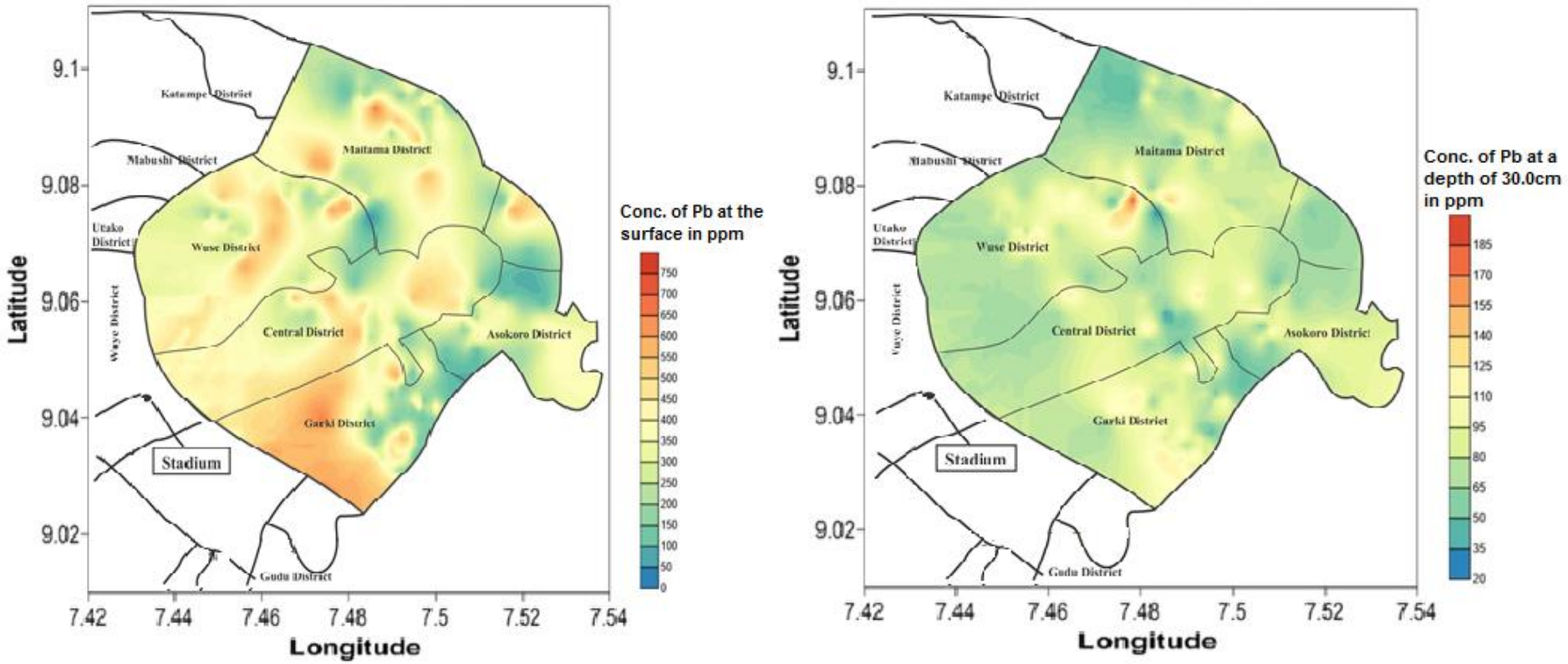
Although, Lead it is not a nutritionally essential element, its monitoring is important because of its toxicity to human health. Most of the lead produced in metallic form, in batteries, cable sheathing, sheets and pipes, etc., is recovered and recycled, but most lead used in compound form, like paints and petrol additives is lost to the environment, eventually ending up in the aquatic environment. Lead compounds, similar to the ones used in petrol additives are reportedly being used in the production of mercurial fungicides (Martinez and Motto, 2000).

Lead from vehicle exhausts, in the form oftetraethyl Pb, was, until recently, a significant source of contamination. In urban environments, road dusts can contain very high levels of Pb (Archer and Barret 1976), although the introduction of unleaded petrol has reduced this potentially toxic hazard in developed industrialized countries.

Anthropogenic sources of pollution may cause local enhancement of Pb levels in surface water by an order of magnitude compared to background values (Banett and Mallory, 1971).

The median total Pb content (ICP-MS analysis) in subsoil is 17.2 mg kg^{-1} and in topsoil 22.6 mg kg^{-1}; the range of Pb values varies from <3 to 938 mg kg^{-1} in subsoil and from 5.3 to 970 mg kg^{-1} in topsoil.

In the study area, (Figure 5.4a) lead is clearly found on the surface soil in large concentration of about 700.0mg/l especially in places with high commercial activities, like around market places, gas stations and around road networks. High concentration of Lead within these places is generally attributed to the use of petroleum in cars and generator. Given the Chemistry of Pb, high concentrations have been thought to exist in the very near surface soil, and rapidly droped with depth (Adriano, 2001). However it has been observed here that reasonable concentration of Pb was found at a depth of 30.0cm below the soil surface(Figure 5.4b). This suggests possible mechanism for downward transport in some environments, and may have implications for remediation. Generally, high concentration of Lead in the surface and sub-surface soil may be attributed to anthropogenic activities mostly by emission from vehicles still using unleaded fuel.



(a) (b)

Figure 5.4: (a) Lead (Pb) distribution maps showing high Pb concentrations at the surface soil and (b) at depth of 30.0cm in Abuja

5.1.5 Concentration of Zinc (Zn) within Abuja Surface and Subsurface Soil

Zinc is the heaviest member of the first row transition series of elements, consisting of Sc, Ti, V, Cr, Mn, Fe, Co, Ni, Cu and Zn, and belongs to group 12 of the periodic table, along with Cd and Hg. The element has an atomic number of 30, an atomic mass of 65, one main oxidation state (+2) and five naturally occurring isotopes (^{64}Zn, ^{66}Zn, ^{67}Zn, ^{68}Zn and ^{70}Zn), of which ^{64}Zn, ^{66}Zn and ^{68}Zn are the most abundant at 48.6%, 27.9% and 18.8% respectively of the total mass.

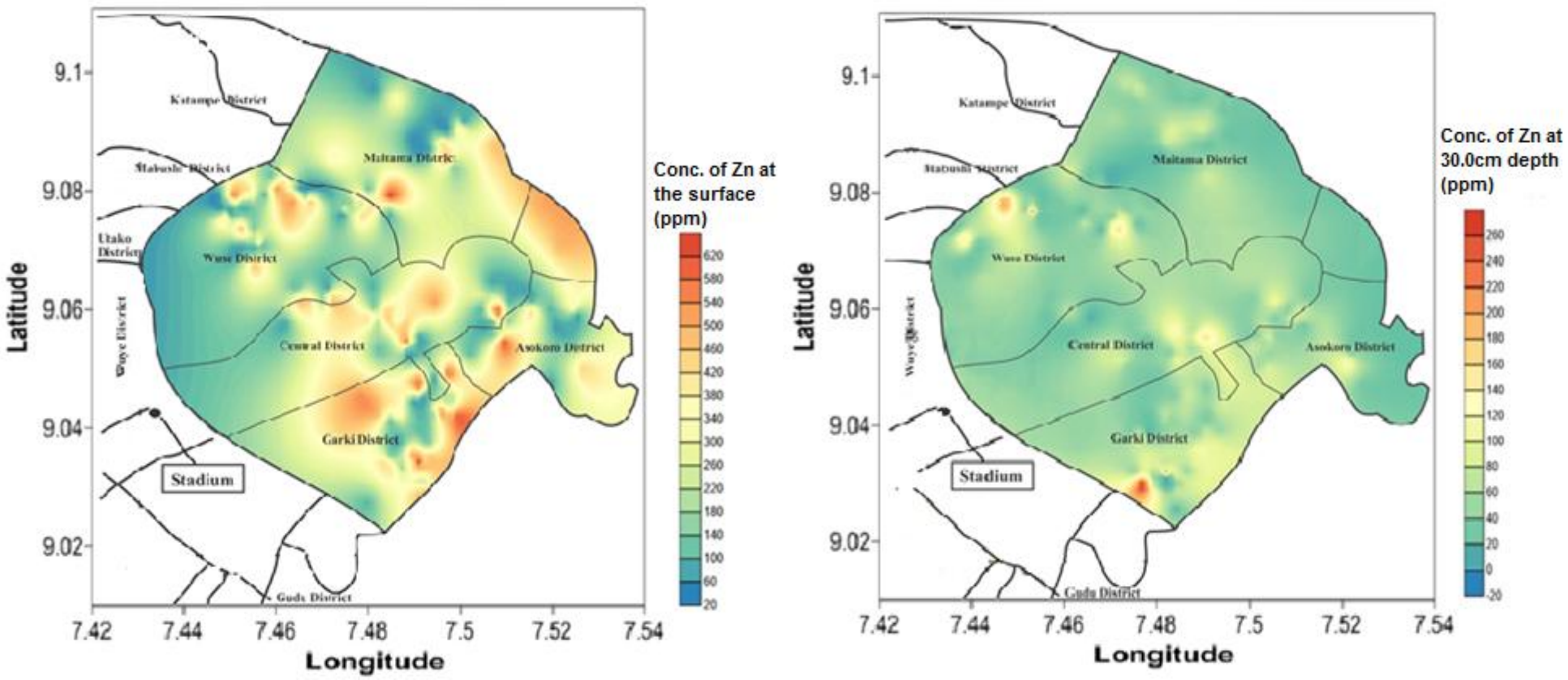
The Zn content in soil depends on the nature of parent rocks, texture, organic matter and pH, and ranges from 10 to 300 mg kg^{-1} (Mihaljevic 1999) with an estimated global average of 64 mg kg^{-1} (Kabata-Pendias *et al*., 1992).

Anthropogenic sources of zinc are significant, arising mainly from industrial activities such as mining, coal, waste combustion, and steel processing. A major use of Zn is as an anti-corrosion coating. It is also used as a constituent of brass, as a white pigment (ZnO) in paint and rubber products, and in the manufacture of dry batteries.

The median total Zn content (XRF analysis) is 47 mg kg^{-1} in subsoil and 52 mg kg^{-1} in topsoil; the range of values vary from <3 to 3060 in subsoil and from <3 to 2900 mg kg^{-1} in topsoil. The average ratio topsoil/subsoil is 1.075.

The concentration of Zinc at the surface (Figure 5.5a) shows a relatively high localized concentration scattered around the districts between(500.0-700.0)mg/l. Generally for the result and Google map of the localized spots with high concentrations corresponds to the places used mostly by ware houses, building material markets, spare parts market and general Motor Park. Places with medium concentration between 200.0 and 400.0mg/l

correspond to places with average commercial activities, residential building, plaza, government offices e.t.c., while places with low concentration between 20.0mg/l to 150.0mg/l are places dominated mostly by residential houses, estates, and reserve areas. At a depth of 30.0cm, (Figure 5.5b), it is observed that the maximum concentration recorded is about 300.0mg/l in about two distinct location (Wuse and Garki). Aside these two prominent features, most of the areas have concentration almost as the background concentration. No much virtual correlation between the surface concentration map and the surface magnetic susceptibility. This implies that Zinc might not have contributed significantly to the magnetic susceptibility enhancement within the study area.



(a) (b)

Figure 5.5: (a) Zinc (Zn) distribution maps showing Zn concentrationat the surface soil and (b) at depth of 30.0cm in Abuja

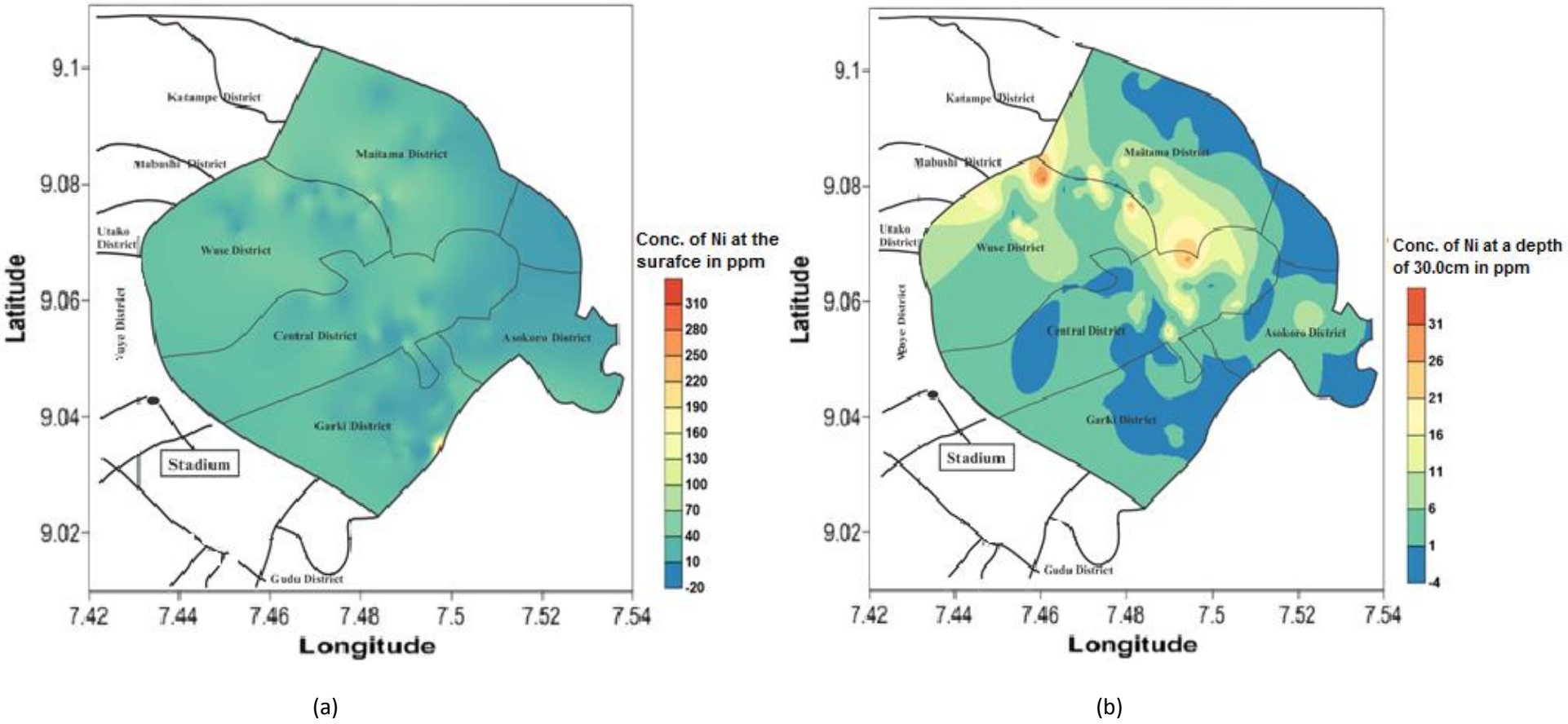
5.1.6 Concentration of Nickel (Ni) within Abuja Surface and Subsurface Soil

Nickel is one of many trace metals widely distributed in the environment, being released from both natural sources and anthropogenic activity, with input from both stationary and mobile sources. It is present in the air, water, soil and biological material. Natural sources of atmospheric nickel levels include wind-blown dust, derived from the weathering of rocks and soils, volcanic emissions, forest fires and vegetation.

Anthropogenic sources of nickel include fertilisers, steel works, metal plating and coinage, fuel combustion and detergents (Reimann and de Caritat 1998).

The median total Ni content (ICP-MS analysis) is 21.8 mg kg-1 in subsoil and 18.0 mg kg^{-1} in topsoil, with a range from <2 to 2400 mg kg^{-1} in subsoil and up to 2690 mg kg^{-1} in topsoil. The average ratio topsoil/subsoil is 0.918.

Nickel is generally distributed uniformly through the soil profile but typically accumulates at the surface from deposition by industrial and agricultural activities. Nickel may present a major problem in land near towns, in industrial areas, or even in agricultural land receiving wastes such as sewage sludge. The concentration of Nickel on the surface soil is between 0 and 100.0mg/l and at a depth of 30.0cm between 0 and 34.0mg/l (Figure 5.6). This is low when compared with the median total content of Nickel.



(a) (b)

Figure 5.6: Nickel (Ni) distribution maps showing Ni concentrations at the surface soil (b) at a depth of 30.0cm

5.2 CORRELATION BETWEEN MAGNETIC SUSCEPTIBILITY AND HEAVY METALS CONCENTRATION

One of the simple statistical methods used to investigate the linear relationship between two variables that are continuous is the correlation method (Mukaka, 2012). Correlationis generally measured by a statisticsfactorcalled the correlation coefficient, which represents the strength of the linear relationship between the variables in question. It is a dimensionless quantity that takes a value in the range -1 to +1. A correlation coefficient of zero indicates that no linear relationship exists between two continuous variables, and a correlation coefficient of -1 or +1 indicates a perfect linear relationship. The strength of relationship can be anywhere between -1 and +1. The stronger the correlation, the closer the correlation coefficient comes to ±1. If the coefficient is a positive number, the variables are directly related (i.e., as the value of one variable goes up, the value of the other also tends to do same). If, on the other hand, the coefficient is a negative number, the variables are inversely related (i.e., as the value of one variable goes up, the value of the other tends to go down).

In the study, the Pearson correlation method was used to investigate the relationship between magnetic susceptibility and the concentration of heavy metal within the study area.

The Pearson correlation coefficient is given by the expression

$$R = \frac{\sum_i (x_i - x)(y_i - y)}{\sqrt{\left[\sum_i^n (x_i - x)^2 \sum_i^n (y_i - y)^2\right]}} \qquad 5.1$$

where x_i and y_i are the values of x and y for the i_{th} level. Another important information from this statistical method in explaining relationship is the coefficient of determination "r^2". This parameter gives the proportion of the variance (fluctuation) of one variable that is

predictable from the other variable. The coefficient of determination is the ratio of the explained variation to the total variation.

The coefficient of determination represents the percentage of the data that is the closest to the line of best fit. For example, if r = 0.922, then r^2 = 0.850, which means that 85% of the total variation in y can be explained by the linear relationship between x and y (Equation 5.2). The other 15% of the total variation in y remains unexplained.

$$y = a + bx \qquad 5.2$$

The coefficient of determination is a measure of how well the regression line represents the data. If the regression line passes exactly through every point on the scatter plot, it would be able to explain all of the variation. The further the line is away from the points, the less it is able to explain.

Figure 5.7 shows a positive coefficient of determination between the selected heavy metals (Fe, Cr, Ni, Cd, Zn and Pb) and magnetic susceptibility within the study area. From the plots, a pronounced positive and significant coefficient wasfound between the concentration of heavy metal elements Fe, Pb and Cd and magnetic susceptibility. There is a very weakcorrelation with Ni. Table 5.2 show the correlation between the heavy metals and magnetic susceptibility, a strong correlation exist between Fe, Pb and Cd, while Cr and Zn have an average correlation, Ni has the least correlation coefficient of about 0.0831.

Table 5.2 Correlation parameters of selected heavy metals with magnetic susceptibility measurements in Abuja Phase 1

Element	Correlation Coefficient (R)	Coefficient of Determination (R^2)
Fe	0.9366	0.8772
Cd	0.9103	0.8287
Ni	0.0831	0.0069
Cr	0.6011	0.3613
Pb	0.9566	0.9151
Zn	0.5513	0.3039

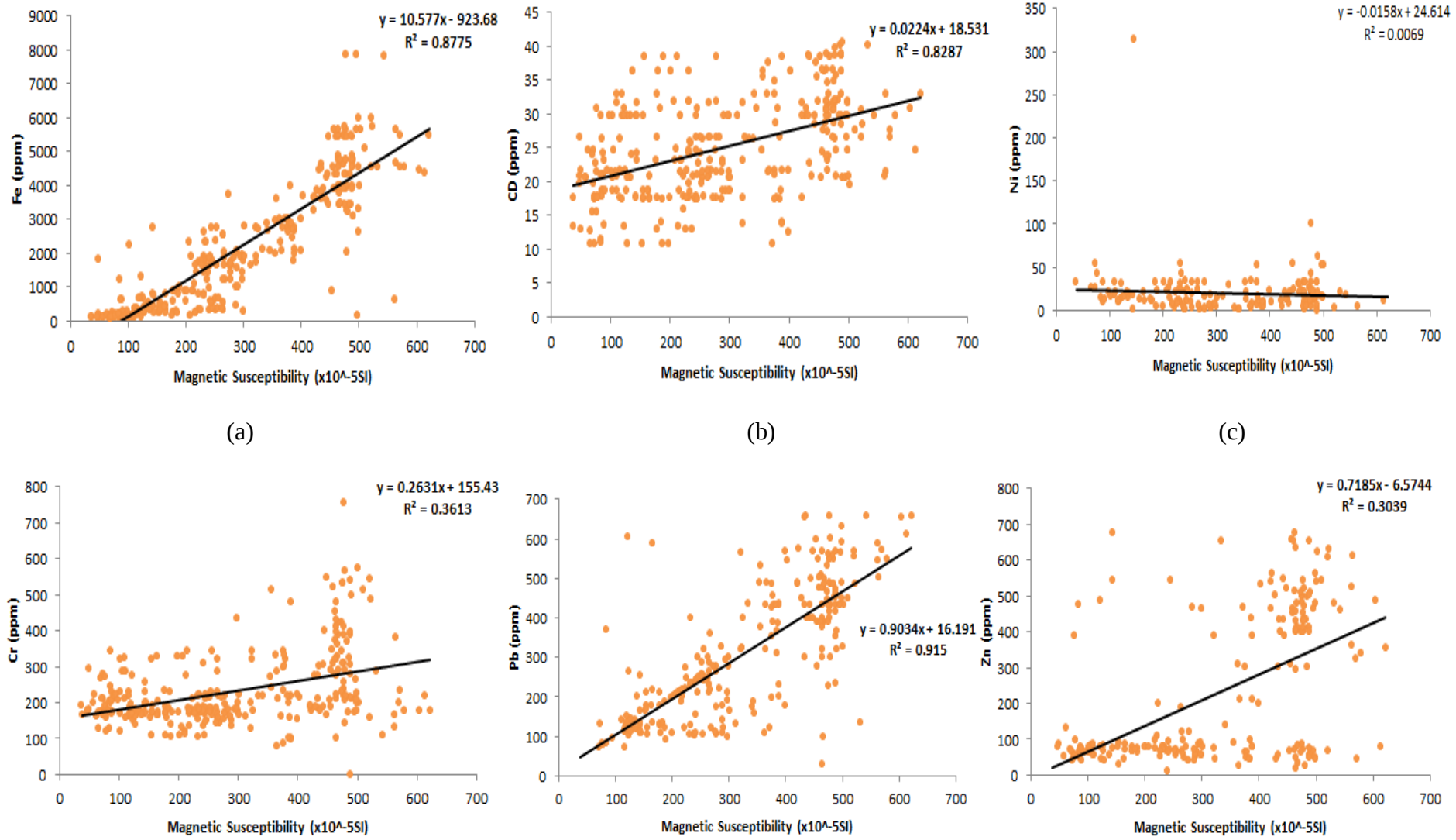


Figure 5.7: Correlation plots between Magnetic Susceptibility and concentration of (a) Fe, (b) Cd, (c) Ni, (d) Cr, (e) Pb and (f) Zn at the surface soil

CHAPTER SIX

DISCUSSION,CONCLUSION AND RECOMMEDATION

6.1 DISCUSSION

In this study, magnetic susceptibility mapping and Atomic Absrption Spectrometer analysis have been successfully carried out on the soil of Abuja metropolis (Phase 1),North central Nigeria. The major rock types within the study area are the migmatite and the biotite gneiss with an average magnetic susceptibility of about 112.5 x 10^{-5}SI. This is in conformity with previous works carried out within the area (Kogo *et al.*, 2009; Longpia *et al*., 2013 and Idehai *et al*., 2014). In general, the magnetic properties of the residual soil depend largely on the lithological structure and the weathering process of the parent rocks within the area. As expected the background magnetic susceptibility mapping conducted within virgin areas around the city indicates an average susceptibility value of about 45.0 x 10^{-5}SI less than that of the parent rocks located within the area.The linear trend observed from the graph plots of the background values indicates no external influence on the distribution of the magnetic susceptibility at any point (see Figure 4.3). The background magnetic susceptibility of the vertical profiles obtained from undisturbed locations at the 5 district shows evidence of linear trends without any external influence from anthropogenic grains (see Figure 4.14). Most of the magnetic susceptibility signal obtained here arise from lithological processes especially from the parent rocks. In order to evaluate the magnetic susceptibility values obtained in this work, we consider the average magnetic susceptibility of the parent rocks and the soil as the natural background susceptibility of the area and the susceptibility classification in Table 6.1 which assigned soil neutral to severe impact on the environment.

Table 6.1 Classification of magnetic susceptibility effect on the Environment (Preetz*etal.*, 2009)

Classification	Magnetic Susceptibility ($x10^{-5}SI$)
Neutral	0-50.0
Moderate	50.0-500.0
Severe	500.0-2000.0
Very severe	>2000

6.1.1 Discussion on Magnetic Susceptibility Mapping

Magnetic susceptibility measurements on surface soil and subsoil along road networks quantify the degree and the effect of environmental pollution related to vehicular emission. The high magnetic susceptibility values of about (450.0-650.0) x 10^{-5}SI occur at 0–2.0 m from the road pavement and excessively recorded in areas with high business activities. Roads leading to residential areas show low magnetic susceptibility of about (200.0-300.0) x 10^{-5}SI, with magnetic signal mostly contributed by lithological processes.

The magnetic susceptibility values obtained along the road segments decreases with increased distance from the road pavements. This may be connected to the fact that vehicular activities contribute to the pollution along the road network (see Figures 4.4, 4.6, 4.8, 4.10 and 4.12.)

The localized, narrow trend of susceptibility enhancements parallel to the road pavement, results from the deposition of traffic-related particles. These particles accumulate in the close vicinity of the road immediately after discharge into the environment as described by Petrovsky and Ellwood (1999). The compacted soil as a result of the use of track by passengers result in irregular evolution of magnetic susceptibility exhibited in some of the

contour maps with zones of high value and others with low value (see Figures 4.5c and 4.11b). Moreover, a small enhancement of magnetic susceptibility values observed at distance from the road pavement may have resultedfrom the continuous atmospheric deposition by various particle-transport mechanisms (see Figures 4.7a, 4.7b and 4.9b). It is interesting to note furthermore, that the width of the contaminated area in this case does not change within the investigated area and the highest signal is always obtained immediately after the road pavement (see Figures 4.5, 4.7, 4.9, 4.11 and 4.13).

Wuse district recorded the highest magnetic susceptibility values of about 720.0 x 10^{-5}SIthan any other area in Abuja. This may be attributed to the fact that business activities are concentrated in the area, and hence vehicles movement within the district is high. Maitama and Asokoro have low values of magnetic susceptibilities. The values obtained there indicated that business activities and influx of vehicles within the areas are limited, as the areas are home to residential buildings.

From the Table 6.1, most of the areas near the road pavement having magnetic susceptibility of about 500.0 x 10^{-5}SI aside road C_1 in Central district, M_1, M_2 and M_4 in Maitama district and all the roads mapped in Asokoro are considered to have severe effect on the environment.

The vertical soil profiles obtained from the vicinity of the roads pavement shows magnetic susceptibility enhancement of about (400.0-650.0) x 10^{-5}SI at the top soil to a depth of about 20.0cm (see Figure 4.15, 4.16, 4.17, 4.18 and 4.19). The enhancement of magnetic susceptibility decreases from the topsoil with depth. This is attributed to anthropogenic activities where the roadside dusts are deposited directly on the top soil. Reoccurrence of enhanced magnetic susceptibility at depth of 20.0-30.0cm may indicate further deposition of

magnetic grains or presence of metallic particle at such depths (see Figure 4.15a and 4.17c. Evidence of layers occurs in the soil profiles with some showing high magnetic susceptibility values with depth. This can be traced to the anthropogenic activities with time within the area. Most of the road side dusts that are not washed away by water or deposited far away from the road are gradually buried with time within the areas and this can be used as evidence of long time activities in the areas.

From the 2D contour maps at different depth, high magnetic susceptibility of about (400.0-600.0) x 10^{-5}SI is clearly observed at the surface maps (Figure 4.20). The magnetic susceptibility enhancement occurred mostly at the boundaries of the various districts. High enhancement in this case is attributed to the fact that the boundaries between these districts are made of major road network linking both districts and residential area together. In the Northern part of the Central district and eastern part of Wuse district, low magnetic susceptibility are observed, in Wuse district the low magnetic susceptibility values observed are attributed to the terrain of the area which is sloppy and hence most of the magnetic grains deposition are easily transported to a nearby river in the area. The low susceptibility observed in the Central district is majorly due to the fact that the 3arm division situated there is a highly restricted area for commercial and traffic related activities.

At the subsurface (see Figure 4.21, 4.22, 4.23 and 4.24), it is clearly observed that magnetic susceptibility decreases with depth, although some places indicate high values even at depth, but conclusively, the decrease in magnetic susceptibility with depth is due to the fact that magnetic pollutants have less penetrating factor and also most of them are easily transported and deposited either in the river, lakes e.t.c.

According to Preetz *et al*., (2009), the surface soil of Abuja is considered to have moderate to severe effect on the environment. At the depth of 10.0cm, severe effects of magnetic susceptibility are still observed in the maps even though with reduced surface coverage mostly close to roads and commercial places. At 20.0cm and 30.0cm, magnetic susceptibility enhancement is greatly reduced. We can infer here that the boundary between anthropogenic enhanced magnetic susceptibility and lithogenic influenced susceptibility is about 20.0-30.0cm. The implication of this is that, most of the anthropogenic begins of recent when compared with the anthropogenic boundaries of other cities across the world (Table 6.2). Thus the thickness of soil considered to have moderate/severe effect to the environment is about 30.0cm. Reoccurrence of enhanced magnetic susceptibility below this depth may therefore results from anomalous body.

Table 6.2: Comparison of Anthropogenic Boundaries in some Cities across the World with present study

Cities	Anthropogenic Boundary	Source
Abuja (Nigeria)	**30.0cm**	**Present study**
Beijing (China)	70.0cm	Zhang et al., 2006
Denizli (Turkey)	40.0cm	Aydin and Akyol, 2015
Tubingen (Germany)	30.0cm	Blaha *et al*., 2008
Prahova (Romania)	15.0cm	George and Dumitru, 2010
Zambia	80.0cm	Bohdan *et al*., 2010
Beni Mellal (Morocco)	20.0cm	Mohammed et al., 2010
Shanghai (China)	75.0cm	Yang et al., 2007
Lishui (China)	40.0cm	Shenggao et al., 2010
Thessaloniki (Greece)	25.0cm	Zananiri et al., 2006
Silesian (Poland)	20.0cm	Zawadzki et al., 2011

The magnetic susceptibility profile lines running from the east to west indicate clearly the anthropogenic depth of about 20.0-30.0cm, with enhanced magnetic susceptibility mostly at the surface and at a depth of 10.0cm. The profile lines also highlighted the nature of penetration of these magnetic grains. Most of the grains happen to have less ability to

penetrate deeper into the soil. This is a clear indication that the major source of these pollutions is mostly due to depositional factor rather than long time activities.

Frequency-dependent magnetic susceptibility distributions of fine grain are irregular along most of the road pavements (see Figure 4.27-4.31). The distribution of frequency-dependence susceptibility of less than 5.0 percent dominated the plot from the road pavements to a distance of about 8.0m in some cases. This indicates the presence of coarse multidomain and single state domain grain in the roadside dust rather than super paramagnetic grain (Jordanova, 2013). In the road in Asokoro district (see Figure 4.31), frequency-dependence susceptibility greater than 5.0 percent is predominantly found there, an indication of super paramagnetic grains. Single State domain and multidomain grains are mostly released from anthropogenic sources while super paramagnetic grains are found from pedogenic source, hence from this observation, it should be of interest to know that most of the roadside dust are covered with magnetic dust from anthropogenic sources.

The scattergram plot of magnetic susceptibility with frequency-dependence susceptibility (see Figure 4.34-38) clearly shows the distribution of the magnetic grains according to their sizes. From the plot it is obvious that the percent of super paramagnetic grains is less when compared to multidomain and single state domain grains.

In the 2D surface frequency-dependent susceptibility contour maps of Abuja city (see Figure 4.32), it is clearly observed that the surface and topsoil is predominantly covered by magnetic grains with frequency-dependence susceptibility of about 0-5.0 percent. This indicates that vehicular/industrial activities are responsible for the release of these grains since they mostly fall within the region of multidomian and single state domain. At the sub-surface (depth of 30.0cm), it is observed that the frequency-dependence susceptibility varies

mostly between 7.0-11.0 percent, these percentage clearly indicate the presence of super paramagnetic grains as a dominant contributor. Generally super paramagnetic grains are mostly from pedogenic rather than anthropogenic sources. From this, we can conclude that multidomian and single state domain grain mostly accumulate at the surface and hardly do they find their way to depth of 30.0cm.

The presence of anthropogenic magnetite in topsoil samples from polluted areas is been determined by low-temperature k measurement (e.g. Magiera *et al.* 2008). Magnetite undergoes Verwey transition at about –150°C (see Figure3.37). Magnetic concentrates prepared from the raw samples of topsoil and magnetically enhanced layers exhibit a prominent Verwey transition, indicating the presence of coarse MD magnetite, likely of anthropogenic origin.

Changes in the magnetic properties at slightly higher temperatures (-25°C) as seen in Figure 4.40e, point to the presence of pyrrhotite, siderite and/or rhodochrosite, respectively. These minerals are paramagnetic at room temperature but become magnetic at low temperatures. At high temperature (see Figure 4.41a, d,f and h), susceptibility drop at 400°C indicates monoclinic pyrrhotite as a major contributor. The curve independent of temperature from room temperature to about 250°C is an indication of the presence of multidomain minerals (see Figure 4.41d, g and i) while susceptibility drop above 500°C is as a result of the magnetite or hematite in the samples (see Figure 4.41b, e and f) (Wolfers *et al.*, 2011).

Predominance of minerals with Curie temperature of 575 to 580^{o}C in both road dust and soil points to magnetite as both lithogenic mineral grains and spherules of anthropogenic origin.

6.1.2 Discussion on Atomic Absorption Spectrometer Analysis

Atomic Absorption Spectrometer analysis reveals Fe, Cr, Cd, Ni, Zn and Pb as anthropogenic magnetic grains predominantly found on Abuja soil both at the surface and sub-surface.

Fe with a maximum concentration of 8000.0mg/l found mostly in Wuse, Maitama and Central districts. Asokoro and upper part of Central areas indicates low values of Fe of about 1200.0mg/l. At the depth of 30.0cm, the maximum concentration recorded was 6500.0mg/l in Wuse and Maitama. The surface and subsurface distributionof Fe show some correlation with the magnetic susceptibility 2D maps both at the surface and the sub-surface.

Cadmium is clearly observed in the entire surface map of the area with a concentration of about 40.0mg/l, the concentration reduces with depth. At 30.0cm depth, the concentration is generally less than 20mg/l and may not contribute significantly to the values of magnetic susceptibility observed at that depth.

Chromium has maximum concentration at the surface soil in theCentral district; this concentration is about 700.0mg/l. In most of the other districts, it is observed that the concentration is of lithological origin. At the depth of 30.0cm, the maximum concentration is about 130.0mg/l.

The evidence of Lead at the surface is likely due to the presence of petroleum products on the soil, with maximum concentration of about 600.0mg/l evenly spread across Maitama, central area and Garki where most of the gas stations are located. At a depth of 30.0cm the concentration reduced to about 130mg/l, this reduction of lead at the subsurface is attributed to the fact that anthropogenic activities is the major factor that contribute significantly to the surface concentration. There is also a correlation between the

concentration of lead and the magnetic susceptibility map both at the surface and sub-surface.

High concentration of Zinc was found in Wusedistrict at the surface and at depth of 30.0cm with a maximum concentration of about 700.0mg/l.

The concentration of Nickel at the surface and depth of 30.0cm is generally low and in some place not seen.

The distribution of heavy metals across Abuja surface soil and subsurface can be generally attributed to anthropogenic activities within the area with Fe, Pb and Cr as the major contributors to the high magnetic susceptibility values obtained in the study area. This is due to the fact that in all cases, concentration decreases with depth.

The source of Fe in the surface and sub-surface soil may be attributed to the abrasive vehicular wear in particular brake linings, while zinc particles may be attributed to the abrasion of tyres (Birmili *et al*., 2006). Pb may be attributed to petroleum products.

From the correlation plots, a pronounced positive and significant coefficient was found between the concentration of heavy metal elements Fe, Pb and Cd and magnetic susceptibility of about of 0.9366, 0.9103 and 0.9566 respectively. There is a very weak correlation with Ni of 0.0831. From these results, it is evident that magnetic susceptibility can be used as a guideline to find contaminated urban areas with high Fe, Pb and Cd value.

6.2 CONCLUSION

Previous studies showed that magnetic susceptibility variations are caused by differences in geology (lithogenic/geogenic), soil forming processes (pedogenesis) and anthropogenic input of magnetic material (Dearing *et al.*, 1996 and Thompson and Oldfield, 1986). The high magnetic enhancement in the top soil is attributed to anthropogenic inputs of magnetic minerals/grains.

From the magnetic susceptibility results, it is observed that the soil of Abuja has high magnetic susceptibility compared with the background parent rocks values. This indicates that anthropogenic activities results in the increase of the magnetic susceptibility observed on the surface soil of Abuja and the major reason for the difference must especially at the surface. High magnetic susceptibility enhancement around road networks most have resulted from anthropogenic influence due to vehicles activities.

Spatial distributions with depth can be very useful in delineating areas where the enhancement is as a result of anthropogenic pollution from those of lithogenic origin. From the results obtained, the spatial distribution with depth shows that the magnetic susceptibility at the top 20.0cm of soil is the most affected by anthropogenic pollutants. It was concluded that the boundary between anthropogenic enhanced magnetic susceptibility and pedogenic magnetic susceptibility occurs at 30.0cm.

The decrease in magnetic susceptibility towards deeper soil horizon is an indication that the magnetic grains accumulate in the topsoil as a result of anthropogenic dust fall. Also, from the spatial distribution with depth it is possible to investigate where the volumes of soil with heightened magnetic susceptibility are located in the soil profile and in this way investigate which characteristics type of soil profile it is.

Frequency dependent susceptibility helps in discriminating magnetic grains due to anthropogenic sources from those that originate from lithogenic processes. From the result, it was concluded that the frequency dependent values obtained immediately after the road pavements and on the surface soil of Abuja arise mostly from anthropogenic dust falls of metallic pollutants released mostly from vehicular and industrial activities. While at a distance of about 8.0m and depth of 40cm most of the recorded frequency dependent values arise from the lithological processes of the parent rocks. From the results obtained, it was clearly shown that the major contributor to the surface magnetic susceptibility in Abuja city arised from the continual deposition of magnetic grains from anthropogenic sources.

The temperature dependent susceptibility measurement carried out on the samples collected across the city shows evidence of magnetic grains like migmatite in them.

The results from the AAS analysis indicate the high concentration of Fe, Pb, Cr, Ni, Cd and Zn at the surface soil. These concentration are more than the allowed concentrationin soil and hence poses a risk to the environment.

The positive and pronounced correlation between Fe, Pb and Cd with magnetic susceptibility measuements make the magnetic susceptibility measurement a reliable tool in quick evaluation of environmental contamination by these metals.

6.3 RECOMMENDATION

Many challenging problems remain untouched because of the limitation of time for sampling and experimental measurements/facilities during the development of this thesis work. Some of the aspects that can be investigated in future using this thesis work as the basis are summarized below. The outcome of the road dust analysis could serve as a basis for future planning of the city, as well as in providing precedence for urban coastal cities to

follow. It is hoped that the results of road dust analysis will assist the relevant industries and authorities in designing appropriate preventive measures to ensure the environmental quality of the roads to be improved. The relevant data will make available to the appropriate authorities for decision making and implementing various environmental protection measures in problematic areas, within and outside the state.

Recommendation for Future Studies

i. Source material characterization can be extended and their detailed analysis may help in modelling urban dust composition, easy outlining and regulation of specific dust components for environmental checks.
ii. Tree leaves providing a non-magnetic background for collecting particulates near road corridor can be used as an indicator for better monitoring of traffic derived particulates, and its subsequent control strategies.
iii. The nature of the deposited particulate matter on sediments, soils and road dusts and their magnetic and chemical properties can be undertaken seasonally, as part of health related studies in the investigated area.
iv. Establishment of non-magnetic quartz sand pads at selective sites can quantify vehicle derived particulates, and can help in understanding the mobility of pollutants in the environment.
v. Historical data regarding metal accumulation in sediments and soils in published literature is limited. Hence, temporal/historical monitoring of impact of metal inputs due to industrialization and urbanization can be magnetically studied using lake, mudflat and mangrove sediment cores from economically important regions.

REFERENCES

Akinroye L. (2013). Cardiovascular Disease is Big Threat to MDGs. Vanguard *Newspaper 8th May; 34*

Adriano D. C. (2001).Trace Elements in Terrestrial Environments.2e, Springer, New York.

Abu-Allaban M., Gillies J.A., Gertler A.W., Clayton R. and Proffitt D. (2003).Tailpipe, Resuspended Road Dust, and Brake-wear Emission factors from on-road Vehicles.*Atmospheric Environment*, 37(37), 5283-5293.

Ahmad I., Hayat S., Ahmad A. and Samiullah I. (2005).Effect of Heavy Metal on Survival of certain groups of Indigenous Soil Mocrobial Population. Journal of Applied Scinece Environment Management; 9; 115-121.

Amereih S., Meisel T., Scholger R. and Wegscheider W. (2005).Antimony Speciation in Soil Samples along two Austrian Motorways by HPLC-ID-ICP-MS, Journal of Environmental. Monitoring, 7, 1200-1206.

AnagnostopoulouM. A. and Day J.P. (2006). Lead Concentrations and Isotope Ratios in Street dust in major Cities in Greece in Relation to the use of Lead in Petrol. *Science of The Total Environment*, 367(2-3), 791-799.

Adyin A. and Akyol E. (2015).Observing Urban Soil Pollution using Magnetic Susceptibility. International Journal of Environmental Research, 9 (1); 295-302.

Aydin A. and Gelisli K.(1996).Magnetic Studies in Saruhan–Bayburt Scarn Zone.Jeofizik 10 (1–2), 40–49 in Turkish.

Archer A, and Barratt R. S. (1976). Lead in the Environment: Monitoring for Lead. Sci. Total Environ., 96: 173-176.

Banerjee A.D.K. (2003).Heavy Metal Levels and Solid Phase Speciation in Street Dusts of Delhi, India.*Environmental Pollution*, 123(1), 95-105.

Barnett P. R., and Mallory E. C.(1971). Determination of Minor Elements in Water by Emission Spectroscopy: U.S. Geol. Survey Techniques Water-Resources Inv. TWI 5-A2, pp 31.

Bartington Instruments Ltd. (2010). Operation Manual for MS2 Magnetic Susceptibility System (OM0408 Issue 48), Bartington Instruments Ltd., Oxford, U. K, 71.

Basavaiah N. and Aniruddha S. K. (2004).Environmental Magnetism and its Implication towards Palaeomonsoon Reconstruction. Journal of Indian Geophysics Union, 8(1), 1-14.

Basavaiah N (2011). Geomagnetism: Solid Earth and Upper Atmosphere Perspectives: Springer Publisher, 486 pages.

Basavaiah N., Blaha U., Das P.K., Deenadayalan K., Sadashiv M.B. and Schulz H. (2012). Evaluation of Environmental Magnetic Pollution screening in Soils of Basaltic origin: Results from Nashik Thermal Power Station, Maharashtra, India. Environmental Science and Pollution Research, 19, 3028–3038.

Beckwith P.R., Ellis J.B., Revitt D.M., and Oldfield, F. (1986).Heavy Metals and Magnetic Relationships for Urban Source Sediments. Physics of the Earth and Planetary Interiors, 42, 67–75.

Birmili, W., Allen, A.G., Bary, F. and Harrison, R.M., (2006). Trace Metal Concentrations and Water Solubility in Size-fractionated Atmospheric Particles and influence of Road Traffic. *Environmental Science and Technology*, 40, 1144–1153.

Blaha U, Appel E, Stanjek H. Determination of anthropogenic boundary depth in industrially polluted soil and semi-quantification of heavy metal loads using magnetic susceptibility. Environmental Pollution. 2008;156:278–289. doi: 10.1016/j.envpol.2008.02.013.

Booth, C.A., Shilton, V., Fullen, M.A., Walden, J., Worsley, A.T. and Power, A.L. (2006). Environmental Magnetism: Measuring, Monitoring and Modelling Urban Street Dust Pollution. In: J.W.S. Longhurst and C.A. Brebbia (Eds) *Air Pollution XIV*. Wessex Institute of Technology (WIT) Press, Southampton 333-342.

Bourliva A., Kautiranis N., Papadopoulou L., Aidona E., Christoforidis C. and Kollias P. (2011). On the Morphology, Geochemical Characteristics and Magnetic Properties of Urban Road dust Particles from the Historic Center of the City of Thessaloniki, Greece. Proceeding of the 12th International Conference on Environmental Science and Technology, Rhodes, Greece.

Briggs, D.J., Collins, S., Elliott, P., Ficher. P., Kingham, S., Lebret, E., Pryl, K., van Reeuwijk, H., Smallbone, K., and van der Veen, A., (1997). Mapping Urban Air Pollution using GIS: a regression-based approach.*International Journal of Geographical InformationScience*, 11, 699–718.

Chameides, W.L., Yu, H., Liu, S.C., Bergin, M.N., Zhou, X., Mearns, L., Wang, G., Kiang, C.S., Saylor, R.D., Luo, C., Huang, Y., Steiner, A. and Giorgi, F. (1999) Case study of the effects of atmospheric aerosols and regional haze on agriculture: An opportunity to enhance crop yields in China through emission controls?" *In Proceedings of the National Academy of Sciences of the United States of America*, 96(24).

Chaparro, M. A. E., Sinito, A. M., Ramasamy, V., Marinelli, C., Chaparro,M. A. E., Mullainathan, S. and Murugesan, S. (2008). Magnetic Measurements and Pollutants of Sediments from Cauvery and Palaru River, India.Environmental Geology, 56 (2), 425-437.

Chaparro M. A.E., Lirio J. M., Nuñez H., Gogorza C. S. G. and Sinito A. M. (2005).Preliminary Magnetic Studies of Lagoon and Stream Sediments from Chascomus Srea (Argentina)-Magnetic Parameters as Pollution Indicators and some results of using an Experimental Method to Separate Magnetic Phases. Enviromental Geology, 49(1):30–43

Chaparro M. A. E., Gogorza C. S. G., Chaparro M. A. E., Irurzun M. A. and Sinito A. M. (2006). Review of Magnetism and Heavy Metal Pollution Studies of various Environments in Argentina. Earth Planets Space 58(10):1411-1422

Charlesworth, S.M., and Lees, J.A. (2001).The Application of some Mineral Magnetic Measurements and Heavy Metal Analysis for CharacterizingFine Sediments in an Urban Catchment, Coventry, UK.Journal of Applied Geophysics, 48, 113–125.

Charlesworth S., Everett M., McCarthy R., Ordonez A. and De Miguel E. A. (2003). Comparative Study of Heavy Metal Concentration and Distribution in Deposited Street Dusts in a large and a small Urban Area: Birmingham and Coventry, West Midlands, UK, *Environmental International*, 29, 563-573.

Chadima M. (2012). Magnetic Susceptibility and its Variation with Temperature.Institute of Geology, Academy of Science.

Chen, X., Xia, X., Zhao, Y. and Zhang, P. (2010) Heavy metal concentrations in roadside soils and correlation with urban traffic in Beijing, China.*Journal of Hazardous Materials*, 181, 640-646.

Chen, Y. and Xie, S. (2012) Temporal and Spatial Visibility Trends in the Sichuan Basin, China, 1973 to 2010.*Atmospheric Research*, 112, 25-34.

Christopher, J. C. (2012). Application of Mineral Magnetic Measurements as a Pollution Proxy for Urban Road Deposited Sediment. Unpublished Ph.D Thesis, University of Wolverhampton.

Committee on the Medical Effects of Air Pollutants (COMEAP).(2001). Long-term effects of particles on mortality. Oxford: Health Protection Agency Chemical Hazards and Poisons Division.

Committee on the Medical Effects of Air Pollutants (COMEAP) (2009). Long-Term Exposure to Air Pollution: Effect on Mortality. Oxford: Health Protection Agency Chemical Hazards and Poisons Division.

Committee on the Medical Effects of Air Pollutants (COMEAP) (2010). The Mortality Effects of Long term exposure to particulate air pollution in the United Kingdom. Oxford: Health Protection Agency Chemical Hazards and Poisons Division.

Currie, R.G. and Bornhold, B. D. (1983). The Magnetic Susceptibility of Continental-shelf Sediments, West Coast Vancouver Island, Canada. Marine Geology 51, 115-27.

Dearing J. A. (1999). Environmental Magnetic Susceptibility: Using the Bartington MS2 System, Chi Publishing, Kenilworth, U. K, 104.

Dearing J.A., Hay K., Baban S., Huddleston A.S., Wellington E.M.H. and Loveland P.J., (1996). Magnetic Susceptibility of Topsoils: a Test of Conflicting Theories using a National Database. Geophysical Journal International 127, 728-734.

Dekkers, M.J. and Pietersen, H.S. (1992). Magnetic Properties of Low-Ca fly ash: a rapid tool for Fe-assessment and a Proxy for Environmental Hazard. In: F.P. Glasser et al. (eds.), Advanced Cementitious Systems: Mechanisms and Properties. Mat. Res. Soc. Symposium Proceedings, 245, 37-47.

Débora M. C., Chaparro M. A. E., Gogorza C. S. G., Navas A. and Sinito A. M. (2010). Vehicle-derived Emissions and Pollution on the Road Autovia 2 investigated by Rock-magnetic Parameters: A case study from Argentina. Studia Geophysica et Geodaetica 54 (1): 135-152.

Dockery D., C. A. Pope X., Xiping J., Spengler J., Ware M., Fay B. and Speizer F. (1993). An Association between Air Pollution and Mortality in Six U.S. Cities.New England Journal of Medicine 329(24): 1753–59.

Doran J. W., Liebig M. A. and Santana D. P. (1998).Soil Health and Global Sustainability. In: Proceedings of the 16th World Congress of Soil Science. Montepellier, France, 20–26 August 1998.

Dunlop D. J. and Özdemir, Ö. (1997).Rock magnetism: Fundamentals and Frontiers. Cambridge University Press, Cambridge, England, 573.

Enahoro I. A.and Ogbonnaya I. (2015). Sub-Soil Investigation of a Proposed Construction Site at Kyami District, Abuja, Nigeria. Journal of Applied Geology and Geophysics, 3, 2: 1; 54-58

Evans M. E. and Heller F. (2003).Environmental Magnetism: Principles and Applications of Enviromagnetics. International Geophysics Series, 86, Academic Press, 299.

Eyre J. K. (1997). Frequency Dependence of Magnetic Susceptibility for Population of Single-domain Grains. Geophysical Journal International, 129; 2009-2011.

Faiz Y., Tufail M., Javed M.T., Chaudhry M.M. and Siddique N. (2009).Road Dust Pollution of Cd, Cu, Ni, Pb and Zn along Islamabad Expressway, Pakistan. Microchem Journal,92, 186–192.

France D. E. and Oldfield F. (2000).Identifying Goethite and Hematite from Rock Magnetic measurements of Soils and Sediments.Journal of Geophysical Research; vol 105; pp 2781-2795.

Frederichs T., von Dobeneck T., Bleil U., and Dekkers M. J. (2003). Towards the Identification of Siderite, Rhodochrosite, and Vivianite in Sediments by their Low-temperature Magnetic Properties, Phys. Chem. Earth, 28, 669–679.

Forsberg B., Hansson H.C., Johansson C., Aureskoug H., Persson K., and Järvholm B. (2005). Comparative Health Impact Assessment of Local and Regional Particulate Air Pollutants in Scandinavia.*Ambio,* 34, 11–19.

Galadima A., Muhammad N. U. and Garba Z. N. (2010).Spectroscopic Investigation of Heavy Metals in Waste Water from University Students' Halls of Residence. International Journal of Chemistry, 20(4): 239-244.

Gautam P., Blaha U., Appel E. and Neupane G. (2004).Environmental Magnetic Approach towards the Quantification of Pollution in Kathmandu Urban Area, Nepal. Physics and Chemistry of the Earth, Parts A/B/C 29, 973–984.

Gautam P., Blaha U. and Appel E. (2005).Magnetic susceptibility of dust-loaded leaves as a proxy of traffic-related heavy metal pollution in Kathmandu City, Nepal.*Atmospheric Environment,* 39(12), 2201-2211.

George G. N. and Egbelehulu O. P. (2012).Measurement of Magnetic Suceptibility of some Rocks and Soil Samples in Dede and Kubwa in Bwari Area Council of the Federal Capital Territory, Abuja.International Journal of Basics and Applied Sciences. 1; (2); 166-167.

George F. G and Dumitru I. (2010).Geophysical Mapping of Soils; New Data on Romanian Soils based on MagneticSusceptibility. Géophysique / Rom. Geophys.J., Tome 54, P. 83–95, Bucureşti.

Georgeaud V. M., Rochette P., Ambrosi J.P., Vandamme D. and Williamson D. (1997). Relationship between Heavy Metals and Magnetic Properties in a Large Polluted Catchment: the Etang de Berre (South of France). Phys Chem. Earth, 22(1–2), 211–214.

Giugliano M., Lonati G., Butelli P., Romele L., Tardivo R. and Grosso, M. (2005) Fine particulate (PM2.5-PM1) at urban sites with different traffic exposure.*Atmospheric Environment,* 39(13), 2421-2431.

González C.M. and Aristizábal B.H. (2012) Acid Rain and Particulate Matter Dynamics in a mid-sized Andean city: The effect of rain intensity on ion scavenging. *Atmospheric Environment,* 60, 164-171.

Greenwood N. N. and Earnshaw A. (1984).Chemistry of the Elements. Pergamon Press, Oxford.

Hakon F. (2008). Magnetic and Spectroscopic Investigations of Mineral Transformations in mixed-valence oxides and magnesium silicates.Ph.D Dissertation; Swiss Federal Institute of Technology, Zürich.

Hanesch M., Scholger R. and Rey, D. (2003).Mapping Dust Distribution around an Industrial site by measuring Magnetic Parameters of Tree Leaves.Atmospheric Environment 37, 5125–5133.

Hanesch M. and Scholger R. (2002).Mapping of Heavy Metals Loadings by means of Magnetic Susceptibility Measurements. Environ Geol 42(8):857–870.

Hanesch M., Scholger R., and Dekkers M. J. (2001). The Application of Fuzzy c-means Cluster Analysis and Non-linear Mapping to a Soil Data Set for the Detection of Polluted Sites. Phys. Chem. Earth, Part A Solid Earth Geodesy. 26(11-12): 885-891.

Hannam, J. and Heller, F. (2001).Magnetic Investigations of Roadside Leaves in Z¨urich, Switzerland, *MAGazine Newsletter*, 4, 4.

Harrison R.M., Laxen D. and Wilson S. (1981). Chemical Associations of Lead, Cadmium, Copper, and Zinc in Street Dusts and Roadside Soils.*Environmental Science and Technology*, 15(11), 1378-1383.

Harrison R.M., Deacon A.R., Jones M.R. and Appleby R.S.(1997).Sources and Processes affecting Concentrations of PM10 and PM2.5 Particulate Matter in Birmingham.Atmospheric Environment31, 4103–4117.

Haugland T., Ottesen R.T. and Volde T. (2007) Lead and Polycyclic Aromatic Hydrocarbons (PAHs) in surface Soil from day care centres in the city of Bergen, Norway. *Environmental Pollution*, 153(2), 266-272.

Hetland R.B., Schwarze P.E., Johansen B.V., Myran T., Uthus N. and Refsnes M. (2001) Silica-induced cytokine release from A549 cells: importance of surface area versus size. *Human and Experimental Toxicology*, 20, 46-55.

Hoffmann V., Knab M. and Appel E. (1999).Magnetic Susceptibility Mapping of Roadside Pollution. Journal of Geochemical Exploration 66, 313–326.

Hilton J. and Lishman J.P. (1985).The effects of Redox changes on the Magnetic Susceptibility of Sediments from a seasonally anoxic lake.*Limnology and Oceanography*, 30, 907-909.

Hunt A., Jones J., and Oldfield F. (1984). Magnetic Measurements and Heavy Metals in Atmospheric Particulates of Anthropogenic Origin. Science of the Total Environment 33, 129–139.

Idehai I. M., Egai, A. O. and Okiotor M. E. (2014).Comparative Assessment of the Geotechnical Properties of Residual Soils in part of Awka and Abuja of Nigeria.Nigerian Journal of Technology (NIJOTECH), 33(4), 595-603.

Ingo G.M., D'uffizi M., Falso G., Bultrini G., and Padeletti G. (2004).Thermal and Microchemical Investigation of Automotive Brake Pad Wear Residues.*Thermochimica Acta*, 418, 61–68.

Jacobson M.Z. (1997). Development and Application of a New Air Pollution Modeling System—II.Aerosol module structure and design.*Atmospheric Environment*, 31(2), 131-144.

Johnston M. J. S. and Stacey F. D. (1969). Transient Magnetic Anomalies accompanying Volcanic Eruptions in New Zealand. Nature 224, 1289-90.

Jordanova D, Hoffmann V, and Fehr K. T. (2004). Mineral Magnetic Characterization of Anthropogenic Magnetic Phases in the Danube river sediments, Earth planet. Sci. Lett. 221: 71-89.

Jordanova D., Jordanova N. and Werban U. (2013).Environmental Significance of Magnetic Properties of Gley Soils near Rosslau (Germany), Environmental Earth Sciences, 69 (5), 1719-1732.

Jordanova N.V., Jordanova D.V., Veneva L., Yorova K. and Petrovsky E. (2003).Magnetic Response of Soils and Vegetation to Heavy Metal Pollution – A case study.

Ju Y., Wang S., Zhang Q., Wang L. and Deng C. (2004). Mineral Magnetic Properties of Polluted Top-soils: A Case Study in Fujian Province, Southeast China. Chinese Journal of Geophysics, 47 (2) 314-321.

Kabata-Pendias A., Dudka S. and Chlopecka A.(1992). Background Levels and Environmental Influences on Trace Metals in Soils of the Temperate Humid Zone of Europe. p. 61-84. In D.C. Adriano (ed). Biogeochemistry of trace metals. CRC Press, Boca Raton, FL

Kelly F.J. and Fussell J.C. (2012).Size, Source and Chemical Composition as determinants of toxicity attributable to Ambient Particulate Matter.*Atmospheric Environment*, 60, 504-526.

Ketzel M., Omstedt G., Johansson C., During I., Pohjola M., Oettl M., Gidhagen L., Lohmeyer A., Berkowicz R. and Wlhlin, P. (2007). Estimation and Validation of PM2.5/PM10 Exhausted and non-exhausted Emission Factors for Practical Street Pollution Modelling.*Atmospheric Environment*, 41, 9370–9385.

Kim, W., Doh, S.J., Park, Y.H., and Yun, S.T. (2007). Two-year Magnetic Monitoring in Conjunction with Geochemical and Electron Microscopic Data of Roadside Dust in Seoul, Korea. Atmospheric Environment, 41, 7627–7641.

Knab M., Appel E. and Hoffmann V. (2001).Separation of the Anthropogenic Portion of Heavy Metal Contents along a Highway by means of Magnetic Susceptibility and Fizzy c-means Cluster Analysis. European Journal of Environmental Engineering and Geophysics 6, 125–140.

Knox E.G. (2006).Roads, railways and childhood cancers. Journal of Epidemiology and Community Health 60, 136–141.

Knutsen S., Shavlik D., Chen L. H., BeesonW.L., Ghamsary M. and Petersen, F. (2004). The Association between Ambient Particulate Air Pollution Levels and Risk of Cardiopulmonary and All-cause Mortality during 22 years follow-up of a Non-smoking Cohort. Results from the AHSMOG Study.Epidemiology 15, S45.

Kogbe CA (1976). The Cretaceous and Paleogene sediments of southern Nigeria.In C. A. Kogbe (Ed.) Geology of Nigeria. pp. 325- 334

Kogo, B. E., Gajere, E. N., Ogunmola J. K. and Ogbole, J. O. (2009). Neutron Activation Analysis of Soil Samples from Different Parts of Abuja Metropolis. Middle-East Journal of Scientific Research 4 (4), 254-262.

Kokinou E. (2014). Magnetic Susceptibility as a Proxy Method to Characterize Geological Formation.Proceeding of the 2nd WSEAS International Conference on Engineering Mechanics Structure and Engineering Geology.

Kumar P. and Britter R. (2005) *Particulate Matter: Importance, regulations and its historical perspective.* University of Cambridge, UK.

Kucer N., Sabikoglu I. and Can N. (2011). Measurements of Environmental Pollution in Industrial Area using Magnetic Susceptibility Method. Acta Physica Polonia, 121 (1), 20-23.

Li Y., Xu B., Shenyang Y. and Liu W. (2015).Simulation of Magnetic Hysteresis Loops and Magnetic Barkhausen noise of iron containing non magnetic particles.American Journal of Physics, vol 5; (7), 761-778.

Lin C.C., Chen S.J., Huang K.L., Hwang W.I., Chang-Chien G.P. and Lin W.Y. (2005). Characteristics of Metals in Nano/ultrafine/fine/coarse Particles collected beside a heavily Trafficked Road. *Environmental Science and Technology*, 39 (21), 8113-8122.

Longpia, C.B., Ashano E.C. and Pam B.G. (2013).Geophysical Investigation for Engineering Site Development around Galadimawa-Aleita Area, Abuja, North Central Nigeria.Journal of Applied Geology and Geophysics, 1(6), 1-11

Lough G.C., Schauer J.J., Park J.-S., Shafer M.M., Deminter J.T., and Weinstein J.P. (2005). Emissions of Metals associated with Motor Vehicle Roadways. *Environmental Scienceand Technology*, 39, 826–836.

Lowrie, W. (1990).Identification of ferromagnetic minerals in a rock by coercivity and unblocking Temperatures Properties. Geophysical Research Letter, 17(2), 159-162.

Lu S., Bai S., Cai, J. and Xu C. (2005). Magnetic Properties and Heavy Metal Contents of Automobile Emission Particulates.Journal Zhejiang University Science, 6B (8),731-735.

Lu S. and Bai S. (2008).Magnetic Characterization and Magnetic Mineralogy of the Hangzhou Urban Soils and its Environmental Implications. Chinese Journal of Geophysics, 51 (3) 549-557.

Lu S.G., Zhu L., Yu J.Y. (2012).Mineral Magnetic Properties of Chinese Paddy Soils and its Pedogenic Implications. Catena, 93: 9–17.

Luo X., Yu S., Li X. (2011). Distribution, Availability, and Sources of Trace Metals in different Particle size fractions of Urban Soils in Hong Kong: Implications for assessing the risk to human health. *Environmental Pollution*, 159(5), 1317-1326.

Maher B. A., Moore C. and Matzka J. (2008).Spatial Variation in Vehicle-derived Metal Pollution identified by Magnetic and Elemental Analysis of Roadside Tree Leaves. Atmospheric Environment 42 (2), 364–373.

Maher B. A. and Thompson R. (1999).Quaternary climates, environments and magnetism. Cambridge University Press: Cambridge, UK; New York.

Maher B. A. (1988). Magnetic Properties of some Synthetic Sub-micron Magnetites. Geophysical Journal, 94, 83-96.

Maher, B. A. (1986). Characterization of Soils by Mineral Magnetic Measurements.Physics of the Earth and Planetary Interiors, 42, 76– 92.

Maria J., Agata H., Magdalena K., Barbara K., Anatotiy S., Ksenija B. and Zhana M. (2008).Magnetic Structure of Polluted Soil Profiles from Eastern Ukraine. Acta Geophysica DOI: 10.2478/s11600-008-0036-8.

Martínez C. E. and Motto H. L, (2000).Solubility of Lead, Zinc and Copper added to Mineral Soils. Environmental Pollution, vol. 107, no. 1, pp. 153–158

Matzka J. and Maher B. A. (1999). Magnetic Bio-monitoring of Roadside Tree Leaves: Identification of Spatial and Temporal Variations in Vehicle-derived Particulates. Atmospheric Environment 33, 4565–4569.

Magiera T., Stryszcz Z., Kapička A., Petrovský E. (2006). Discrimination of Lithogenic and Anthropogenic influences on Topsoil Magnetic Susceptibility in Central Europe. Geoderma, 130, 299-311.

Michal S. B. (2012). Application of Magnetic, Geochemical and Micro-morphological Methods in Environmental Studies of Urban Pollution Generated by Road Traffic.PhD Dissertation, Department of Physics, University of Helsinki.

Miguel A.G., Cass G.R., Glovsky M.M., and Weiss J., (1999).Allergens in Paved Road Dust and Airborne Particles.*Environmental Science and Technology*, 33, 4159–4168.

Mihaljevic M. (1999). Zinc. In: C. P. Marshall & R. W. Fairbridge (eds.), Encyclopedia of Geochemistry. Kluwer Academic Publisher, Dordrecht, Germany.674-675.

Minyuk P. S., Subbotnikova T. V., Brown L. L., and Murdock K. J. (2012). Thermomagnetic Properties of Vivianite Nodules, Lake El'gygytgyn, Northeast Russia, Clim. Past Discuss., 8, 4989– 5027, doi:10.5194/cpd-8-4989-2012.

Mitra A.P. and Sharma C. (2002). Indian aerosols: present status. *Chemosphere*, 49(9), 1175-1190.

Mitsuo Y., Ifihar M. K., Mirza N. A. and Huma A. (1998). Magnetic Propertices of Suspended Particulate Matter (SPM) in Atmosphere; Proceedings of the 8th Symposium on Geo-Environments and Geo-Technices, Page 235-240.

Mohammed E. B., Barakat A, Agouriane E, Sajieddine M (2010) Soil magnetic susceptibility as a proxy to detect urban pollution in Beni Mellal City (Morocco). In: 10e`me Confe´rence Internationale en Physique de la Matie`re Condense´e et Physique Statistique, Beni Mellal, 25–26 , p 92

Mohamed E. B., Khalid J., Ahmed B. and Yahya B. (2011).Magnetic Susceptibility and Heavy Metal Contamination in Agricultural Soil of Tadla plain.*J. Mater. Environ. Sci. 2 (S1) (2011) 513-519*

Mohammed M. S. (2012). Bio-monitoring of Particulates Matter by Magnetic Properties of Ulmus carpiniflolia Leaves. African Journal of Biotechnology, 11 (73), 13827-13830.

Mooney H. M. and Bleifuss R. (1953).Magnetic Susceptibility Measurements in Minnesota. Part II: analysis of field results. Geophysics XVIII, 383-93.

Morawska L. and (Jim) Zhang J. (2002).Combustion Sources of Particles. 1. Health Relevance and Source Signatures. *Chemosphere*, 49, 1045–1058.

Moreno E., Sagnotti L., Turrell J., Winkler A. and Cascella A. (2003). Biomonitoring of Traffic Air Pollution in Rome using Magnetic Properties of Tree Leaves. Atmospheric Environment 37, 2967–2977.

Morris W. A., Versteeg J. K., Bryant D.W., Legzdins A. E., Mccarry B. E. and Marvin, C. H. (1995). Preliminary Comparisons between Mutagenicity and Magnetic Susceptibility of Respirable Airborne Particulate.Atmospheric Environment 29, 3441–3450.

Mukaka M. M. (2012). A guide to appropriate use of correlation coefficient in medical research.Malawi Med Journal; vol 24; pp 69–71.

Mullins, C. E. (1977). Magnetic Susceptibility of the Soil and its Significance in Soil Science: A review. Journal of Soil Science, 28, 223– 246

O'Reilly.W. (1976). Magnetic Mineral in the Crust of the Earth. Reports Prg. Phys., 39, 857-908.

Oches E. A. and Banerjee S. K. (1996). Rock-magnetic proxies of climate change from loess-paleosol sediments of the Czech Republic. Stud. Geophys.Geodaet., 40, 287-300.

Oniku, S. A., Osazuwa, I. B. And Meludu, O. C. (2008).Preliminary Report On Magnetic Susceptibility Measurements on Rocks Within The Zaria Granite Batholith, Nigeria. Geofizika, 25(2), 203-213.

Ozdemir O. and Dunlop D. J. (1998).Single-domain-like behavior in a 3-mm natural single crystal of magnetite. Journal of Geophysical Research, 103(B3): 2549-2562.

Palmgren F., Waahlin P., Kildesó J., Afshari A. and Fogh C. L. (2003).Characterisation of Particle Emissions from the Driving Car Fleet and the Contribution to Ambient and Indoor Particle Concentrations. Phys. Chem. Earth, 28: 327-334.

Parthasaradhy P. and Ranganayakulu S. V. (2014). Hysteresis and Eddy Current Losses of Magnetic Material by Epstein frame method-novel approach. International Journal of Engineering and Science; pp 85-93.

Perera F.P. (2008). Children are likely to suffer from our fossil fuel addiction. *Environmental Health Perspectives*, 116(8) 987-990.

Peters N.E., Meyers T.P. and Aulenbach B.T. (2002). Status and Trends in Atmospheric Deposition and Emissions near Atlanta, Georgia, 1986–99.*Atmospheric Environment*, 36(10) 1577-1588.

Petrovsky E. and Ellwood B.B. (1999).Magnetic Monitoring of Pollution of Air, Land and Waters. In: Maher, B.A., Thompson, R. (Eds.), Quaternary Climates, Environments and Magnetism. Cambridge University Press, Cambridge, 279– 322.

Petrovsky E., Kapicka A., Zapletal K., Sebestova E., Spanila T., Dekkers M.J., and Rochette P. (1998). Correlation between Magnetic Parameters and Chemical Composition of Lake Sediments from Northern Bohemia - Preliminary Study. Physics and Chemistry of the Earth, 23, 1123–1126.

Petrovsky E., Kapicka A., Jordanova N. and Boruvka L. (2001). Magnetic Properties of Alluvial Soils Contaminated with Lead, Zinc and Cadmium. Journal ofApplied Geophysics.48: 127-136.

Pope C.A., Burnett R.T., Thun M.J., Calle E.E., Krewski D., Kazuhiko, I. and Thurston, G.D. (2002). Lung Cancer, Cardiopulmonary Mortality, and Long-term: Exposure to Fine Particulate Air Pollution. Journal of American Medical Association 287, 1132–1141.

Pöschl U. (2005). Atmospheric Aerosols: Composition, Transformation, Climate and Health Effects. *Angewandte Chemie International Edition*, 44, 7520–7540.

PreetzH., Altfelderb S., Volker Henningsb V. and Igela J.(2009). Classification of Soil Magnetic Susceptibility and Prediction of Metal Detector performance – case study of Angola.Proc. of SPIE Vol. 7303 730313-1.

Puranen R. (1977). Magnetic Susceptibility and its Anisotrophy in the study of Glacial Transport in northern Finland. In *Prospecting in areras of Glaciated Terrain, L. K. Lawrence (ed)*, 111-19. London: Institution of Mining and Metallurgy.

Rai U. N., Dwivedi S., Tripathi R. D. Shukla O. P. and Singh N. K. (2005). Algal Biomass: An Economical Method for Removal of Chromium from Tannery Effluent Bulletin of Environmental Contamination and Toxicology, 75:297–303.

Reimann C, de Caritat P. (1999). Chemical elements in the environment— factsheets for the geochemist and environmental scientist.Berlin, Germany7 Springer-Verlag; 1998.ISBN 3-540-63670-6.

Ricci P.F., Catalano J.A. and Kelsh M.D. (1996). Time series (1963–1991) of Mortality and Ambient Air Pollution in California: An Assessment with Annual Data. *Inhalation Toxicology*, 9, 95–106.

Rose A. W., Hawkes H. E. and Webb J. S. (1979).Geochemistry in Mineral Exploration. Academic Press, New York, N.Y., pp. 490-517.

Salonen R.O., Halinen A.I., Pennanen A.S., Hirvonen M.-R., Sillanpaa M., Hillamo R., Shi T., Borm P., Sandell E., Koskentalo T. and Aarnio P., (2004). Chemical and in Vitro Toxicologic Characterization of Wintertime and Springtime Urban-air Particles with an Aerodynamic Diameter below 10 µm in Helsinki.*Scandinavian Journal of Work, Environmentand Health*, 30, 80–90.

Sangode S. J., Vhatkar K., Patil S. K., Meshram D. C., Pawar N. J., Gudadhe S. S., Badekar A. G and Kumararel V. (2010). Magnetic Susceptibility Distribution in the Soil of Pune

Metropolitan Region: Implications to Soil Magnetometry of Anthropogenic Loading. Current Science, 98, (4) 516-527.

Schmidt A., Yarnold R., Hill M. and Ashmore M. (2005). Magnetic Susceptibility as Proxy for Heavy Metal Pollution: A site study, Journal of Geochemical Exploration 85: 109–117.

Scholger R. (1998). Heavy metal Pollution Monitoring by Magnetic Susceptibility Measurements applied to Sediments of the River Mur (Styria, Austria). European Journal of Environmental and Engineering Geophysics 3, 25–37.

Schon, J. H. (1996). Physical Properties of Rocks: Fundamentals and Principle of Petrophysics. In Klaus, H. and Sven, T. (Eds): Handbook of geophysical exploration, Vol.18, Pergamon Press, London, 583.

Schwartz J., Dockery D. W. and Neas L. M. (1996). Is daily mortality associated specifically with fine particles? Journal of Air and Waste Management Association, 46, 927-939.

Seaton A., MacNee W. and Donaldson K. (1995).Particulate Air Pollution and Acute Health Effects. Lancet 345, 176–178.

Semelova V., Fialova H., Kapička A. and Kacalek D. (2009).Magnetometric Method as a Tool of Measuring Pollution of Forest Soils by Heavy Metals – Example of the Orlické Hory Mts. Lesnícky časopis – Forestry Journal ročnik 55, čislo 4, 385–393.

Sharma A. P. and Tripathi B.D. (2008).Magnetic Mapping of Fly-ash Pollution and Heavy Metals from Soil Samples around a Point Source in a dry Tropical Environment.Env.Monit. Assess, 138, 31−39.

Shen M. J., Hu S. Y. and Blaha U. (2006).A magnetic study of a polluted soil profile at the Shijingshan industrial area, Western Beijing, China. Chinese Journal of Geophysics. (in Chinese), 49(6): 1665-1673.

Shenggao L., Hongyan W. and Junling G. (2010). Magnetic response of heavy metals pollution in urban soils: magnetic proxy parameters as an indicator of heavy metals pollution. 19th World Congress of Soil Science, Soil Solutions for a Changing World 1 – 6 August 2010, Brisbane, Australia.

Shilton V.F., Booth C.A., Smith J.P., Giess P., Mitchell D.J. and Williams, C.D. (2005).Magnetic Properties of Urban Street Dust and their Relationship with Organic Matter Content in the West Midlands, UK.*Atmosphercic Environment*, 39, 3651–3659.

Spiteri C., Kalinski V., Rösler W., Hoffmann V. and Appel, E. (2005). Magnetic Screening of a Pollution Hotspot in the Lausitz area, Eastern Germany: Correlation Analysis between

Magnetic Proxies and Heavy Metal Contamination in Soils, *Environmental Geology, 49 (1),* 1-9.

Sioutas C., Delfino R.J., and Singh M. (2005).Exposure Assessment for Atmospheric Ultrafine Particles (UFPs) and Implications in Epidemiologic Research.*Environmental HealthPerspectives*, 113, 947–955.

Smith L.A., Means J. L. and Chen A. (1995). Remedial Options for Metals-Contaminated Sites.Lewis Publishers, Boca Raton, Fla, USA.

Snowball I.F. and Thompson R. (1988).The Occurrence of Greigite in Sediments from Loch Lomond.*Journal of Quaternary Science*, 3, 121-125.

Sternbeck J., Sjödin Å., and Andréasson K. (2002). Metal Emissions from Road Traffic and the influence of Re-suspension; results from two tunnel studies. *Atmospheric Environment*, 36, 4735–4744.

Sutherland R. A. and Tolosa C.A. (2000).Multi-element analysis of road-deposited Sediment in an Urban Drainage Basin, Honolulu, Hawaii.*Environmental Pollution*, 110(3), 483-495.

Sylwia K. D. (2014). The use of Magnetic Method to Study the Spread of Anthropogenic Pollution in Model Soil Profiles-Preliminary Results.Castle Meeting New trends on Paleo, Rock and Environmental Magnetism.

Strzyszcz Z. and Magiera T. (1993) Distribution of Ferromagnetics in Forest Soils of some Polish German Regions in Relation to their Origin. Mitteilungen der Deutschen Bodenkundlichen Gesellschaft, v 72:1309–1312.

Strzyszcz Z. and Magiera T. (1998).Magnetic Susceptibility and Heavy Metal Contamination in Soil of Southern Poland. Physics and Chemistry of the Earth, 23; 9-10; 1127-1131.

Tadeusz S., Michal G., Bogumil G., Katarzyna B., Ryszard S., Marzena T. and Monika S. (2013). Chemical, Magnetic and Mossbauer Effect Analysis of Road dust from Expreeway. Nukleonika, 58(1): 109-112.

Tarling D.H. (1971). Gondwanaland, Palaemagnetism and Continental Drift. Nature, 229; 17-21.

Thompson R. and Oldfield F. (1986). Environmental Magnetsim, George Allen and Unwin, London.

Verosub K. L. and Roberts A. (1995). Environmental Magnetism: Past, Present and Future. Journal of Geophysical Research, 100, 2175-2192.

Vassilev S. (1992). Phase Mineralogy Studies of Solid Waste Products from Coal burning at some Bulgarian Thermoelectric Power Plants. Fuel, 71, 625-633.

Walden J., Oldfield F. and Smith J. P. (1999).*Environmental Magnetism: A Practical Guide.* Quaternary Research Association, London.

Wehland F., Panaiotu C., Appel E., Hoffmann V., Jordanova D. Jordanova N. and Denut I. (2002). The Dam Breakage of Baia Mare - A Pilot Study of Magnetic Screening. Physics and Chemistry of the Earth 27, 1371–1376.

Williams R.D. and Cooper J.R. (1990). Location Soil Boundary using Magnetic Susceptibility. Soil Science; 150(6); 889-895.

Wolfers P., Fillion G., Ouladdiaf B., Ballou R., and Rochette P. (2011).The Pyrrhotite 32K Magnetic Transition. Solid State Phenomenon, 170, 174-179.

Wróbel A., Rokita E., and Maenhaut W., (2000).Transport of Traffic-related Aerosols in Urban Areas.*Science of the Total Environment*, 257, 199–211.

Yang T, Liu Q, Chan L,andCao G. (2007).Magnetic investigation of heavy metals contamination in urban topsoils around the East Lake, Wuhan, China. Geophys J Int 171:603–612.

Yang T., Liu Q., Li H., Zeng Q. and Chan L. (2010) Anthropogenic Magnetic Particles and Heavy Metals in the Road dust: Magnetic identification and its implications. *Atmospheric Environment*, 44(9), 1175-1185.

Yin J., Allen A.G., Harrison R.M., Jennings S.G., Wright E., Fitzpatrick M., Healy T., Barry E., Ceburnis D. and McCusker D. (2005).Major Component Composition of Urban PM10 and PM2.5 in Ireland.*Atmospheric Research*, 78(3- 4), 149-165.

Yoshida, M. and Gautam.P. (1988). Magnetostratigraphy of Plio-Pleistocene Lacustrine Deposits in the Kathmandu Valley, central Nepal. Proc. Indian Natural Science Academy. 3, 410-417.

Zawadzki, J., Magiera, T., Fabijańczyk, P., & Kusza, G. (2012).Geostatistical 3-dimensional integration of measurements of soil magnetic susceptibility. *Environmental Monitoring and Assessment, 184*(5), 3267–3278.

Zananiri I., Kondopoulou D. and Spassov S. 2010. The application of environmental magnetism techniques for pollution assessment in urban and suburban areas in Greece: State of the art and case studies, Bull. Geol. Soc. Greece, XLIII/4, 1972-1982.

Zhang C., Huang B., Li Z. and Liu, H. (2006).Magnetic Properties of Highroad-side Pine Tree Leaves in Beijing and their Environmental Significance. Chinese Science Bulletin, 51(24):3041-3052.

Zhao H., Li X., Wang X. and Tian D. (2010). Grain size Distribution of Road-Deposited Sediment and its Contribution to Heavy Metal Pollution in Urban run-off in Beijing, China. *Journal of Hazardous Materials*, 183(1–3), 203-210.

APPENDIX A Magnetic Susceptibility Data obtained along Roads in Central District

Distance along the Road (m)	Distance from the Road (m)	Magnetic Susceptibility X10^-6 SI CA1	Magnetic Susceptibility X10^-6 SI CA2	Magnetic. Susceptibility X10^-6 SI CA3	Magnetic Susceptibility X10^-6 SI CA4
0	0	435.7	546.5	456.3	245.0
10	0	477.5	478.5	365.4	233.8
20	0	487.7	534.8	466.9	276.4
30	0	497.4	488.5	452.7	277.6
40	0	534.8	543.2	466.3	301.4
50	0	618.4	499.6	431.2	299.6
60	0	477.3	512.7	421.0	314.2
70	0	452.8	494.3	342.8	278.4
80	0	567.4	398.6	365.4	289.5
90	0	546.3	400.7	411.8	304.7
0	1	436.8	577.5	478.3	264.3
10	1	478.6	503.7	423.1	309.8
20	1	523.1	555.1	476.5	298.5
30	1	534.1	503.9	466	365.1
40	1	512.9	565.9	435.2	354.2
50	1	578.4	500.4	455.3	345.2
60	1	487.5	536.9	433.4	345.4
70	1	466.7	501.4	435.2	356.4
80	1	577.2	485.4	389.6	300.5
90	1	546.7	412.5	456.4	303.9
0	2	434.3	521.8	527.4	364.9
10	2	476.4	436.5	462.8	275.1
20	2	509.7	478.5	465.4	288.9
30	2	521.8	498.6	471.9	278.4
40	2	465.3	438.5	477	244.1
50	2	423.1	437.9	462	289.5
60	2	484.2	462.1	454.9	333.6
70	2	478.4	478.4	455.4	321.3
80	2	512.5	485.6	432.9	333.8
90	2	432.1	408.6	467.3	289.5
0	3	411.8	438.6	674.9	302.8
10	3	444.2	384.1	441.5	208.8
20	3	489.5	384.9	377.6	277.4
30	3	489.4	365.2	388.3	165.4
40	3	387.1	352.1	372.1	178.4
50	3	378.4	378.4	211	160

60	3	452.9	400.5	207.4	166
70	3	388.4	352.8	375.4	177.5
80	3	438.6	367.8	366.5	176.4
90	3	378.5	365.2	376.4	176.5
0	4	378.4	324.5	432.1	222.8
10	4	421.9	328.3	658.4	256.3
20	4	476.2	333.1	421.3	147.3
30	4	421.9	277.6	364.2	198.5
40	4	333.9	203.7	173.2	109.5
50	4	339.8	312.5	176.5	131
60	4	376.4	326.6	145	154.3
70	4	342.7	298.5	200.1	152.9
80	4	400.3	312.4	241	163.9
90	4	342.1	298.5	244.8	133
0	5	375.1	288.5	237.8	217.5
10	5	398.6	312.3	356.4	177.3
20	5	456.3	275.8	602	175.5
30	5	389.4	214	411.9	162.1
40	5	276.4	187.4	378.5	167.3
50	5	277.4	256.3	167.4	98.6
60	5	312.8	209.6	145.3	105.3
70	5	312.5	222.5	167.4	132.2
80	5	321.8	206.8	166.4	112.4
90	5	288.5	247.5	188.5	98.5
0	6	349.3	212.5	164.3	121.9
10	6	364.1	193.2	173.2	165.3
20	6	401.3	201.4	377	143.8
30	6	276.4	162.9	589.6	201.4
40	6	266.4	193.2	435.2	78.3
50	6	243.1	169.3	156.3	131.3
60	6	265.4	178.4	145.2	97.5
70	6	275.3	155.4	155.4	78.5
80	6	277.4	183.2	138.8	102.7
90	6	213.8	183.7	143.2	105.9
0	6	287.4	175.9	133.9	78.4
10	7	308.9	166.5	155.3	105.9
20	7	378.5	199.5	284.3	123.2
30	7	244.3	145.6	365.2	110.2
40	7	243.1	177.4	623.2	146.3
50	7	194.2	171.4	177.3	68.9
60	7	222.4	141.9	143.8	104.7
70	7	243.8	146.3	136.5	
80	7	204.7	138.6	121.4	

90	7	165.3	162.1	123.5
0	8	263.9		133.8
10	8	277.4		147.2
20	8	345.2		183
30	8	201.4		251.8
40	8	189.4		367.4
50	8	162.8		121.4
60	8	199.5		126.8
70	8	196.3		123.2
80	8	187.4		110.7
90	8	134.7		111.4
0	9	243.6		
10	9	238.4		
20	9	301.7		
30	9	198.4		
40	9	177.4		
50	9	137.9		
60	9	166.3		
70	9	183.5		
80	9	166.3		
90	9	122.1		
0	10	224.7		
10	10	238.4		
20	10	267.4		
30	10	209.8		
40	10	162.9		
50	10	112.4		
60	10	173.9		
70	10	185.3		
80	10	184.9		
90	10	118.4		
0	11	198.5		
10	11	187.9		
20	11	212.6		
30	11	183.7		
40	11	143.2		
50	11	100.4		
60	11	152.4		
70	11	210.6		
80	11	152.6		
90	11	147.9		
0	12	158.4		
10	12	165.3		

20	12	200.4
30	12	177.3
40	12	138.5
50	12	111.4
60	12	144.7
70	12	173.9
80	12	144.8
90	12	100.4

APPENDIX B Magnetic Susceptibility Data obtained along Roads in Garki District

Distance along the Road (m)	Distance from the Road (m)	Magnetic Susceptibility $X10^{-5}$ SI G_1	Magnetic Susceptibility $X10^{-5}$ SI G_2	Magnetic. Susceptibility $X10^{-5}$ SI G_3	Magnetic Susceptibility $X10^{-5}$ SI G_4
0	0	431.7	398.5	543.7	555.4
10	0	444.6	387.6	533.9	543.9
20	0	431.7	376.2	489.7	526.8
30	0	462.6	345.2	521.7	436.9
40	0	463.9	453.6	492.4	477.2
50	0	411.0	365.8	565.7	436.7
60	0	399.6	435.2	485.5	522.7
70	0	434.7	425.7	531.8	432.4
80	0	389.6	378.3	488.4	453.6
90	0	428.6	406.6	521.7	522.4
0	1	426.3	423.8	523.9	647.3
10	1	418.6	411.3	511.8	566.8
20	1	365.1	389.5	563.7	544.2
30	1	423.7	412.4	511.3	533.9
40	1	369.3	342.6	422.1	435.6
50	1	423.9	433.2	463.2	345.2
60	1	356.9	475.9	456.2	435.3
70	1	421.8	412.4	512.8	453.8
80	1	356.4	367.4	478.3	411.3
90	1	364.9	352.1	523.0	467.4
0	2	356.4	341.7	366.1	589.5
10	2	324.3	378.5	376.8	526.9
20	2	342.1	321.4	276.4	511.0
30	2	418.5	341.9	273.9	286.0
40	2	322.4	412.8	277.4	381.0
50	2	367.4	400.8	265.3	319.0
60	2	342.1	367.5	266.1	355.2
70	2	265.8	367.3	310.8	412.8
80	2	274.9	264.8	254.3	377.2
90	2	264.9	248.6	341.8	413.2
0	3	312.0	287.5	265.9	435.9
10	3	264.9	254.3	288.6	466.7
20	3	311.0	233.8	178.4	364.8
30	3	361.9	265.3	201.8	245.3
40	3	310.4	233.8	174.3	333.5
50	3	331.7	333.8	201.3	253.7
60	3	263.9	273.9	176.3	241.9

70	3	218.5	233.5	222.7	276.4
80	3	243.1	211.6	128.3	321.4
90	3	231.8	176.5	176.3	344.2
0	4	243.2	223.7	565.0	277.1
10	4	216.4	192.6	534.2	312.6
20	4	259.3	178.4	522.8	231.7
30	4	333.9	176.9	511.7	213.8
40	4	263.9	231.5	498.7	263.2
50	4	273.6	256.4	488.6	219.7
60	4	175.9	361.7	500.8	228.7
70	4	173.9	162.1	151.9	234.8
80	4	222.5	156.3	478.5	246.3
90	4	221.7	132.1	407.3	319.8
0	5	164.8	143.8	379.3	164.8
10	5	153.0	149.5	276.4	200.9
20	5	222.8	132.1	201.4	166.4
30	5	267.3	133.9	200.9	178.6
40	5	177.3	167.5	178.4	212.7
50	5	133.2	200.5	263.2	178.5
60	5	143.6	243.9	211.5	174.9
70	5	166.2	122.4	478.4	221.1
80	5	158.4	121.7	208.8	231.8
90	5	201.9	113.6	312.7	260.9
0	6	112.8	275.9	176.3	134.2
10	6	131.7	235.1	176.3	131.7
20	6	167.3	277.3	103.0	132.0
30	6	213.8	278.5	143.2	152.6
40	6	130.2	289.6	146.7	167.4
50	6	117.8	175.0	142.1	147.7
60	6	133.5	276.9	102.3	144.8
70	6	121.8	264.8	251.8	178.4
80	6	152.5	267.3	153.2	216.6
90	6	143.9	274.3	178.4	238.4
0	6	100.8	127.4	122.7	121.5
10	7	98.7	122.5	107.3	116.0
20	7	141.9	138.4	82.7	119.7
30	7	187.5	117.4	127.5	137.5
40	7	100.0	217.5	107.5	131.8
50	7	98.0	167.4	113.8	133.2
60	7	99.0	165.6	92.5	117.5
70	7	109.5	135.7	173.9	120.6
80	7	109.6	125.8	111.0	163.9
90	7	132.1	134.2	120.6	170.0

0	8	89.5	98.5	110.9
10	8	87.5	104.8	126.5
20	8	121.9	111.9	114.8
30	8	144.2	104.2	108.7
40	8	101.3	118.2	103.2
50	8	104.0	121.6	104.8
60	8	78.8	144.0	101.2
70	8	76.0	109.4	113.4
80	8	93.2	111.0	120.0
90	8	104.2	93.7	143.8

APPENDIX C Magnetic Susceptibility Data obtained along Roads in Wuse District

Distance along the Road (m)	Distance from the Road (m)	Magnetic Susceptibility $X10^{-5}$ SI W_1	Magnetic Susceptibility $X10^{-5}$ SI W_2	Magnetic. Susceptibility $X10^{-5}$ SI W_3	Magnetic Susceptibility $X10^{-5}$ SI W_4
0	0	675.9	666.3	705.8	473
10	0	684.3	577.4	689.4	504.8
20	0	655.9	632.8	718.5	488.4
30	0	657.4	643.8	704.8	472.4
40	0	558.9	577.3	669	521.4
50	0	677.4	583.2	673.2	477.4
60	0	583.5	512.8	683.2	536.3
70	0	673.2	477.3	731	495.3
80	0	627.4	470.4	699.4	512.4
90	0	599.8	466.4	678.4	504.8
0	1	643.8	574.9	678.4	452.8
10	1	657.6	583.9	653.7	467.3
20	1	678.6	547.8	673.9	480.5
30	1	633.9	622.9	677.4	436.8
40	1	536.4	643.2	632.1	456.3
50	1	634.2	538.3	633.1	421
60	1	577.5	473.9	641.9	464.2
70	1	644.7	438.5	673.9	401.2
80	1	619.5	421.9	639.7	453.2
90	1	600.4	421.9	578.4	436.2
0	2	677.5	521.8	643.8	410.7
10	2	637.5	525.3	544.3	437.5
20	2	633.2	538.4	633.1	378.5
30	2	567.4	548.0	573.6	361.0
40	2	438.5	534.9	564.3	412.0
50	2	533.7	462.9	560.3	382.4
60	2	437.5	423.1	611.2	378.4
70	2	611.4	444.2	641.9	351.4
80	2	612.8	388.4	563.2	377.0
90	2	612.4	378.4	521.5	377.1
0	3	665.2	463.8	611.9	364.9
10	3	599.0	462.1	519.8	370.0
20	3	578.5	462.8	572.9	331.7
30	3	528.5	512.8	513.7	322.9
40	3	411.8	478.3	520.4	388.4
50	3	487.5	444.5	538.2	274.0
60	3	389.5	377.4	583.0	284.3

70	3	577.5	377.4	539.7	251.8
80	3	539.5	352.7	487.9	315.2
90	3	548.6	344.1	472.0	307.8
0	4	547.6	412.8	453.9	328.5
10	4	531.8	400.0	435.9	342.1
20	4	539.0	467.2	511.4	273.8
30	4	466.8	437.5	437.2	254.3
40	4	328.5	439.0	477.5	341.4
50	4	451.9	373.6	473.8	231.6
60	4	364.5	274.9	519.4	261.0
70	4	549.0	352.1	476.1	204.8
80	4	519.0	311.4	451.3	264.2
90	4	518.5	298.4	420.0	241.0
0	5	532.1	388.4	452.8	266.8
10	5	453.9	378.4	411.7	264.3
20	5	522.8	429.6	455.9	230.9
30	5	431.7	387.5	421.9	231.9
40	5	277.5	330.4	378.4	274.7
50	5	433.5	328.4	466.1	200.4
60	5	329.5	213.2	456.3	183.8
70	5	487.5	219.4	422.5	172.7
80	5	477.3	207.4	378.4	201.8
90	5	463.8	197.3	382.5	200.0
0	6	423.9	346.2	388.5	213.7
10	6	411.8	322.7	363.7	244.8
20	6	466.9	372.9	414.7	179.3
30	6	369.5	273.9	353.0	183.0
40	6	285.9	276.4	349.0	233.8
50	6	376.5	277.4	388.4	183.2
60	6	270.5	189.4	387.5	164.0
70	6	437.5	175.4	380.5	153.0
80	6	438.5	173.2	356.4	166.4
90	6	411.7	156.3	363.1	176.4
0	6	367.5	322.8	321.7	
10	7	387.5	256.4	342.1	
20	7	426.5	261.4	355.0	
30	7	338.2	216.4	312.7	
40	7	234.5	249.0	312.8	
50	7	311.3	206.0	319.5	
60	7	253.0	164.8	329.7	
70	7	411.8	134.4	361.4	
80	7	419.5	134.0	278.4	
90	7	382.0	144.3	287.0	

0	8	344.9	257.3	337.6
10	8	312.8	239.0	309.7
20	8	364.9	230.0	304.8
30	8	273.2	183.9	277.4
40	8	221.1	163.2	307.5
50	8	264.3	183.9	300.8
60	8	222.9	138.4	278.5
70	8	378.5	122.4	289.4
80	8	374.6	121.8	241.9
90	8	352.1	110.8	238.0
0	9	209.6		
10	9	277.4		
20	9	333.0		
30	9	266.4		
40	9	208.5		
50	9	233.2		
60	9	189.5		
70	9	362.1		
80	9	327.4		
90	9	274.9		
0	10	178.6		
10	10	253.5		
20	10	263.7		
30	10	212.8		
40	10	177.4		
50	10	102.5		
60	10	164.0		
70	10	277.4		
80	10	200.8		
90	10	163.0		

APPENDIX D Magnetic Susceptibility Data obtained along Roads in Maitama District

Distance along the Road (m)	Distance from the Road (m)	Magnetic Susceptibility $X10^{-5}$ SI M_1	Magnetic Susceptibility $X10^{-5}$ SI M_2	Magnetic. Susceptibility $X10^{-5}$ SI M_3	Magnetic Susceptibility $X10^{-5}$ SI M_4
0	0	342.6	432.3	231.6	276.4
10	0	332.9	421.4	241.4	241.3
20	0	278.4	382.1	204.8	273.8
30	0	301.3	375.4	224.8	233.7
40	0	321.4	366.2	247.5	231.8
50	0	333.0	324.7	251.4	241.3
60	0	317.5	317.5	226.4	226.4
70	0	299.6	307.4	231.8	241.3
80	0	314.3	285.9	247.4	276.4
90	0	338.5	231.6	237.4	251.7
0	1	276.4	411.3	178.4	214.4
10	1	243.1	417.4	204.8	209.5
20	1	231.4	362.7	183.8	212.0
30	1	288.4	341.7	195.2	194.3
40	1	257.4	321.4	300.8	207.0
50	1	279.0	301.4	213.8	207.5
60	1	222.4	301.3	199.6	199.6
70	1	235.6	268.3	163.0	222.8
80	1	267.4	244.7	208.7	204.4
90	1	289.0	178.5	178.5	206.3
0	2	201.4	400.9	132.1	182.0
10	2	184.3	403.0	164.3	145.2
20	2	204.3	312.4	153.8	177.1
30	2	231.4	312.6	164.2	162.8
40	2	212.7	300.0	278.4	173.2
50	2	231.4	267.4	175.3	188.4
60	2	182.5	264.2	172.5	172.5
70	2	200.8	241.9	121.4	162.1
80	2	213.9	212.9	183.2	138.2
90	2	201.9	152.5	147.8	178.3
0	3	156.3	378.5	109.8	156.3
10	3	144.2	356.3	138.5	103.8
20	3	167.4	309.5	121.4	121.8
30	3	183.9	309.5	128.7	121.9
40	3	157.3	267.4	217.5	139.0
50	3	203.8	231.4	136.0	132.8
60	3	123.5	230.9	148.7	148.7

70	3	175.9	177.3	114.9	122.3
80	3	189.5	175.9	147.3	110.5
90	3	182.1	113.5	113.5	144.2
0	4	132.1	374.2	99.3	110.9
10	4	106.3	367.4	102.8	90.4
20	4	98.5	301.4	108.4	102.4
30	4	134.2	283.8	93.7	108.4
40	4	112.3	254.3	174.0	103.7
50	4	185.9	212.9	120.5	104.8
60	4	95.0	210.4	102.6	102.6
70	4	124.1	136.2	109.5	100.4
80	4	145.3	132.9	129.0	108.0
90	4	132.9	98.6	109.4	109.4
0	5	90.4	364.5	81.3	98.0
10	5	78.4	353.9	74.3	83.2
20	5	78.4	278.4	88.3	97.4
30	5	109.5	237.4	80.5	100.8
40	5	87.5	221.8	130	93.8
50	5	138.4	178.4	90.6	100.4
60	5	76.9	163.2	100.5	100.5
70	5	109.5	123.1	96.3	94.8
80	5	118.6	100.3	104.2	79.4
90	5	107.6	87.3	87.3	91.0
0	6	76.5	363.6	73.9	
10	6	67.3	324.9	70.3	
20	6	74.1	267.4	78.4	
30	6	89.0	212.3	77.4	
40	6	67.9	209.5	112.3	
50	6	105.2	167.4	84.3	
60	6	67.0	134.2	95.4	
70	6	82.0	109.0	78.5	
80	6	98.9	93.8	81.3	
90	6	91.3	75.0	78.2	
			360.5	70.4	
			312.6	70.2	
			253.7	70.4	
			200.7	69.0	
			198.7	82.4	
			134.2	81.8	
			121.8	70.0	
			79.4	70.4	
			89.6	76.4	
			74.0	76.4	

APPENDIX EMagnetic Susceptibility Data obtained along Roads in Asokoro District

Distance along the Road (m)	Distance from the Road (m)	Magnetic Susceptibility $X10^{-5}$ SI A_1	Magnetic Susceptibility $X10^{-5}$ SI A_2	Magnetic. Susceptibility $X10^{-5}$ SI A_3	Magnetic Susceptibility $X10^{-5}$ SI A_4
0	0	187.4	209.7	178.5	124.0
10	0	195.4	206.4	187.4	139.4
20	0	189.5	204.3	194.3	133.0
30	0	183.9	194.7	186.5	131.8
40	0	193.7	193.7	189.5	127.5
50	0	190.5	210.5	184.3	130.4
60	0	195.3	209.5	194.3	131.3
70	0	184.3	204.8	188.5	125.4
80	0	195.0	198.0	184.3	130.4
90	0	185.7	203.5	175.4	122.6
0	1	167.3	234.2	146.3	109.7
10	1	162.8	225.4	153.8	128.5
20	1	155.2	230.7	167.5	123.9
30	1	166.4	228.5	163.0	116.3
40	1	167.4	231.8	165.5	104.0
50	1	167.3	241.9	163.2	103.7
60	1	177.2	239.5	177.5	118.7
70	1	153.8	236.5	174.3	100.7
80	1	167.4	231.5	156.3	112.4
90	1	163.2	241.5	162.9	109.0
0	2	109.4	209.4	103.8	78.3
10	2	121.0	201.8	121.8	98.6
20	2	131.8	206.4	142.8	89.8
30	2	127.3	203.8	134.5	101.6
40	2	152.9	209.4	137.5	102.1
50	2	131.5	212.4	131.8	98.4
60	2	136.7	213.5	140.9	101.3
70	2	121.8	214.7	164.3	100.4
80	2	142.1	203.5	134.2	109.4
90	2	145.3	213.8	127.5	93.7
0	3	104.2	174.9	97.5	72.9
10	3	100.4	167.4	109.5	94.4
20	3	106.4	167.4	121.5	85.4
30	3	111.9	174.3	121.5	94.3
40	3	133.0	184.5	129.9	95.2
50	3	113.0	182.4	104.8	96.4
60	3	129.3	167.4	136.4	92.1
70	3	109.5	178.5	142.9	89.4

80	3	121.8	165.2	130.5	99.4
90	3	127.5	177.5	106.3	87.6
0	4	91.8	142.1	79.7	71.9
10	4	82.9	138.5	84.2	84.2
20	4	94.5	132.6	109.5	80.9
30	4	111.8	130.9	106.4	90.6
40	4	112.8	139.8	105.8	91.1
50	4	109.6	169.7	100.5	91.9
60	4	109.4	142.1	104.7	83.1
70	4	93.1	151.5	121.1	84.2
80	4	100.3	132.1	132.1	87.4
90	4	104.5	142.1	98.7	70.3
0	5	88.4	102.6	77.9	70.8
10	5	80.5	108.5	78.4	78.4
20	5	87.8	102.9	92.4	80.1
30	5	83.7	110.6	97.9	81.4
40	5	93.7	118.2	100.5	84.2
50	5	105.3	132.1	94.3	81.9
60	5	76.5	109.8	78.6	78.4
70	5	85.3	102.5	103.8	80.4
80	5	78.0	109.7	109.7	81.3
90	5	96.4	109.6	85.4	60.7
0	6	75.2	98.6	77.5	70.5
10	6	76.5	100.9	75.4	75.4
20	6	80.5	97.5	87.5	79.4
30	6	72.1	98.4	85.1	80.4
40	6	85.0	109.9	99.5	80.4
50	6	95.0	109.5	88.2	80.3
60	6	74.3	97.0	75.8	74.9
70	6	73.0	77.6	85.0	74.9
80	6	76.4	83.2	83.2	76.3
90	6	88.6	90.7	69.0	60.1
					70.2
					72.3
					74.0
					78.5
					76.5
					73.2
					70.3
					67.1
					65.4
					59.7

Appendix F Low Frequency magnetic Susceptibility measurements along vertical soil profiles near road pavements

Sampling station	**WI**	**W2**	**W3**	**W4**	**C1**	**C2**	**C3**	**C4**	**G1**	**G2**	**G3**	**G4**	**A1**	**A2**	**A3**	**A4**	**M1**	**M2**	**M3**	**M4**
Depth (cm)	**Magnetic Susceptibility (x10^{-5}SI)**																			
0	620.7	570.4	660.2	575.8	540.8	430.4	450.2	430.6	540.3	576.3	465.7	432.8	239.8	243.7	211.7	207.4	341.0	343.8	303.0	231.6
5.0	489.5	376.5	589.5	507.4	511.4	390.5	383.2	276.4	350.1	601.8	271.3	278.4	171.3	213.5	165.0	93.8	189.5	177.4	269.6	154.6
10.0	296.4	299.7	322.7	349.8	258.7	231.3	202.0	199.8	198.7	241.3	178.9	178.4	129.8	98.9	100.0	85.4	145.6	91.4	187.8	102.7
15.0	199.7	191.3	240.9	243.1	362.4	167.8	372.8	165.3	146.3	101.8	126.7	126.3	111.9	157.4	162.7	68.9	99.7	80.9	127.6	86.4
20.0	189.3	153.2	201.5	160.5	150.3	119.0	351.2	151.8	118.9	106.2	99.6	98.7	78.6	124.6	123.1	60.2	96.5	81.2	71.4	63.0
25.0	154.2	100.8	189.7	503.3	103.9	108.4	319.2	100.0	109.8	97.6	91.8	87.9	64.3	100.9	98.6	55.3	102.5	81.3	63.2	51.3
30.0	103.8	80.7	121.7	94.2	98.7	103.2	297.6	99.8	97.8	94.0	78.6	76.3	50.8	70.7	70.7	50.8	95.4	78.5	52.1	40.2

Appendix G: Magnetic Susceptibility values obtained from different points within Abuja

Long.	Lat.	Low Frequency Magnetic Susceptibility at the surface	Low Frequency Magnetic Susceptibility at 10.0cm depth	Low Frequency Magnetic Susceptibility at 20.0cm depth	Low Frequency Magnetic Susceptibility at 30.0cm depth	Low Frequency Magnetic Susceptibility at 40.0cm depth	High Frequency Magnetic Susceptibility at the surface	High Frequency Magnetic Susceptibility at 30.0cm depth	Frequency Dependence at the surface (%)	Frequency Dependence at 30.0cm depth (%)
9.073681	**7.481779**	**465.3**	**378.0**	**271.5**	**130.6**	**121.5**	**459.7164**	**117.1482**	**1.2**	**10.3**
9.076213	7.484424	532.4	421.0	322.5	200.8	163.2	519.0900	181.9248	2.5	9.4
9.076808	7.482168	488.5	478.0	213.6	103.5	143.2	479.7070	93.3570	1.8	9.8
9.077341	7.484430	489.5	560.0	366.8	176.5	121.4	472.8570	159.7325	3.4	9.5
9.077341	7.479881	477.8	351.0	266.8	100.9	100.3	451.0432	91.1127	5.6	9.7
9.074972	7.476855	543.2	210.0	172.5	108.5	100.4	513.8672	98.8435	5.4	8.9
9.072683	7.474644	478.5	321.0	299.5	175.4	165.4	458.4030	168.0332	4.2	4.2
9.076198	7.474644	476.5	109.0	98.5	90.7	93.2	461.7285	79.9974	3.1	11.8
9.075275	7.471677	453.4	219.6	155.3	104.3	98.5	436.1708	93.9743	3.8	9.9
9.073363	7.470695	487.5	276.9	132.4	99.5	95.4	473.8500	91.0425	2.8	8.5
9.077671	7.462521	496.0	353.9	188.5	128.6	103.2	475.1680	118.5692	4.2	7.8
9.076429	7.462785	501.3	422.9	382.1	170.8	122.1	494.2818	156.1112	1.4	8.6
9.076677	7.459130	503.4	412.8	274.6	120.9	111.5	493.3320	110.6235	2.0	8.5
9.076812	7.458447	485.3	342.5	277.8	131.6	114.2	474.1381	121.2036	2.3	7.9
9.078598	7.453452	443.6	321.9	211.0	125.7	100.9	432.5100	115.2669	2.5	8.3
9.080819	7.455996	477.5	388.4	284.3	167.8	100.5	467.4725	151.5234	2.1	9.7
9.077560	7.447706	487.0	121.9	111.4	94.6	96.5	460.7020	86.5590	5.4	8.5
9.076572	7.443155	456.5	219.8	129.5	102.8	98.5	425.0015	94.9872	6.9	7.6
9.072470	7.440409	463.2	211.3	132.3	109.9	102.4	418.7328	102.3169	9.6	6.9
9.071697	7.440491	473.4	299.8	133.6	121.8	119.6	433.6344	111.3252	8.4	8.6
9.069964	7.445664	466.5	439.8	319.4	219.0	174.3	431.9790	197.9760	7.4	9.6
9.070632	7.444910	458.5	422.9	382.5	238.5	165.4	426.8635	218.2275	6.9	8.5
9.069228	7.446278	487.5	476.3	284.3	209.6	209.5	473.3625	193.6704	2.9	7.6
9.067384	7.449656	466.5	433.2	377.5	254.3	234.2	459.5025	228.1071	1.5	10.3
9.064804	7.446374	483.6	421.9	326.4	267.4	243.2	476.8296	233.4402	1.4	12.7

9.065094	7.445207	443.5	387.6	235.6	187.5	189.5	432.4125	184.1250	2.5	1.8
9.057507	7.465734	447.5	381.9	212.6	167.4	167.5	437.2075	146.6424	2.3	12.4
9.056496	7.459535	448.3	439.8	324.5	188.6	189.5	436.1959	162.3846	2.7	13.9
9.055051	7.459401	475.4	456.3	325.6	325.4	374.5	433.0894	296.4394	8.9	8.9
9.054770	7.462397	482.4	433.9	300.7	267.4	223.5	432.7128	239.8578	10.3	10.3
9.054442	7.471757	488.5	488.8	288.6	205.8	268.4	426.4605	179.6634	12.7	12.7
9.053280	7.478512	490.5	443.2	285.7	207.5	208.1	481.6710	203.7650	1.8	1.8
9.052837	7.480108	476.4	478.4	304.7	178.5	155.3	417.3264	156.3660	12.4	12.4
9.050811	7.477634	427.5	472.0	307.2	243.5	209.7	368.0775	209.6535	13.9	13.9
9.050589	7.481573	478.5	490.5	388.4	213.0	176.8	460.7955	202.9890	3.7	4.7
9.052186	7.482909	465.3	301.5	266.4	177.4	133.7	450.4104	165.3368	3.2	6.8
9.050230	7.484378	388.7	284.1	209.6	153.2	109.6	378.5938	142.0164	2.6	7.3
9.046001	7.482575	399.8	201.9	132.1	105.8	99.4	388.6056	98.4998	2.8	6.9
9.044127	7.479303	388.6	198.5	271.0	207.4	144.2	371.1130	189.5636	4.5	8.6
9.047006	7.489011	365.0	133.8	111.9	99.0	97.6	341.2750	89.5950	6.5	9.5
9.042339	7.486849	384.0	453.2	523.1	512.8	473.2	359.4240	473.8272	6.4	7.6
9.044761	7.486608	375.9	684.3	658.7	564.8	376.5	349.9629	528.6528	6.9	6.4
9.045516	7.486396	333.5	406.2	543.9	545.8	302.8	311.8225	500.4986	6.5	8.3
9.055305	7.499241	375.8	388.5	276.9	133.7	109.5	342.7296	122.2018	8.8	8.6
9.049093	7.508286	367.4	209.5	159.8	111.4	109.5	339.4776	100.7056	7.6	9.6
9.050606	7.511377	385.4	388.5	206.8	136.5	12.8	351.0994	124.3515	8.9	8.9
9.055149	7.504595	463.8	200.6	133.8	96.4	98.4	423.4494	88.0132	8.7	8.7
9.038107	7.487980	475.9	275.4	166.4	132.6	105.4	436.4003	121.5942	8.3	8.3
9.037939	7.490125	422.7	499.6	377.9	231.5	177.5	389.3067	215.5265	7.9	6.9
9.033668	7.485888	433.7	305.6	230.8	170.6	121.4	404.6421	152.1752	6.7	10.8
9.030395	7.480170	443.6	365.0	222.6	186.0	164.3	414.7660	169.4460	6.5	8.9
9.030214	7.484067	488.6	404.9	205.8	206.4	188.3	452.4436	191.1264	7.4	7.4
9.031277	7.477823	463.6	355.9	218.7	177.5	204.3	445.9832	170.7550	3.8	3.8
9.021089	7.481219	468.5	376.0	211.7	109.5	110.9	453.9765	106.1055	3.1	3.1
9.023130	7.487936	459.6	321.8	117.6	97.5	104.3	450.8676	92.8200	1.9	4.8
9.021199	7.485924	454.8	200.7	121.8	89.6	90.5	447.9780	83.5968	1.5	6.7

9.021135	7.488005	437.6	309.6	222.7	140.7	132.1	429.7232	130.4289	1.8	7.3
9.018950	7.483200	444.9	200.9	122.4	77.5	109.4	443.1204	73.3150	0.4	5.4
9.018432	7.488323	476.5	377.9	166.9	109.3	132.1	473.6410	107.3326	0.6	1.8
9.021558	7.487805	448.0	384.3	143.1	120.5	118.5	445.3120	112.6675	0.6	6.5
9.018767	7.490119	478.6	295.0	166.3	153.9	133.1	474.7712	144.9738	0.8	5.8
9.020832	7.489221	461.3	333.8	176.9	169.3	118.5	452.9966	162.1894	1.8	4.2
9.018977	7.491157	463.9	376.8	211.5	162.1	109.5	454.1581	153.0224	2.1	5.6
9.014435	7.489950	473.9	387.9	238.4	177.6	109.7	467.2654	162.1488	1.4	8.7
9.021807	7.492161	475.8	457.9	365.9	189.7	137.4	465.8082	171.1094	2.1	9.8
9.020828	7.490683	463.7	435.8	398.4	364.8	288.7	453.4986	337.0752	2.2	7.6
9.030815	7.494895	510.7	433.9	333.2	275.4	209.5	489.7613	256.3974	4.1	6.9
9.039520	7.496497	523.5	543.9	543.2	473.2	477.9	476.9085	433.4512	8.9	8.4
9.030376	7.499324	563.8	577.9	382.5	320.7	298.7	555.9068	302.7408	1.4	5.6
9.031231	7.494104	521.6	321.9	285.1	241.5	231.4	514.2976	220.4895	1.4	8.7
9.030795	7.493743	388.6	443.6	390.5	300.9	277.5	382.3824	271.4118	1.6	9.8
9.033837	7.497271	341.0	300.7	205.8	137.5	138.5	336.9080	127.0500	1.2	7.6
9.031999	7.496124	362.8	200.4	121.6	109.7	104.3	354.0928	104.9829	2.4	4.3
9.044334	7.507939	463.8	109.8	96.8	96.4	93.2	451.7412	91.1944	2.6	5.4
9.046047	7.510234	464.8	307.6	266.8	209.5	189.6	450.3912	195.8825	3.1	6.5
9.050420	7.507510	462.8	209.5	125.8	107.4	105.1	451.2300	101.8152	2.5	5.2
9.049907	7.504965	477.9	290.3	188.7	132.6	121.6	467.8641	125.8374	2.1	5.1
9.054054	7.504993	467.4	322.7	244.8	185.4	175.4	441.2256	173.3490	5.6	6.5
9.058199	7.507030	487.6	453.8	341.4	328.7	288.5	445.1788	303.0614	8.7	7.8
9.049001	7.526857	488.9	288.7	203.5	175.4	167.8	440.9878	165.2268	9.8	5.8
9.046576	7.527391	467.3	298.6	167.3	106.3	103.2	431.7852	97.0519	7.6	8.7
9.054437	7.511315	474.9	244.7	166.8	108.2	105.4	465.4020	102.4654	2.0	5.3
9.097056	7.500249	387.6	365.8	201.6	132.1	131.8	373.2588	123.5135	3.7	6.5
9.101848	7.499028	355.4	300.9	177.4	109.7	100.8	342.9610	101.4725	3.5	7.5
9.100297	7.501287	380.0	354.8	207.5	131.9	104.2	363.2800	120.4247	4.4	8.7
9.099965	7.499104	376.6	322.0	222.4	148.4	122.1	356.6402	137.4184	5.3	7.4
9.102256	7.493623	498.6	433.9	232.5	166.3	132.5	479.6532	154.9916	3.8	6.8

9.099018	7.496601	499.0	367.8	199.5	163.2	133.7	470.0580	153.7344	5.8	5.8
9.103294	7.492071	463.7	453.2	333.1	189.4	175.4	441.4424	175.3844	4.8	7.4
9.104012	7.487123	287.6	302.6	212.4	133.9	122.8	276.3836	122.3846	3.9	8.6
9.105296	7.492815	289.7	252.1	174.1	121.0	105.3	281.5884	111.4410	2.8	7.9
9.106364	7.490806	342.7	201.4	130.7	106.4	100.8	313.2278	97.9944	8.6	7.9
9.103876	7.483477	345.2	277.4	187.4	98.3	96.4	314.4772	89.9445	8.9	8.5
9.100114	7.481241	277.4	190.8	143.2	122.0	100.5	247.7182	110.0440	10.7	9.8
9.102565	7.477354	231.4	163.9	121.9	117.4	104.3	205.0204	108.1254	11.4	7.9
9.099307	7.476823	298.4	184.2	195.0	178.3	164.8	259.0112	163.5011	13.2	8.3
9.109478	7.480233	265.7	186.8	131.5	126.4	107.3	263.3087	119.5744	0.9	5.4
9.112614	7.477990	365.4	233.8	174.9	121.9	199.7	343.8414	112.5137	5.9	7.7
9.083840	7.492430	376.3	285.4	299.5	197.8	219.4	325.4995	178.8112	13.5	9.6
9.086094	7.494054	356.2	401.9	329.5	209.5	233.7	347.6512	190.8545	2.4	8.9
9.092014	7.494263	354.7	300.9	209.4	142.1	154.9	344.7684	131.4425	2.8	7.5
9.089464	7.493834	378.2	365.2	235.1	177.5	164.2	367.9886	162.0575	2.7	8.7
9.092936	7.485492	488.6	322.8	255.8	189.3	187.5	473.4534	176.9955	3.1	6.5
9.082166	7.474198	456.2	377.5	233.8	177.3	166.5	432.4776	164.1798	5.2	7.4
9.078391	7.469853	463.7	432.1	207.6	132.1	128.4	423.8218	120.7394	8.6	8.6
9.077093	7.473231	278.4	246.9	177.4	177.0	154.3	248.0544	162.1320	10.9	8.4
9.082980	7.475624	376.4	366.8	189.4	167.4	156.8	351.5576	167.4000	6.6	0.0
9.073841	7.466484	265.3	231.4	139.4	121.8	108.5	233.9946	121.8000	11.8	0.0
9.077756	7.462583	456.3	288.5	205.4	189.6	157.3	442.1547	179.3616	3.1	5.4
9.071623	7.465216	477.4	341.3	253.1	189.4	164.3	464.0328	175.3844	2.8	7.4
9.075440	7.459899	485.4	377.8	145.3	106.3	98.6	475.2066	97.1582	2.1	8.6
9.082776	7.462818	488.9	427.4	253.8	148.2	138.5	468.3662	139.3080	4.2	6.0
9.073003	7.453046	463.2	412.8	277.5	200.4	165.4	443.2824	180.9612	4.3	9.7
9.060920	7.453542	484.7	399.8	271.9	131.6	103.6	459.4956	120.5456	5.2	8.4
9.054690	7.465302	356.0	309.8	217.5	132.9	121.5	329.3000	122.9325	7.5	7.5
9.075243	7.480365	231.2	178.6	147.6	109.7	122.6	210.3920	99.4979	9.0	9.3
9.075990	7.478857	212.6	183.8	105.4	94.3	100.8	189.6392	85.9073	10.8	8.9
9.076070	7.478252	197.6	98.8	98.1	78.5	77.5	171.5168	70.9640	13.2	9.6

9.073271	7.477253	232.6	152.3	100.5	87.4	89.6	206.0836	77.9608	11.4	10.8
9.076361	7.478491	233.6	137.4	121.5	118.5	109.5	204.6336	108.1905	12.4	8.7
9.078166	7.480183	212.7	142.8	136.4	127.3	121.9	189.5157	116.4795	10.9	8.5
9.076347	7.471090	222.8	210.8	177.5	151.0	138.6	202.9708	138.9200	8.9	8.0
9.075608	7.469944	214.7	165.2	139.5	138.6	120.3	198.5975	126.8190	7.5	8.5
9.076954	7.470370	209.8	173.2	168.3	156.3	150.8	190.9180	142.7019	9.0	8.7
9.078078	7.471057	205.7	122.7	104.2	117.3	106.9	194.5922	108.5025	5.4	7.5
9.078747	7.465411	210.9	165.4	152.1	138.6	127.4	198.6678	126.6804	5.8	8.6
9.079144	7.467091	200.9	130.7	122.1	113.8	107.6	187.2388	106.0616	6.8	6.8
9.077453	7.464361	177.6	126.3	111.8	94.3	95.1	164.1024	86.0959	7.6	8.7
9.077080	7.460032	187.6	109.7	94.3	92.1	95.1	169.4028	83.2584	9.7	9.6
9.079887	7.461191	231.8	122.5	109.6	99.8	99.5	213.4878	89.0216	7.9	10.8
9.080823	7.452888	321.9	254.9	213.2	167.3	132.0	310.9554	152.7449	3.4	8.7
9.075575	7.448104	301.3	302.6	267.5	240.9	288.5	286.8376	237.7683	4.8	1.3
9.078506	7.444356	289.4	166.5	147.2	132.7	176.2	253.5144	118.3684	12.4	10.8
9.075153	7.442464	299.7	299.5	287.0	230.8	215.4	260.1396	208.6432	13.2	9.6
9.072559	7.442207	294.3	256.4	233.5	198.7	175.4	287.2368	184.9897	2.4	6.9
9.073561	7.444282	297.4	213.8	200.6	178.4	162.0	280.1508	164.6632	5.8	7.7
9.073142	7.440013	178.4	143.7	137.5	133.2	100.6	163.2360	121.7448	8.5	8.6
9.072684	7.443118	123.8	165.8	144.8	122.4	100.5	113.4008	113.0976	8.4	7.6
9.066914	7.443150	233.7	229.7	188.5	102.7	98.6	222.7161	92.6354	4.7	9.8
9.066995	7.445515	243.2	231.8	219.6	144.8	155.9	230.5536	134.2296	5.2	7.3
9.069923	7.447326	253.8	186.9	174.2	109.7	146.5	226.3896	97.8524	10.8	10.8
9.068420	7.448777	264.9	176.9	168.4	125.7	152.4	241.3239	114.5127	8.9	8.9
9.068823	7.449974	244.3	147.4	120.5	98.6	138.6	225.9775	90.1204	7.5	8.6
9.064494	7.447843	253.8	188.7	174.3	105.6	153.1	237.3030	97.5744	6.5	7.6
9.064244	7.443750	255.3	185.6	177.5	125.4	105.3	236.6631	118.0014	7.3	5.9
9.058733	7.464771	266.3	204.6	184.9	121.8	105.8	254.8491	112.6650	4.3	7.5
9.058181	7.463661	231.3	196.4	177.3	109.6	100.7	223.4358	102.5856	3.4	6.4
9.058737	7.465310	241.3	200.9	188.6	133.5	103.2	233.8197	123.6210	3.1	7.4
9.057979	7.463708	277.4	231.7	189.6	127.4	132.8	271.5746	120.6478	2.1	5.3

9.057072	7.460777	322.3	266.2	201.3	159.7	121.7	314.2425	149.4792	2.5	6.4
9.051665	7.462459	243.2	209.8	186.2	130.8	132.1	234.2016	120.9900	3.7	7.5
9.051552	7.467035	301.3	278.5	258.6	189.7	189.5	288.9467	173.5755	4.1	8.5
9.045200	7.490140	312.8	274.9	264.3	168.4	164.3	292.7808	155.7700	6.4	7.5
9.048329	7.490836	277.4	178.9	167.4	88.6	109.7	262.4204	84.3472	5.4	4.8
9.050098	7.488786	245.3	132.5	107.5	89.7	84.1	237.4504	82.9725	3.2	7.5
9.056203	7.503446	233.3	133.6	109.6	96.5	78.6	223.2681	88.2975	4.3	8.5
9.046909	7.507601	203.0	127.6	98.6	96.9	90.9	196.5040	89.5356	3.2	7.6
9.050334	7.513114	277.4	176.0	163.2	120.3	112.5	274.0712	115.1271	1.2	4.3
9.043231	7.501706	199.8	121.0	105.3	99.7	98.5	181.8180	91.1258	9.0	8.6
9.057279	7.511548	186.4	105.7	98.6	97.4	98.0	170.5560	88.8288	8.5	8.8
9.054806	7.517094	253.9	193.6	176.3	156.9	122.1	242.4745	146.7015	4.5	6.5
9.055201	7.513058	255.0	183.9	173.8	165.8	169.4	245.3100	153.5308	3.8	7.4
9.041303	7.486009	233.4	133.8	121.6	111.0	110.5	225.9312	105.1170	3.2	5.3
9.037287	7.491209	231.8	144.7	110.2	105.3	100.9	222.0644	99.5085	4.2	5.5
9.038749	7.493214	238.7	128.6	113.7	109.8	100.7	233.6873	102.8826	2.1	6.3
9.037195	7.492037	237.4	175.4	145.7	123.2	105.8	230.5154	115.1920	2.9	6.5
9.032968	7.489152	298.4	205.8	167.8	147.3	130.8	289.1496	140.0823	3.1	4.9
9.034669	7.490561	288.7	342.6	199.8	177.9	154.7	277.7294	167.9376	3.8	5.6
9.033780	7.487233	276.1	339.8	175.3	163.2	138.9	260.0862	150.7968	5.8	7.6
9.029677	7.482534	268.4	200.5	174.8	167.3	160.9	245.5860	153.0795	8.5	8.5
9.029734	7.480719	257.4	197.5	133.7	131.0	105.2	235.0062	119.6030	8.7	8.7
9.024371	7.483078	288.4	463.8	453.7	309.8	288.5	276.2872	296.7884	4.2	4.2
9.024941	7.485201	231.0	186.4	167.6	156.2	138.6	226.1490	147.4528	2.1	5.6
9.022537	7.483483	222.0	132.0	105.8	98.0	100.8	218.2260	89.4740	1.7	8.7
9.026931	7.489214	241.3	348.2	323.8	219.8	209.5	233.8197	198.2596	3.1	9.8
9.022154	7.482012	265.3	201.9	184.6	105.4	93.2	258.1369	97.3896	2.7	7.6
9.019674	7.485140	266.3	198.5	143.7	102.5	98.5	258.0447	93.5825	3.1	8.7
9.016627	7.490020	277.3	176.5	122.7	110.6	109.5	266.7626	99.7612	3.8	9.8
9.015791	7.489754	188.9	204.4	186.4	144.2	133.6	184.9331	133.2408	2.1	7.6
9.015538	7.492471	179.6	210.9	188.9	175.3	155.7	174.3916	167.7621	2.9	4.3

9.017482	7.490421	165.3	253.9	213.6	178.4	165.2	160.8369	172.8696	2.7	3.1
9.020313	7.494693	155.3	177.9	169.8	167.3	177.2	150.7963	159.6042	2.9	4.6
9.019728	7.493428	143.2	100.9	78.6	78.1	78.5	132.4600	71.9301	7.5	7.9
9.020719	7.496298	144.2	132.8	112.8	83.2	80.8	132.9524	76.7936	7.8	7.7
9.023659	7.494485	133.9	199.0	144.6	122.9	107.2	121.1795	112.2077	9.5	8.7
9.024238	7.496687	126.8	97.9	96.8	90.5	90.5	115.6416	83.3505	8.8	7.9
9.026401	7.498111	119.7	87.9	86.9	85.0	83.2	108.5679	75.8200	9.3	10.8
9.027083	7.495192	118.7	86.5	87.6	64.3	66.5	104.4560	58.3201	12.0	9.3
9.027864	7.499020	115.3	67.9	68.4	68.4	68.9	100.0804	62.3124	13.2	8.9
9.029023	7.495932	135.2	84.9	86.9	86.1	87.4	116.0016	76.8012	14.2	10.8
9.030708	7.496481	142.7	96.8	89.4	87.6	86.0	127.4311	79.1904	10.7	9.6
9.029387	7.494438	132.9	234.9	177.6	165.4	144.8	117.6165	155.8068	11.5	5.8
9.031486	7.501014	110.9	321.9	265.8	178.6	175.2	98.3683	163.2404	11.3	8.6
9.034988	7.499412	71.6	89.7	86.3	566.2	121.8	62.1488	511.2786	13.2	9.7
9.040682	7.500133	115.2	97.9	87.6	86.0	87.5	104.9472	80.0660	8.9	6.9
9.043758	7.509865	116.2	109.8	83.5	123.8	109.6	105.2772	113.0294	9.4	8.7
9.048586	7.507019	118.5	113.9	76.8	76.7	85.4	107.2425	70.0271	9.5	8.7
9.050276	7.509973	119.7	120.8	100.2	132.1	108.4	111.0816	119.4184	7.2	9.6
9.052877	7.508569	143.2	132.7	100.6	96.5	95.8	131.1712	89.1660	8.4	7.6
9.051503	7.508696	142.7	123.8	99.5	97.6	79.8	129.7143	89.1088	9.1	8.7
9.042634	7.521853	154.3	153.8	107.3	94.3	90.4	137.6356	85.3415	10.8	9.5
9.045066	7.527044	143.8	134.7	129.4	105.3	100.4	128.4134	95.4018	10.7	9.4
9.043022	7.520690	123.1	122.8	98.5	97.6	96.2	112.1441	89.1088	8.9	8.7
9.046165	7.517689	213.8	198.7	106.4	104.3	1004.0	209.3102	96.4775	2.1	7.5
9.047742	7.526889	251.3	250.8	247.5	188.5	177.3	243.5097	175.4935	3.1	6.9
9.049261	7.522920	122.8	99.0	103.6	100.5	3.1	117.6424	96.3795	4.2	4.1
9.052934	7.521889	241.3	221.8	138.5	126.9	106.3	233.8197	119.5398	3.1	5.8
9.055717	7.514148	152.9	132.6	94.2	98.6	96.5	142.5028	91.2050	6.8	7.5
9.098420	7.505125	127.9	98.8	96.8	76.9	79.0	118.3075	70.2866	7.5	8.6
9.097506	7.501655	165.4	321.8	493.5	476.3	398.5	151.1756	438.6723	8.6	7.9
9.099603	7.499404	177.3	122.6	92.5	90.8	97.5	164.1798	82.0832	7.4	9.6

9.099088	7.501681	255.1	224.8	113.5	109.6	104.3	244.3858	99.9552	4.2	8.8
9.098113	7.502323	273.8	231.8	169.4	132.5	121.6	257.9196	122.6950	5.8	7.4
9.100207	7.499660	277.3	122.9	93.6	277.3	175.3	259.8301	257.0571	6.3	7.3
9.100502	7.500816	287.4	167.9	96.4	96.6	95.3	273.6048	89.3550	4.8	7.5
9.100408	7.497999	265.3	228.7	115.3	108.5	98.5	255.2186	99.9285	3.8	7.9
9.100328	7.496928	153.8	123.5	86.5	86.7	76.5	145.8024	78.4635	5.2	9.5
9.100116	7.496691	163.9	155.8	103.5	96.4	87.2	160.6220	89.1700	2.0	7.5
9.099098	7.501811	127.0	111.9	89.5	89.1	88.7	115.5700	82.0611	9.0	7.9
9.098243	7.500069	177.3	115.9	81.5	80.6	78.5	162.2295	74.4744	8.5	7.6
9.102084	7.495520	183.2	122.0	85.2	87.6	88.4	166.7120	80.5920	9.0	8.0
9.103163	7.494381	153.8	98.5	95.1	94.2	94.7	141.6498	90.1494	7.9	4.3
9.100286	7.494359	127.3	94.8	96.5	93.8	92.5	113.5516	86.6712	10.8	7.6
9.100993	7.491321	263.4	218.7	118.4	98.6	97.6	254.9712	92.3882	3.2	6.3
9.102267	7.489348	222.3	157.7	100.5	100.2	99.7	219.6324	94.7892	1.2	5.4
9.105528	7.488224	225.8	166.4	129.4	114.3	109.8	217.4454	106.8705	3.7	6.5
9.104285	7.488938	216.4	277.0	322.6	286.8	222.0	211.2064	265.2900	2.4	7.5
9.102420	7.486690	217.3	213.9	184.3	138.6	146.3	211.6502	133.6104	2.6	3.6
9.102509	7.485730	231.8	188.9	138.6	108.6	109.4	224.6142	100.4550	3.1	7.5
9.104269	7.485365	341.8	213.7	134.5	129.6	121.9	333.5968	118.4544	2.4	8.6
9.102601	7.483122	266.3	231.9	185.4	122.4	133.7	262.8381	114.0768	1.3	6.8
9.102437	7.485801	274.2	187.4	111.6	87.5	100.5	269.8128	82.7750	1.6	5.4
9.100102	7.478567	231.8	177.4	106.4	89.7	95.4	224.3824	84.0489	3.2	6.3
9.103122	7.479014	263.6	342.1	345.2	256.4	231.4	246.4660	239.9904	6.5	6.4
9.102210	7.479916	247.3	352.1	354.2	178.5	166.8	225.2903	161.0070	8.9	9.8
9.096145	7.477224	251.9	253.1	196.4	189.7	184.3	235.5265	172.8167	6.5	8.9
9.084179	7.495696	256.3	219.0	188.4	188.1	177.5	240.1531	171.9234	6.3	8.6
9.083590	7.496681	241.9	210.4	199.2	196.5	178.5	234.1592	183.1380	3.2	6.8
9.084056	7.494565	245.3	211.2	129.5	126.3	108.3	227.1478	116.7012	7.4	7.6
9.084496	7.496003	244.3	152.4	130.6	126.5	109.5	231.8407	117.0125	5.1	7.5
9.082489	7.496762	448.3	341.5	120.5	121.5	109.5	433.9544	112.5090	3.2	7.4
9.084375	7.495384	215.3	199.4	129.5	120.5	107.3	200.6596	112.1855	6.8	6.9

9.087344	7.494546	189.9	276.8	212.8	200.9	188.5	175.8474	184.0244	7.4	8.4
9.088389	7.497239	176.4	111.8	78.9	78.6	89.5	163.5228	73.0980	7.3	7.0
9.087518	7.492804	230.9	123.7	100.9	100.0	99.2	220.9713	94.6000	4.3	5.4
9.087329	7.490226	234.2	352.8	233.5	231.8	200.5	219.2112	214.1832	6.4	7.6
9.084903	7.488469	227.4	165.8	108.7	107.5	100.8	210.7998	96.9650	7.3	9.8
9.090221	7.496107	227.3	145.7	108.9	108.3	104.3	212.7528	100.3941	6.4	7.3
9.087557	7.489283	287.3	133.8	122.3	117.9	107.5	263.7414	107.7606	8.2	8.6
9.086630	7.492958	251.3	234.9	168.4	160.8	143.2	246.2740	148.9008	2.0	7.4
9.091785	7.497360	218.4	199.8	128.5	121.3	109.7	213.8136	113.5368	2.1	6.4
9.090381	7.497152	217.3	215.8	177.5	156.4	133.7	215.5616	142.9496	0.8	8.6
9.094713	7.492656	117.4	209.8	129.5	108.3	106.4	116.9304	100.2858	0.4	7.4
9.096389	7.494538	187.3	123.4	198.5	105.2	96.5	183.3667	98.4672	2.1	6.4
9.097186	7.496850	156.3	142.8	111.0	88.6	89.6	155.5185	83.9928	0.5	5.2
9.093873	7.495704	137.3	121.8	109.5	99.5	98.2	123.8446	91.6395	9.8	7.9
9.091738	7.488010	142.8	122.8	121.4	98.8	95.1	131.5188	90.3032	7.9	8.6
9.093734	7.489394	164.8	111.5	82.3	81.0	95.3	150.7920	74.1150	8.5	8.5
9.100749	7.484451	145.2	221.4	166.8	148.6	121.5	132.7128	137.3064	8.6	7.6
9.098843	7.479662	176.4	193.8	173.8	132.9	100.8	163.6992	121.6035	7.2	8.5
9.098682	7.480539	273.1	127.3	118.4	87.9	86.5	248.2479	82.9776	9.1	5.6
9.098664	7.485123	243.3	172.1	127.5	76.8	75.2	222.6195	71.5776	8.5	6.8
9.101299	7.496524	153.0	100.6	98.5	78.4	77.6	139.9950	72.6768	8.5	7.3
9.096906	7.495683	163.2	121.5	93.2	88.9	87.6	149.1648	82.7659	8.6	6.9
9.082973	7.478730	177.3	153.2	97.6	94.3	92.8	160.1019	85.2472	9.7	9.6
9.082419	7.470900	167.3	157.8	136.5	108.4	104.3	163.7867	99.5112	2.1	8.2
9.079801	7.480944	129.4	217.0	177.3	170.6	167.8	123.0594	157.6344	4.9	7.6
9.076716	7.466748	219.0	89.8	89.2	90.5	91.0	204.1080	85.2510	6.8	5.8
9.081395	7.469868	224.9	211.8	144.4	145.6	109.6	217.7032	129.8752	3.2	10.8
9.070039	7.462391	189.4	109.0	105.4	145.2	132.1	173.1116	134.1648	8.6	7.6
9.056411	7.459630	100.9	100.2	99.5	231.5	200.5	91.3145	211.8225	9.5	8.5
9.059156	7.464349	104.2	100.3	99.8	92.0	86.5	92.9464	83.8120	10.8	8.9
9.053035	7.461722	213.2	104.2	100.0	96.4	93.1	192.7328	88.1096	9.6	8.6

9.077015	7.482716	78.5	78.2	79.4	76.0	77.9	72.2200	70.3000	8.0	7.5
9.077118	7.484202	483.9	381.3	117.5	111.5	89.6	416.6379	104.3640	13.9	6.4
9.075857	7.485513	46.5	45.2	56.4	55.4	56.4	40.3620	50.0262	13.2	9.7
9.074094	7.486191	78.6	162.5	234.1	244.3	205.8	69.9540	223.2902	11.0	8.6
9.073113	7.481237	104.2	95.6	95.4	90.8	78.6	100.8656	82.9004	3.2	8.7
9.070756	7.475924	190.5	154.8	178.6	109.0	105.2	184.4040	96.0290	3.2	11.9
9.075446	7.474904	87.4	87.2	85.4	67.8	65.4	79.0096	61.9014	9.6	8.7
9.078232	7.476987	88.4	84.8	81.8	76.5	76.5	80.6208	71.3745	8.8	6.7
9.073544	7.470244	83.2	132.7	154.3	132.0	121.9	75.2960	120.6480	9.5	8.6
9.077572	7.467334	84.3	85.3	78.5	77.6	78.6	77.3031	70.0728	8.3	9.7
9.078021	7.458853	102.4	95.2	85.4	84.3	82.9	95.3344	77.0502	6.9	8.6
9.077431	7.450733	110.5	98.7	87.9	88.6	87.6	106.9640	81.0690	3.2	8.5
9.075403	7.446420	49.5	56.5	57.4	56.8	57.4	46.6290	52.1992	5.8	8.1
9.077053	7.450966	69.5	65.2	65.3	65.8	75.9	65.0520	60.2728	6.4	8.4
9.075132	7.445563	72.9	71.8	70.8	70.1	78.6	65.7558	64.0714	9.8	8.6
9.077756	7.439922	58.4	60.2	60.5	59.9	60.8	57.8160	56.7253	1.0	5.3
9.078493	7.436763	85.9	76.9	76.5	76.7	77.2	85.4705	73.0184	0.5	4.8
9.072620	7.444292	100.5	82.1	83.2	82.3	80.5	91.5555	74.4815	8.9	9.5
9.073895	7.437549	120.0	154.2	154.3	130.2	110.9	109.3200	119.9142	8.9	7.9
9.074303	7.443823	105.4	89.7	87.5	85.2	82.1	95.4924	75.9984	9.4	10.8
9.071204	7.436921	99.7	67.4	68.5	65.4	63.2	88.9324	59.6448	10.8	8.8
9.070029	7.439173	93.2	78.4	78.2	70.8	68.9	82.5752	64.0032	11.4	9.6
9.068604	7.444834	91.5	78.2	79.0	69.7	66.5	82.4415	63.7058	9.9	8.6
9.071138	7.448197	104.9	84.3	83.9	75.1	73.2	92.8365	69.9181	11.5	6.9
9.066640	7.448272	104.3	97.3	88.5	86.4	83.5	94.2872	78.7968	9.6	8.8
9.066924	7.450471	84.3	95.1	87.5	88.4	78.6	77.0502	80.7092	8.6	8.7
9.064946	7.448545	78.5	78.9	78.6	76.3	75.1	72.6125	71.0353	7.5	6.9
9.063272	7.443539	72.1.0	70.2	72.4	70.7	75.9	65.1784	65.6803	9.6	7.1
9.057203	7.466829	108.0	83.2	80.5	271.4	200.8	98.7120	250.7736	8.6	7.6
9.054849	7.466031	109.4	152.7	154.3	152.9	109.6	101.3044	142.9615	7.4	6.5
9.056806	7.458890	121.7	122.1	98.6	78.5	89.6	115.2499	71.9060	5.3	8.4

9.050250	7.478486	109.4	78.3	75.6	77.4	80.6	106.0086	75.0006	3.1	3.1
9.050895	7.484444	102.1	87.5	86.3	84.3	86.4	101.6916	79.5792	0.4	5.6
9.046807	7.479423	496.5	254.9	138.5	107.8	5.4	493.5210	98.5292	0.6	8.6
9.045996	7.477715	76.3	67.9	67.5	68.1	95.4	69.6619	62.3796	8.7	8.4
9.047199	7.481762	72.9	54.8	54.8	54.3	342.0	68.5260	50.1732	6.0	7.6
9.044550	7.487390	71.9	63.1	67.3	65.9	78.6	65.1414	59.5736	9.4	9.6
9.051569	7.489788	75.4	212.1	233.2	211.7	205.8	71.9316	201.9618	4.6	4.6
9.049857	7.495770	83.7	103.2	98.5	90.8	89.8	78.2595	84.8980	6.5	6.5
9.048174	7.495252	97.5	87.4	78.5	70.2	77.6	91.8450	64.9350	5.8	7.5
9.048332	7.493458	86.3	45.3	63.2	64.3	74.3	78.3604	58.9631	9.2	8.3
9.051574	7.493867	65.0	65.9	68.3	69.6	70.6	62.6600	63.6144	3.6	8.6
9.054144	7.492289	325.3	120.8	95.1	77.6	75.4	299.6013	71.7800	7.9	7.5
9.056182	7.491021	65.4	76.5	78.5	68.9	69.8	61.8684	62.3545	5.4	9.5
9.055705	7.495504	47.4	69.8	68.6	70.2	65.2	46.1384	66.4794	2.6	5.3
9.046945	7.547490	63.2	73.8	68.4	73.5	70.7	57.7648	67.9875	8.6	7.5
9.056773	7.519774	55.1	64.3	86.5	60.8	58.9	49.9206	56.6048	9.4	6.9
9.054552	7.514584	37.4	64.9	68.3	47.9	58.9	33.3234	43.7806	10.9	8.6
9.059961	7.493051	36.2	45.3	96.4	60.5	71.5	32.0732	54.8130	11.4	9.4
9.062137	7.503717	64.9	56.2	67.3	72.8	70.5	58.5398	67.0488	9.8	7.9
9.033982	7.491936	56.4	65.9	69.5	70.6	68.4	49.3500	63.9636	12.5	9.4
9.023190	7.481622	47.3	47.6	48.5	76.9	78.2	41.8605	70.2866	11.5	8.6
9.022262	7.489722	49.2	53.9	56.3	77.4	75.9	44.9196	69.0408	8.7	10.8
9.025360	7.488420	47.5	45.3	48.5	45.7	58.9	42.0375	40.9015	11.5	10.5
9.021075	7.483555	43.0	43.1	52.9	50.3	50.9	37.5820	45.5718	12.6	9.4
9.023119	7.490609	42.8	41.0	2.0	48.5	50.8	38.2632	43.8440	10.6	9.6
9.016624	7.427820	40.8	40.9	49.5	60.2	71.3	36.8832	53.6984	9.6	10.8
9.015332	7.495284	57.9	54.3	58.6	64.3	63.4	53.4417	58.1272	7.7	9.6
9.013913	7.488007	50.3	50.0	51.6	49.8	121.8	46.1251	45.8658	8.3	7.9
9.021035	7.493364	265.4	160.9	98.6	77.6	76.3	261.9498	71.1592	1.3	8.3
9.021964	7.496924	78.9	67.8	76.5	60.9	64.3	71.4045	55.4799	9.5	8.9
9.025063	7.495560	96.4	78.5	78.5	70.2	69.5	93.3152	64.1628	3.2	8.6

9.023444	7.493563	87.4	77.1	77.3	73.5	67.4	83.9914	66.4440	3.9	9.6
9.027018	7.496413	67.4	58.5	58.6	60.8	60.8	64.5018	56.0576	4.3	7.8
9.033276	7.499622	36.9	40.9	43.8	47.9	60.5	33.3945	42.7268	9.5	10.8
9.032075	7.498712	57.9	56.5	50.5	60.5	57.4	52.7469	55.4180	8.9	8.4
9.037501	7.500221	88.2	78.5	73.1	72.8	72.0	80.6148	66.5392	8.6	8.6
9.038915	7.498522	77.4	75.9	71.6	70.6	70.5	69.8148	64.6696	9.8	8.4
9.055011	7.502796	70.4	75.3	75.1	76.9	75.4	65.6128	70.2866	6.8	8.6
9.056161	7.508522	63.9	78.9	78.6	77.4	77.4	56.3598	70.6662	11.8	8.7
9.057336	7.497120	48.8	192.9	198.5	178.0	98.5	44.1152	161.4460	9.6	9.3
9.055093	7.497597	45.9	67.4	58.3	56.7	63.2	41.9526	51.8238	8.6	8.6
9.045060	7.524055	73.8	73.7	73.9	70.6	78.5	68.4126	65.4462	7.3	7.3
9.046558	7.521602	78.3	76.8	76.4	76.1	74.3	71.1747	70.9252	9.1	6.8
9.042764	7.518623	75.9	74.7	75.2	76.0	74.3	68.6895	69.6920	9.5	8.3
9.043271	7.522887	62.9	60.4	61.0	60.9	60.5	57.4906	56.1498	8.6	7.8
9.041745	7.529432	58.0	76.9	75.4	73.9	72.2	53.7080	67.0273	7.4	9.3
9.039287	7.527794	87.9	84.3	82.4	80.8	82.8	80.6043	74.6592	8.3	7.6
9.038510	7.525044	89.3	78.6	76.0	78.6	77.6	83.4955	72.0762	6.5	8.3
9.040821	7.522070	72.1	79.0	77.5	77.1	78.9	65.8994	70.6236	8.6	8.4
9.035168	7.522241	64.3	64.3	65.0	65.4	67.5	63.4641	60.1026	1.3	8.1
9.041682	7.521440	337.5	340.1	209.5	189.7	113.2	334.8000	173.7652	0.8	8.4
9.037412	7.516341	77.4	73.8	73.9	73.7	77.8	73.2204	67.6566	5.4	8.2
9.042206	7.516762	37.4	46.3	46.5	47.8	56.4	34.8194	43.7370	6.9	8.5
9.042098	7.519328	61.9	60.4	61.9	60.9	61.7	57.1956	56.3325	7.6	7.5
9.045684	7.521311	60.8	56.4	56.3	56.0	57.9	55.1456	51.7440	9.3	7.6
9.047720	7.525163	74.3	100.8	95.4	95.2	98.7	67.9102	86.8224	8.6	8.8
9.049710	7.524812	67.0	64.3	68.5	68.2	67.5	59.9650	61.6528	10.5	9.6
9.054425	7.519465	66.3	67.4	68.5	67.2	66.8	58.4103	61.2192	11.9	8.9
9.055065	7.514179	72.9	71.4	83.9	83.0	82.3	63.7146	73.4550	12.6	11.5
9.063928	7.515098	48.7	47.9	48.4	48.7	54.8	42.2716	43.4404	13.2	10.8
9.094634	7.506178	103.6	76.8	75.2	74.8	73.7	90.5464	67.3948	12.6	9.9
9.098036	7.506799	103.2	177.3	104.3	100.5	97.8	95.1504	92.6610	7.8	7.8

9.098033	7.494193	99.8	78.3	79.4	79.4	78.7	91.9158	72.5716	7.9	8.6
9.099421	7.494998	90.7	103.2	83.2	83.6	80.5	83.8068	76.5776	7.6	8.4
9.098230	7.492615	87.4	120.5	93.9	94.2	90.8	80.5828	86.0988	7.8	8.6
9.101778	7.492800	87.6	110.5	93.2	94.5	109.8	81.9060	86.7510	6.5	8.2
9.102180	7.489827	532.2	232.9	130.2	116.1	97.8	525.2814	106.2315	1.3	8.5
9.100333	7.490773	63.9	65.4	65.5	67.5	65.4	59.0436	61.6275	7.6	8.7
9.104742	7.489744	88.3	67.3	68.6	65.9	65.8	76.9976	59.4418	12.8	9.8
9.103979	7.484511	73.2	76.2	75.9	74.3	73.1	72.1020	71.9967	1.5	3.1
9.102499	7.482071	87.5	80.4	67.9	67.8	65.8	86.7125	60.4776	0.9	10.8
9.102483	7.480655	62.4	60.9	54.8	56.4	54.7	57.0336	50.9856	8.6	9.6
9.099335	7.474782	68.5	63.3	51.6	50.8	57.6	63.1570	46.2788	7.8	8.9
9.109594	7.478318	74.8	72.1	56.8	57.6	56.9	67.7688	52.1280	9.4	9.5
9.107810	7.478879	47.3	53.7	65.9	65.4	66.5	42.1916	60.9528	10.8	6.8
9.083295	7.497847	77.2	67.3	63.9	63.7	65.8	69.8660	57.6485	9.5	9.5
9.094561	7.494682	76.5	66.8	45.8	46.5	73.1	68.0850	41.9430	11.0	9.8
9.092068	7.491043	87.5	78.4	73.7	73.2	65.8	78.9250	66.0264	9.8	9.8
9.096832	7.490398	65.3	63.2	62.9	60.7	54.7	59.8148	56.5724	8.4	6.8
9.082820	7.481426	63.9	64.4	67.3	66.5	57.6	58.7241	61.5790	8.1	7.4
9.074306	7.456603	89.5	67.4	70.0	68.9	56.9	81.9820	63.8703	8.4	7.3
9.064445	7.460636	71.9	69.4	70.8	67.5	66.5	64.9976	62.0325	9.6	8.1
9.052627	7.458290	73.9	76.3	76.9	76.1	65.8	68.3575	70.5447	7.5	7.3
9.120253	7.414471	80.7	78.4	76.8	76.7	54.7	75.8580	72.4048	6.0	5.6
9.118028	7.563542	241.0	233.8	94.8	93.7	57.6	233.5290	91.7323	3.1	2.1
9.000917	7.419911	266.8	163.0	116.7	98.6	56.9	260.1300	92.2896	2.5	6.4
9.002940	7.559937	231.9	133.7	88.8	88.2	66.5	228.6534	80.6148	1.4	8.6
9.027364	7.469396	435.1	233.7	111.9	93.2	65.8	431.1841	90.3108	0.9	3.1
9.034927	7.474982	402.7	174.8	117.4	98.6	73.1	395.4514	94.4588	1.8	4.2
9.036175	7.489390	421.8	212.7	133.9	106.4	65.8	416.7384	102.6760	1.2	3.5
9.039476	7.482886	245.1	177.5	115.5	113.9	54.7	237.5019	105.0158	3.1	7.8
9.050798	7.485437	476.7	275.9	154.9	135.5	120.9	460.0155	128.3185	3.5	5.3
9.045771	7.495935	176.4	120.4	112.4	98.6	93.2	157.8780	90.2190	10.5	8.5

9.044881	7.472156	184.6	106.8	75.1	75.0	76.4	167.0630	68.3250	9.5	8.9
9.035187	7.466374	162.4	102.7	78.6	78.1	72.4	145.5104	71.3834	10.4	8.6
9.046926	7.474055	90.7	98.7	73.5	73.2	74.3	80.5416	67.0512	11.2	8.4
9.026354	7.468882	398.7	211.6	119.5	76.4	72.1	393.5169	70.0588	1.3	8.3
9.021201	7.487771	465.3	287.9	168.4	104.3	88.5	462.5082	101.0667	0.6	3.1
9.031183	7.495746	433.6	211.8	129.8	109.6	99.8	422.7600	102.5856	2.5	6.4
9.044832	7.478671	84.8	87.9	88.5	88.1	94.3	83.1888	83.4307	1.9	5.3
9.051951	7.482784	102.3	67.8	68.9	68.5	78.5	96.5712	64.6640	5.6	5.6
9.054371	7.493256	562.1	321.8	155.9	103.8	108.7	557.0411	94.8732	0.9	8.6
9.060759	7.469613	103.7	88.4	90.5	89.6	94.1	100.0705	84.1344	3.5	6.1
9.055333	7.467073	498.4	200.7	105.8	101.4	110.8	485.9400	96.0258	2.5	5.3
9.062724	7.448590	478.4	222.6	154.9	122.5	132.7	470.2672	110.6175	1.7	9.7
9.069679	7.456565	321.8	288.7	200.9	176.5	163.9	316.0076	161.4975	1.8	8.5
9.064039	7.476874	273.4	143.8	123.7	117.5	100.8	269.8458	108.9225	1.3	7.3
9.070951	7.458161	381.2	189.8	121.8	96.5	100.7	376.6256	90.4205	1.2	6.3
9.073847	7.470654	578.7	273.8	236.8	214.3	177.4	573.4917	205.0851	0.9	4.3
9.084683	7.467383	563.1	121.6	123.9	98.6	96.5	538.8867	92.7826	4.3	5.9
9.072591	7.456232	421.9	100.8	109.8	95.3	92.1	385.6166	85.8653	8.6	9.9
9.077502	7.480309	321.8	174.9	121.8	89.6	87.6	315.6858	86.8224	1.9	3.1
9.071019	7.484335	274.3	122.8	109.8	88.6	87.8	269.3626	84.4358	1.8	4.7
9.079646	7.492366	443.2	265.9	177.5	120.5	113.0	433.8928	112.9085	2.1	6.3
9.072810	7.489743	117.4	98.7	99.5	99.6	100.8	112.8214	95.7156	3.9	3.9
9.088621	7.497866	94.7	95.2	98.5	98.6	100.4	85.7035	89.2330	9.5	9.5
9.079627	7.499619	102.1	89.7	78.2	76.9	75.6	93.4215	70.3635	8.5	8.5
9.075921	7.499445	421.8	300.8	210.5	153.8	133.7	395.2266	144.1106	6.3	6.3
9.086164	7.490366	206.9	166.8	147.3	140.8	128.5	200.4861	136.4352	3.1	3.1
9.092033	7.498065	174.7	108.9	96.2	95.3	92.1	166.8385	91.0115	4.5	4.5
9.086998	7.492707	231.0	176.9	89.5	86.5	84.3	215.9850	80.2720	6.5	7.2
9.085236	7.496763	431.8	208.6	105.9	89.4	84.8	424.8912	82.6056	1.6	7.6
9.092781	7.501275	94.3	95.0	87.5	88.1	85.9	86.1902	80.5234	8.6	8.6
9.085085	7.502252	306.9	284.9	122.1	111.9	100.3	295.8516	107.8716	3.6	3.6

9.075853	7.500998	289.4	254.8	207.1	185.3	138.6	274.0618	168.8083	5.3	8.9
9.093480	7.498256	84.2	87.6	89.5	88.5	85.3	77.8008	80.0925	7.6	9.5
9.100067	7.496450	102.4	78.6	76.5	77.5	78.6	95.3344	70.7575	6.9	8.7
9.094056	7.483936	207.5	179.8	118.5	95.6	93.2	199.6150	87.0916	3.8	8.9
9.099197	7.484080	301.0	208.7	157.4	100.0	97.5	294.6790	89.2000	2.1	10.8
9.091185	7.482701	276.9	138.1	119.5	100.5	96.3	263.8857	92.5605	4.7	7.9
9.092492	7.476894	344.5	198.6	123.1	104.3	100.3	333.8205	95.4345	3.1	8.5
9.091783	7.499797	495.3	210.9	98.5	98.4	87.7	481.4316	89.2488	2.8	9.3
9.088194	7.494737	299.2	134.1	87.6	86.8	88.5	292.9168	83.5016	2.1	3.8
9.103227	7.495023	498.8	327.6	153.2	101.8	89.4	488.3252	96.4046	2.1	5.3
9.088115	7.507926	283.7	258.7	142.8	105.6	101.4	278.5934	101.5872	1.8	3.8
9.087847	7.520558	603.8	477.8	230.8	603.9	643.9	550.0618	545.9256	8.9	9.6
9.074488	7.519304	121.7	120.9	113.7	98.6	100.8	113.4244	92.8812	6.8	5.8
9.065707	7.524034	371.4	287.5	176.8	89.5	78.6	355.8012	85.7410	4.2	4.2
9.052882	7.517239	83.6	87.7	89.7	88.5	71.3	75.4072	79.8270	9.8	9.8
9.053283	7.527728	76.9	78.6	76.8	73.2	70.5	70.3635	67.0512	8.5	8.4
9.048239	7.526313	247.8	209.6	160.6	95.3	89.4	224.2590	87.8666	9.5	7.8
9.040428	7.529805	387.0	345.8	213.7	174.9	132.1	381.5820	167.3793	1.4	4.3
9.035647	7.521757	621.6	509.8	444.6	267.5	123.1	556.3320	241.5525	10.5	9.7
9.042645	7.518672	121.8	342.6	266.8	194.3	102.3	111.4470	177.7845	8.5	8.5
9.097482	7.483568	621.7	544.0	665.9	589.5	432.1	616.1047	568.8675	0.9	3.5
9.089988	7.495371	521.5	389.7	198.7	188.1	121.7	482.9090	174.1806	7.4	7.4
9.097634	7.495022	89.5	90.5	72.6	70.6	71.2	82.7875	65.3050	7.5	7.5
9.103598	7.493250	473.1	274.9	121.8	97.6	93.2	460.3263	93.4032	2.7	4.3
9.099028	7.478762	382.0	241.4	166.8	95.4	95.3	377.4160	91.1070	1.2	4.5
9.066722	7.443342	273.0	185.3	99.6	77.1	77.3	263.4450	74.9412	3.5	2.8
9.050038	7.456370	430.0	243.9	121.4	109.5	103.9	417.9600	106.1055	2.8	3.1
9.012432	7.476846	300.8	162.3	98.5	90.6	88.4	287.8656	88.3350	4.3	2.5
9.037117	7.521849	480.0	288.5	221.4	92.5	104.2	456.4800	88.9850	4.9	3.8
9.052316	7.528390	571.0	465.1	210.8	187.5	152.1	541.3080	169.1250	5.2	9.8
9.054494	7.517269	100.9	84.6	85.3	89.0	76.4	94.4424	83.3040	6.4	6.4

9.047780	7.508348	207.5	158.3	109.6	85.4	100.3	200.0300	77.2016	3.6	9.6
9.021240	7.491230	273.7	174.9	100.2	82.9	80.4	262.4783	79.5011	4.1	4.1
9.024262	7.491400	612.9	512.0	320.8	200.9	153.2	606.1581	194.0694	1.1	3.4
9.057846	7.477743	94.8	103.2	95.6	87.5	88.4	93.0936	81.9000	1.8	6.4
9.092233	7.500329	433.9	377.5	210.6	178.6	132.1	428.2593	173.0634	1.3	3.1
9.100232	7.490234	70.9	71.4	73.8	71.0	71.2	63.8809	63.3320	9.9	10.8
9.089200	7.486908	322.3	277.3	110.7	98.5	88.9	319.3993	93.8705	0.9	4.7
9.076258	7.517256	77.4	89.4	89.6	84.3	87.2	69.1182	75.2799	10.7	10.7
9.058644	7.518354	82.8	78.4	78.5	75.2	76.3	72.1188	66.4016	12.9	11.7
9.083934	7.471143	570.6	432.1	208.5	185.4	102.4	543.2112	171.6804	4.8	7.4
9.150000	7.540000	78.0	78.0	78.0	78.0	78.0	69.5760	71.0580	10.8	8.9

APPENDIX H **Concentration of Heavy Metals at different locations at the surface and depth of 30.0cm (mg/l)**

LONG	LAT	FE (0)	FE(0)	CD (0)	CD (0)	CR (0)	CR (10)	PB (0)	PB (30)	ZN (0)	ZN (30)	NI (0)	NI (30)
9.11702	**7.42978**	**309.786**	**3977.758**	**23.110**	**8.779**	**100.000**	**100.000**	**30.000**	**10.978**	**20.000**	**10.000**	**10.000**	**3.000**
9.07110	7.46708	400.786	6785.490	40.162	12.543	286.458	121.657	134.771	154.390	98.765	45.390	21.982	8.987
9.07841	7.46945	3096.700	2008.433	38.665	17.300	305.674	120.543	232.878	121.688	67.776	43.675	0.000	0.000
9.08056	7.46450	7865.879	6453.664	20.676	19.554	499.765	253.200	320.786	109.684	87.765	23.865	62.180	21.675
9.07574	7.48990	7821.333	2006.665	38.600	10.879	308.789	176.490	659.032	100.865	89.870	19.067	100.253	0.000
9.09401	7.49034	2045.669	2097.799	29.776	9.780	109.543	60.343	657.890	121.544	54.460	21.097	18.328	8.665
9.04000	7.48000	5655.377			5.362						0.000	0.000	0.000
9.06273	7.46762	889.098	2097.600	30.876	13.266	754.658	209.600	548.760	198.600	43.877	45.342	32.722	0.000
9.05897	7.46319	4895.696	3006.455	38.559	10.700	208.500	105.607	598.786	98.776	67.980	34.995	31.621	12.332
9.04863	7.46434	7867.665	3654.675	36.407	9.770	178.644	100.655	453.655	132.665	56.870	48.564	17.280	9.897
9.06354	7.47761	3995.800	2001.500	20.650	6.876	209.700	132.776	125.809	100.675	65.776	21.543	16.772	0.000
9.06426	7.48669	786.778	3096.800	20.776	7.980	574.886	152.664	327.687	97.660	76.898	23.543	52.388	12.543
9.06983	7.46048	786.984	3343.966	19.490	13.223	200.655	102.573	100.980	98.430	623.879	299.443	0.000	0.000
9.03000	7.48000	5109.988	304.748								0.000	0.000	0.000
9.04603	7.48562	5233.588	4553.600	28.559	12.543	305.688	105.776	432.876	104.374	547.667	231.665	54.780	34.808
9.04213	7.46606	3096.431	3007.656	39.650	13.877	238.500	129.697		78.668	78.980	34.250	42.120	21.879
9.04539	7.48223	2000.798	5467.500	40.110	9.669	323.600	131.223	453.987	60.860	78.998	35.480	14.320	6.990
9.02110	7.48753	3096.588	2865.400	24.355	9.374	345.499	158.409	157.879	96.409	89.786	43.211	21.762	7.843
9.02696	7.49772	2435.882	6555.800	36.554	8.589	375.400	176.905	509.908	91.570	675.343	0.000	32.830	21.576
9.03203	7.49484	3099.600	2786.500	30.668	10.430	343.200	239.706	121.776	80.675	76.338	23.552	26.349	13.225
9.04765	7.50383	2090.655	3000.600	23.887	8.660	329.665	159.490	98.786	78.690	329.675	105.488	0.000	0.000
9.04409	7.52223	6045.300	3023.600	27.554	6.097	309.700	103.200	198.790	90.883	342.775	188.343	0.000	0.000
9.03934	7.51904	5448.900	3444.323	28.430	12.995	390.600	159.300	354.880	118.755	100.865	45.776	32.100	28.780
9.04735	7.51126	4354.540	3788.544	31.530	10.400	361.550	106.500	476.980	119.740	99.742	38.678	32.196	17.544
9.05208	7.50548	2007.540	398.600	30.769	11.558	309.700	100.650	228.709	123.100	129.543	32.597	10.877	0.000
9.05941	7.51885	5224.500	4440.866	32.143	12.113	371.500	98.788	100.978	100.212	119.554	13.299	12.654	0.000
9.03000	7.47000	4988.565						567.480			0.000	0.000	0.000
9.06904	7.51801	783.031	4555.786	40.629	13.228	209.599	119.675	365.897	90.876	56.876	32.657	21.543	0.000

9.03610	7.47371	6027.492	5660.700	28.654	9.665	256.334	110.669	547.889	60.870	67.854	23.443	21.654	9.089
9.09638	7.49013	879.662	3576.500	29.760	8.967	275.496	137.648	100.987	78.654	75.436	41.430	21.675	7.095
9.08309	7.50885	4566.768	6775.477	35.700	13.285	144.780	89.765	34.700	65.488	62.098	22.775	10.659	5.890
9.06343	7.49037	987.889	3440.675	27.500	12.976	210.769	121.675	321.987	56.480	43.786	32.125	9.807	0.000
9.01329	7.45798	2004.656	100.000	14.000	5.000	100.000	100.000	50.000	10.000	76.907	10.000	8.798	0.000
9.05572	7.49837	897.400	657.965	12.543	6.077	152.765	89.786	70.980	65.780	43.765	33.647	0.000	0.000
9.03621	7.47526	560.788	440.322	13.860	5.769	98.760	98.760	435.786	57.668	78.665	31.869	5.897	0.000
9.06241	7.49570	1000.807	654.966	9.000	7.998	78.968	100.675	432.890	50.760	23.965	19.865	2.543	0.000
9.04080	7.50541	886.400	568.709	32.700	10.783	100.786	89.540	365.887	40.879	43.865	23.443	3.884	0.000
9.04765	7.50383	550.386	360.879	38.553	10.743	87.708	89.706	425.997	47.685	64.570	31.660	7.848	4.656
9.06000	7.51000	455.887	190.635	38.685	10.574			436.229	56.489	653.854	41.847	3.085	0.000
9.05000	7.54000	3776.453	456.387	32.886	8.687			485.460	79.584	300.574	42.847	6.387	0.000
9.05000	7.50700	4553.871	562.734	21.662	9.876			488.392	109.885	209.578	41.843	7.384	0.000
9.07000	7.53000	4356.834	466.837	17.327	11.432			309.675	92.194	98.584	32.985	3.993	0.000
9.08000	7.51000	3766.309	300.983	31.865	12.423	321.854	89.675	400.886	121.005	295.934	30.992	4.384	0.000
9.08500	7.46000	4332.670	203.434	31.723	11.976	12.540	12.349	562.654	98.586	498.986	28.564	7.998	0.000
9.02000	7.42000	1000.654	400.810	29.771	10.767			574.944	121.473	564.380	28.365	3.954	0.000